AN ELECTRONICALLY FOCUSED MULTIPLE BEAM SIDE SCAN SONAR

Peter Fox

August 1985

Submitted to the University of Cape Town in fulfilment of the requirements for the degree of Doctor of Philosophy.

ABSTRACT

Phased arrays have been in use since World War II but their commercial application has been constrained by the bulk and cost of the beam forming system. High resolution side scan sonar systems have many operational parameters that may only be extended with the aid of phased arrays, the resolution and the imaging rate being the most important. This thesis describes a microprocessor controlled dynamically focused side scan sonar where high resolution and high image acquisition rates are achieved. Dynamic focusing prevents the depth of field limitations of fixed focus arrays by updating the array phases at regular intervals so as to create a focal point which receeds from the array in synchronism with the returning echoes from the transmitted pulse. A high image acquisition rate is achieved through the simultaneous formation of multiple beams. Using a microprocessor as a low cost controller demands rapidly executable software and a little specialized hardware. Programmable quadrature phase shifters give phase and amplitude control. A beam forming board combines the phase shifted signals into a beam and samples it. A 'time domain multiplexed' transmitter solves the problem of efficient insonification of swaths. The system timing is complex; while image samples are captured data is formatted and presented for recording on a chart recorder. This occurs in real-time, while the focus of each of the multiple

beams is changed almost every two meters. Tank tests of the completed system provide confirmation of the resolution predicted with theory and computer simulation. Sea trials confirm that resolution close to that predicted may be obtained under operational circumstances. The results obtained fully justify the assertion that low cost microprocessor controlled dynamically focused multiple beam phased arrays are both an attainable and an attractive solution to the problems faced by the designer of high resolution side scan sonar systems.

DECLARATION

I, Peter Fox, submit this thesis in fulfilment of the requirements for the degree of Doctor of Philosophy. I claim that it is my original work and that it has not been submitted in this or in similar form for a degree at any University.

Signed: Signed by candidate

15 th day of August, 1985.

ACKNOWLEDGEMENTS

I would like to thank Professor Denbigh for the many discussions and useful supervision which I received, the Institute of Maritime Technology for the support and use of the "Shirley-T" and the tank facility, and Steve Miller for the transducer and the seemingly endless wiring looms.

TABLE OF CONTENTS

ABSTRACT ii

DECLARATION iv

PREFACE iv

TABLE OF CONTENTS v

LIST OF ILLUSTRATIONS ix

LIST OF TABLES xi

LIST OF ABBREVIATIONS xii

1 INTRODUCTION 1

2 LITERATURE SURVEY

2.1 Introduction 7
2.2 Phased arrays 7
2.3 Electronic scanning 8
2.4 Fresnel zone scanning 9
2.5 Dynamic focusing 11
2.6 Beam forming systems 13
2.6.1 Digital beam forming 13
2.6.2 Digitally controlled delays 15
2.6.3 Digital delays 15
2.6.4 Analog delay lines 16
2.6.4.1 Charge coupled devices 17
2.6.4.2 Surface acoustic wave devices 18
2.6.4.3 Lumped constant LC delay lines 19
2.6.5 Phase shift beam forming 19

3 SYSTEM PARAMETERS

3.1 Introduction 21
3.2 Basic system parameters 23
3.2.1 Frequency 23
3.2.1.1 Attenuation 23
3.2.1.2 Noise 24
3.2.1.3 Backscattering strength 24
3.2.2 Resolution 27
3.2.2.1 Along-track 27
3.2.2.2 Range Resolution 29
3.2.3 Transducer 29
3.2.3.1 Near field effects 29
3.2.3.2 Dynamic focusing 30
3.2.3.3 Array elements 31
3.2.3.4 Grating sidelobes 33
3.2.3.5 Scanning 35
3.2.3.6 Construction 36

TABLE OF CONTENTS

4	FOCUSING, STEERING AND SHADING	
4.1	Introduction	38
4.2	Focused apertures	38
4.2.1	Continuous focusing	40
4.2.2	Scanning	41
4.2.3	Depth of field	41
4.3	Discretely focused array	42
4.3.1	Array bounds	42
4.3.2	Computer modelling	49
4.4	Final beam forming configuration	54
5	PHASE SHIFTS	
5.1	Introduction	61
5.2	Digitally controlled analog phase shifters	61
5.2.1	Programmable gain amplifiers	63
5.2.2	Phase coefficient determination	67
5.3	Calibration and testing of phase shifters	72
5.3.1	Static performance	72
5.3.2	Dynamic range	72
5.3.3	Dynamic performance	74
5.4	Phase errors	79
6	SUMMING, DETECTION AND A/D CONVERSION	
6.1	Introduction	83
6.2	Time varying gain	83
6.3	Detection	83
6.4	A/D conversion	85
7	TRANSMITTER	
7.1	Introduction	87
7.2	Transmitter transducer	87
7.2.1	Required insonification	87
7.2.2	Large uniform aperture	88
7.2.3	Large phased aperture	89
7.2.4	Small aperture	91
7.2.5	Multiple transmitting subarrays	92
7.2.6	Receiver considerations	95
7.3	Transmitter hardware	96
7.3.1	Sequencer	96
7.3.2	Power drivers	96

TABLE OF CONTENTS

8 PREAMPLIFIERS

8.1 Introduction 99
8.2 Input stage 99
8.2.1 Transducer matching 100
8.2.2 Front end tuning 103
8.3 Line drivers 104

9 TIMING

9.1 Introduction 106
9.2 Overall timing 107
9.2.1 Parallel to serial swath conversion 107
9.2.2 Range sampling 108
9.2.3 Data output timing 110
9.3 Timing and output hardware 111

10 CONTROLLER: SOFTWARE AND HARDWARE

10.1 Introduction 116
10.2 Program overview 117
10.3 Software description 119
10.3.1 Main routine 119
10.3.1.1 Time varying gain 119
10.3.1.2 Time keeping setup 121
10.3.1.3 Dynamic memory allocation 122
10.3.1.4 Initial output 124
10.3.1.5 Initial phases 124
10.3.2 Phase setting 125
10.3.3 Range sampling 126
10.3.4 Data output 129
10.4 Memory map 132
10.4.1 Program memory 132
10.4.2 Preset data storage 132
10.4.3 Random access memory 132
10.5 Address allocation 134
10.6 Input/output ports 135
10.7 Hardware 136

TABLE OF CONTENTS

11	RESULTS	
11.1	Introduction	139
11.2	Beamwidth measurement	139
11.2.1	Experimental setup	140
11.2.2	Measurement accuracy	143
11.3	Beamwidths	144
11.4	Vertical beamwidth	148
11.5	Reservoir tests	154
11.6	Sea trials	156
12	CONCLUSIONS	
12.1	Conclusions	167
12.2	Developmental possibilities	169

APPENDICES

Appendix I	Analysis of field of array	172
Appendix II	Field modelling	176
Appendix III	Phase determination	181
Appendix IV	Controller software	186
Appendix V	Circuit diagrams	202
Appendix VI	Publication	208

LIST OF REFERENCES 218

LIST OF ILLUSTRATIONS

Figure 3.1 System parameters 22
3.2 Frequency and attenuation 25
3.3 Ambient noise spectral density 25
3.4 Backscattering strength 25
3.5 Incomplete surveying at high speed ... 28
3.6 Multiple beams imaging parallel swaths 28
3.7 Beamwidths of focused and unfocused apertures .. 30
3.8 Array geometry 32
3.9 Far field beam pattern 32
3.10 Photograph of transducer 37

Figure 4.1 Transducer and field geometry 39
4.2 Far field beam pattern of transducer . 39
4.3 Array and element patterns superimposed 43
4.4 Field intensity; 3 element array at 10 m 50
4.5 Field intensity; 3 element array at 10 m, steered 50
4.6 Field intensity; 4 elements at 10 m 52
4.7 Field intensity; 4 elements at 10 m, steered 52
4.8 Array growth 55
4.9 Field intensity; centre beam, 10 m to 55 m, "3-D" 58
4.10 Field intensity; centre beam, contour plot 58
4.11 Field intensity; beam no. 2, 10 m to 55 m, "3-D" 59
4.12 Field intensity; beam no. 2, contour plot 59
4.13 Field intensity; beam no. 1, 10 to 55 m, contour 60

Figure 5.1 Quadrature power divider 62
5.2 Phase and amplitude response 62
5.3 Block diagram of phase shifter 64
5.4 Photograph of phase shifter 65
5.5 Phase shift test circuit 76
5.6 Phase shift test results 76,77
5.7 Field intensity; 5 element array at 21 m 81
5.8 Field intensity; 5 phase errors 81
5.9 Field intensity; 10 phase errors 82

LIST OF ILLUSTRATIONS

Figure	6.1	Beam forming block diagram	84
	6.2	Detector performance	84
	6.3	Photograph of beam forming board	86
Figure	7.1	Beam necking	90
	7.2	Low directivity insonification	90
	7.3	Non overlapping outward bound pulses .	94
	7.4	Transmitter beam coverage	94
	7.5	Block diagram of transmitter	97
	7.6	Photograph of transmit sequencer and driver ..	98
Figure	8.1	Block diagram of preamplifier	101
	8.2	Equivalent circuit of transducer	101
	8.3	Circle diagram, element 10	102
	8.4	Circle diagrams of all elements	102
	8.5	Photograph of preamplifier	105
Figure	9.1	System timing diagram	109
	9.2	Measured timing, beam 1	112
	9.3	Measured timing, beam 2	112
	9.4	Block diagram of timing board	113
	9.5	Photograph of timing board	115
Figure	10.1	Main routine flow chart	120
	10.2	Dynamic memory allocation	123
	10.3	Phase setting flow chart	127
	10.4	Range sampling flow chart	128
	10.5	Data output flow chart	131
	10.7	Photograph of controller	138

LIST OF ILLUSTRATIONS

Figure 11.1 Tank experimental set up 142
11.2 Simulated echo timing system 142
11.3 Directivity; beam no. 1 at 10 m 145
11.4 Directivity; beam no. 2 at 10 m 145
11.5 Directivity; beam no. 1 at 14 m 149
11.6 Directivity; beam no. 3 at 16,8 m ... 149
11.7 Directivity; beam no. 1 at 16,8 m ... 150
11.8 Directivity; beam no. 1 at 17 m 150
11.9 Vertical beam pattern 152
11.10 Vertical beam pattern with baffle ... 153
11.11 Geometry of baffle 153
11.12 Polar scan of reservoir 155
11.13 Array mounting frame on vessel 158
11.14 Sidescan record of wreck 160
11.15 Record of wreck made with improved TVG profile 161
11.16 Record of base of tower 163
11.17 More sand ripples 163
11.18 Sand hillock 164
11.19 Sand hillock, reduced contrast 165
11.20 Sand hillock, expanded 166

LIST OF TABLES

Table 4.1 Binary beam shading 48
4.2 Subarray length and resolution 54

5.1 Beam no. 1 phases 70
5.2 Phases arranged for transfer 71
5.3 Static phase shifter test results ... 73
5.4 Beam no. 5 phases 78

8.1 Resonant frequencies of elements 100

10.1 Memory allocation 134
10.2 Input/output port mapping 135

ABBREVIATIONS AND NOMENCLATURE

A/D .... Analog to digital converter

β ..... Propagation constant (rads/m)

C ..... Coefficient, cosine channel of phase shifter

CCD .... Charge coupled device

d ..... Element spacing (m)

D ..... Overall array length (m)

FFT .... Fast Fourier Transform

FIFO ... First in first out buffer

FIR .... Finite Impulse Response

λ ..... Wavelength (m)

P( )..... Field amplitude

S ..... Coefficient, sine channel of phase shifter

S(n).... Discrete aperture illumination

Sa(x)... sin(x)/x

w ..... Width of element (m)

x ..... Azimuth (m)

x_f ..... Focal azimuth (m)

x_n ..... Azimuth of centre of n th element (m)

z ..... Range (m)

"...upon the unplumbed, salt, estranging sea."

Matthew Arnold, 'To Marguerite' 1863

INTRODUCTION

The history of hydrographic survey, beginning with the circumnavigation of the globe by James Cook, predates the appointment of the first British Naval Hydrographer (in 1795) by some 25 years. From these early beginnings until the 1920's surveys were made with a lead and line. Around 1925 the first ultrasonic echo sounders were introduced and pronounced an instant success by the Hydrographer of the time.

The technique of continuous echo sounding along transit lines has the obvious disadvantage of leaving large tracts of the sea bed between the transit lines unsurveyed. An unexpected pinnacle of rock may lurk in one of these gaps awaiting the unlucky passage of a vessel overhead.

The realization of echo sounding systems was accomplished before the development of useful side scan sonar systems. The concept of side scan sonars (originally known as horizontal echosounders) was however, the seed from which echo sounders developed. A patent application dated May 10, 1912 filed by Richardson (1) referred to a patent filed earlier the same year describing an apparatus "for detecting the echo from a large object when the sound travels through the air" and suggested "an adaptation of this method so as to make it work under water". The title "Apparatus for Warning a Ship at Sea of its Nearness to Large Objects Wholly or Partly under Water" suggests that the

germination of this idea lay not in the field of echo sounding but rather in the sinking of the Titanic the previous month after a collision with an iceberg.

World War I and the production of the submarine provided the impetus for the development of sonar (an achronym derived from Sound Navigation and Ranging) as a possible countermeasure. During this period Fessenden (2) constructed a moving coil acoustic transducer for submarine communications and echo ranging. The device was not particularly suitable for sonar. In 1916 Langevin developed an acoustic transducer utilizing the piezoelectric effect (3). The device was (and remains) most suitable, capable of producing large outgoing acoustic power while remaining extremely sensitive to the very small echoes returning. The emerging electronics technology of that time, the vacuum tube, enabled the tiny voltages produced by the transducer to be amplified and detected and the practical implementation of Richardson´s invention was possible.

World War II saw extensive field deployment of active sonars and led to the observation by ASDIC (Anti-Submarine Detection Investigation Committee) operators that there was a close correlation between the intensity of echoes returning from the sea bed and the topography. In 1954 Urick (4,5) decribed backscattering of sound from a harbour floor. In 1955 Ahrens (6) described the use of horizontal echo

sounding for the location of fish and later, in a lecture delivered at the International Meeting on Radiolocation in Hamburg during 1957 produced some results on the application of the technique to wreck detection (7). At the same meeting Kunze (8) described a device developed by a colleague, Dr. Kietz, which produced images of the sea bed on both sides of a towed body. This was the first side scan sonar and its ability to delineate objects on the sea floor that might warrant further attention was clearly demonstrated to the meeting with a side scan record of a wreck. The cartographic type of image produced by Kietz stimulated interest in side scan sonars outside the domain of civil and military mariners.

Experiments conducted by Chesterman, Clynick and Stride (9) left little doubt as to the usefullness to marine geologists of side scan sonar as an instrument for surveying the sea bed. The Kelvin Hughes company displayed a commercial instrument known as a "Surveying Asdic" at the 8th International Hydrographic Conference in May 1962 (10). Their results were not as striking as those obtained by Kietz but the system was a major advance in that the transducer was mounted on a towed body. Gyrostabilization of the tranducer mount to counteract the pitch and roll of the vessel was no longer required. Furthermore, the transducer could be towed closer to the sea bed, increasing coverage while reducing the interfering effects of aeration and propeller noise.

After that the development of side scan sonars was rapid and varied. Side scan sonar systems have been described with a wide spectrum of operating parameters, ranging from the long range system known by the acronym GLORIA (11) with an operating range of over 20 km to a short range high resolution system with a maximum range of 15 m (12). GLORIA is an impressive system with a 5 m long transducer mounted in a towed body weighing 3,5 tons in water. The transmitted frequency is 6,5 kHz at a power level of 50 kW and the beamwidth is approximately 2,7°, giving a resolution of 1 km at the maximum range. At the other extreme is the short range high resolution system achieving 50 mm resolution at 15 m range with multiplicative processing of the signals from an array operating at 750 kHz.

Between these extremes is a variety of commercially available side scan sonars with ranges from 100 m to 2400 m (13). At the longer ranges attenuation places restrictions on the maximum frequency and thus the attainable resolution while at shorter ranges higher frequencies of operation are possible. Unfortunately at these higher frequencies the beam formed by a uniform aperture remains collimated and the finest resolution is approximately equal to the transducer size.

To achieve high resolutions at short ranges requires the use of transducer apertures which may be controlled. By focusing an aperture the beam

collimation may be avoided and the resolution is significantly enhanced. A further complication with high resolution side scan sonars is that the towing speed of the array is limited by the need to provide surveying of contiguous swaths without any gaps between them. This problem may be solved by the use of electronic scanning to image more than one area simultaneously at a given range. The possible towing speed increases linearly with the number of beams formed.

Electronic beam forming, focusing and scanning may all be accomplished with phased arrays, the theory of which dates back to Schelnukoff's work at Bell Labs during World War II (14). For many years the application of the theory was hampered by the difficulty and cost of its physical implementation.

The difficulty lay mainly in two areas; the time delays (or phase shifts) and the beam former (or controller). The trade-offs involve the number of units, their complexity, control, bulk and cost; all considered within the context of the available technologies.

Over the past fifteen years rapid advances have been made in analog and digital integrated circuits. Although the complexity of phased arrays has in no way diminished as a result of these developments, the cost and difficulty of their implementation has. The desired high resolution and high imaging rates can now

be attained with phased array sonars that are portable and easy to handle without being prohibitively costly.

The objective of this thesis is to demonstrate the validity of the above statement by designing, constructing and evaluating a high resolution electronically focused multiple beam side scan sonar which is portable and within the financial reach of every serious investigator of the sea bed.

Literature Survey

2.1 Introduction

A brief history of the application of phased arrays to sonar systems (particularly side scan sonar) is followed by a survey of the techniques and the technologies available to a designer of such a system today.

2.2 Phased arrays

Schelkunoff (14) presented a classic paper in 1943 on the mathematical theory of linear arrays and Woodward in 1946 (15) described a method for calculating the aperture illumination required to produce a given polar diagram. Beam forming with phase shifters had been realized prior to the end of World War II. The U.S.A., Great Britain and Germany all used phased array radars using mechanically actuated phase shifters to accomplish beam steering (16). The mechanical phase shifters could be altered only relatively slowly and the beam angle was varied discretely from pulse to pulse rather than dynamically within the interpulse period. The realization of electronic phase shifters which could be altered rapidly was the key to the real-time multiple beam formation required by high resolution sonar systems and simultaneously would allow arrays to be focused and

thus achieve the desired high resolutions.

2.3 Electronic scanning

The first application of real-time phased arrays in sonar was a within-pulse sector scanning sonar for fish detection and location. Electronic sector scanning was developed independently by Tucker at the University of Birmingham and Voglis at the Admiralty Research Laboratories (17). In 1958 Tucker, Welsby and Kendell (18) described a practical implementation of electronic sector scanning utilizing an appropriate frequency modulation technique (19) and a lumped constant LC delay line to produce the necessary time-varying aperture illumination. The method of implementation lent itself to the generation of the linear phase tapers required for beam steering, but did not allow for the often complicated aperture illuminations required in high resolution systems. Results of the sea trials of this horizontal echo ranger were presented by Tucker et.al. (20) in 1959. Although the primary application of this equipment was the detection and location of fish one of the images shown was a side scan sonar type record of the outer breakwater of Portland harbour. Welsby (21) suggested the use of multiplicative processing to enhance the resolution and some results of this approach were presented by McCartney (22) who also described an improved method of controlling the phases although the basic limitations

of the frequency modulation technique remained.

In 1963 Welsby and Dunn (23) described a high resolution sonar with electronic sector scanning. The system had some similarities (in terms of operating frequency and range resolution) to the system described in this thesis. Resolutions of 20 cm at 12 m range were achieved with multiplicative processing. Resolution at greater ranges was not discussed but is almost certain to have degraded linearly with range; while the resolution obtained with this system remains essentially constant over a significant portion of the operating range.

Multiplicative processing certainly enhances resolution in some systems, but may produce undesireable responses in a multiple target environment due to a form of intermodulation resulting from the inherent non-linearity of the beam forming process. This may cause targets seemingly to disappear and result in an image with a granular texture (24). These spurious responses may be reduced with incoherent pulse to pulse integration (25). This requires multiple pulses on target and reduces the scanning rate.

2.4 Fresnel zone scanning

The medical profession and materials engineers had a requirement for non-invasive short range high resolution ultrasonic inspection instruments which

could best be met by transducers operating in their near field. The sound field of a rectangular transducer in the near field had been approximated and theoretically examined by Freedman (26) in 1959. In 1964 Kay and Bishop (27) presented a paper on near field beam steering. In the ensuing discussion they mentioned that electronic focusing was being considered and noted that it would be necessary to vary both the focal length and the focal direction to make such a system useful. This would have involved considerable complexity in the electronics and was not thought to be a viable proposition. Kay did however suggest that the aperture of an electronically focused array might necessarily be small in terms of wavelengths and that the resolution would thus be somewhat restricted. Welsby (28) gave a simple proof in 1968 that under certain practical conditions the effect of focusing is simply to shift the normal far field directional pattern of an array from infinity onto the focal surface. Tucker (29) then showed that the resolution advantages to be gained from multiplicative processing were even greater in the near field than in the far field, although the restrictions on the scanning rate and pulse repetition frequency remained.

Around this time the first reports of the utilization of electronic beamforming in medical imaging were published. Somer (30) in 1968 described an electronic sector scanning ultrasonic imaging instrument and later reported resolution improvements

using nonlinear processing (31). In 1971 Gazey and Creasey (12) described a high resolution short range sonar using multiplicative processing since, as they noted "focusing would be unacceptable because of either complexity or the small depth of focus". Welsby, Creasey and Barnickle (25) applied mechanical prefocusing to a multiplicative array to improve the resolution but the system was obviously limited in its depth of field. While discussing this problem they noted the possibility of automatically varying the focal distance so as to resolve the depth of field problem for systems in which the operating range extends from close to the array to well into the far field. High resolution is a desirable goal since it increases the amount of information, and in some systems this goal may only be achieved with the aid of dynamic focusing.

2.5 Dynamic focusing

By the early seventies the development of analog and digital integrated circuits had profoundly altered the technological environment within which research into high resolution short range ultrasonic imaging was conducted. The emerging integrated circuit technology not only reduced analog circuit complexity but also made the use of programmable digital controllers for phased arrays a practicality. The problem of electronic complexity was diminished by these

developments in such a dramatic fashion that not only did electronic focusing become a relatively simple process but dynamically variable focusing was also feasible.

In 1973 Thurstone and Von Ramm (32) described an ultrasonic imaging system using a phased array transducer to provide not only electronic sector scanning but dynamic focusing which permitted the receiver to be focused at a range that increases with time, tracking the increasing two way propagation time of the returning ultrasonic echos. It is the primary factor responsible for the improved resolution of the system.

The system of Thurstone and Von Ramm was for diagnostic use in evaluating the dynamic behavior of the heart and required very high data rates. To this end a PDP-11 minicomputer was the dedicated controller. A computer of this size is not readily transportable, and instead of putting to sea the dynamically focused phased array remained confined to the medical diagnostic laboratories.

For high resolution side scan sonars with dynamic focusing to be available to marine geologists and geophysicists the instruments would have to be of reasonable cost and physical transportability. The late seventies saw the phenomenal development of microprocessors and large scale integration with the concommitent plummeting of the costs of these devices.

These are the prerequisite tools for the realization of a portable dynamically focused side scan sonar.

2.6 Beam forming systems

There exist a wide variety of ways in which beam forming and focusing may be achieved. These range over a continuum from wholly digital to wholly analog methods with almost any combination of the two technologies (32,33,34,35,36,37,38). The various available techniques are examined primarily for their applicability to a dynamically focused side scan sonar and secondarily with respect to cost and/or complexity.

2.6.1 Digital beam forming

The digital methods involve the sampling and A/D conversion of the signals and their subsequent algorithmic processing. Sampling is usually performed at the Nyquist rate, although bandpass signals such as those normally encountered in sonar systems may be sampled at the lower rate of approximately twice the signal bandwidth. If the spatial processing (beam forming) is carried out before the temporal processing the system is known as a phased array, while when the reverse is true it is termed a holographic system (39). In an all digital beam former it makes little difference which calculations are performed first.

The attraction of the wholly digital methods lie primarily in the declining size and cost of the hardware and in the use of the Cooley-Tukey algorithm (40), or Fast Fourier Transform (FFT), to reduce the number of computations. The advantage to be gained from the FFT is not available in the case of a focused array. The discrete Fourier transform used in far field imaging with arrays to compute the wavenumber (and hence angle of arrival) of an incoming wavefront is not applicable in the near field where the spatial frequency of an incoming wavefront is not constant over the array face. In the near field the transformation from the samples of the wavefront to the angle of arrival is described by the Fresnel integral (26,41) A matrix may be set up which transforms a vector input of wavefront samples into a vector output of samples of the echo intensity within the range cells, but the matrix lacks the symmetry and linearity of the discrete Fourier transform and must be computed exhaustively. Some researchers have utilized the rather limited symmetry of the matrix to optimise the processing algorithm (42). Even on relatively powerful minicomputers the optimized processing of each scan takes some seconds (if not minutes).

The amount of processing done in software may be reduced at the expense of introducing more hardware.

2.6.2 Digitally controlled delays

The time consuming complex multiplications required in digital beam forming may be circumvented using digitally controlled delays or phase shifts. Again the techniques may be divided broadly into those dealing with analog samples and those dealing with digital samples. Digital delay lines and phase shifters operate by converting the analog sample of the output of each element into a digital value and storing the values in some type of memory for further processing.

2.6.3 Digital delays

If the signal samples are stored in a random access memory (RAM) and read out from the storage locations with appropriately differing base addresses delays may be realized. A medical imaging system utilizing the RAM method has been constructed (43). The signal is sampled at twice the maximum frequency and the constraints placed on the A/D converters and the data acquisition rates are severe. Since the fractional bandwidths of side scan sonar systems are significantly less than those of medical imaging systems there is some advantage to be gained by sub-Nyquist sampling.

Sub-Nyquist sampling allows signals to be sampled at rates consistent only with their bandwidth. Complex sampling techniques are required to prevent aliasing (44,45). A variety of methods exist using the Hilbert

transform, second order sampling or quadrature sampling. All result in significant reductions in the conversion times required of the A/D convertors.

The samples may be processed in the frequency domain to form the beams as in the digital shifted sideband beam former (46) or in the time domain. Unfortunately an input sampling rate of between five and ten times that required for waveform reconstruction is needed to achieve acceptable approximations to the exact focusing and steering delays (47). The sampling rate may be reduced by inserting Finite Impulse Respone (FIR) digital filters between the A/D converters and the subsequent processing. In this way the bandlimited waveform may be sampled at the sub-Nyqist rate, padded with zeroes and reconstructed by interpolation to produce samples at the rates required by beam forming.

2.6.4 Analog delay lines

The use of digitally controlled analog delay lines has been widespread both in medical imaging and in sonar systems. In some systems the waveform is sampled at discrete intervals and the analog samples are delayed using a bucket brigade device such as a charge coupled device (CCD) (48) or a switched capacitor filter (49). Other systems do not sample the waveform but provide identical delayed versions of the input signal. The delays are not continuously variable; an analog multiplexer selects the delay by selecting one

of the taps provided at various intervals on the delay line.

2.6.4.1 Charge coupled devices

With unfocused beam forming a single CCD allows the formation of a single steered beam in real-time by using the taps as inputs and controlling the clock frequency to achieve the required interelement delays (48). Another method is the use of a bank of CCD´s, one per element (50). Such an arrangement can provide focusing, although the circuitry to generate the clock frequencies in a dynamically focused system in which the required delays do not vary linearly with time would be complex. The sampling rate within the CCD would normally be at least the Nyquist rate although a system of quadrature sampling has been implemented (51) which results in a significant reduction in the required sampling rate without the need for mixers.

The generation of the clocks may be considerably eased by utilizing more specialized CCD devices. A cascade charge coupled device (C3D) has been described (52,53) which combines a pair of linearly tapered CCDś to achieve the linear delays required by beamsteering, with a pair of quadratically tapered CCD´s to achieve focusing. The clocking rates of the CCD´s determine the scan angle and the focal length. The system is elegant and promising but it does require access to custom made CCD´s, which are very expensive in low

volume production runs.

2.6.4.2 Surface acoustic wave devices

Continuous analog delay lines have been widely applied in beam forming systems. Surface acoustic wave devices have been used in beam steering applications (54) as well as focusing. An ingenious focused array has been described (55) using a chirp signal travelling on a surface acoustic wave device simultaneously to focus and scan an acoustic transducer array by mixing time translates of the chirp waveform with the signals from the array elements. The system described performed imaging in one direction only (azimuth) although range resolution could be implemented with little difficulty. The chirp signals (one for each different focal distance) required for dynamic focusing would be difficult to generate; they might be stored digitally and read out at the appropriate times (once per range cell). This would require considerable storage and high data transfer rates. Another disadvantage is that mixers are rather difficult to match in a multi-element array that is highly sensitive to phase and amplitude (51).

2.6.4.3 Lumped constant LC delay lines

Lumped constant delay lines utilizing inductors and capacitors to simulate transmission lines with low propagation velocities were applied to the construction of the first dynamically focused imaging system (32) after having been used for some years in within pulse electronic sector scanning instruments (18,20). While providing a large dynamic range the lumped constant delay lines are physically large, expensive and subject to switching transients (51). They also have a drawback in common with other delay lines in which the delay is determined by the selection of one of the multiple taps. The number of taps required for efficient beam focusing is large and the analog multiplexer performing the selection is also prone to switching transients.

2.6.5 Phase shift beam forming

One of the major advantages of side scan sonar systems is the narrow fractional bandwidth. At small scan angles the required time bandwidth product of the delay lines is small, typically less than one. True time delays are unnecessary since the pulse length is many times greater than the maximum delay, and phase shifters would provide adequate control of the signal phases. A small distortion is expected to arise from not using true time delays but this is confined to within a few cycles of the leading and trailing edges

of the pulse. Narrow band phase shifters providing eight bits of phase control while simultaneously allowing shading to be applied are relatively simple to construct and inexpensive. While the cost of providing one phase shifter for each element used in forming each beam may be relatively large it is certainly not prohibitive and is greatly offset by the reduced cost of the controller. The controller is relieved of all the mathematical operations involved in the beam forming process and is only concerned with providing data to the phase shifters and orchestrating the process.

SYSTEM DESIGN

3.1 Introduction

The design of a dynamically focused side scan sonar involves the consideration of a large number of interelated parameters. Some of the system constraints are imposed by the available technologies and their relative costs and complexities. Other constraints are imposed by the medium through which the signal propagates and the motion of the platform bearing the array.

The major factors that are considered in the design and a map of their relationships with one another is shown in fig. 3.1. After the basic system parameters are fixed the problem is simply to achieve the highest possible resolution without incurring excessive costs.

This chapter outlines the reasoning involved in the determination of the configuration of the array and beam forming system.

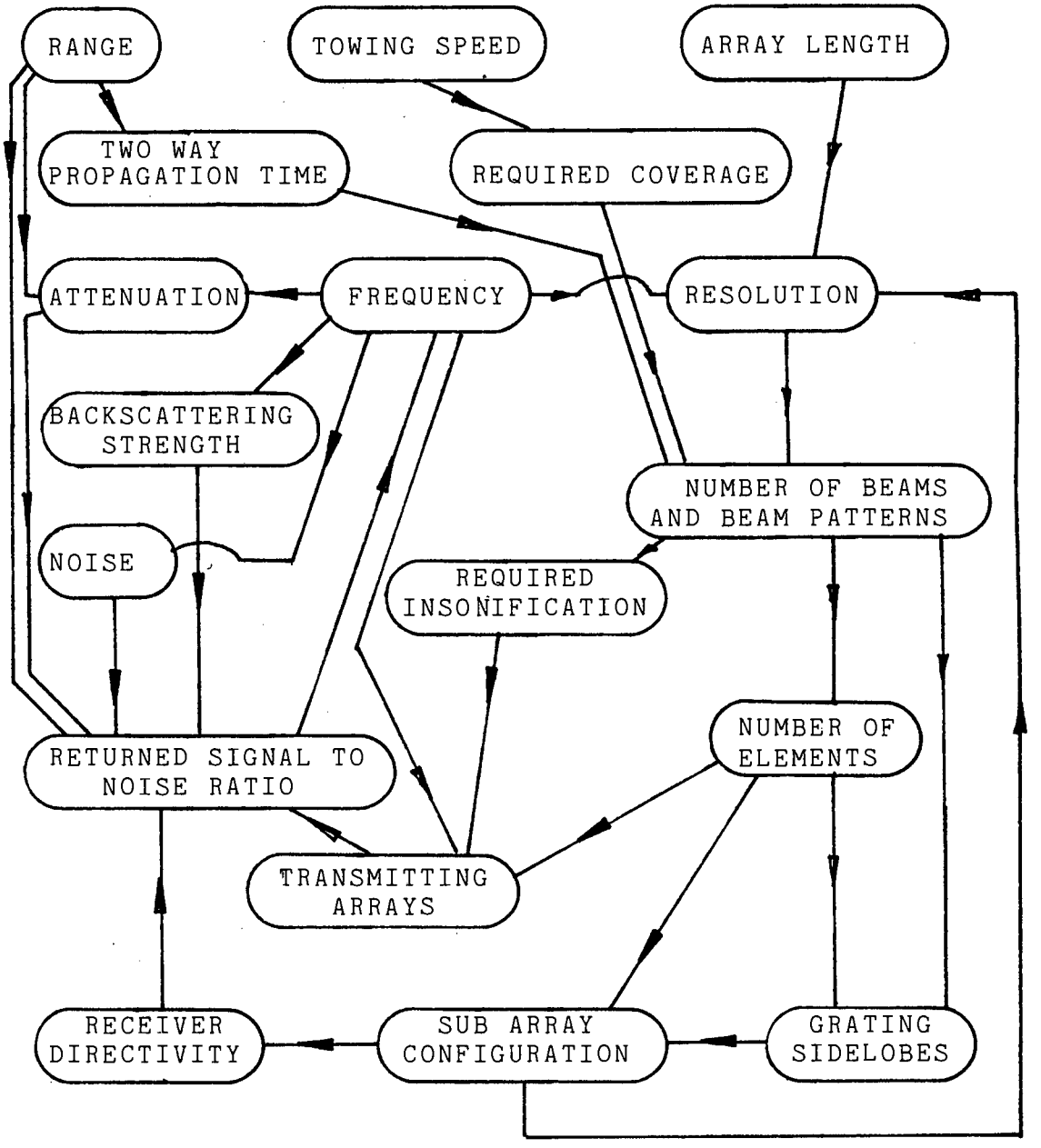

Fig. 3.1: The interrelated system parameters

3.2 Basic System Parameters

The side scan sonar is designed to have an operating range of 10 m to 150 m and to produce continuous high resolution images while being towed at a speed of 10 knots. As a portable instrument the maximum array length is restricted for ease of handling to about 1 m. A resolution of 0,2 m is considered desirable over much of the operating range, and at least out to 40 m.

3.2.1 Frequency

High frequencies give high resolution without placing too severe demands on the aperture size. The maximum frequency is determined by a number of factors dealt with below.

3.2.1.1 Attenuation

Examining the relationship between frequency and attenuation shown in fig. 3.2 it is clear that the attenuation increases over most of the frequency spectrum shown as the square of the frequency (56). At a frequency near 300 kHz the attenuation is aproximately 0,1 dB per meter. At 150 m range the two way transmission loss due to attenuation is 30 dB.

3.2.1.2 Noise

The ambient noise level in the sea at coastal locations consists of a number of identifiable components (57). Wind and wave action produce noise, as does shipping. The associated noise spectra decrease with increasing frequency. Above 100 kHz the dominant noise source is thermal noise, and the ambient noise power spectral density increases from its minimum level of 28 dB re 1 Pa (in a 1 Hz bandwidth) at a rate of 6 dB per octave, as shown in fig. 3.3.

At high frequencies thermal noise in the ocean and receiver front end noise are the major contributors to the noise component of the signals presented to the beam former.

3.2.1.3 Backscattering strength

The backscattering strength of the sea bed as a function of frequency and angle of incidence is shown in fig. 3.4.

Towing a sonar 20 m above the sea bed and projecting sound at a point 150 m away results in an angle of incidence of 10°. At such angles and at frequencies around 300 kHz the backscattering strengths vary from -40 dB to -25 dB (58).

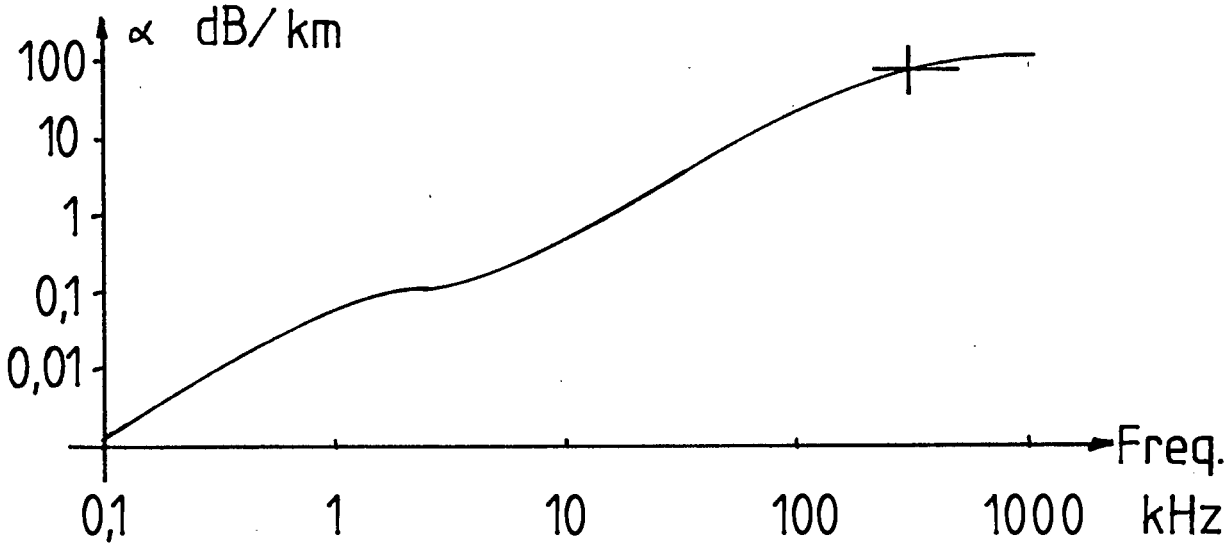

Fig. 3.2: Attenuation coefficient.

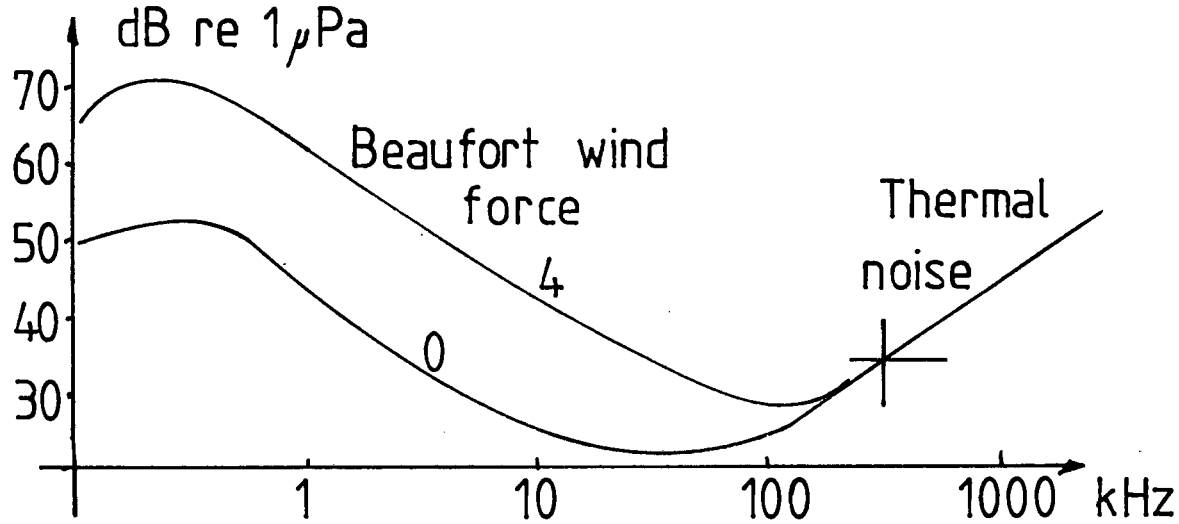

Fig. 3.3: Ambient noise spectral density.

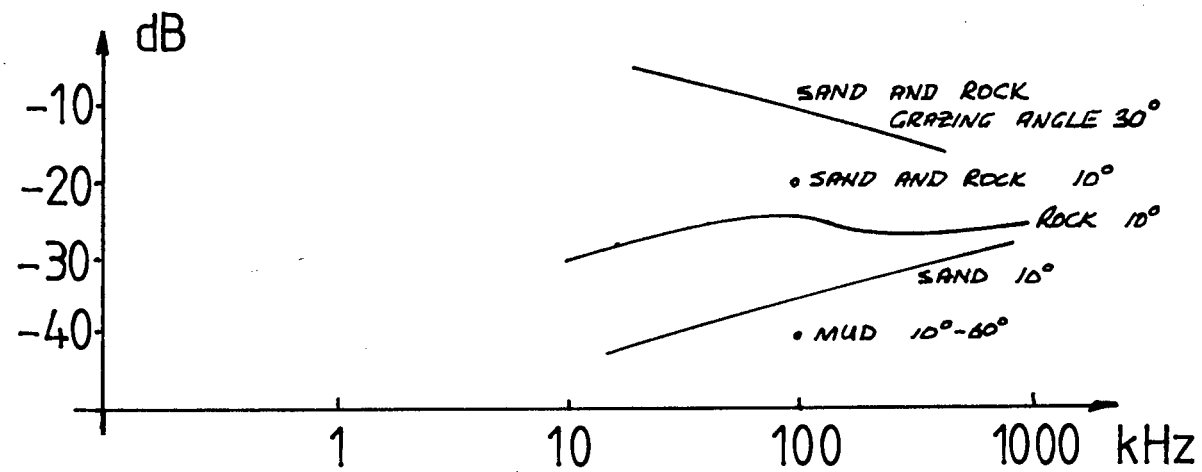

Fig. 3.4: Backscattering strength.

The high attenuation at 300 kHz is clearly the dominating factor in signal to noise ratio calculations at long ranges. For this reason the system operating frequency was chosen to be close to 300 kHz. The exact value of 308 kHz actually used was found after determining the resonant frequency of the completed transducer.

Curves and tables (60) are available for the rapid determination of the maximum operating range that may be expected of a typical side scan sonar operating at 300 kHz. With a minimum signal to noise ratio of 15 dB, a fractional bandwidth of 0,1 and a backscattering strength of -35 dB an operating range of 160 m is predicted using a source level of 228 dB re 1 Pa, and an azimuthul beamwidth of 0,33 rads. The beamwidth of the side scan sonar system described here is at least an order of magnitude narrower than this 'typical' value.

With the high directivity index of the 208 wavelength array on both transmit and receive (26 dB each way) an acoustic power output of 200 W will suffice and the transmitter is designed accordingly, as discussed in chapter 7.

3.2.2 Resolution

3.2.2.1 Along-track

The along-track resolution, the required towing speed and the maximum range together determine the number of beams that must be formed. Figure 3.5 shows the effect of towing a high resolution side scan sonar at a rate faster than the width of one resolution cell width per interpulse period.

The interpulse period is determined by the maximum operating range. At 150 m range returning echoes take 200 ms. With a resolution of 20 cm this restricts the towing speed to 1 m/s, or close to 2 knots. At the desired towing speed of 10 knots there would be gaps of 80 cm left unsurveyed between each imaged swath.

With the formation of multiple simultaneous beams the gaps may also be surveyed within the allotted time. Such a system is shown in fig. 3.6 where the parallel swaths are shown along with two resolution cells (shaded) of two of the beams. The formation of multiple parallel beams allows the surveying rate to be increased proportionately. For the towing speed of 10 knots the required number of beams is 5.

At lower towing speeds it is not necessary to turn off any of the beams so as to prevent overlap. The image is still a set of 5 swaths totalling 1 m width but the interval between transmitted pulses may be increased to the appropriate value by slowing down the

chart recorder. This is discussed in some detail in the chapter on system timing along with a method for maintaining an even flow of data, swath by swath, to the chart recorder.

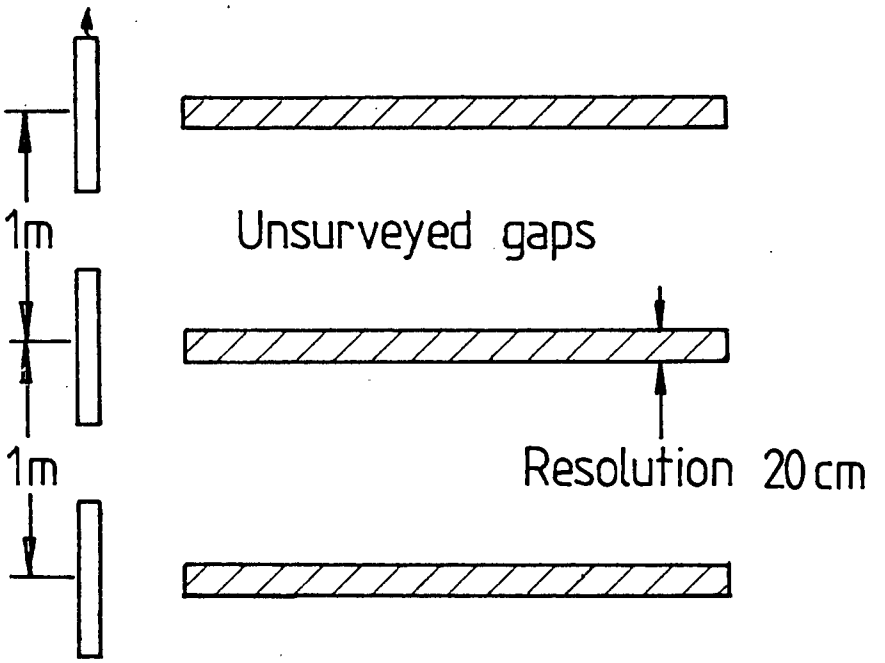

Fig. 3.5: Incomplete surveying with high resolution

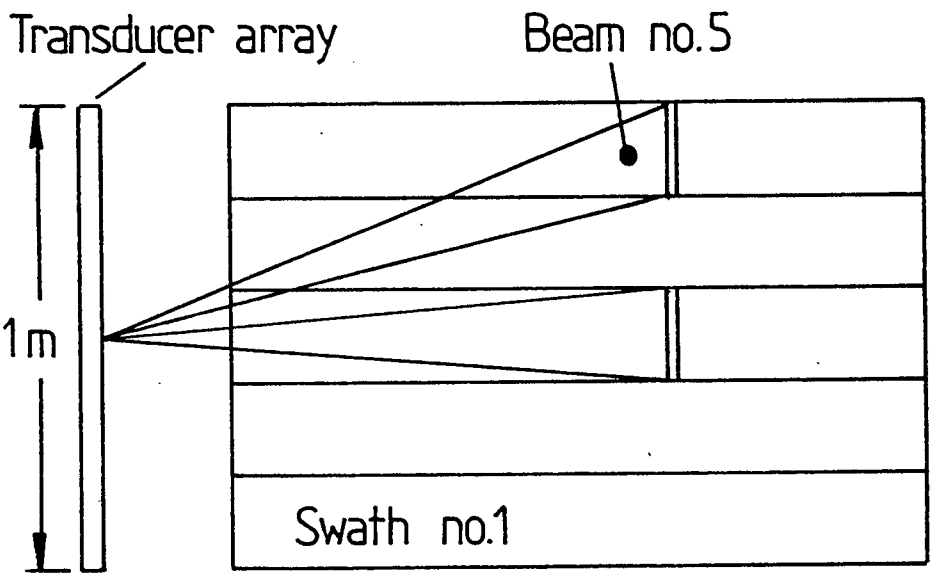

Fig. 3.6: Multiple beams imaging parallel swaths.

3.2.2.2 Range Resolution

The ultimate limit on the range resolution is the resolution of the display. Since few chart recorders (or other suitable displays) will resolve more than 1000 pixels there is little advantage to be gained by designing for resolutions better than this. The system is designed to produce a range resolution of 13,7 cm, corresponding to 1024 pixels per swath (the base 2 number is chosen to optimize the processing time of some of the microprocessor subroutines).

3.2.3 Transducer

3.2.3.1 Near field effects

Using a transducer of the maximum length (1 m) at a frequency of 308 kHz results in a near field which extends to a range far greater than the maximum operating range. Since the beam of a uniformly excited transducer in its near field is essentially collimated and thus approximately equal to the transducer length it is apparent that focusing is necessary to achieve the desired resolution of 0,2 m with a 1 m transducer. The situation is depicted in fig. 3.7 where the approximate -3 dB contours of an unfocused beam and a focused beam are drawn for comparison.

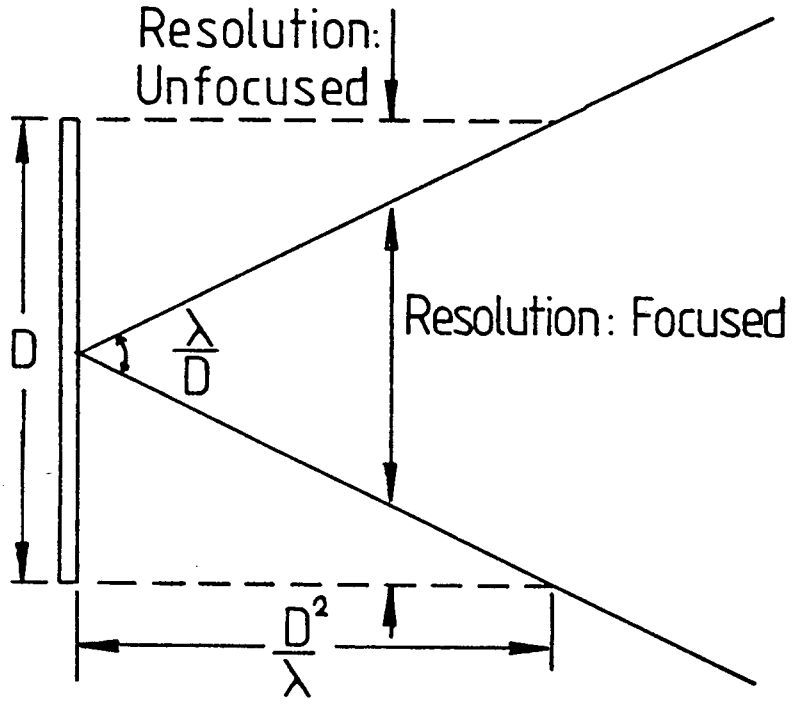

Fig. 3.7: Beamwidths of focused and unfocused apertures

3.2.3.2 Dynamic focusing

With focusing the beam formed by an aperture subtends an angle in radians that is the inverse of the aperture length in wavelengths. Well known from optics is the fact that while large apertures provide improved resolution, they also have less depth of field than small apertures. A single point focus would result in improved lateral resolution at the focal range at the expense of degraded resolution at ranges very different from that (60). An advantage of single point focus is simplicity; focusing can be achieved with a fixed device such as a plexiglass acoustic lens (61).

To realize the significant advantages to be gained from focusing the array would have to remain focused at all ranges. A dynamically focused array 200 wavelengths long with a focal point that recedes in range synchronously with the range cell from which the echo is returning will have a resolution of 5 cm at 10 m range, degrading linearly to 20 cm at 40 m range and ultimately to 75 cm at the maximum range.

3.2.3.3 Array elements

After the determination of the maximum operating frequency and the maximum aperture the problem remains of how to fill that aperture. The number of elements into which the array is divided is the dominant factor determining the cost of the system hardware, and must be kept to a minimum.

The element length and spacing determines the distribution and amplitude of the grating sidelobes. Grating sidelobes (and indeed all sidelobes) may cause ambiguity in the determination of a wavefronts angle of arrival. Figures 3.8 and 3.9 show the geometry of an array and the resulting beam pattern respectively (61). The beam pattern is shown for both a steered beam (dashed line) and an unsteered beam (solid line).

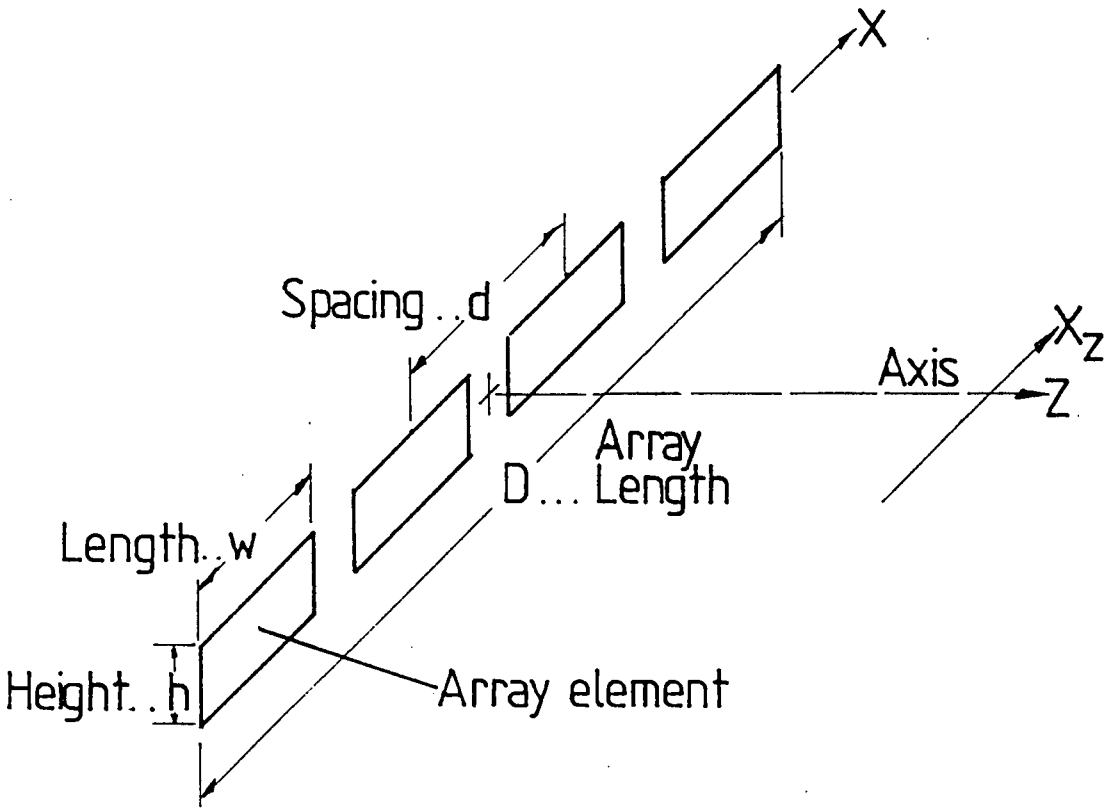

Fig. 3.8: Array Geometry

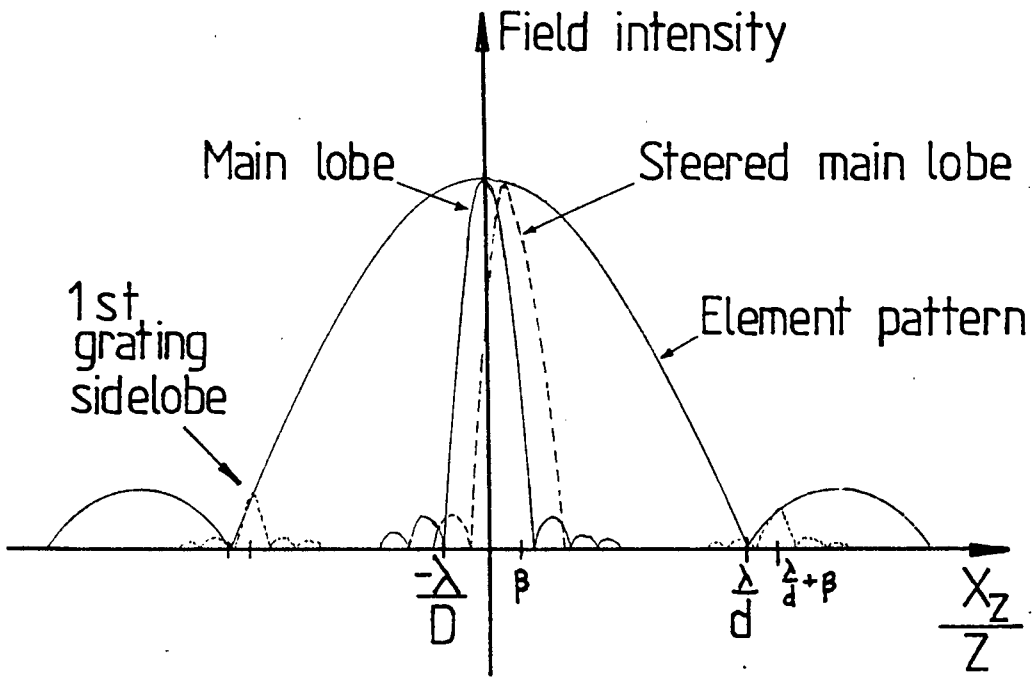

Fig. 3.9: Far field beam pattern

The sidelobes on the main beam may be reduced by sacrificing array gain and applying an appropriate aperture shading. This shading function can only be approximated in a piecewise linear fashion by a discrete array, and the number of elements required to achieved a sufficiently good approximation is prohibitively large. Although shading of a sort is implemented in this system, the mechanism by which the sidelobes are affected is somewhat different from that of far field beam forming.

3.2.3.4 Grating sidelobes

The control of grating sidelobes is achieved through the appropriate choice of element size and spacing, both of which influence the beam forming hardware and software.

To prevent the appearance of the grating sidelobes anywhere within the visible space of the array completely the incoming wavefronts must be unambiguously sampled. This requires an element spacing of less than one wavelength, clearly a costly and complex solution in an array of over 200 wavelenths. As the spacing of the elements is increased the grating sidelobes move closer to the main lobe. The maximum spacing is limited by the need to keep the grating sidelobes out of the insonified area.

The insonification of the region may be limited to only those areas within which the steered beams lie, by shaping the transmitted beam. This method was considered and rejected. The problem of maintaining an adequate insonification of the whole area to be surveyed at short ranges and simultaneously providing sufficient transmitter directivity to allow the use of reasonable transmit powers is discussed in greater depth in the chapter concerning the transmitter.

Making the array elements equal in width to the spacing forms a continuous aperture, albeit with a discontinuous phase and amplitude distribution. In this way the grating sidelobes are forced to remain in the vicinity of the nulls in the element pattern (for small steering angles) and are thus insignificant. This only holds true in the far field.

In the near field the situation is very different. The element spacing chosen is the maximum value consistent with the beam steering and grating sidelobe requirements. The resulting element width may be such that the beamwidth of the individual element at short ranges is significantly less than the array length. The point to be imaged with the focused beam must lie within the individual beams of all the elements used in forming that beam (25). At short ranges it is advantageous to form a beam using only a small subarray.

3.2.3.5 Scanning

The use of subarrays at short ranges has the advantage of reducing the required beam steering angle. The beam steering angle is determined by the distance between the subarray axis and the focal point. Choosing the subarray elements to be as close to the focal point as possible results in a minimum beam steering angle.

An upper bound is placed on the element spacing by the fact that unambiguous scanning may only be accomplished to an angle (in radians) that is the reciprocal of the spacing (expressed in wavelengths). An alternative statement of the same limitation is to require that the array does not undersample the incoming wavefront for all angles of incidence of interest. The maximum beam steering angle (without using subarrays) is 0,045 rads and may be achieved using an array with an element spacing of slightly larger than 20 wavelengths. The use of subarrays would allow an increased element spacing were it not for the use of a contiguous array to control grating sidelobes.

The minimum beamwidth that an element may have (and thus its maximum size) may be determined by noting that the steering of a beam requires at least two elements while crude focusing can be accomplished with three. At the minimum range the beams of at least three elements must overlap.

A contiguous array with an element spacing of 10 cm operated as subarrays at short ranges fulfills the requirements of steering, focusing, resolution and grating sidelobe control.

3.2.3.6 Construction

Using the maximum manageable length of 1 m the final transducer is a ten element array. Each of the 10 elements is composed of four transducers measuring 25 mm by 5 mm and operating in parallel to form a uniform element of 10 cm length. With the element height of just over one wavelength the beam is fan shaped with a vertical beamwidth of close to one radian. Mutual coupling is small due to the relatively small interface area between element ends.

A photograph of the completed transducer is shown in fig. 3.10. Mechanical rigidity is maintained by mounting the transducers on a closed cell foam backing within an aluminium channel section. The face of the array is protected from the sea water with a thin layer of epoxy resin.

Details on the bandwidth and impedance of the array elements are given in the chapter on the receiver.

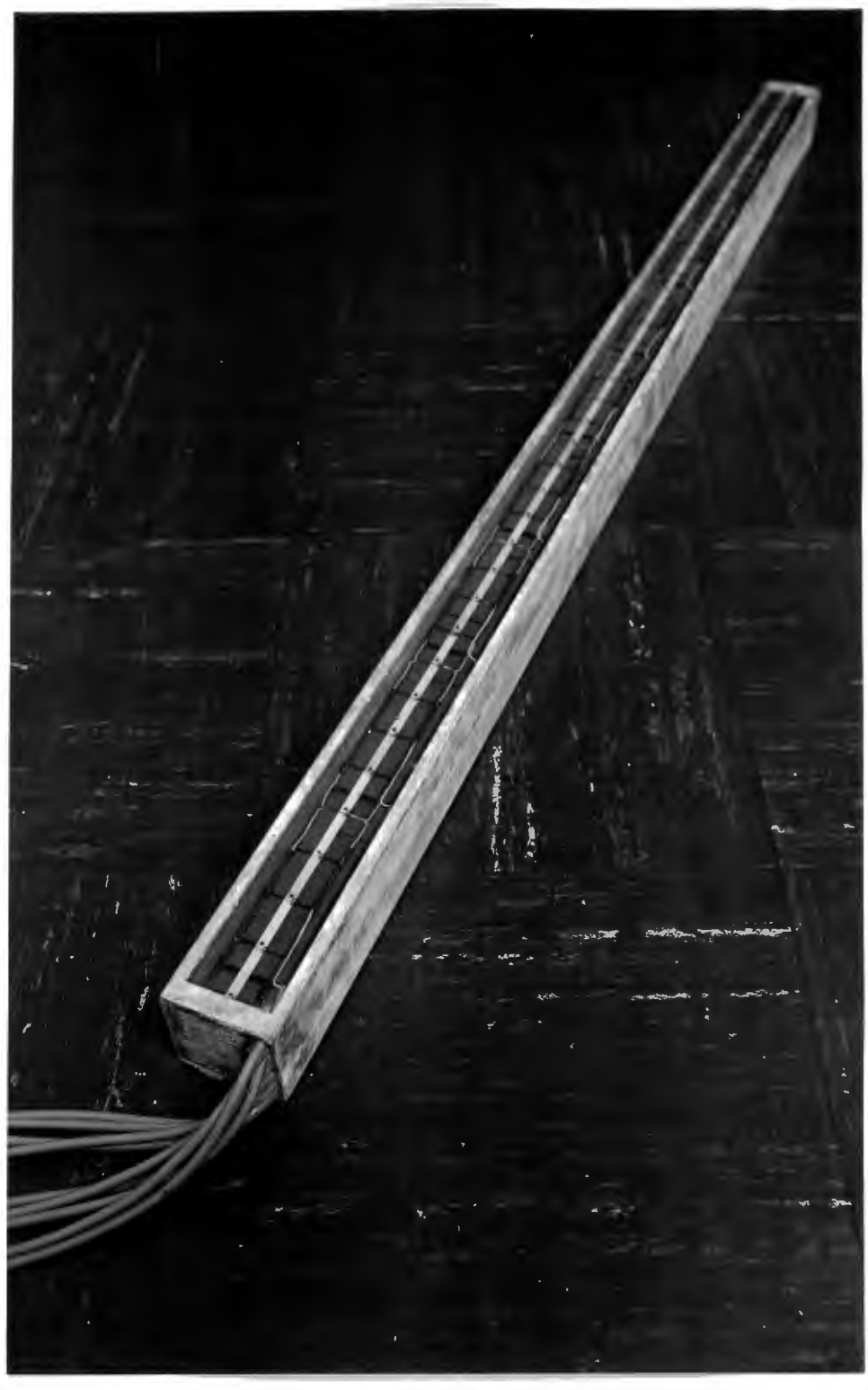

Fig. 3.10 Photograph of transducer

FOCUSING, STEERING AND SHADING

4.1 Introduction

The selection of phases and amplitudes for optimum resolution is discussed. The properties of continuously focused apertures are described. The approximation of the continuous aperture with a discrete line array results in an upper bound on the extent of the aperture. A expression is derived for the determination of these bounds and the results are verified with computer modelling. The effects of beam steering are shown in some detail. The entire field of the discretely focused, steered beam is then modelled and the results discussed.

4.2 Focused apertures

The geometry of the array is shown in fig. 4.1. The following definitions are used:

Element length	w=0,1 m
Element spacing	d=0,1 m
Array length	D=1,0 m

The far field beam pattern of the array, steered to an angle 0,01 rads is shown in fig. 4.2.

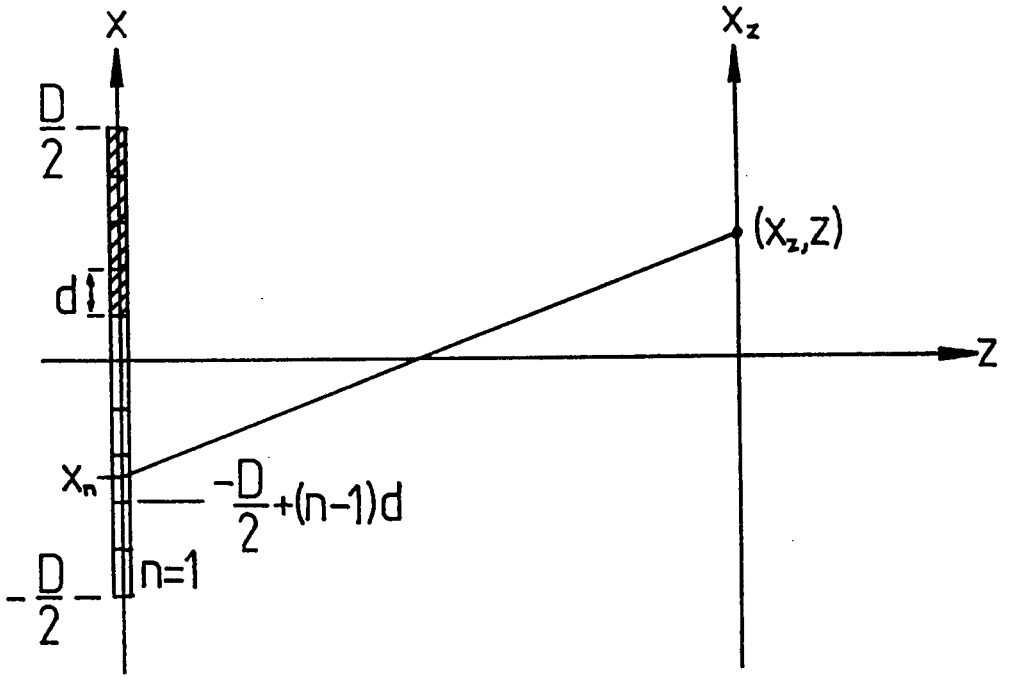

Fig. 4.1: Array geometry

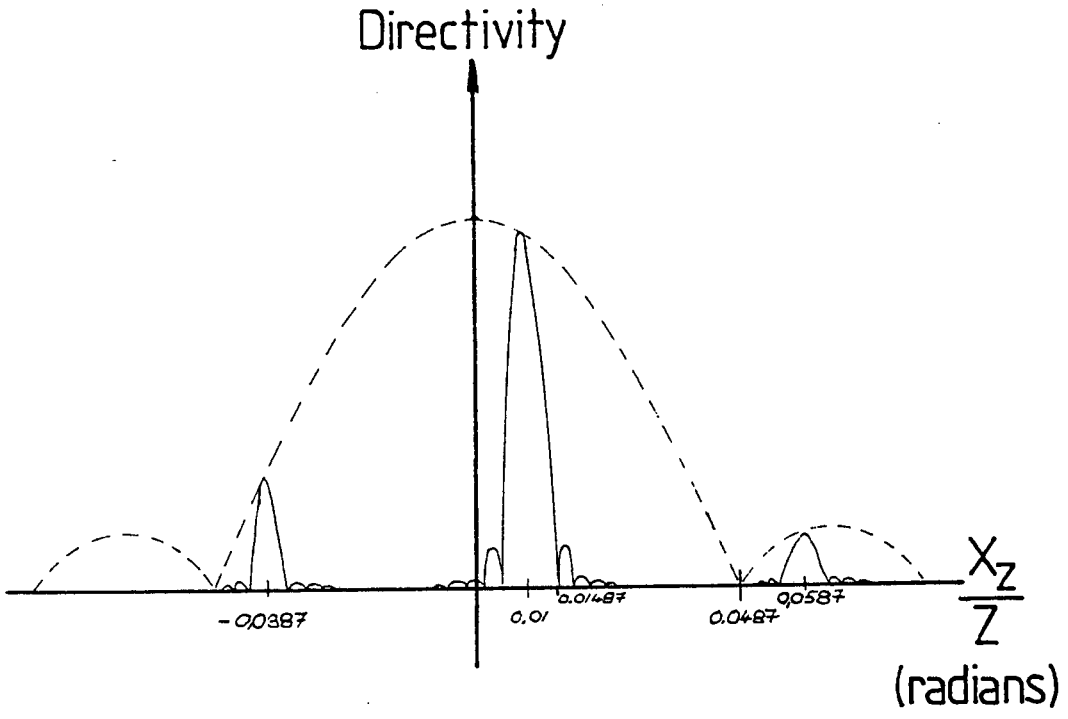

Fig. 4.2: Field intensity

There are two distinct zones of operation of the array. At ranges greater than 44 m all ten elements of the array are active and only focusing and steering need be applied. The beam pattern of the array behaves in very much the same fashion as that of a continuously focused aperture and will be discussed under that heading. At ranges between 10 m and 44 m the discrete nature of the array is apparent in the beam pattern.

4.2.1 Continuous focusing

In the focal plane near the axis of a continuously focused rectangular aperture the field intensity has all the properties of the far field. The angular resolution is the same as that of an unfocused aperture in its far field. Within a limited zone around the focal point a close approximation to the variation of field intensity with azimuth within the main lobe is given by the expression (41).

$$P(x_z, z) = \left[\frac{\sin(\frac{\pi D x_z}{\lambda z})}{(\frac{\pi D x_z}{\lambda z})} \right]^2 \qquad 4.1$$

Comparing this expression with that of a rectangular aperture of uniform phase and amplitude we conclude that the sidelobe levels have remained unchanged by focusing, while the width of the lobes and their positions are simply scaled down. This gives rise to the enhanced resolution.

4.2.2 Scanning

A simple geometrical argument (28,29) leads to the conclusion that the far field beam steering accomplished by the application of a linear phase taper to an aperture is also reproduced on the focal plane of a continuously focused aperture.

4.2.3 Depth of field

Although the far field beam pattern is essentially projected from infinity onto the curved focal surface the results above are only valid within a limited zone around the focal surface (the depth of field) and are thus valid on a focal plane of constant z if the distance between this plane and the actual focal surface does not exceed the depth of field. As the range departs from the focal distance the field pattern becomes progressively more distorted. At the limits of the depth of field the maximum phase error incurred between the extremities of the array are limited to less than $\pi/2$ radians.

The depth of field may be expressed in terms of the focal range Zf and the aperture size (in wavelengths) (25,28).

$$\left(\frac{z_f}{1+\frac{z_f 4\lambda}{D^2}}\right) \leq z \leq \left(\frac{z_f}{1-\frac{z_f 4\lambda}{D^2}}\right) \qquad 4.2$$

At ranges greater than 50 m the depth of field is large and the beam forming system does not have to refocus very often. At the shorter ranges the depth of field is very much less, refocusing must be performed at intervals close to 2 m. This sets a limit on the time available to the microprocessor within which it has to refocus. This topic is dealt with in detail in the chapters on the system timing and the microprocessor.

Clearly the determination of the aperture phase distribution is a relatively simple matter if the number and spacing of the elements is such that the above description of the beams is valid.

4.3 Discretely focused array

4.3.1 Array bounds

The effects of the beamwidths of the individual elements is noticeable at short ranges. Figure 4.3 is a reproduction of the far field beam pattern of the array (fig. 4.1) with the beam pattern of a single element superimposed on it. When large elements are used in a focused and steered array it is essential that the focal point is within the directional patterns of all the elements. A geometric argument (25) yields bounds on the array length expressed in terms of the beam-widths of the individual elements.

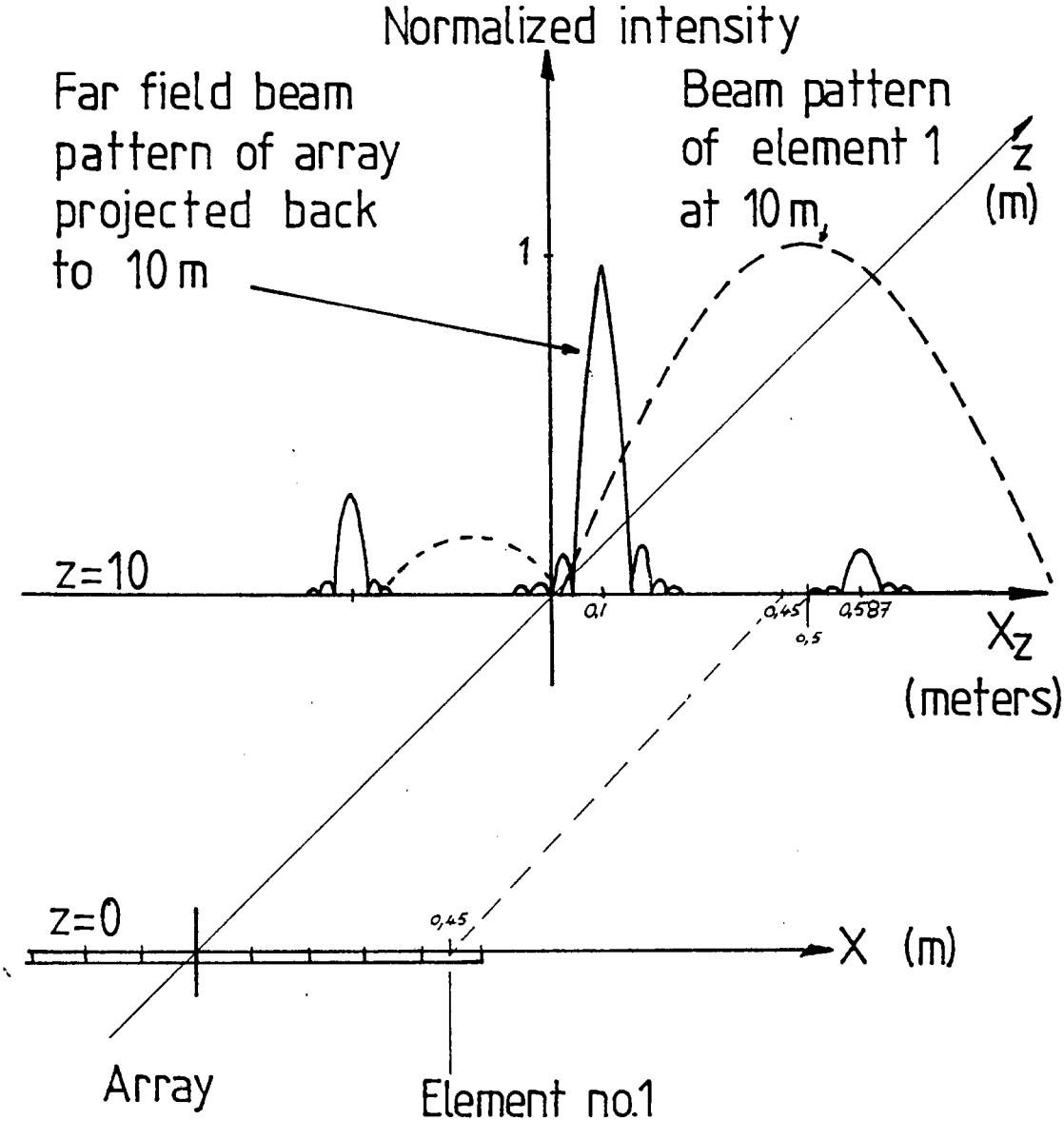

Fig. 4.3: Field intensity of element and array

It has been suggested (25) that the useful array length may be extended by reducing the length of the elements at the shorter ranges, thereby broadening their individual beams. Besides the electronic complexity of including intra-element switching circuitry and having dynamically varying element sizes there are also the sidelobes to be considered. Reducing the element size of such a sparse array as that described here causes a marked increase in the amplitude of the first grating sidelobe. Noting that this grating sidelobe is at an angle of only 0,0487 rads from the main beam as shown in fig. 4.2 it is clear that it must be kept under control.

Inter-element switching is far easier to implement. If an element does not make a significant contribution to the total field strength at the focal point, its output is ignored in the process of beam forming.

The contribution of each element must be determined for all focal ranges and steering angles and the appropriate binary element shading is applied. The contribution of a particular element to the field intensity is modified when the beam is steered off axis as required in a multiple parallel beam system. When the beam is steered to another point on the image plane the contribution of those elements on the side of the axis of symmetry to which the beam is steered increases. Given the range and the focal point the problem to be solved is the determination of the number

of elements of which a focused subarray should be composed so as to optimize the resolution.

This discussion refers to the geometry of fig. 4.1. As shown in appendix I, the field intensity set up by an aperture with an illumination of S(x), may be approximated by the familiar Fresnel zone approximation (63).

$$|P(x_z,z)|^2 = \left| \frac{ke^{-j\beta z}}{z} \int_{Array} S(x) e^{-j\beta (x_z - x)^2/2z} \, dx \right|^2 \qquad 4.3$$

For a discrete array of N elements, each of width d and operating in its far field the integral above may be written more explicitly as the sum of the effects of the elements. The field at an azimuth of Xz (from the array axis) and a range z is given by

$$P(x_z,z) = \frac{ke^{-j\beta z}}{z} \sum_{n=1}^{N} S(n) e^{-j\beta (x_z - x_n)^2/2z} \, d.Sa\left(\frac{\beta d (x_z - x_n)}{2z}\right) \qquad 4.4$$

The term S(n) represents the discrete aperture illumination, the phase and amplitude of which is the same over the extent of an element and is under the control of the microprocessor. To achieve focusing the phases of S(n) are selected to cancel the quadratic phase term for a particular value of Xz; the focal point, denoted Xf;

$$\angle S(n) = e^{-j\beta (x_z - x_n)^2/2z} \qquad 4.5$$

The contribution of each element is modified by the element patterns given by the terms

$$Sa\left(\frac{\beta d(x_f - x_n)}{2z}\right) \qquad 4.6$$

A particular element centred at Xn contributes significantly to the field at the focal point only if the point lies within the halfpower limits of that element´s beam. The resulting bound on the azimuthal distance between an element´s axis and the focal point is derived in appendix I and reproduced here.

$$|(x_f - x_n)| \leq \frac{\pi z}{2\beta d} \qquad 4.7$$

Thus at 10 m range with an element length of 21,4 wavelengths the inequality is

$$|(x_f - x_n)| \leq 0,238$$

and is satisfied (approximately) by

$$n = 1,2,3$$

Incidentally the inequality is also satisfied by n=0 but there is no element corresponding to this value of n.

A similar procedure for a field point at 30 m range steered -0,4 m off the axis of symmetry of the array yields the inequality

$$|(x_f - x_n)| \leq 0,714$$

which is satisfied by values of n ranging from 1 to 8. By this means the useful subarrays are determined for every range and azimuth.

A sample of the output of the program used to determine the binary shading is shown in table 4.1. The program listing is given in appendix I. A "1" in the position of the element indicates that it should be turned on.

Turning elements on or off is a rather abrupt form of aperture shading but does have the advantage that the five beams can be made to have similar characteristics. Were a less abrupt shading to be used on a beam formed primarily by the elements 1,2,3 as for the outermost beams at the closest range, the shading is perforce asymmetrical since there is no element to use outside position 1. A beam formed on a line closer to the center of the array may have a symmetrically shaded source. Such a situation is undesirable from a processing point of view since it might necessitate different time varying gain profiles for the individual beams.

For this reason the number of elements used at each range is the minimum of the maximums determined by the use of the inequality. Thus both the phase and a first approximation to the amplitude of the aperture illumination are determined.

Range= 10

1110000000
0111100000
0001111000
0000011110
0000000111

Range= 12.187

1110000000
0111100000
0001111000
0000011110
0000000111

Range= 14.374

1111000000
1111110000
0011111100
0000111111
0000001111

Range= 16.561

1111100000
1111111000
0111111110
0001111111
0000011111

Range= 18.748

1111100000
1111111000
0111111110
0001111111
0000011111

Range= 20.935

1111110000
1111111100
1111111111
0011111111
0000111111

Range= 23.122

1111110000
1111111100
1111111111
0011111111
0000111111

Range= 25.309

1111111000
1111111110
1111111111
0111111111
0001111111

Range= 27.496

1111111000
1111111110
1111111111
0111111111
0001111111

Range= 29.683

1111111100
1111111111
1111111111
1111111111
0011111111

Range= 31.87

1111111100
1111111111
1111111111
1111111111
0011111111

Range= 34.057

1111111110
1111111111
1111111111
1111111111
0111111111

Range= 36.244

1111111110
1111111111
1111111111
1111111111
0111111111

Range= 38.431

1111111111
1111111111
1111111111
1111111111
1111111111

Range= 40.618

1111111111
1111111111

TABLE 4.1: Binary array shading

4.3.2 Computer modelling

Using the estimated shading determined above the fields are modelled with the aid of a computer using a discrete approximation to the integral in eq. 4.3.

The initial field modelling, written in BASIC for an HP-86 personal computer, is designed to facilitate interaction and produces graphic displays of field intensity over a 1 m width, at a single range. The integral is approximated with between 45 and 50 points.

The performance of the final array configuration adopted is examined with a FORTRAN field modelling program written for a Sperry 1100 series mainframe. The output is in the form of both contour and "3-D" plots of field intensity over a 2 m width with the source integral approximated with 100 points. The modelling is described in appendix II along with the program listing of the BASIC program. The FORTRAN version is almost identical, with a loop to determine the field intensity at each focal zone.

The pattern of a three element array is shown in fig. 4.4. It is clear that the focusing phases applied to the three element array have resulted in an angular beamwidth which is very close to that of a continuously focused aperture of the same length. The continuously focused aperture has a beamwidth of 16,2 cm at 10 m range.

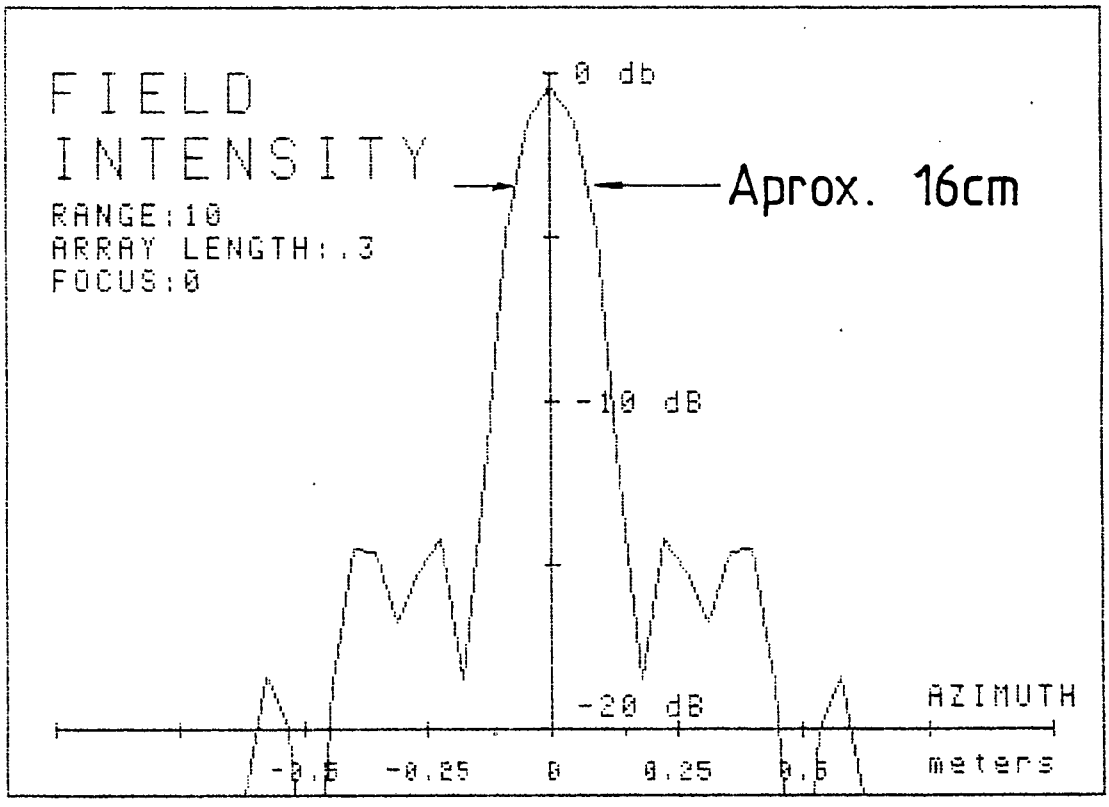

Fig. 4.4: 3 Element array, focused at 10 m

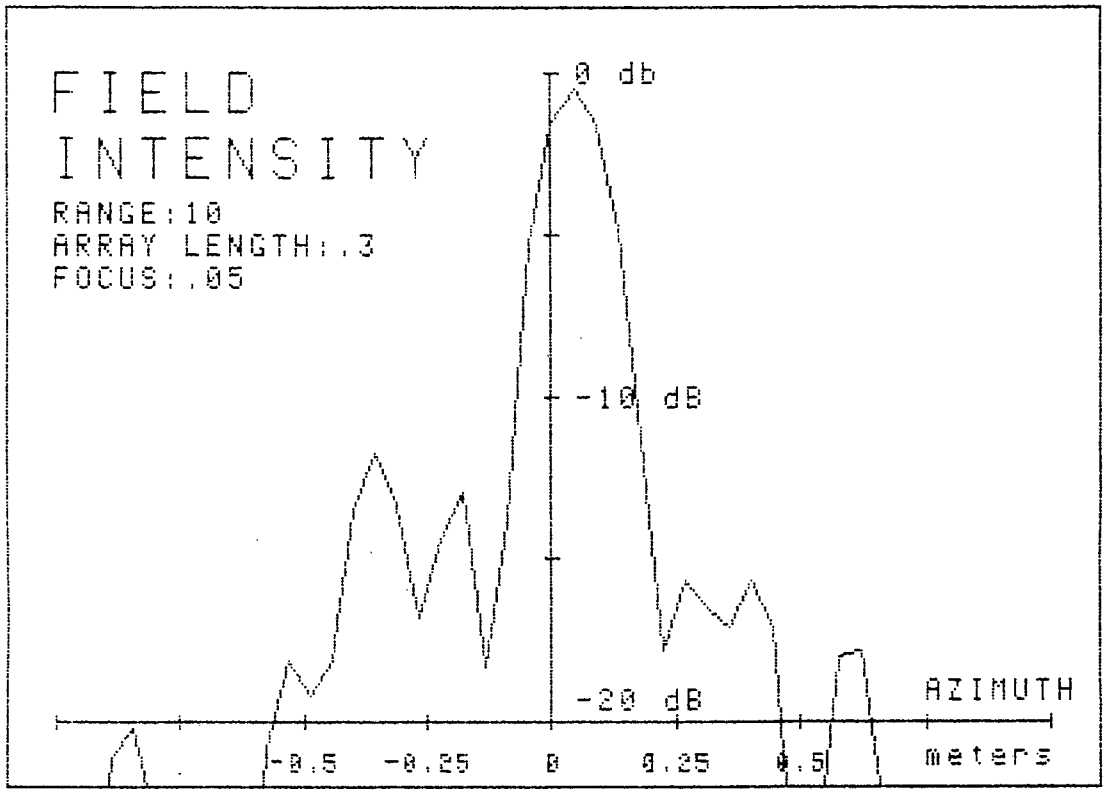

Fig. 4.5: 3 Element array, focused and steered at 10 m

It is of interest to note the effect of beam steering on the three element array at 10 m. Figure 4.5 shows the radiation pattern of the three element array focused on a point at a range of ten meters and a displacement from the array axis of 0,05 m. The field intensity on the side of the symmetry axis away from the beam steering is seen to increase, as shown by the side lobe level increase. The application of the linear phase shift reduces the interaction of the elements somewhat. Those close to the focal azimuth become dominant in the formation of the main beam while those further away, freed from the interference of the other elements, produce increased sidelobes.

The maximum side lobe level of the 3 element focused steered array is seen from fig. 4.5 to be 12 dB down from the principal lobe. These effects of beam steering on the sidelobes are most pronounced at short ranges and the -12 dB levels are considered tolerable. With increasing range the sidelobes approach the typical -13,4 dB levels of uniform far field arrays asymptotically.

The possibility of using more elements in the array than that determined by the aforementioned inequality is investigated. There is a signal to noise ratio advantage to be had from more elements, and possibly enhanced resolution. The radiation pattern of a four element array of total length 0,4 meters is shown in fig. 4.6.

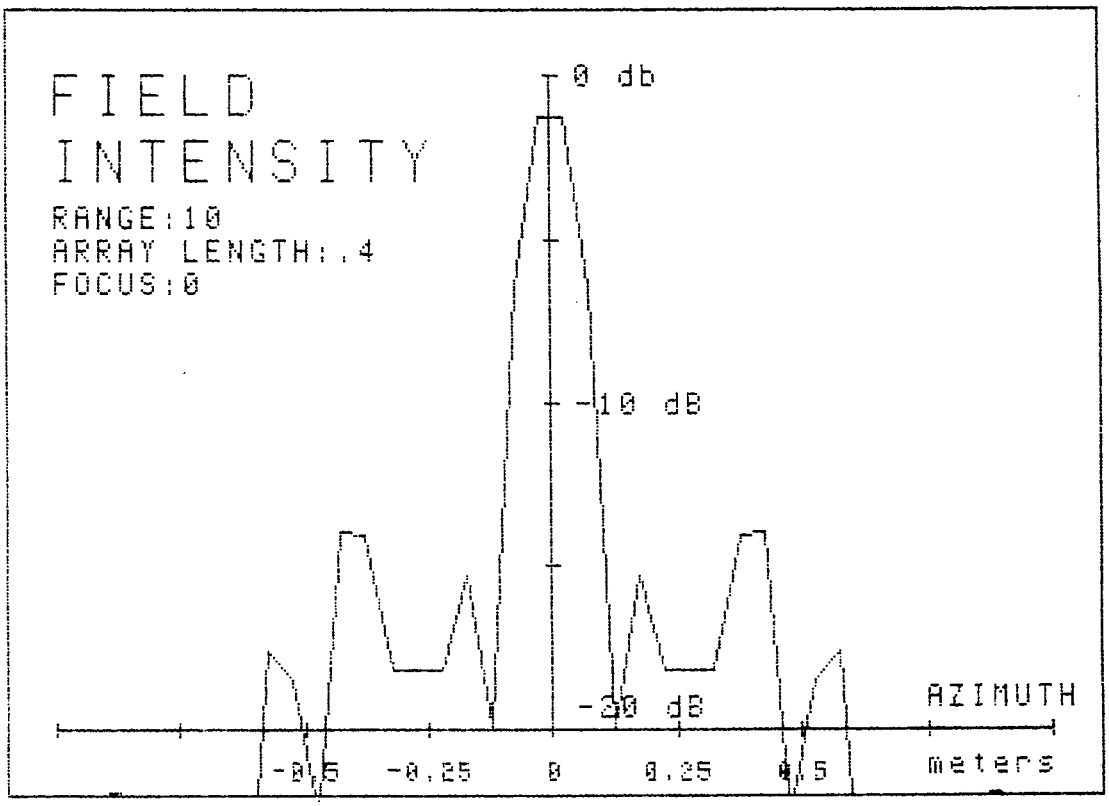

Fig. 4.6: 4 Element array at 10 m

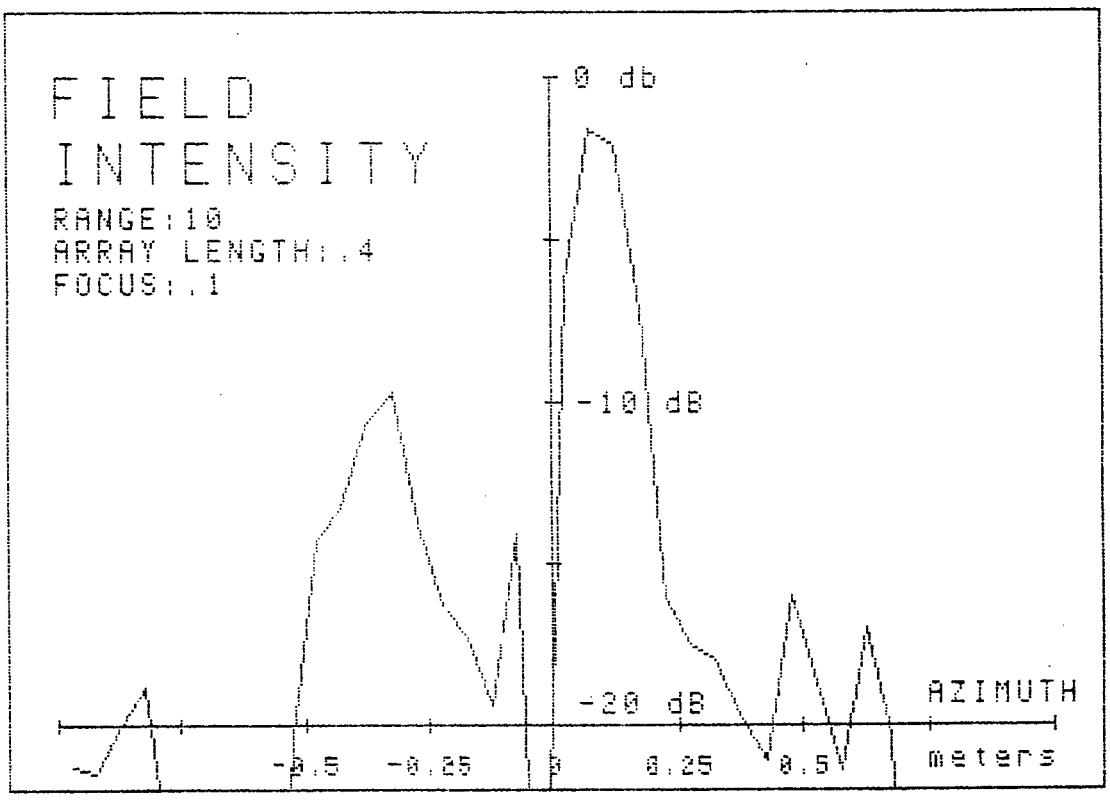

Fig. 4.7: 4 Element array focused and steered at 10 m

Since the extra element's beam is hardly contributing to the main lobe it is expected that the 'gain' will decrease. This is reflected by the slight dip in the peak value of field intensity in the main lobe. The 0 dB mark corresponds to the intensity of a continuously focused aperture. The sidelobes are slightly larger than those of the three element unsteered subarray and they occur at a greater angle. Were it not for the beam steering requirements the longer subarray would yield a higher resolution.

When the beam of the four element subarray is steered onto the point of interest the required steering angle is larger than that of the three element subarray since the axis of symmetry of the former is further from the field point than that of the latter. At the required angle, as shown in fig. 4.7, the sidelobe response to sources off the beam axis becomes marked. Sidelobe levels rise above -10 dB and the first sidelobe broadens, thus contributing a greater part of the recieved energy.

The inequality (eq. 4.7) used above is thus seen to provide a reasonably accurate method of determining which elements should be used to form a beam at a given range.

4.4 Final beam forming configuration.

The required phases (eq. 4.5) and shading of the aperture illumination are thus found and used as input to the mainframe model. Minor adjustments are made to the element shading using this field modelling program and the final result is shown in table 4.2 along with estimates of the resolution at various ranges.

TABLE 4.2

RANGE (meters)	NUMBER OF ELEMENTS	ARRAY LENGTH (meters)	RESOLUTION (meters)
10-14	3	0,3	0,16-0,25
14-17	4	0,4	0,17-0,22
17-25	5	0,5	0,18-0,22
25-31	6	0,6	0,18-0,20
31-34	7	0,7	0,18-0,21
34-37	8	0,8	0,18-0,21
37-44	9	0,9	0,18-0,21
44-150	10	1,0	0,19-0,75

One of the most appealing features of a dynamically expanding focused array is apparent from table 4.2. The resolution is essentially constant over a significant proportion of the operating range.

The growth of the array with time is depicted in the following diagram. Figure 4.8 a shows the situation when producing one of the outermost beams. The vertical bars represent the array at different times. The active portion of the array (i.e. the sub-array) is shown in black. At the shortest range, after a two way round trip time of 13,4 ms, only a small number of elements straddling the swath to be imaged are used. The subarray starts with three

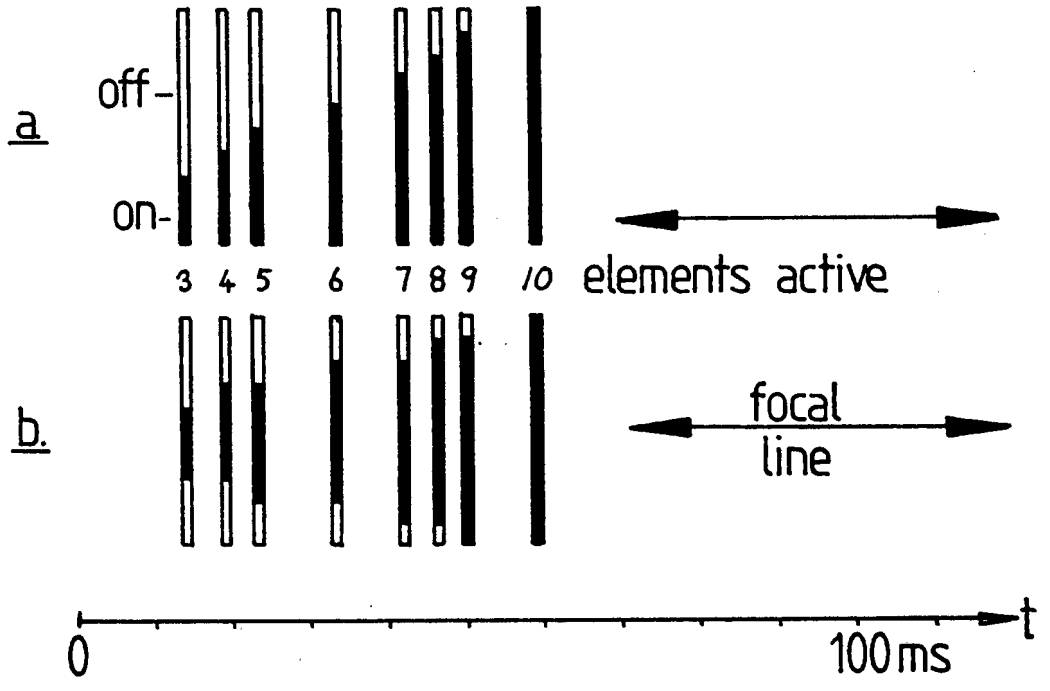

Fig. 4.8: Array growth

elements and 'grows' toward the other end of the array element by element as the increasing two way propagation time indicates that the point to be imaged lies within the half power beamwidth limits of an increasing number of elements. At a range of 44 m all 10 elements have been turned on. Figure 4.8 b shows the situation for the central beam. Rather than growing to only one side the subarray grows outwards. Whenever an odd number of elements is used the subarray lies asymmetrically with respect to the line of focus and beam steering is required. In changing from an even number of elements to an odd there is the choice of which way the asymmetry should go. It has been found that keeping it on one side has negligible effect on the final beam pattern.

A set of five diagrams follows. The first two (figs. 4.9 and 4.10) are a "3-D" depiction and a contour plot of the field intensity of the dynamically focused, steered and shaded central beam formed by the array. Modelling is performed over the range from 10 m to 55 m at which point all ten elements are in use. The ranges at which the number of elements is increased are clearly visible. When elements are switched in the gain of the array increases; this results in a predictable gain modulation which may be be overcome by the initial gain settings to be found in the ROM.

The exposed section in fig. 4.9 should be compared to fig. 4.5. Both are the field intensity produced by an asymmetric 3 element array at 10 m range. The measured directivity of this beam is discussed later and shown in fig. 11.3.

Figures 4.11 and 4.12 ("3-D" and contour plot) show the field intensities of the focused and steered beam in the second swath. The field intensity in the outermost beams is shown in the contour plot of fig. 4.13. A remarkable degree of beam uniformity is achieved, both between the beams and within the beams. The beamwidth remains essentially constant from 10 m to 55 m after which it degrades linearly to 75 cm.

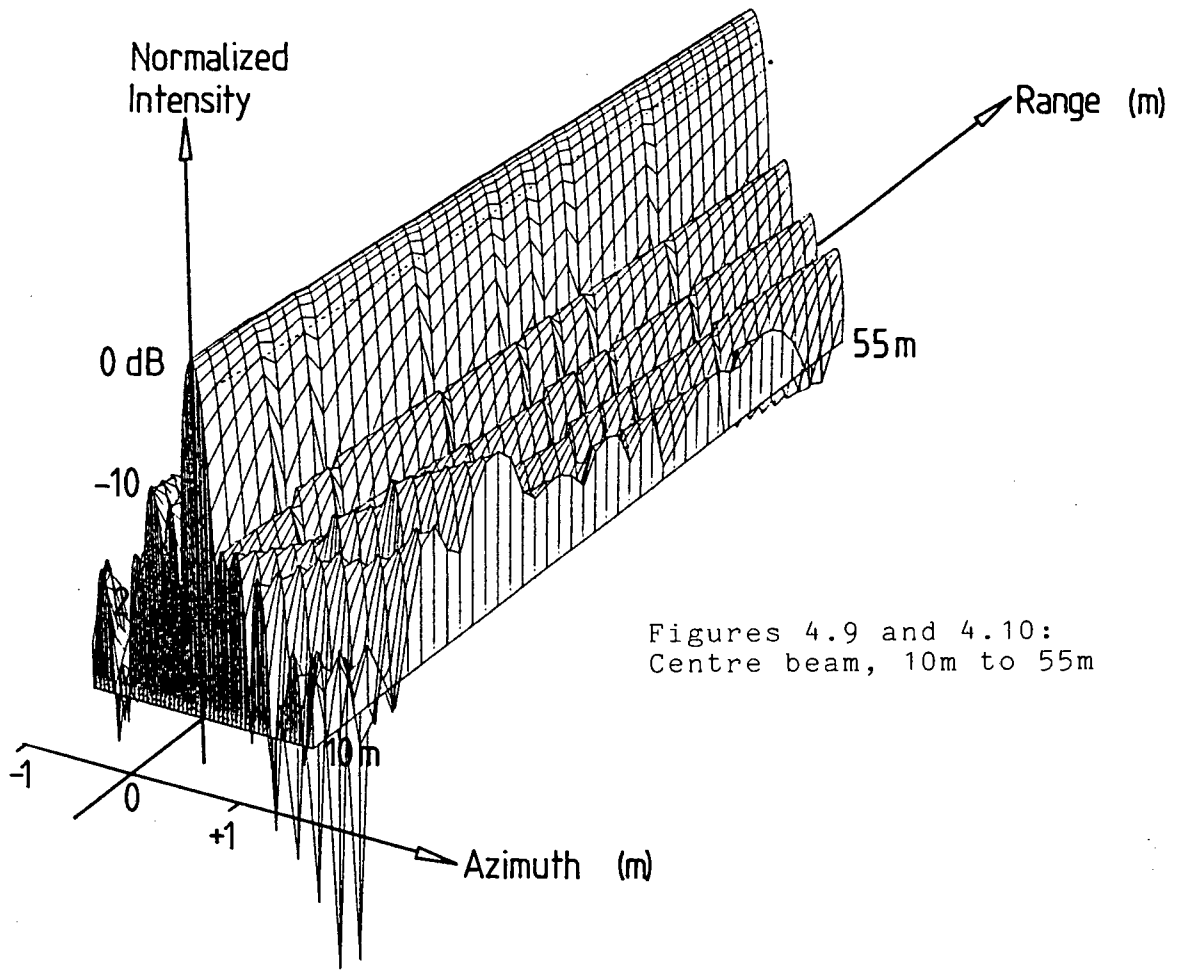

Figures 4.9 and 4.10:
Centre beam, 10m to 55m

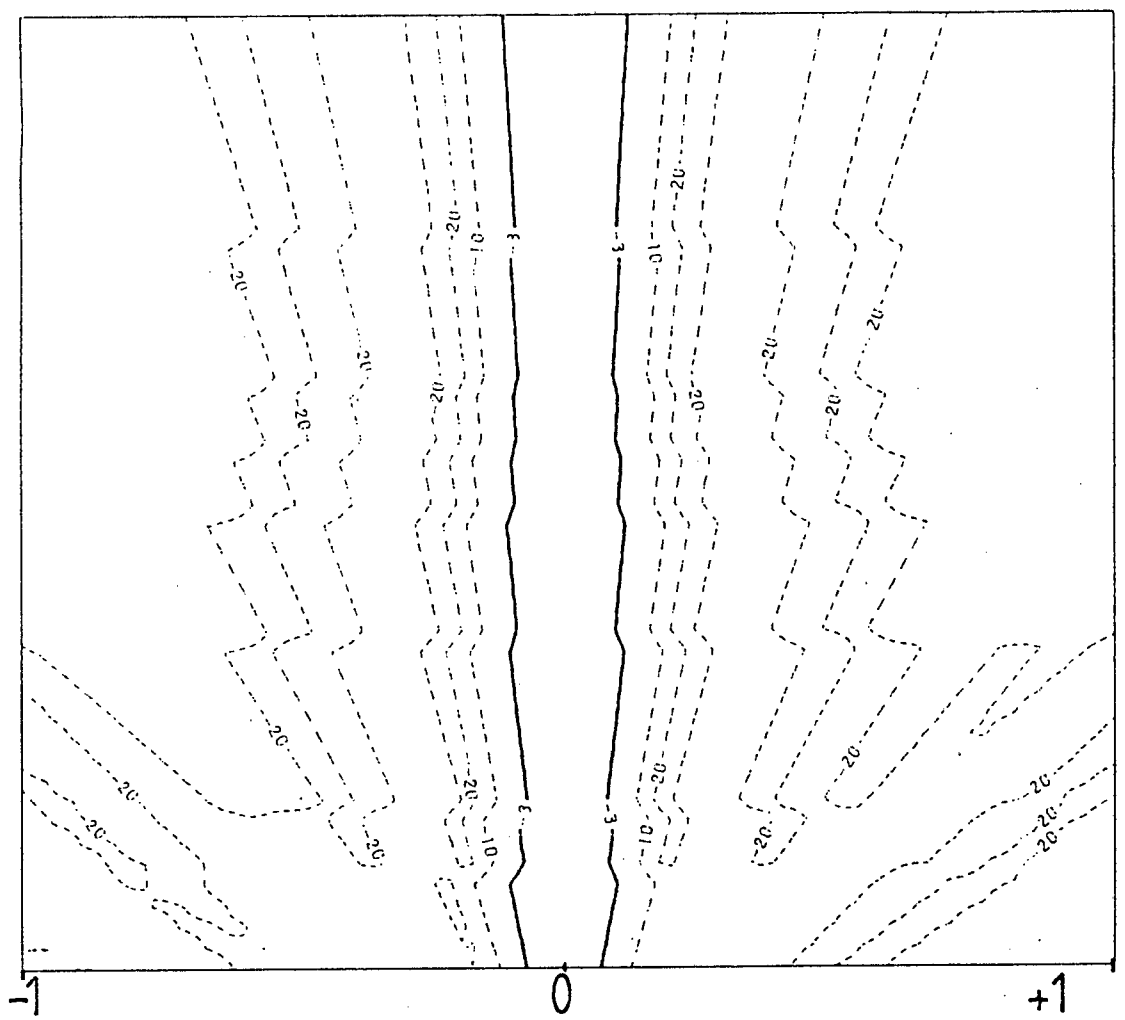

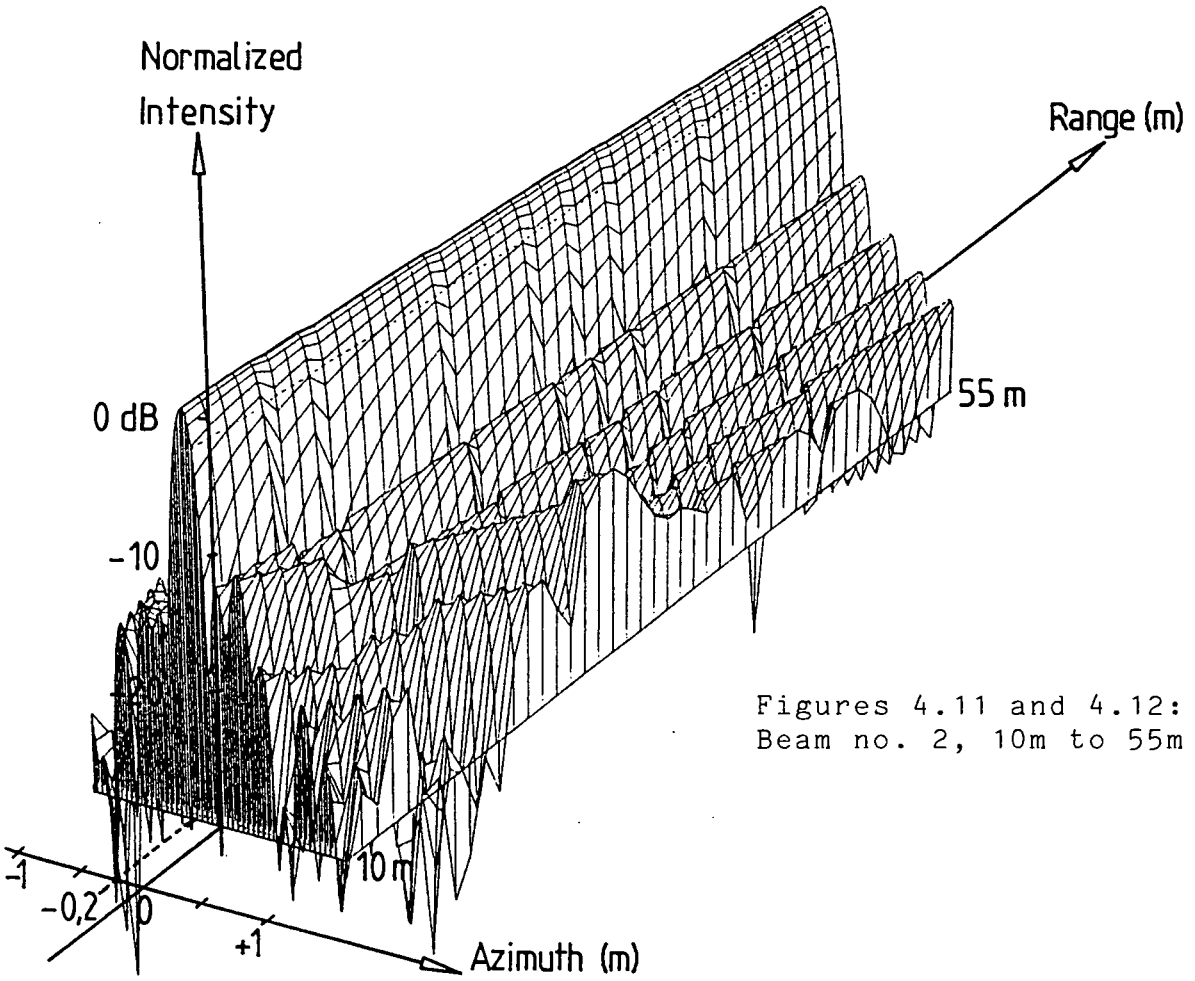

Figures 4.11 and 4.12:
Beam no. 2, 10m to 55m

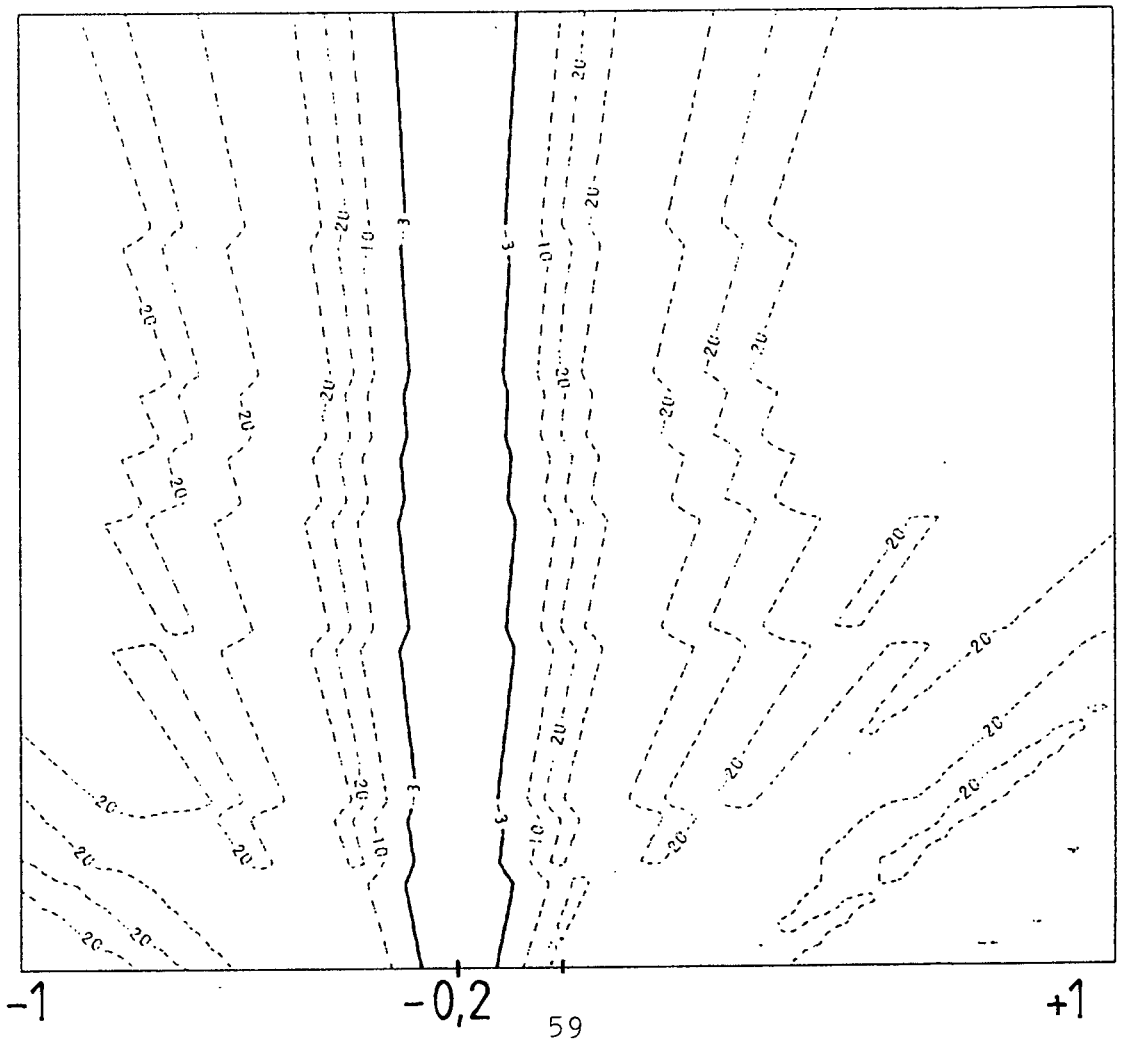

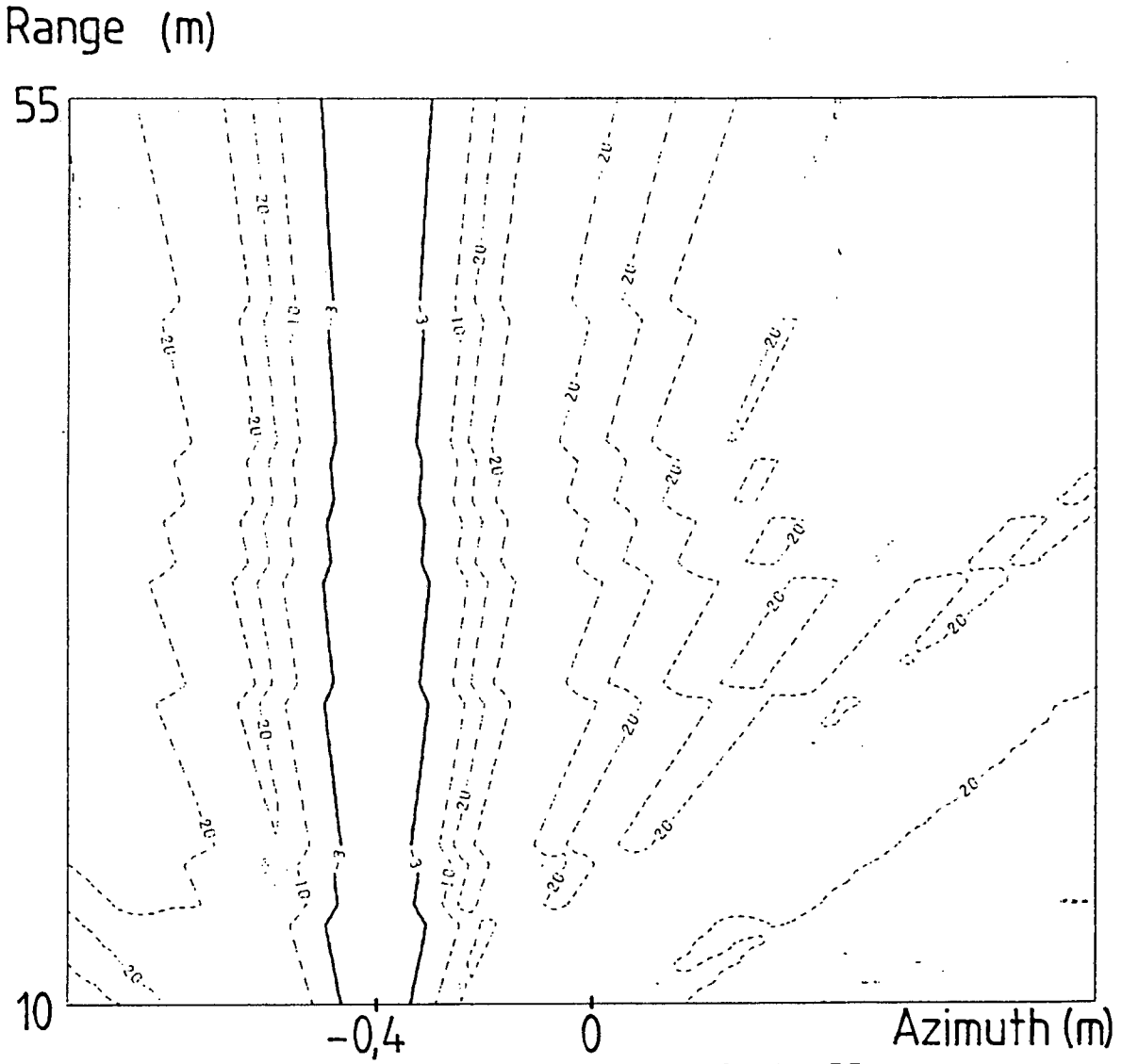

Fig. 4.13: Beam no. 1, 10m to 55m.

PHASE SHIFTERS

5.1 Introduction

Beam forming is accomplished through the use of narrowband analog phase shifters. A quadrature phase shifting technique is implemented with digital control. The design of the phase shifters is described and its performance is evaluated under both static and dynamic conditions.

5.2 Digitally controlled analog phase shifters

The phase shifters are an electronic realization of the familiar trigonometric sum angle formula.

$$\cos(a+b) = \cos(a)\cos(b) - \sin(a)\sin(b) \qquad 5.1$$

The incoming signal is divided into two quadrature components by an RC bridge, as shown in fig. 5.1. The 'sine qua non' of the simplicity of this circuit, and indeed the technique of phase shift beam forming is the small fractional bandwidth.

The range resolution of 13,7 cm dictates a maximum temporal pulse duration of 182 μs, or a baseband bandwidth of 5,5 kHz. The required beam former bandwidth is simply twice that, or 11 kHz. This results in a fractional bandwidth of 3,6 %,

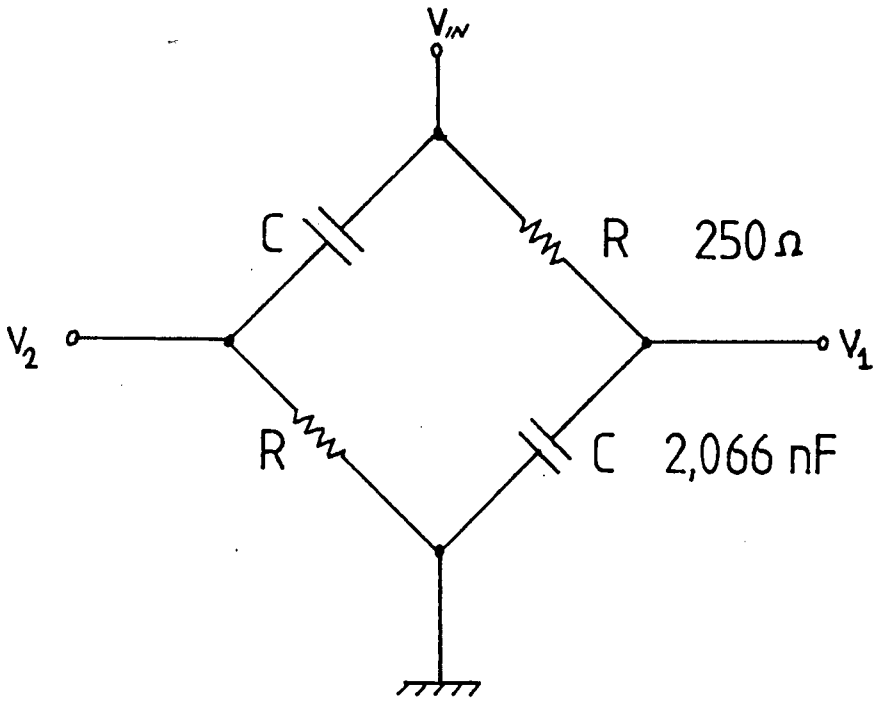

Fig. 5.1: Quadrature power splitter

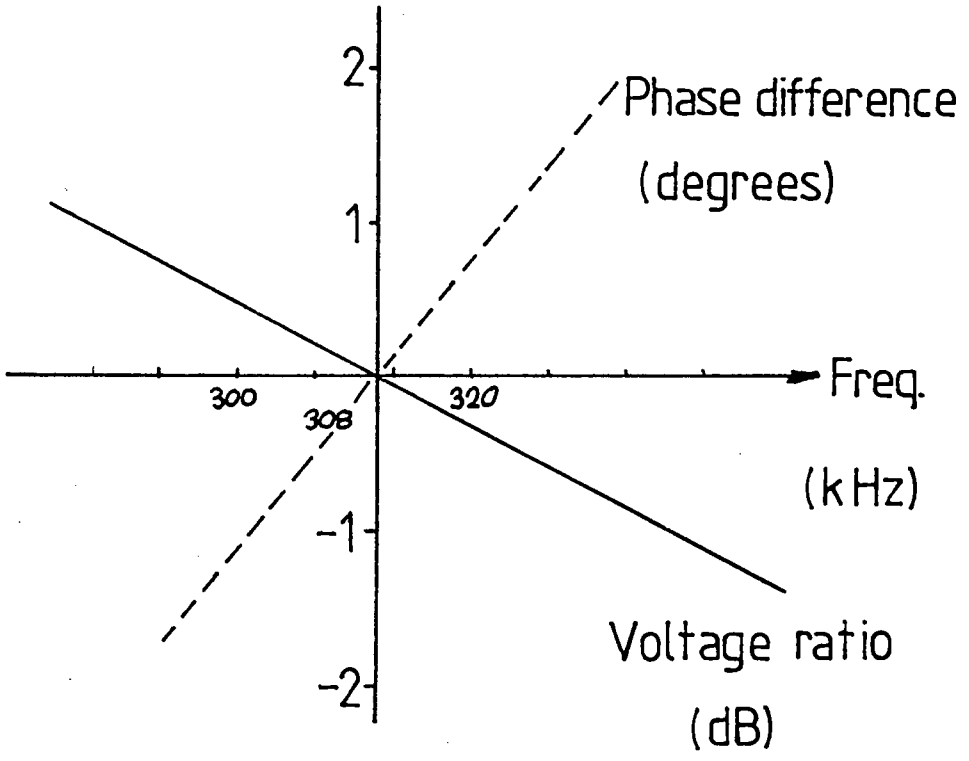

Fig. 5.2: Phase and amplitude response of power splitter

conveniently small. The phase and amplitude response of the fixed quadrature power splitter of fig. 5.1 is shown in fig. 5.2 ; clearly the signals are in phase quadrature to within 0.5° over the bandwidth of interest.

The quadrature components of the signal are then modified by means of the programmable gain amplifiers, as shown in the complete block diagram of the phase shifter (fig. 5.3). Multiplying the signal on the upper branch by cos(b) and the lower by sin(b), where b is the desired phase shift, and adding the results we have the right hand side of eq. 5.1 (to within a constant excess phase). The two coefficients required for the programming of one phase shifter will be referred to as the C and S coefficients because of the terms (sin and cos) on which they operate.

5.2.1 Programmable gain amplifiers

The programmable gain amplifiers must be such that the phase shift through them is not a function of the selected gain; if it were, the determination of the C and S coefficients would be very tedious. Multiplying digital to analog converters provide at their output a binary scaled version of the reference voltage input. Internally these integrated circuits are simply a precision resistor ladder with a series of FET switches. Designed to provide conversion times of the order of microseconds, they may be expected to have

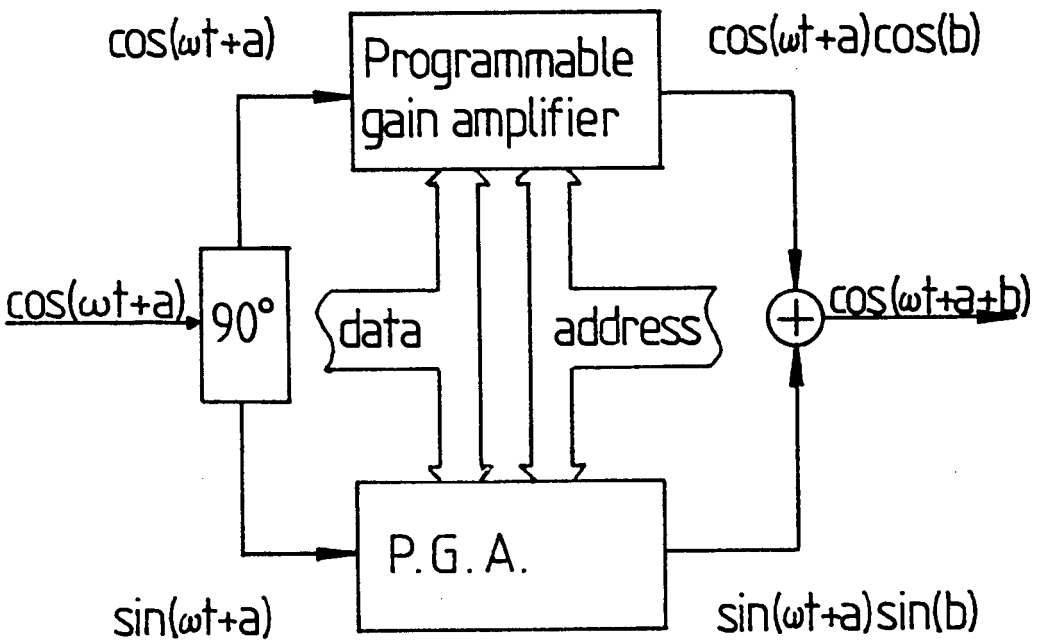

Fig. 5.3: Block diagram of phase shifter

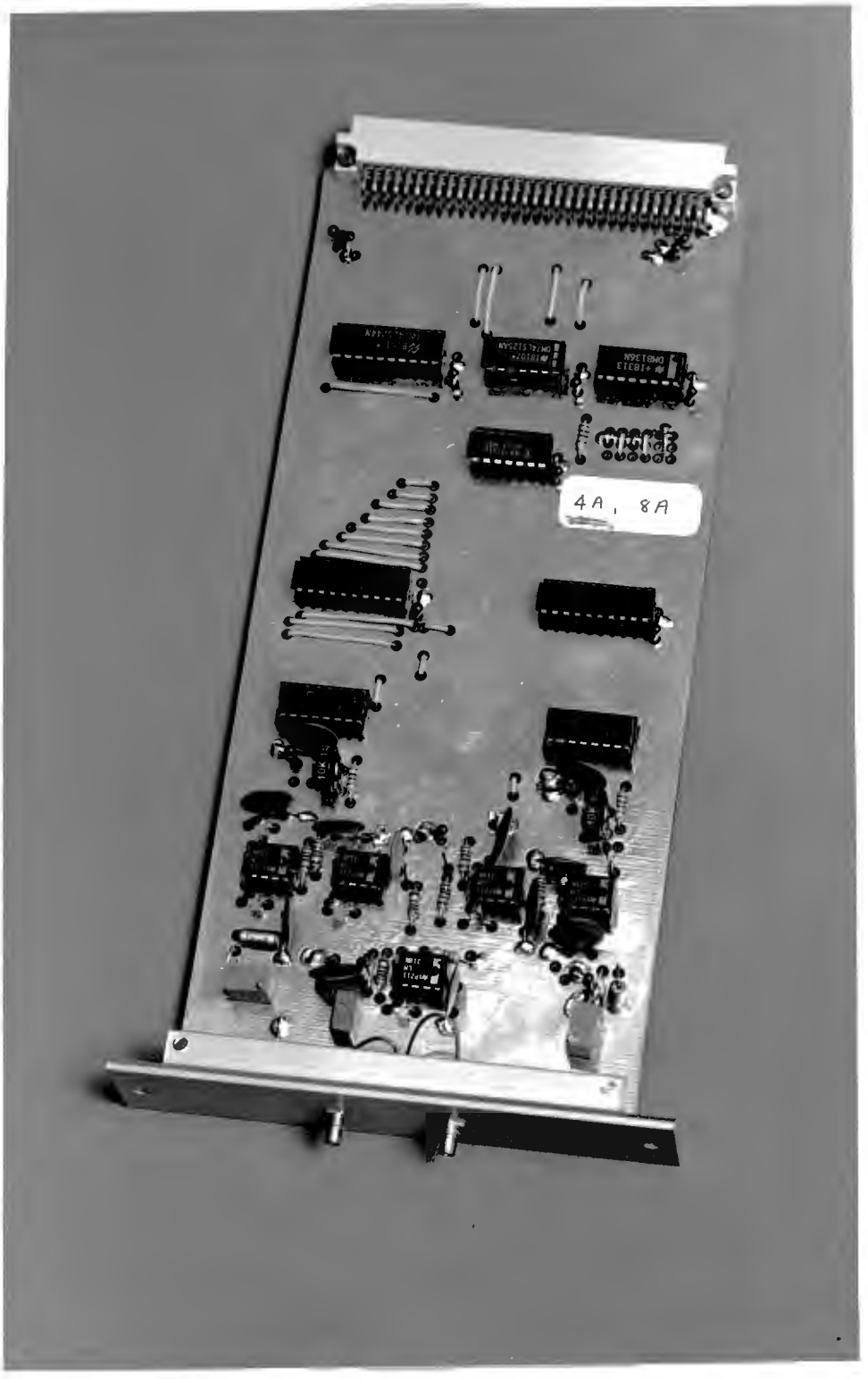

Fig. 5.4: Photograph of phase shifter

order of megaHertz. This is indeed the case with the low cost devices selected for this task. Buffering the outputs with a wideband buffer insures that the small amplifier phase shifts remain small.

Clearly the gains of both amplifiers must change simultaneously. Altering only one at a time would produce spurious output spikes. The A/D's selected have on-chip data buffers; the data on their inputs may change without altering their internal state until a data transfer pulse is sent. An external latch is added to each multiplying A/D to convert it into a "double buffered A/D". With this configuration the next pair of gains required by a phase shifter may be stored at leisure and simultaneously applied by a single transfer pulse.

The multiplying A/D's provide 8 bits of resolution. Although this is more than necessary (see the section on phase errors) it has been retained. The range of the coefficients from -1 to 1 is converted into 255 levels between -127/128 and +127/128. Ignoring the slight scaling we can use the hex FF to program a gain of -1 , hex 80 for a gain of 0 (thus turning the element off) and hex 01 for the +1 coefficient. Intermediate values provide control over both the phase and the amplitude of the the transfer function of the phase shifter.

A photograph of a single phase shifter is shown in fig. 5.4.

5.2.2 Phase coefficient determination

Table 5.1 shows the required phases for beam no. 1 for all ranges between 10 m and 100 m. These are determined using a BASIC program provided in appendix III, which calculates the phase of S(n), given by equation 4.5. These phases cannot be realised exactly due to the inherent quantization in the phase shifting technique, but approximately 8 bits of phase control is possible.

Taking into account the measured excess phase shifts throughout the circuit due to the quadrature power splitter, various buffers and the summing amplifier, an absolute relationship between the desired phase angle and the C and S coefficients is readily obtained. Preset adjustment of both phase and amplitude on each of the quadrature channels is provided to eliminate phase errors due to component variation. This adjustment is performed by first setting the phase difference between the cos and sin channels to 90° and then balancing the gain.

The resultant relationship between the desired phase ϕ and the C and S coefficients is found to be

$$C = 128 - 127\cos(\phi - 181)$$
$$S = 128 + 127\sin(\phi - 181) \qquad 5.2$$

The next step is to convert these decimal coefficients into hexadecimal for storage and use in the beam former. The rest of this procedure is illustrated with an example.

Consider the focusing phases required to form beam no. 1 at a range of 10 m as shown in table 5.1 and reproduced here (in part) for clarity. The phases are:

ELT 1	ELT 2	ELT 3	ELT 4	ELT 5	ELT 6
9.2°	9.2°	83.2°	231.1°	92.6°	28.1°

After the conversion to hex the coefficients appear in pairs. The first two hex characters are sent to the C latch and the second two to the S latch. The data required for three of the focal zone phases (and 5 beams per focal zone) is shown in table 5.2. The first row is pertinent to the example.

ELT 1	ELT 2	ELT 3	ELT 4	ELT 5	ELT 6
FD6D	FD6D	9102	2EE1	17C0	1F14

Note that the data has been arranged in focal zones, ready for linear addressing and easy transfer to the phase shifters.

Aperture shading is readily accomplished by programming the appropriate gains. Not only do the total 16 bits sent to the phase shifter provide 8 bits of phase control; they also permit almost 8 bits (or 48 dB) of amplitude control. In this system however, binary shading has been used for the reasons discussed in chapters 3 and 4. An element is turned off by sending it the coefficient pair 80,80 thus setting the

gains of both amplifiers to zero. After the shading has been applied (in this example the range is short and the shading requirements are that only the leftmost three elements are used) the hex data to be stored for use by the microprocessor is as shown.

ELT 1	ELT 2	ELT 3	ELT 4	ELT 5	ELT 6
FD6D	FD6D	9102	8080	8080	8080

After the required element shading has been applied with the aid of another BASIC program given in appendix III, the data is collected into short records and transferred to a ROM burner in the Intel HEX paper tape format.

FOCUSING PHASES FOR BEAM No. 1

ELEMENT No. RANGE	1	2	3	4	5	6	7	8	9	10
10.000	9.2	9.2	83.2	231.0	92.6	28.1	37.2	120.0	276.1	145.6
12.188	7.6	7.6	68.2	189.5	11.4	253.9	196.9	200.4	264.3	28.5
14.375	6.4	6.4	57.9	160.7	314.9	160.5	57.5	5.8	5.3	56.1
16.563	5.6	5.6	50.2	139.5	273.3	91.8	314.9	222.5	174.6	171.3
18.750	4.9	4.9	44.4	123.2	241.5	39.1	236.2	112.6	28.4	343.5
20.938	4.4	4.4	39.7	110.3	216.2	357.4	173.9	25.7	272.7	194.9
23.125	4.0	4.0	36.0	99.9	195.8	323.6	123.4	315.2	178.8	74.4
25.313	3.7	3.7	32.9	91.3	178.9	295.7	81.7	256.8	101.2	334.7
27.500	3.4	3.4	30.2	84.0	164.6	272.1	46.5	207.8	35.9	250.8
29.688	3.1	3.1	28.0	77.8	152.5	252.1	16.6	166.0	340.2	179.3
31.875	2.9	2.9	26.1	72.5	142.0	234.8	350.7	129.9	292.2	117.6
34.063	2.7	2.7	24.4	67.8	132.9	219.7	328.2	98.4	250.3	63.9
36.250	2.5	2.5	22.9	63.7	124.9	206.5	308.4	70.8	213.5	16.6
38.438	2.4	2.4	21.6	60.1	117.8	194.7	290.9	46.2	180.8	334.7
40.625	2.3	2.3	20.5	56.9	111.4	184.2	275.2	24.4	151.7	297.3
42.813	2.2	2.2	19.4	54.0	105.8	174.8	261.1	4.7	125.6	263.7
45.000	2.1	2.1	18.5	51.3	100.6	166.3	248.5	347.0	102.0	233.4
47.188	2.0	2.0	17.6	49.0	96.0	158.6	236.9	330.9	80.6	205.9
49.375	1.9	1.9	16.8	46.8	91.7	151.6	226.4	316.3	61.1	180.8
51.563	1.8	1.8	16.1	44.8	87.8	145.2	216.8	302.8	43.2	157.9
53.750	1.7	1.7	15.5	43.0	84.2	139.2	208.0	290.5	26.8	136.8
55.938	1.7	1.7	14.9	41.3	80.9	133.8	199.9	279.2	11.7	117.4
58.125	1.6	1.6	14.3	39.7	77.9	128.8	192.4	268.7	357.7	99.4
60.313	1.5	1.5	13.8	38.3	75.1	124.1	185.4	258.9	344.7	82.7
62.500	1.5	1.5	13.3	37.0	72.4	119.8	178.9	249.8	332.6	67.2
64.688	1.4	1.4	12.9	35.7	70.0	115.7	172.8	241.4	321.4	52.8
66.875	1.4	1.4	12.4	34.5	67.7	111.9	167.2	233.5	310.9	39.3
69.063	1.3	1.3	12.0	33.4	65.6	108.4	161.9	226.1	301.0	26.7
71.250	1.3	1.3	11.7	32.4	63.5	105.0	156.9	219.2	291.8	14.8
73.438	1.3	1.3	11.3	31.5	61.7	101.9	152.2	212.6	283.1	3.6
75.625	1.2	1.2	11.0	30.5	59.9	99.0	147.8	206.5	274.9	353.1
77.813	1.2	1.2	10.7	29.7	58.2	96.2	143.7	200.7	267.2	343.2
80.000	1.2	1.2	10.4	28.9	56.6	93.6	139.8	195.2	259.9	333.8

TABLE 5.1: Focusing and steering phases for beam no.1

ZONE No.	BEAM No.	
1	1	FD6DFD6D91022EE17C01F146E63442108BFE1836
1	2	2EE19102FD6DFD6D91022EE17C01F146E6344210
1	3	F1467C012EE19102FD6DFD6D91022EE17C01F146
1	4	4210E634F1467C012EE19102FD6DFD6D91022EE1
1	5	18368BFE4210E634F1467C012EE19102FD6DFD6D
2	1	FE71FE71B10A0292FC695AF905A208AA71FEF045
2	2	0292B10AFE71FE71B10A0292FC695AF905A208AA
2	3	5AF9FC690292B10AFE71FE71B10A0292FC695AF9
2	4	08AA05A25AF9FC690292B10AFE71FE71B10A0292
2	5	F04571FE08AA05A25AF9FC690292B10AFE71FE71
3	1	FE73FE73C5150853D8DB0953C616FE75FE76C817
3	2	0853C515FE73FE73C5150853D8DB0953C616FE75
3	3	0953D8DB0853C515FE73FE73C5150853D8DB0953
3	4	FE75C6160953D8DB0853C515FE73FE73C5150853
3	5	C817FE76FE75C6160953D8DB0853C515FE73FE73
4	1	FE75FE75D21F202B85FE7E01D8DB20D40171026A
4	2	202BD21FFE75FE75D21F202B85FE7E01D8DB20D4
4	3	7E0185FE202BD21FFE75FE75D21F202B85FE7E01
4	4	20D4D8DB7E0185FE202BD21FFE75FE75D21F202B
4	5	026A017120D4D8DB7E0185FE202BD21FFE75FE75
5	1	FE77FE77DC283C1441EEE33137E85109F045F9A6
5	2	3C14DC28FE77FE77DC283C1441EEE33137E85109
5	3	E33141EE3C14DC28FE77FE77DC283C1441EEE331
5	4	510937E8E33141EE3C14DC28FE77FE77DC283C14
5	5	F9A6F045510937E8E33141EE3C14DC28FE77FE77
6	1	FE78FE78E330550818C9FE870170F34B83FE049E
6	2	5508E330FE78FE78E330550818C9FE870170F34B
6	3	FE8718C95508E330FE78FE78E330550818C9FE87
6	4	F34B0170FE8718C95508E330FE78FE78E3305508
6	5	049E83FEF34B0170FE8718C95508E330FE78FE78
7	1	FE79FE79E8376C0205A0E4CD3B14D8DB017BA406
7	2	6C02E837FE79FE79E8376C0205A0E4CD3B14D8DB
7	3	E4CD05A06C02E837FE79FE79E8376C0205A0E4CD
7	4	D8DB3B14E4CD05A06C02E837FE79FE79E8376C02
7	5	A406017BD8DB3B14E4CD05A06C02E837FE79FE79
8	1	FE7AFE7AEB3C7F01017BB4F3940260FB6902F1B8
8	2	7F01EB3CFE7AFE7AEB3C7F01017BB4F3940260FB
8	3	B4F3017B7F01EB3CFE7AFE7AEB3C7F01017BB4F3
8	4	60FB9402B4F3017B7F01EB3CFE7AFE7AEB3C7F01
8	5	F1B8690260FB9402B4F3017B7F01EB3CFE7AFE7A
9	1	FE7AFE7AEE418F01065C82FED8250EB9E83754F7
9	2	8F01EE41FE7AFE7AEE418F01065C82FED8250EB9
9	3	82FE065C8F01EE41FE7AFE7AEE418F01065C82FE
9	4	0EB9D82582FE065C8F01EE41FE7AFE7AEE418F01
9	5	54F7E8370EB9D82582FE065C8F01EE41FE7AFE7A

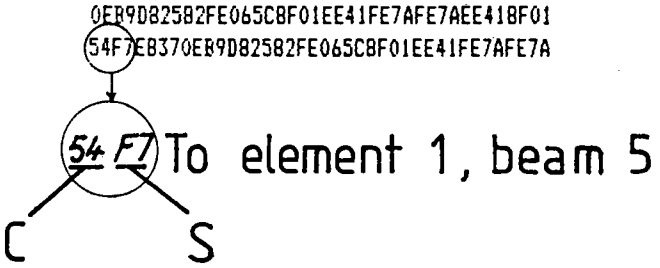

TABLE 5.2: Phase coefficients ready for transfer

5.3 Calibration and testing of phase shifters

5.3.1 Static performance

An accurate measurement of the phase of each phase shifter can only be made under static conditions. A pair of coefficients are sent to a phase shifter and latched. The phase is then measured with a digital phase meter. Four calibration points are applied to each phase shifter and the phase shifts measured. This procedure is carried out for all 50 phase shifters. The measured results are shown in table 5.3 along with the means and variances over the 50 devices. The two bytes of hex in the left hand column are the addresses of the C and S coefficient latches on the various boards.

5.3.2 Dynamic range

Approximately 5 mV of noise is coupled to the phase shifters from the digital circuitry. This could be further reduced with careful attention to layout and decoupling; but even at this level the dynamic range is close to 70 dB. The increasing array gain and method of insonification are expected to keep the dynamic range within this limit.

	FD96	8001	9602	1ED1
4080	349,4	90,6	80,5	214,1
4181	350,2	90,7	80,8	217,6
4282	350,6	90,6	80,7	218,3
4383	349,8	89,5	79,6	216,3
4484	349,9	90,8	80,7	216,7
4585	349,1	90,0	78,9	215,6
4686	349,6	90,6	80,7	216,8
4787	350,5	91,2	81,4	217,8
4888	349,6	89,5	79,6	215,9
4989	349,8	89,9	80,0	216,5
4A8A	349,9	91,0	81,2	217,2
4B8B	350,2	91,2	81,5	218,7
4C8C	350,0	91,4	81,4	216,6
4E8E	349,5	89,9	80,1	216,8
4F8F	350,0	91,0	81,0	217,0
5090	349,7	90,5	80,7	218,0
5191	349,9	90,5	80,4	216,7
5292	350,6	91,7	81,8	217,6
5393	350,7	90,8	81,2	218,3
5494	350,2	91,3	81,5	218,2
5595	350,2	91,4	81,7	217,6
5695	349,5	90,2	80,2	216,1
5797	350,5	90,0	80,8	216,8
5898	350,3	90,9	81,1	218,4
5999	350,0	91,0	81,1	216,9
5A9A	348,8	90,7	81,2	217,8
5B9B	349,5	90,0	80,1	217,2
5C9C	350,3	90,4	80,4	219,1
5D9D	349,5	90,4	80,3	216,8
5E9E	350,5	91,4	81,6	218,8
5F9F	349,1	90,3	80,7	217,8
60A0	349,9	90,6	80,7	217,8
61A1	350,2	91,0	81,0	216,6
62A2	350,3	91,4	81,6	217,6
63A3	350,3	91,3	81,6	217,0
64A4	350,4	90,0	80,4	218,2
65A5	349,6	89,9	80,0	216,7
66A6	350,0	91,5	81,7	218,2
67A7	350,6	91,1	80,9	218,5
68A8	350,3	91,2	81,3	218,3
69A9	350,6	90,7	80,9	218,6
6AAA	350,0	91,3	81,4	216,2
6BAB	350,3	91,4	81,5	218,1
6CAC	350,5	91,3	81,4	218,0
6DAD	349,7	90,1	81,8	218,1
6EAE	350,4	90,8	80,0	218,0
6FAF	350,2	90,5	80,8	218,0
70B0	350,1	90,6	80,7	217,2
71B1	350,0	90,3	80,4	217,7
MEAN	350,0	90,7	80,8	217,4
VARIANCE	0,2	0,3	0,4	0,9

TABLE 5.3: Results of static test of phase shifter

5.3.3 Dynamic performance

Of greater interest is the dynamic performance of the phase shifters when under control of the microprocessor. This measurement of phase cannot be performed with a phase meter since the phases are only constant for 2.9 ms between refocusing.

Fig. 5.5 shows a block diagram of the setup used for this test. The signal at the input of the phase shifter is added to that at the output. When a phase shift of 180° is selected the two signals cancel each other. A phase shift of 0° causes them to add to double the input amplitude. The amplitude at the output of the test circuit is readily expressed in terms of the phase shift. Fig. 5.6 shows the outputs of the the test circuit for beam no. 5. The transmission of a pulse occurs at the origin of the trace. The full extent of the trace covers the 200 ms round trip time to 150 m range. Each phase shift remains constant for slightly less than 3 ms between updates.

The amplitude of the input signal is 1,2 V (or 1,2 divisions on the vertical scale). When the array element is turned off the signal at the output of the test circuit is a constant 1,2 V. When the programmed phase is 0° the output is 2,4 V peak.

Figures 5.6a and 5.6b are the results of the tests on the two elements straddling the swath. As expected their phase remains fairly constant and they are active from the beginning of the swath. Figure 5.6f demonstrates clearly how the shading occurs as well as the range at which the phase is 180° and the output of the test circuit is zero. This element is the sixth to be included in the sub-array at a range of 25 m, or a two way time of 33,3 m s. The point at which the element is turned on is clearly apparent 1,6 divisions from the start of the trace (recall that 1 division is 20 ms). After 53 ms, when the range is 40 m the programmed phase is close to zero, and the test circuit output shows a null. Further away from the swath centreline the elements turn on later and their phases change more rapidly with increasing range.

Comparison of these results with tables of the required phases indicate the correct operation of both the phase shifter hardware and software. Table 5.4 shows some of the required phases for focusing and steering beam no. 5. Note how the elements straddling the swath have little phase variation. Of particular interest is the phase of the element furthest away from the swath centreline. At 150 m the programmed phase of this element is 180°; this should be compared to the test of that element in fig. 5.6j. The points at which the programmed phase shifts are close to 180° have been underlined in table 5.4.

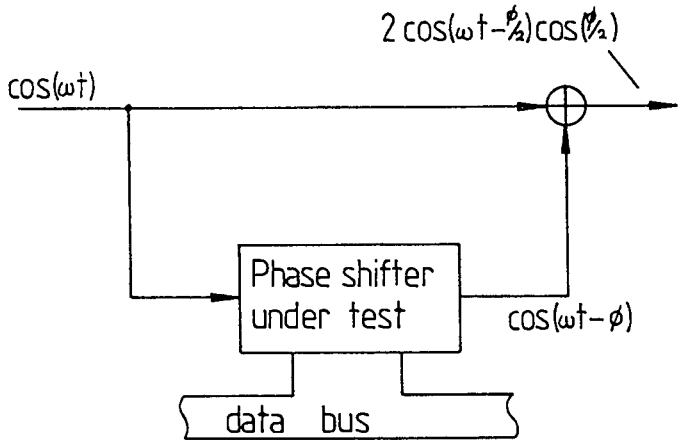

Fig. 5.5: Phase shifter test circuit

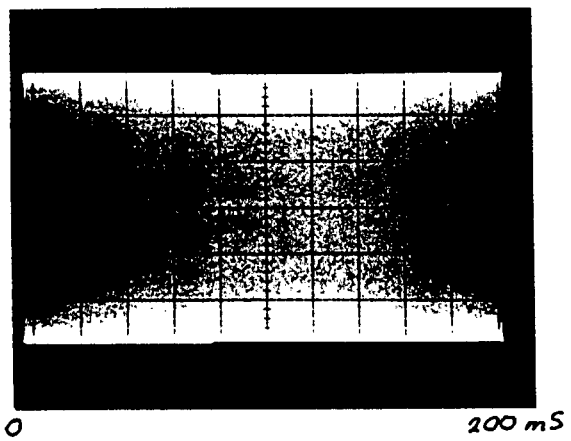

a) Element no. 10

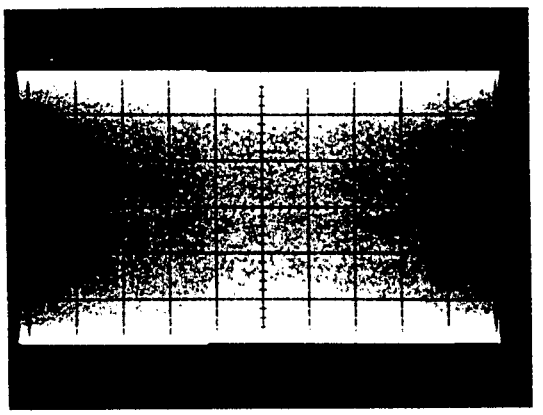

b) Element no. 9

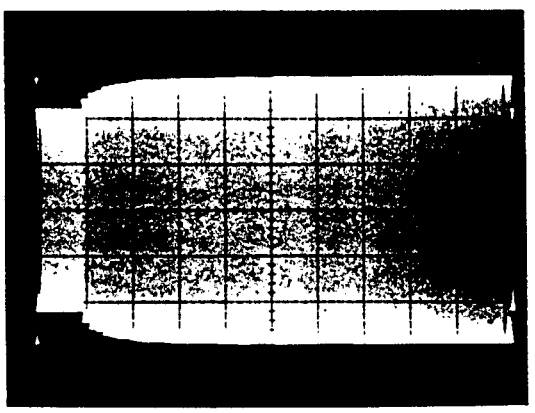

c) Element no. 8

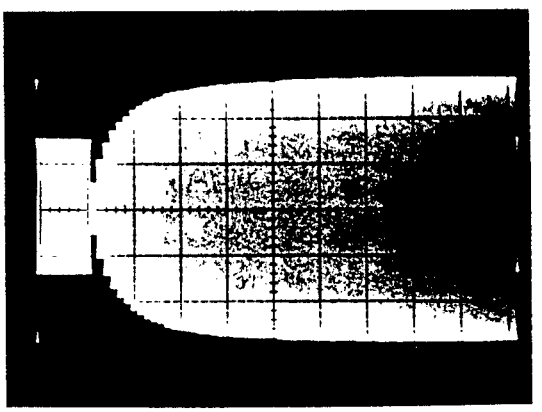

d) Element no. 7

Vertical scale: 1 V/div Horizontal scale: 20 ms/div

Fig. 5.6 Phase shift test results

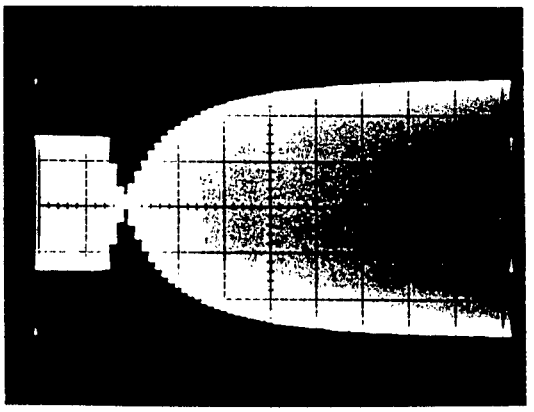

e) Element no. 6

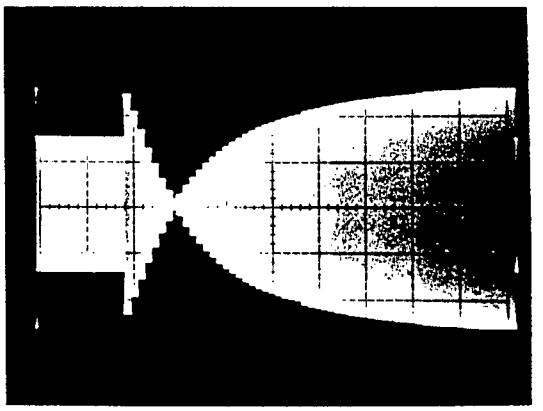

f) Element no. 5

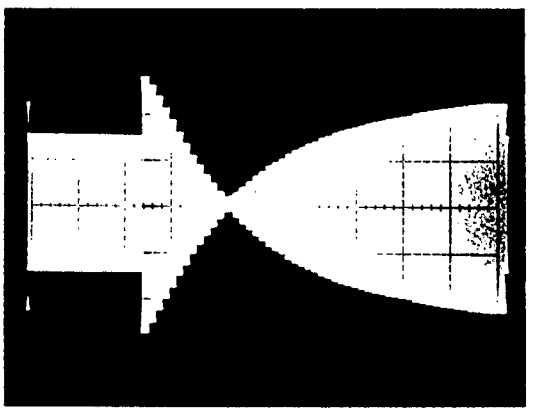

g) Element no. 4

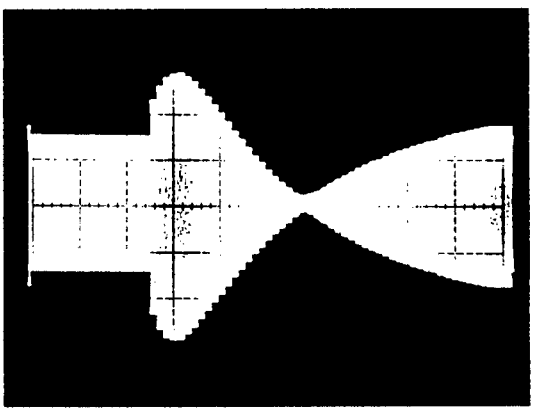

h) Element no. 3

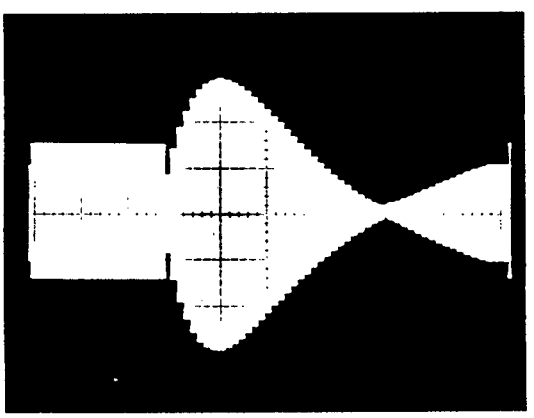

i) Element no. 2

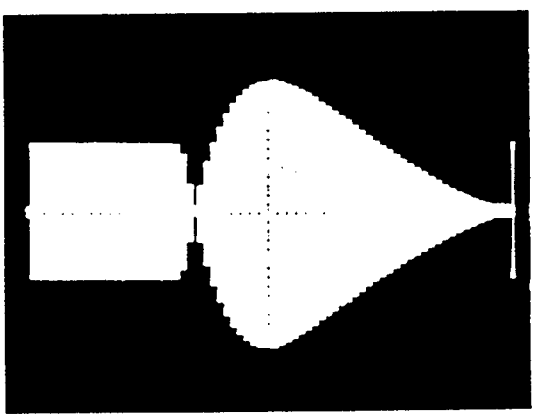

j) Element no. 1

Fig. 5.6: Phase shift test results, contd.

FOCUSING PHASES FOR BEAM No. 5

ELEMENT No. RANGE	1	2	3	4	5	6	7	8	9	10
10.000	145.6	276.1	120.0	37.2	28.1	92.6	231.0	83.2	9.2	9.2
12.188	28.5	264.3	200.4	196.9	253.9	11.4	189.5	68.2	7.6	7.6
14.375	56.1	5.3	5.8	57.5	160.5	314.9	160.7	57.9	6.4	6.4
16.563	171.3	174.6	222.5	314.9	91.8	273.3	139.5	50.2	5.6	5.6
18.750	343.5	28.4	112.6	236.2	39.1	241.5	123.2	44.4	4.9	4.9
20.938	194.9	272.7	25.7	173.9	357.4	216.2	110.3	39.7	4.4	4.4
23.125	74.4	178.8	315.2	123.4	323.6	195.8	99.9	36.0	4.0	4.0
25.313	334.7	101.2	256.8	81.7	295.7	178.9	91.3	32.9	3.7	3.7
27.500	250.8	35.9	207.8	46.5	272.1	164.6	84.0	30.2	3.4	3.4
29.688	179.3	340.2	166.0	16.6	252.1	152.5	77.8	28.0	3.1	3.1
31.875	117.6	292.2	129.9	350.7	234.8	142.0	72.5	26.1	2.9	2.9
34.063	63.9	250.3	98.4	328.2	219.7	132.9	67.8	24.4	2.7	2.7
36.250	16.6	213.5	70.8	308.4	206.5	124.9	63.7	22.9	2.5	2.5
38.438	334.7	180.8	46.2	290.9	194.7	117.8	60.1	21.6	2.4	2.4
40.625	297.3	151.7	24.4	275.2	184.2	111.4	56.9	20.5	2.3	2.3
42.813	263.7	125.6	4.7	261.1	174.8	105.8	54.0	19.4	2.2	2.2
45.000	233.4	102.0	347.0	248.5	166.3	100.6	51.3	18.5	2.1	2.1
47.188	205.9	80.6	330.9	236.9	158.6	96.0	49.0	17.6	2.0	2.0
49.375	180.8	61.1	316.3	226.4	151.6	91.7	46.8	16.8	1.9	1.9
51.563	157.9	43.2	302.8	216.8	145.2	87.8	44.8	16.1	1.8	1.8
53.750	136.8	26.8	290.5	208.0	139.2	84.2	43.0	15.5	1.7	1.7
55.938	117.4	11.7	279.2	199.9	133.8	80.9	41.3	14.9	1.7	1.7
58.125	99.4	357.7	268.7	192.4	128.8	77.9	39.7	14.3	1.6	1.6
60.313	82.7	344.7	258.9	185.4	124.1	75.1	38.3	13.8	1.5	1.5
62.500	67.2	332.6	249.8	178.9	119.8	72.4	37.0	13.3	1.5	1.5
⋮										⋮
101.875	262.1	204.1	153.3	109.7	73.5	44.4	22.7	8.2	0.9	0.9
104.063	256.6	199.8	150.1	107.4	71.9	43.5	22.2	8.0	0.9	0.9
106.250	251.3	195.7	147.0	105.2	70.4	42.6	21.7	7.8	0.9	0.9
108.438	246.3	191.7	144.0	103.1	69.0	41.8	21.3	7.7	0.9	0.9
110.625	241.4	187.9	141.2	101.1	67.7	40.9	20.9	7.5	0.8	0.8
112.813	236.7	184.3	138.4	99.1	66.3	40.1	20.5	7.4	0.8	0.8
115.000	232.2	180.8	135.8	97.2	65.1	39.4	20.1	7.2	0.8	0.8
117.188	227.9	177.4	133.3	95.4	63.9	38.6	19.7	7.1	0.8	0.8
119.375	223.7	174.2	130.8	93.7	62.7	37.9	19.4	7.0	0.8	0.8
121.563	219.7	171.0	128.5	92.0	61.6	37.2	19.0	6.8	0.8	0.8
123.750	215.8	168.0	126.2	90.3	60.5	36.6	18.7	6.7	0.7	0.7
125.938	212.0	165.1	124.0	88.8	59.4	36.0	18.3	6.6	0.7	0.7
128.125	208.4	162.3	121.9	87.3	58.4	35.3	18.0	6.5	0.7	0.7
130.313	204.9	159.5	119.8	85.8	57.4	34.7	17.7	6.4	0.7	0.7
132.500	201.5	156.9	117.9	84.4	56.5	34.2	17.4	6.3	0.7	0.7
134.688	198.3	154.4	115.9	83.0	55.6	33.6	17.2	6.2	0.7	0.7
136.875	195.1	151.9	114.1	81.7	54.7	33.1	16.9	6.1	0.7	0.7
139.063	192.0	149.5	112.3	80.4	53.8	32.6	16.6	6.0	0.7	0.7
141.250	189.1	147.2	110.6	79.2	53.0	32.1	16.4	5.9	0.7	0.7
143.438	186.2	144.9	108.9	77.9	52.2	31.6	16.1	5.8	0.6	0.6
145.625	183.4	142.8	107.2	76.8	51.4	31.1	15.9	5.7	0.6	0.6
147.813	180.7	140.7	105.6	75.6	50.6	30.6	15.6	5.6	0.6	0.6

TABLE 5.4: Phases for beam no. 5

5.4 Phase errors

Errors in the aperture illumination result in deviations in the directivity pattern of an array. The errors may be caused by the physical construction of the array or in the beam forming circuitry. The errors cause loss of gain, quantization sidelobes and beam squint (64).

Satisfactory performance of an array operating in its far field may be ensured by applying the rule-of-thumb criterion that states that the actual phases should not differ from the theoretical ones by more than a sixteenth of a wavelength.

The errors may be classed as either systematic or random. The systematic errors are easily compensated for in a digitally controlled system by simply altering the stored coefficient table. At the operating frequency one sixteenth of a wavelength is slightly smaller than a third of a millimeter. The array is constructed to tolerances far finer than this, with deviation from a straight line of less than 0,1 mm, and systematic errors are expected to be small.

The one sixteenth wavelength criterion is arrived at upon consideration of the far field radiation pattern. A computer simulation of the effect of phase errors in the near field is performed to test the validity of this criterion. The test is specifically

to estimate beam squint. The results are shown in figs. 5.7 to 5.9 . The range is 21 m and 5 elements of the array are active. Figure 5.7 shows the directivity when there are no errors. Figure 5.8 shows the situation where there are 5° errors distributed in such a way as to steer the beam off axis. The resulting squint is less than 1 cm at 20 m range. Fig. 5.9 shows 10° errors with a similar distribution. Although the sidelobe levels are increased the beam squint is less than 2 cm.

Clearly the phase shifters are more than adequate for the task at hand. Other phase errors may occur in the preamplifier stages. Provision is made on these for the adjustment of phase and amplitude to compensate component tolerances.

Random phase errors may be introduced by component temperature coefficients. The preamplifiers are identical and may be expected to have tracking phase errors, which are not a problem. The design of the phase shifters is such that sensitivity to temperature is low; the circuit elements causing phase errors are the quadrature power splitter (with low Q) and the multiplying A/D converters. A worst case 5% deviation in these networks cause phases errors of less than 10°.

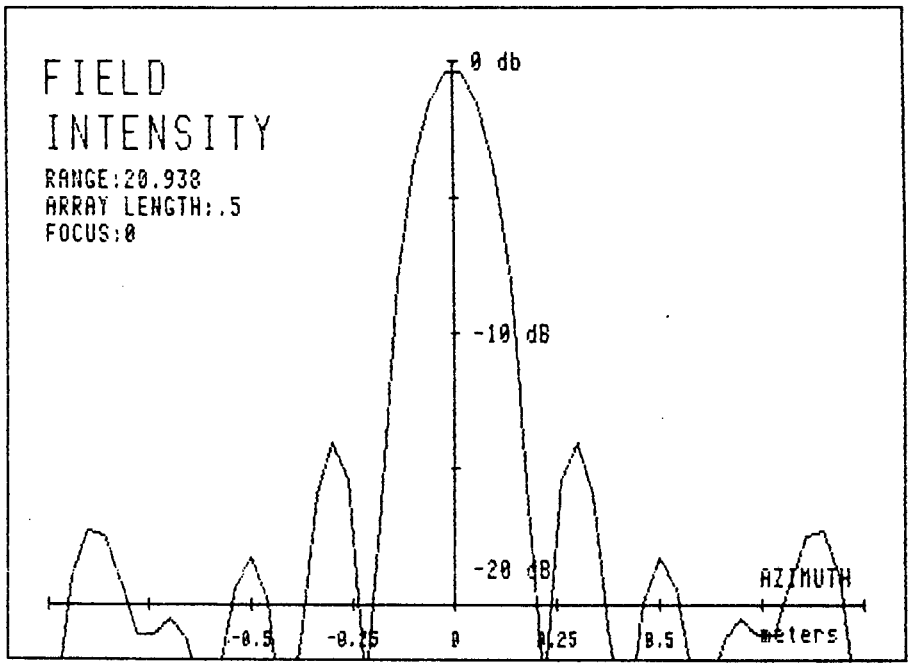

Fig. 5.7: 5 Element array at 20 m, no errors

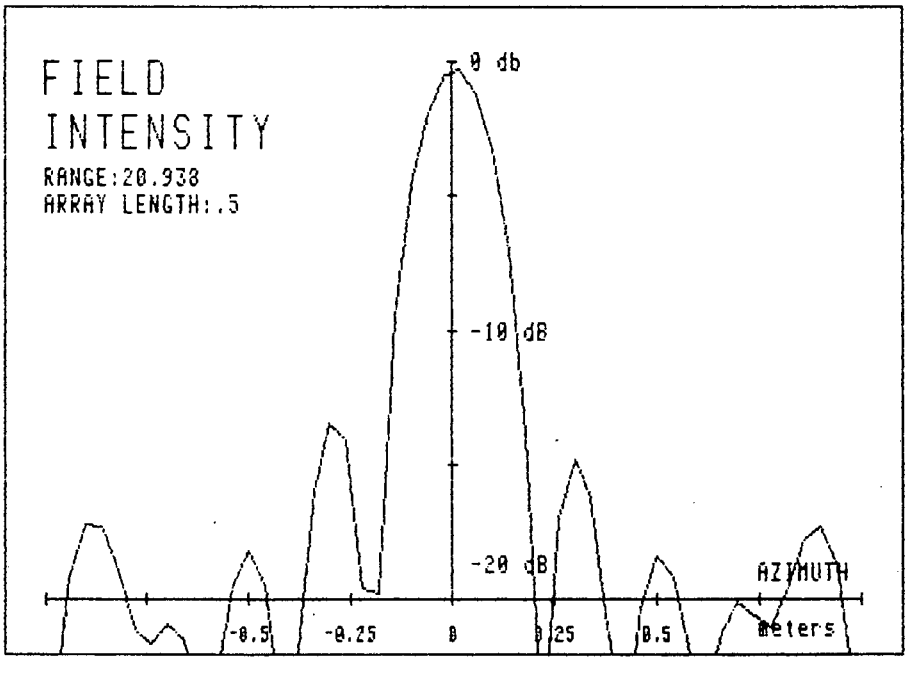

Fig. 5.8: As above, 5° phase errors

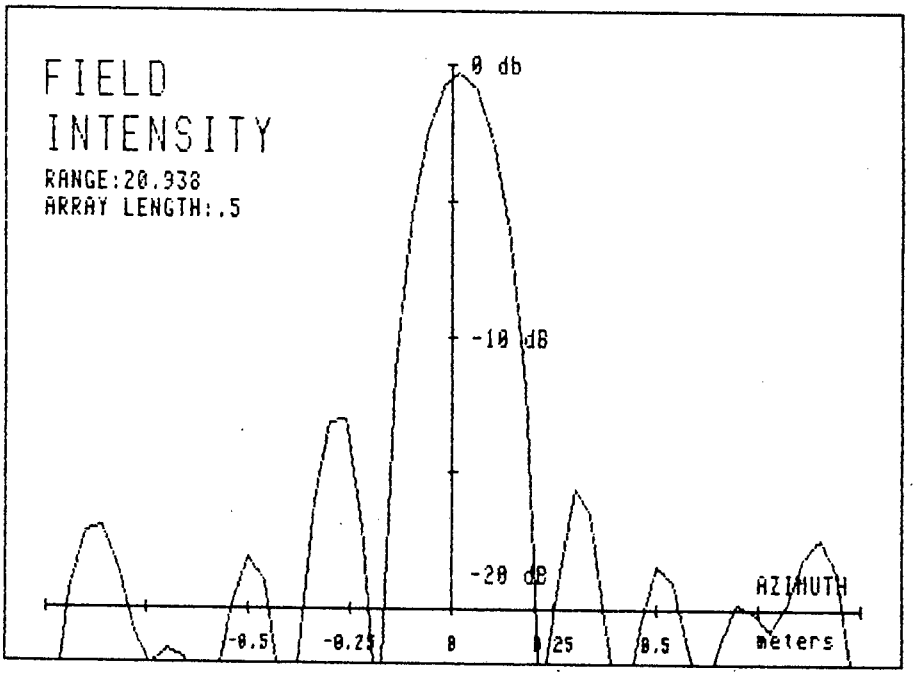

Fig. 5.9: 5 Element array at 20 m range

10° phase errors

BEAM FORMING AND A/D CONVERSION

6.1 Introduction

The actual process of beam forming takes place when the appropriately phase shifted signals from the array elements are summed. The block diagram in fig. 6.1 shows the beam forming summer and the signal processing and analog to digital conversion that follows.

6.2 Time-varying gain

Immediately after the beam former the signal amplitude is adjusted by a programmable gain amplifier to accomodate the effects of increased array length, attenuation and beam spreading. One byte of data is sent to these TVG amplifiers for each focal zone. The values that have been determined empirically are stored in ROM. The manner in which they are handled by the microprocessor is described in paragraph 10.3.1.1.

6.3 Detection

Just prior to detection the signal bandwidth is restricted to eliminate as much of the noise as possible. This is especially important here even though the preamplifiers have a narrowband characteristic since the signals are contaminated with noise from the digital circuitry between the

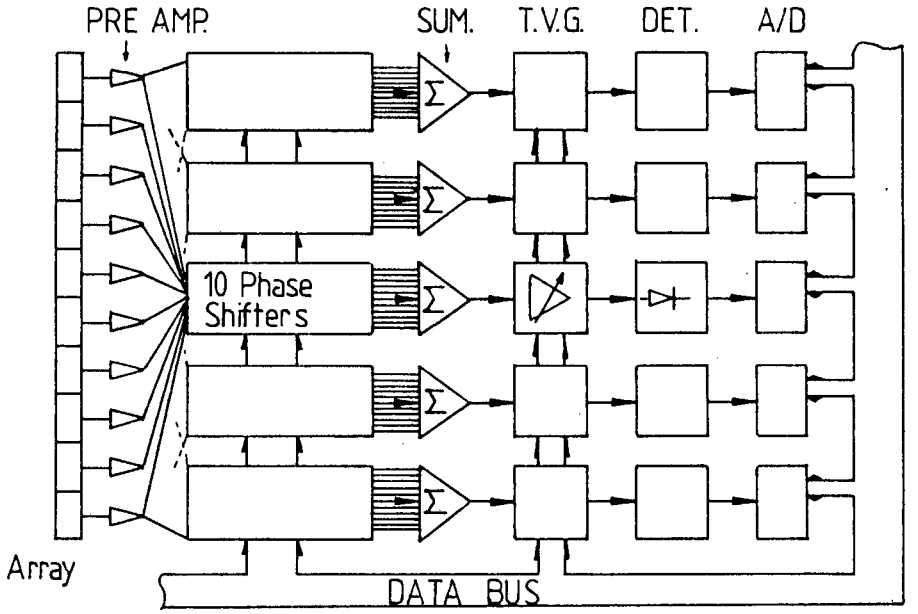

Fig. 6.1: Block diagram of beam forming board

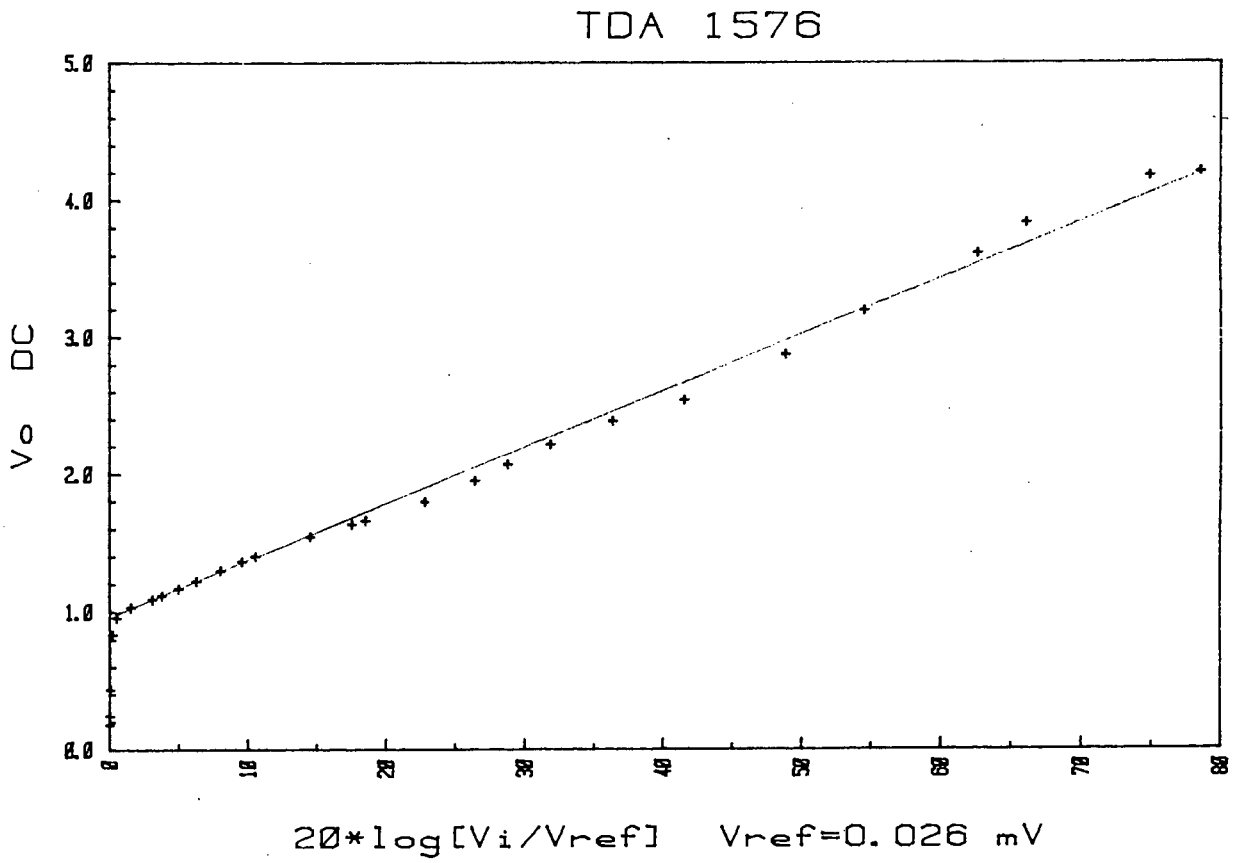

Fig. 6.2: Detector characteristic

preamplifiers and the detector.

The detected signal is then logarithmically compressed prior to A/D conversion. This allows the expected dynamic range of approximately 60 dB to be quantized using 8 bits. The detector and compressor are realized using the signal strength indication output on a FM decoder chip. The sensitivity is excellent as shown by the measured response curve in fig. 6.2 .

6.4 A/D Conversion

The A/D converters are all trigerred simultaneously after having been read individually. The data read at any time is the beam sample from the previous range cell. In this way the A/D timing requirements are relaxed. A full 180 μs are available for the conversion.

A great deal of attention was given to the design and layout of this subsystem to isolate the digital section with its wideband noise from the detector and A/D converter. A photograph of the beam forming board is shown in fig. 6.3.

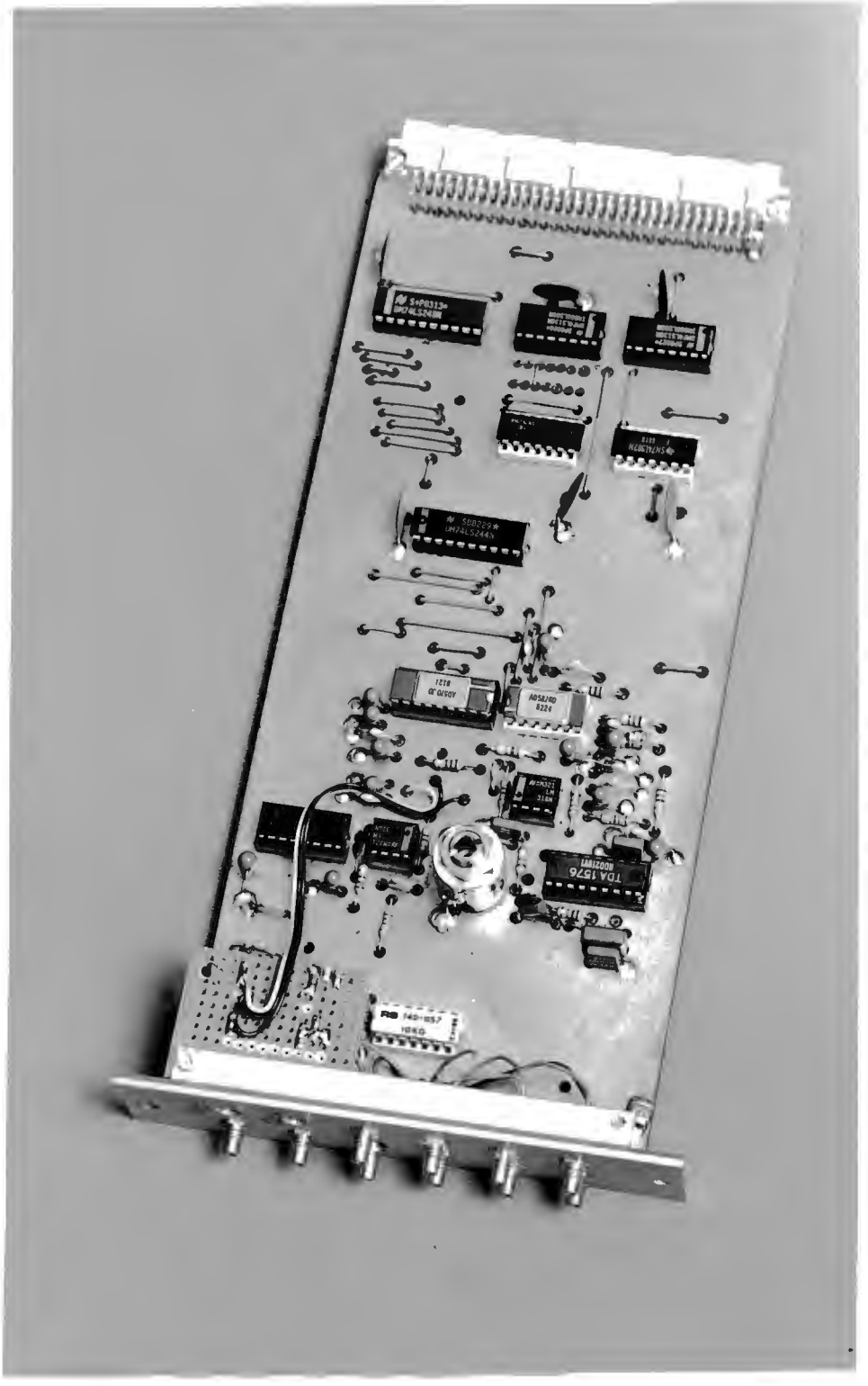

Fig. 6.3: Photograph of beam forming board

TRANSMITTER

7.1 Introduction

The primary requirement of the transmitter is that the area of the sea bed to be imaged must be adequately and uniformly insonified. After the consideration of the simpler options available and their relative merits and demerits a novel 'multiple beam' transmitter, using a form of time domain multiplexing was adopted.

7.2 Transmitter transducer

7.2.1 Required insonification

The required insonification is determined by the the area to be imaged and the towing speed of the array. The receiving array is focused on a line parallel to its axis of symmetry, and this line moves with the array. Relative to the sea bed the locus of the focal point is a line at an angle to the axis of symmetry of the transmitting transducer.

At the correct towing speed of 10 knots the receiver array moves 1 m along track in each pulse repetition interval. The imaged zone is thus a parallelogram with the closest end almost coincident with the array and the farthest end displaced slightly in the direction of towing. It is this area that must

be uniformly illuminated.

An unsteered beam would need to be at least 3 m wide at maximum range to provide the uniform insonification. The transmitter beam may be steered such that its axis is coincident with that of the area to be imaged. In this case the beam may be only 1 m wide at maximum range.

7.2.2 Large uniform aperture

The most obvious choice of transducer for transmission is the whole array. Due to the high directivity that could be obtained the power requirements of the transmitter drivers could be relaxed without incurring degradation in the signal to noise ratio. The beam would be collimated to a range of over 200 m, with a beamwidth of 1 m. Not only is a high directivity obtained but the beam spreading loss is lower; closer to that of cylindrical spreading than that of spherical spreading.

Various studies have indicated that there is a significant reduction in the beam width at ranges comparable to one quarter of the near/far field transition (65), an effect known as beam necking. For the 1 m uniform line source this occurs at approximately 50 m and results in a beamwidth reduction factor of one half. This will result in inadequate insonification of the 1 m wide field at such ranges as

shown in fig. 7.1 .

7.2.3 Large phased aperture

Were it not for beam necking the 1 m transducer might have a fixed linear phase shift applied to steer it in the direction of array motion. Once the implementation of a fixed phasing is considered the possibility arises of using the fixed phases to decollimate the beam in an attempt to counter beam necking. By applying a quadratic phase shift to the transmitting array the transmitted wavefront can be made to appear to be diverging from a point behind the array or converging on a point in front of the array, as in focusing. An investigation into this possibility was performed using the field modelling routines in appendix II.

The method of investigation is briefly as follows. A range of 40 m is chosen since this is where the necking is most severe. The field of a uniform line source of 1 m length is calculated and plotted at this range. Various curvatures are applied interactively to the emitted wavefront (by the appropriate phasing) and the resulting field intensity is plotted. Having obtained a set of transmitter phases which result in an approximately uniform field intensity over 1 m at 40 m range, the field of the transmit beam is then plotted at a variety of other ranges over the operating range of 10 m to 150 m.

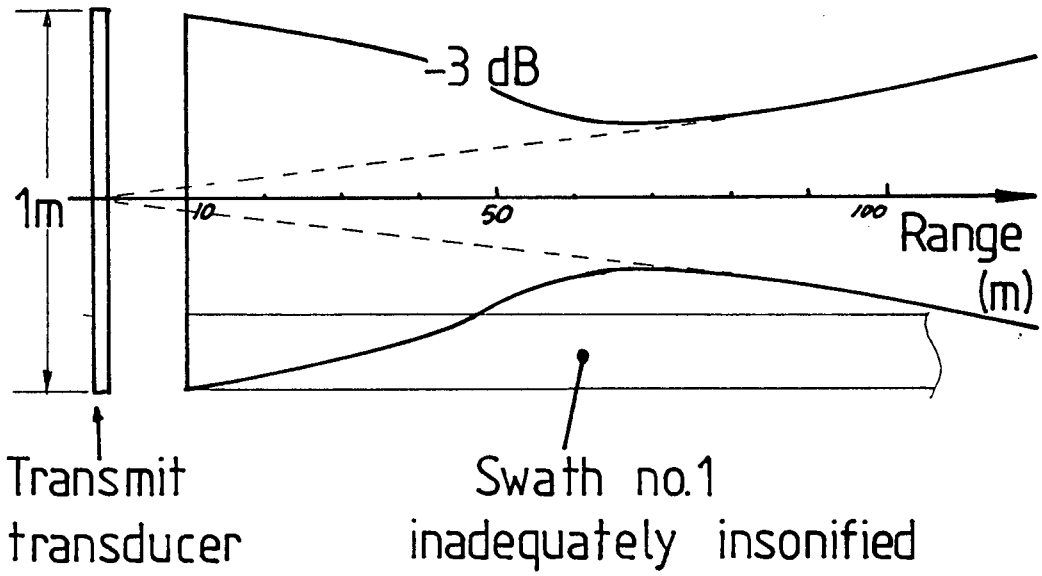

Fig. 7.1: Beam necking

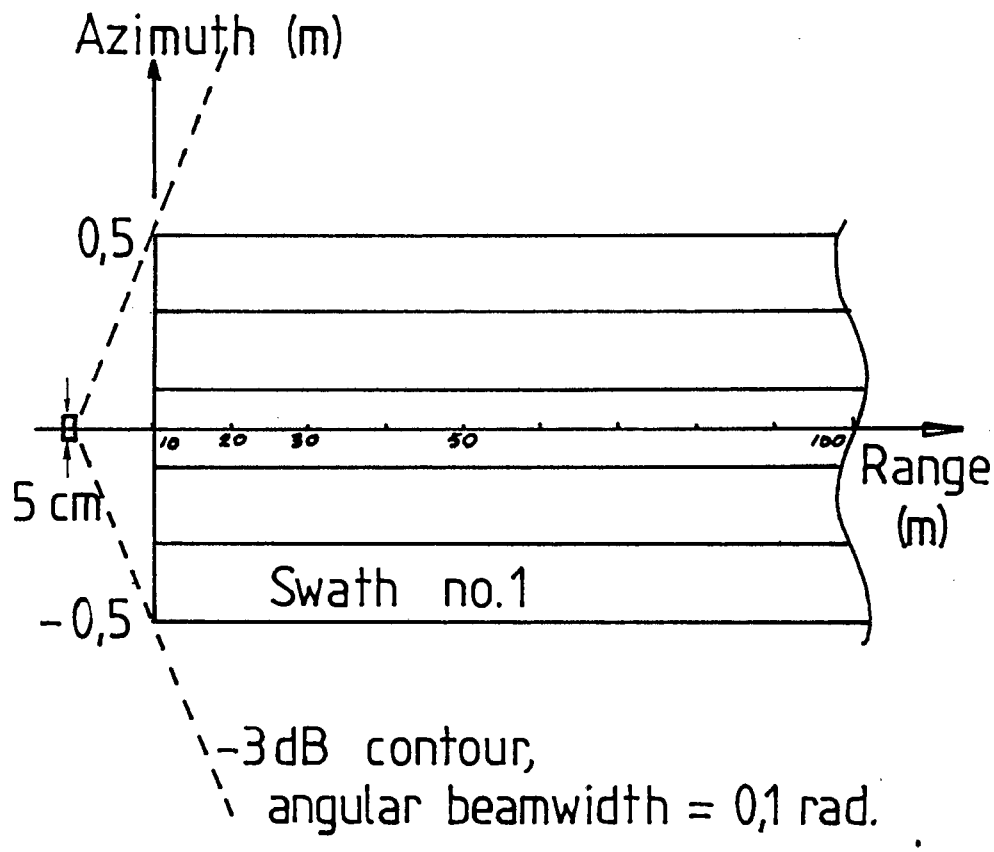

Fig. 7.2: Low directivity insonification

It became apparent that while it is possible to achieve the desired insonification at a given range it is not possible to achieve uniform intensity over the required azimuth at all ranges simultaneously.

7.2.4 Small aperture

At the other extreme of transmitting transducer length is a small transducer of low directivity and spherical spreading. At the minimum range of 10 m the beam width must be at least 1 m, an angular beam width of 0,1 radians. Such a broad beam can only be achieved with a transducer of less than 10 wavelengths, or 5 cm. The approximate -3dB contours of the beam of such a transducer are shown in fig. 7.2.

The directivity is low and the transmitted power must be accordingly increased to maintain adequate signal to noise ratios. At high acoustic power densities cavitation may be a problem. The typical fan beams required in sidescan sonar restrict the height of the element to approximately one wavelength (4,87 mm). As a result the area of the face of a transducer of 5 cm length is only 2,5 cm^2 and the maximum radiated power is limited to 1 kW. Achieving such powers and isolating the sensitive receivers from them is not trivial. Equivalent insonification can be achieved with pulses of only 50 W if the whole array could be used, with concomittent simplification of the power drivers and T/R switching.

Some method is sought whereby the area and the directivity of the transmitting transducer may be made larger than that of the single element.

7.2.5 Multiple transmitting subarrays

The problems with the large aperture are entirely due to the interference of the waves emitted from the various transducers. If the interference could be eliminated the desired insonification can be realized.

A single swath 0,2 m wide would be most adequately insonified by a uniform line source of only 0,2 m length. The near/far field transition of such an array occurs at approximately 10 m, resulting in beam necking around 2,5 m. Each swath would require its own transmitter; in all there must be 5 transmitters with the transducers separated by one swath width. The geometry of the 10 element array is ideal for this purpose. Each pair of elements are 20 cm apart and 20 cm long.

Obviously the 5 sets of transducers (of two elements each) cannot be fired simultaneously since their beams would interfere with each other and the resulting insonification would be the same as that of a 1 m array. Some means must be found whereby each swath may be independently insonified by its 'own' two array elements.

The method whereby the 5 beams are prevented from interfering with each other is similar to time domain multiplexing. The desired range resolution requires a maximum pulse length of 180 μs. Although this specifies the minimum bandwidth of the receiver it does not limit the minimum pulse duration. Minimum pulse length is determined by signal to noise ratios and thus signal energy.

The individual insonification of 5 parallel swaths is achieved by dividing the maximum pulse length into 5 separate pulses of 36 μs each. The pulse energy will be reduced by a factor of 5, but this is shown later to be an effect limited to only the shorter ranges. Using this time domain multiplexing scheme to form multiple transmit beams causes the wavefronts emitted by the two element transmit arrays to be separated in both time and space, the result being no interference between beams. This is depicted diagramatically in fig. 7.3.

Fig. 7.4 shows how the focal point moves off the initial axis of the transmitter transducer. The velocity of the focal point relative to the sea bed is the vector sum of the platform velocity (5 m/s maximum) and the velocity of the receeding point from which the echoes appear to be emanating, namely 750 m/s. The resultant angle between the line of motion of the focal point and the array axis is 0,0667 rads. The beam from the 41 wavelength element has a half divergence angle of 0,244 rads. At 10 m the half beamwidth of the

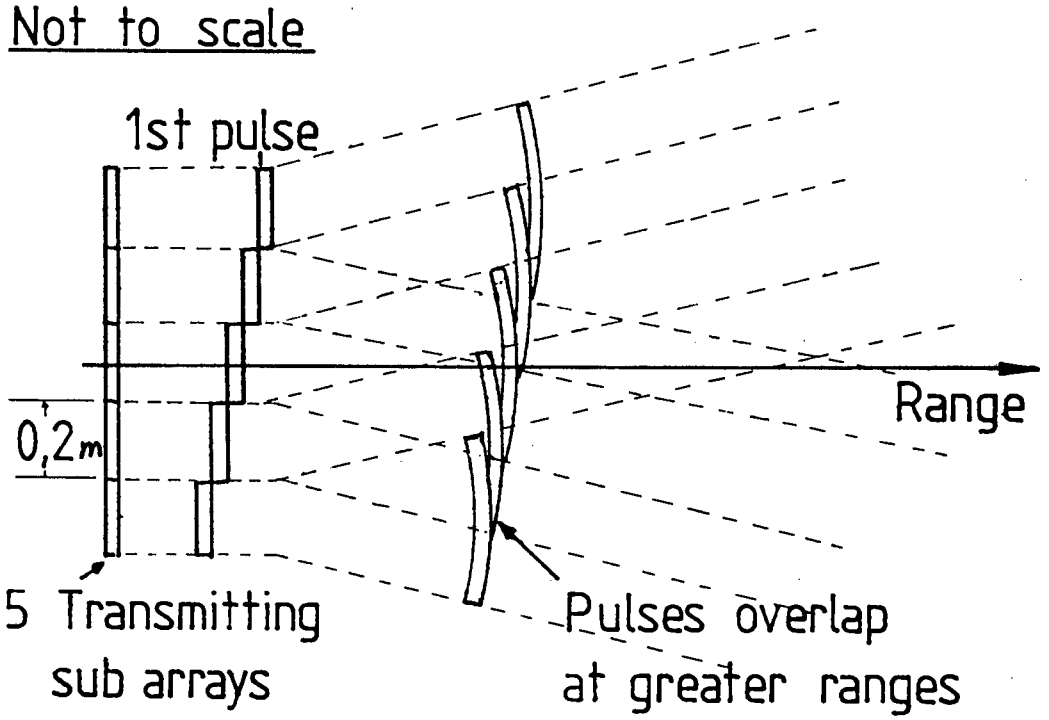

Fig. 7.3: Non overlapping outward bound pulses

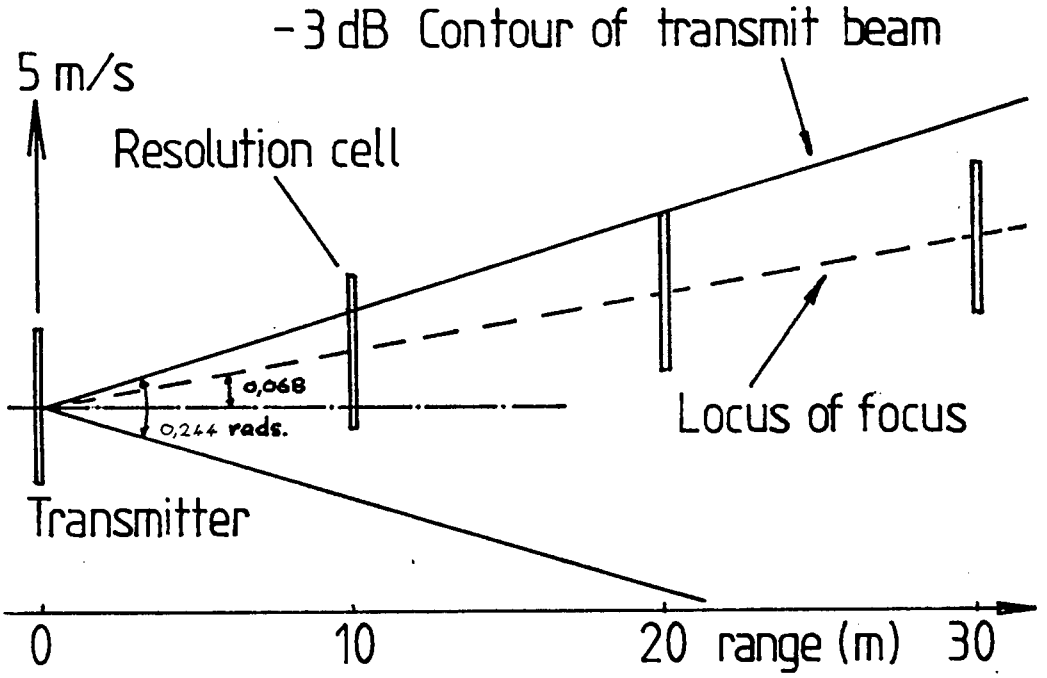

Fig. 7.4: Transmitter beam coverage

element is 12,2 cm while the focal point is displaced by 6,8 cm. This is not considered too serious since the range is short and the signal to noise ratio is large. At 20 m range the situation has improved somewhat. The focal point displacement is 13,3 cm while the half beam width is 24,4 cm. The resolution cell of 10 cm on either side of the focal point is now almost uniformly illuminated. The limits of the insonification and a number of resolution cells at various ranges are also shown in fig. 7.4.

7.2.6 Receiver considerations

On the receiver side the bandwidth is matched to a 180 μs pulse. At short ranges a particular beam 'sees' only one tranmitted pulse of 36 μs. At maximum range however the focal point has been insonified by 5 pulses; their azimuthal beamwidths having broadened to far greater than the required 2 m. The signal recieved in 180 μs from a point at large range is thus a series of 5 reflections. The receiver integrates these 5 pulses to form the sample for that range.

It should be noted that there are two distinct advantages in this method of insonification, namely that the returned signal (ignoring for a moment the spreading loss) actually increases with range due to increasing overlap of the pulses and that the point of interest at greater ranges is illuminated from 5 different angles reducing the possibility of missing

specular reflectors. Combined with the increasing gain of the reciever array due to the growing number of active elements the dynamic range requirements of the receiver are eased and the slope of the time varying gain profile is reduced.

7.3 Transmitter hardware

7.3.1 Sequencer

The block diagram of the transmit sequencer is shown in fig. 7.5 . The transmit trigger is preceded by the T/R pulse which closes the relays connecting the drivers to the elements and turns on the oscillator, allowing it time to settle to its design frequency of 308 kHz. On reception of the TX trigger from the controller this board selectively drives the power amplifiers with short bursts of 7 cycles of 308 kHz as described above, with interleaving dead times of 9,7 μs to prevent spatial overlap and interference. Upon completion of this transmission sequence the relays used for T/R switching are returned to the receive position and the sequencer is reset.

7.3.2 Power drivers

The power amplifiers are VMOS class C drivers capable of delivering a 22 A pulse from a 400 V source. Since the duty cycle is so low the average current

drawn is in the order of 25 mA. The high current is provided by a storage capacitor. The maximum pulse energy required is around 15 mJ and is adequately stored in a 1 μF capacitor. To achieve high turnoff times with the VMOS it is necessary to pull the gate down hard to ground with a small resistor. The current required to raise the gate to the appropriate turn-on voltage is thus large and the 5 V logic input levels are amplified in a three stage preamplifier.

A photograph of the sequencer and power driver is shown in fig. 7.6. The circuit diagram appears in appendix V.

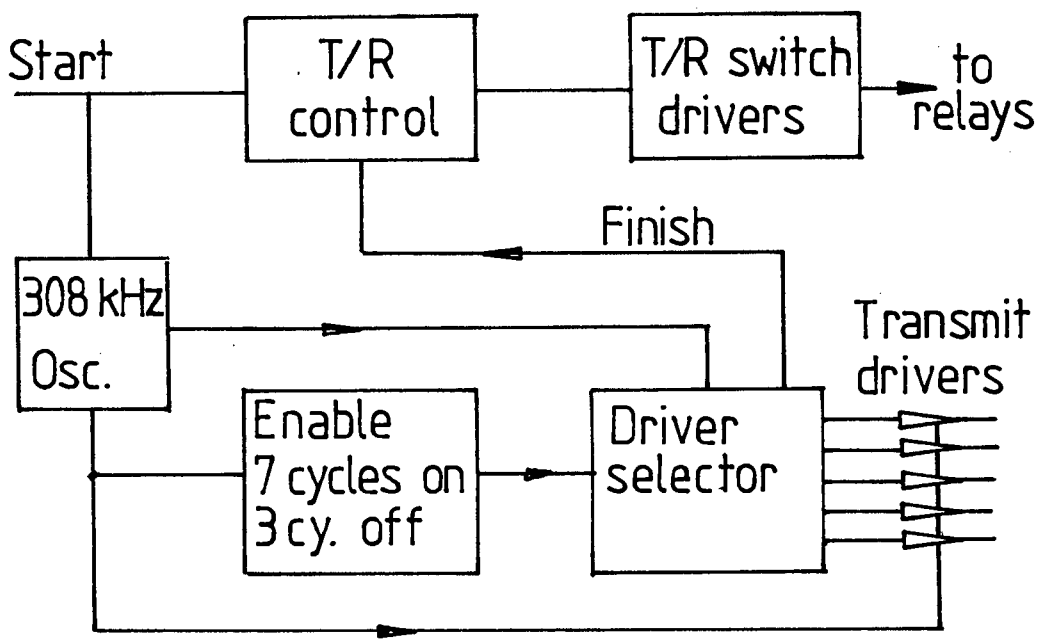

Fig. 7.5: Block diagram of transmitter

Fig. 7.6: Photograph of transmit sequencer and driver

PREAMPLIFIERS

8.1 Introduction

The preamplifiers are conveniently divided into four subsections; a tuned amplifier up front, a high impedance buffer, a digitally controlled attenuator and a line driver. A block diagram is shown in fig. 8.1.

8.2 Input stage

A reasonably low noise high gain tuned amplifier is constructed around an integrated wideband amplifier with a differential input stage. The differential input is driven by a transformer whose primary is tuned to 308 kHz with the combined capacitance of the transducer element and a separate tuning capacitor. The differential input can handle a 5 V difference voltage without sustaining damage. The input is protected from the transmit pulse by a series resistor and a pair of clipping diodes. The series resistance degrades the signal to noise ratio and must be kept small. Due to the large transmitter voltages applied and the step up ratio of the input transformer (used to adjust the source impedance so as to achieve optimum noise performance) the current through the diodes is substantial enough to generate 5 V forward drops. The major effect of this is to drive the amplifier into saturation from which it has ample time (approximately

13 ms) to recover before reception begins.

8.2.1 Transducer matching

The circle diagrams of the elements are plotted to determine the equivalent circuit parameters. The equivalent circuit is shown in fig. 8.2. Figure 8.3 shows that of element 10, annotated in detail, the measured values are typical and are used in the calculations. Figure 8.4 is a plot of the circle diagrams of all ten elements for comparison. The data in table 8.1 are the measured resonant frequencies.

Element no.	Resonant Freq. (kHz)
1	311,6
2	311,9
3	311,7
4	311,0
5	310,9
6	308,9
7	305,9
8	309,4
9	310,0
10	308,6

Table 8.1 Resonant frequencies of elements

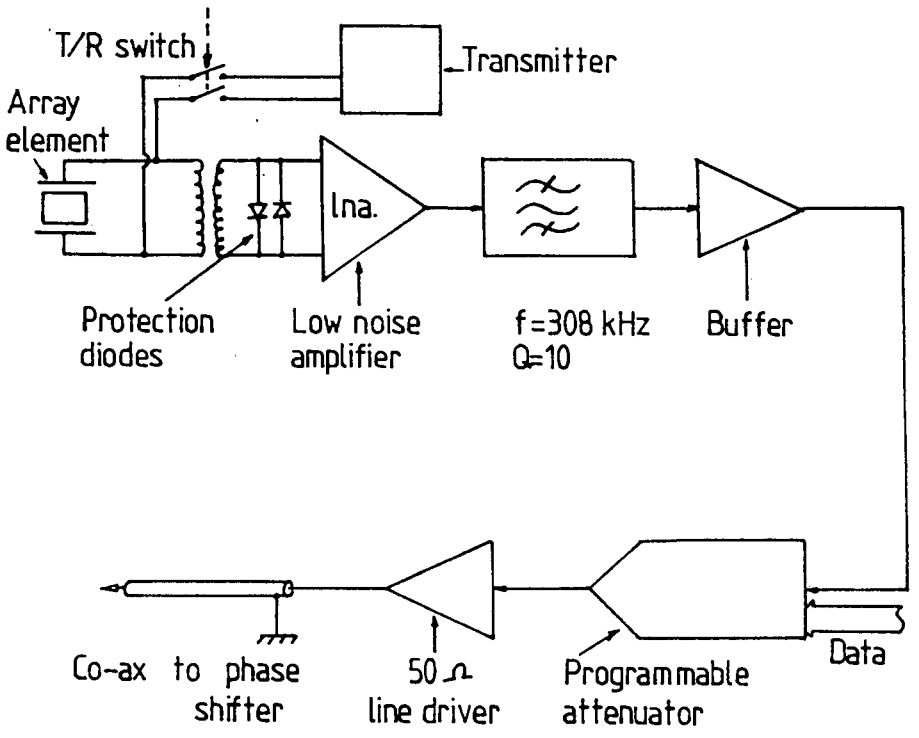

Fig. 8.1: Block diagram of preamplifier

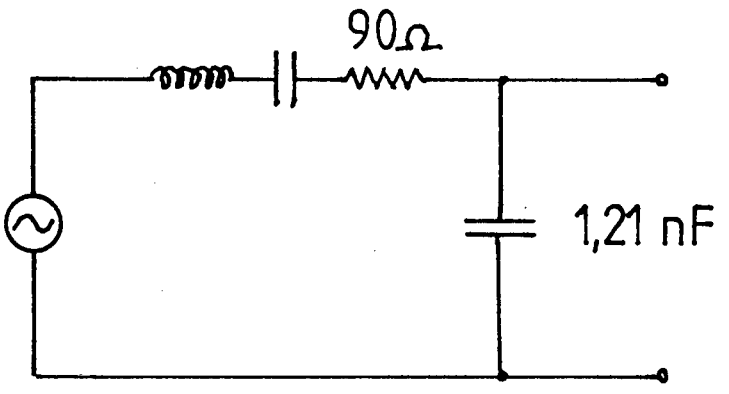

Fig. 8.2: Equivalent circuit of transducer

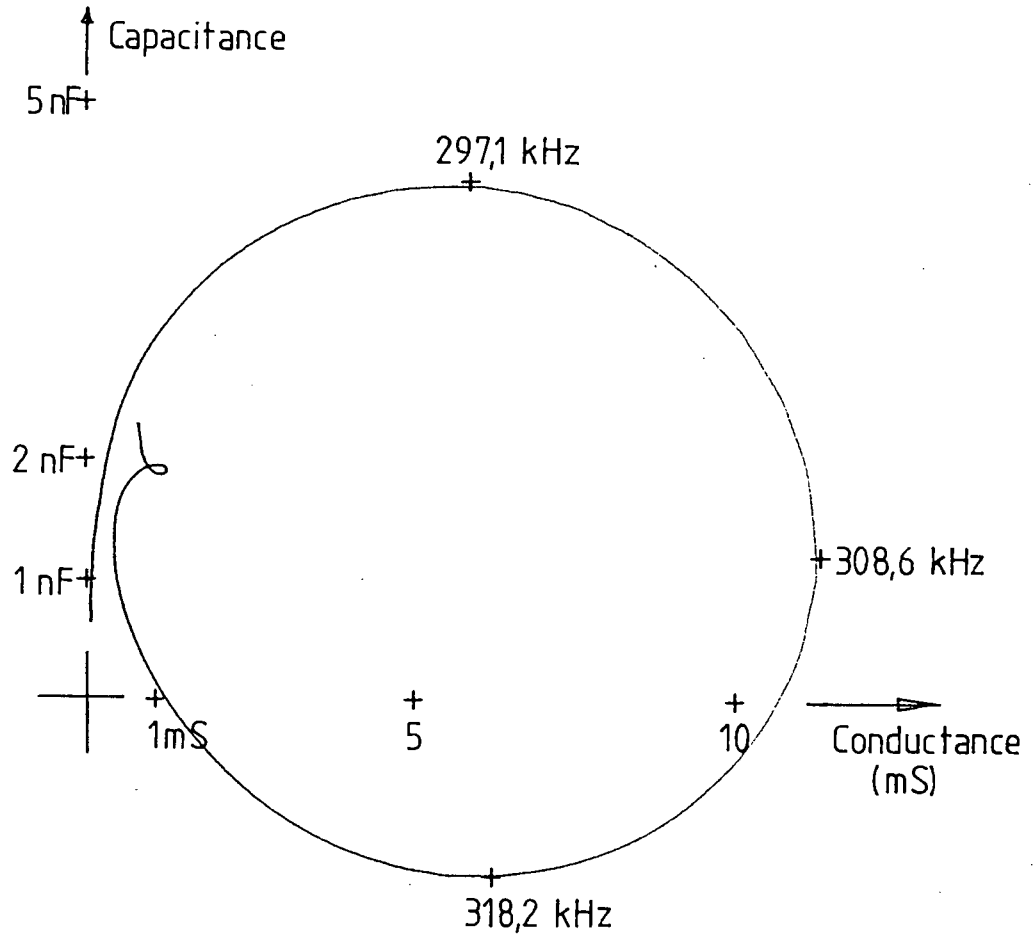

Fig. 8.3: Circle diagram of element 10

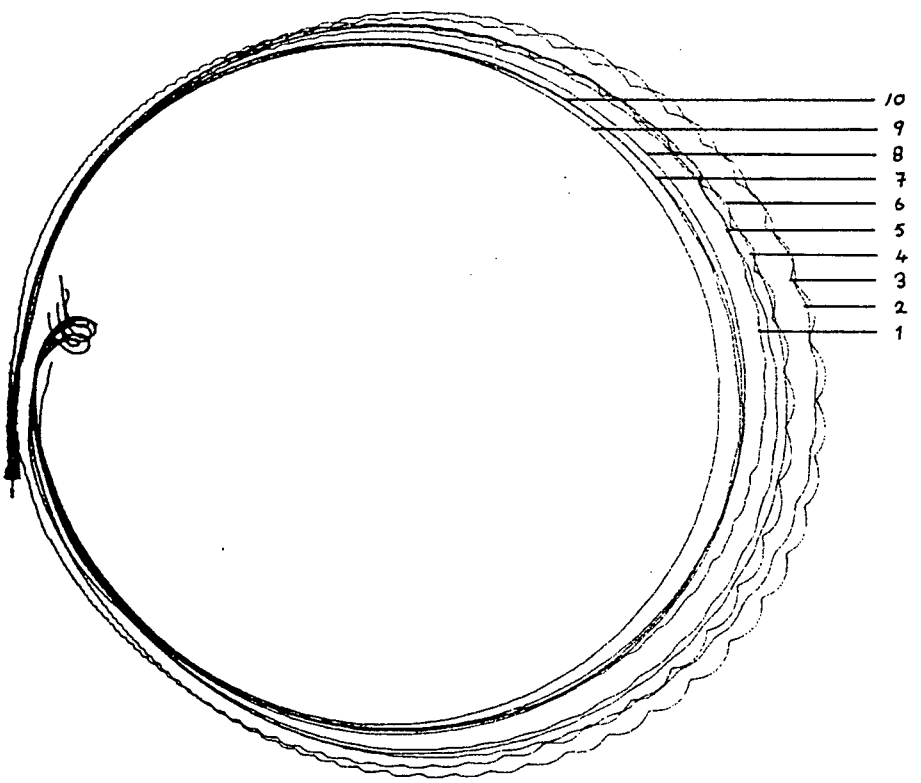

Fig. 8.4: Circle diagrams of all 10 elements

At 308 kHz the radiation resistance is 90Ω and the apparent parallel capacitance if found to be 1,21 nF. The bandwidth is 21 kHz, a fractional bandwidth of 7% (or a Q of 14,7). When the transducer is tuned with 681 μH the damping factor is found to be 0,06. This is severely underdamped; a damping factor of 0,6 would be more suitable. This can be achieved with an additional parallel capacitance of 120 nF. The resulting bandwidth of 17,5 kHz is quite acceptable.

8.2.2 Front end tuning

The output of the integrated amplifier is tuned with a Q of approximately 10 with an adjustable resonant circuit allowing matching of the phases of the ten amplifiers. Loading of the output tuning is prevented by a high input impedance buffer providing an additional 20 dB of gain and allowing a voltage swing of 20 V. The output of the integrated amplifier can only swing 2 V. Gain matching is achieved by adjusting the currents supplied to the AGC control inputs.

Normal AGC is not applied in the front end due to the difficulty of manufacturing AGC amplifiers which track in amplitude and phase. Following the buffer is an 8 bit digitally controlled attenuator providing almost 50 db of presettable reciever gain adjustment over all ten preamplifiers without affecting the relative phase. This circuit is provided with a view to using a standard cable to tow the array. In such a

cable normally there are not the reqired ten coaxial cores to relay the ten signals to the beamformer. Time or frequency multiplexing can be used to relay all the signals over the available cores. Both these techniques have a limited dynamic range over which phase coherence can be maintained, and the signals long term dynamic range should be compressed before sampling or mixing.

8.3 Line drivers

The lines between the preamplifiers and the phase shifters are 50Ω. The input impedance of five phase shifters in parallel is matched to this. Hybrid integrated current drivers capable of providing the 300 mA pulsed currents at the peaks of the returned signal are employed to drive the phase shifters. Due to the relatively short duration of large echoes from the closer ranges the average dissipation of these line drivers is small.

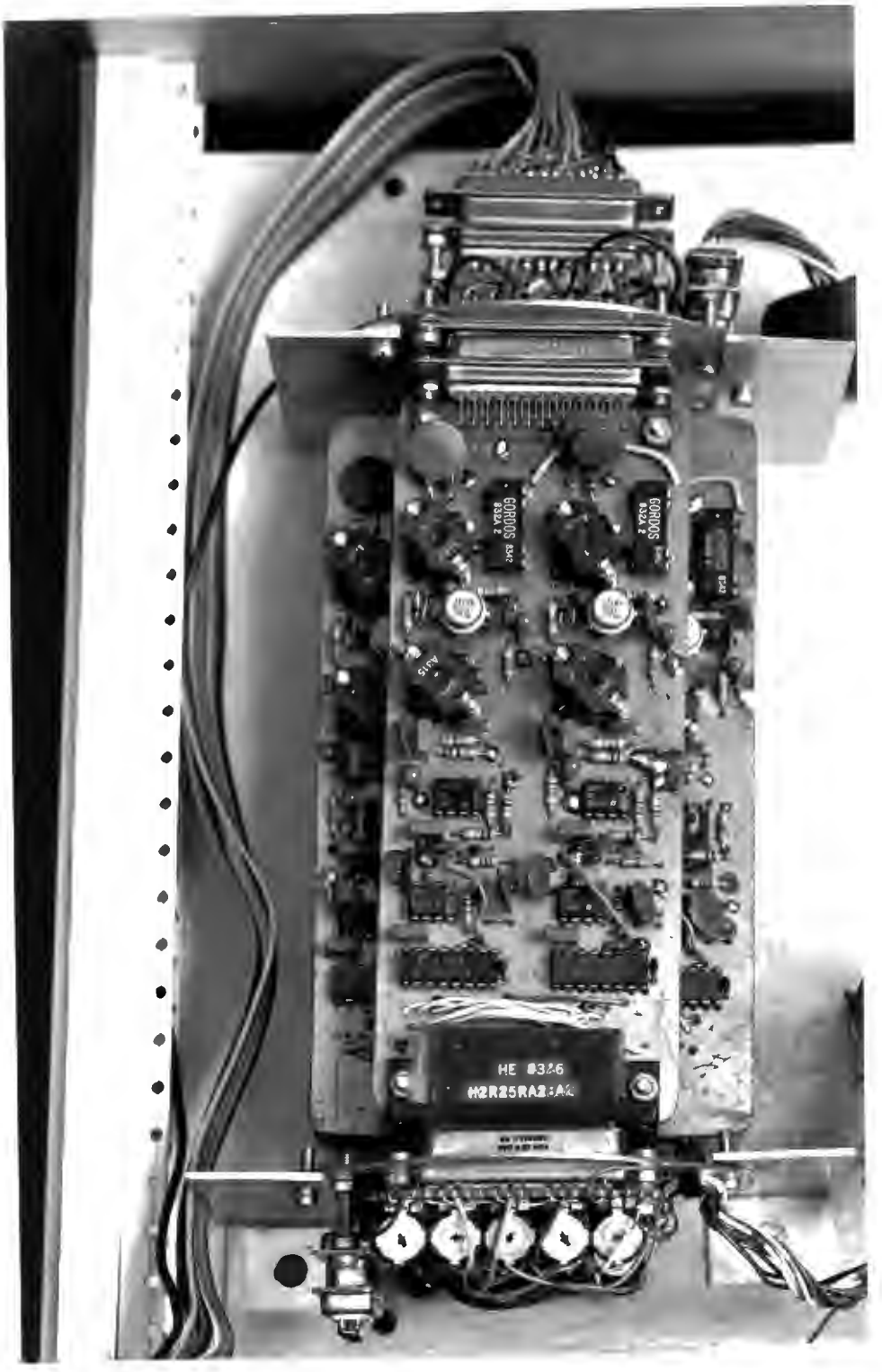

Fig. 8.5: Photograph of preamplifiers

TIMING AND OUTPUT

9.1 Introduction

The functions of data output and system timing are integrated in one subsystem since they are so interactive. Overall system synchronization is provided by the chart recorder. Within each sweep of the chart recorder a single swath is output, after 5 swaths a new transmit pulse is sent. This starts the real time range sampling clock.

This subsystem was developed in parallel with the system software; moving time consuming tasks from software to hardware until the routines are efficient enough to be executed in the available time. This method of reducing software execution time is more advantageous than any method involving the beam forming system. There is only one timing board while there are fifty phase shifters. As a result of the special hardware in this subsystem the task of data output is fully orchestrated here, with only infrequent requests for more data from the microprocessor. These requests are only serviced when higher priority tasks have been completed, not on demand. The timing and output board has been designed to have sufficient patience to wait.

9.2 Overall timing

9.2.1 Parallel to serial swath conversion

The simultaneous formation of multiple beams in a system whose output device is a chart recorder presents some unusual formatting problems. The chart recorder can only record one swath at a time, while the data is entering the system in the form of five parallel swaths. Within each pulse repetition interval there are five swaths to be sent to the recorder. Whereas each range sampling interval acquires five samples simultaneously, these samples must be sent out serially, equally spaced within the range sampling interval.

The problem becomes manifest with the first range cell. The data captured is the first pixel of each of the five swaths. The data which must be sent to the chart recorder before the next range cell are the first five pixels of swath 1; and these are not available yet.

The problem may be circumvented by storing the swath records in temporary storage and fetching them when the records are complete. While one set of swaths is acquired the previous set is sent to the chart recorder. There is thus a brief delay of 0,2 s between data capture and presentation.

9.2.2 Range sampling

Shown at the top of fig. 9.1 are the 'start of line' pulses from the chart recorder. At the maximum towing speed the chart recorder is set to record a new line every 40 ms (1/5 th of the pulse repetition period). On every fifth line a new data acquisition sequence is initiated by activating the transmitter and starting the process of range sampling. The pulse train orchestrating this is derived by dividing the 'start of line' pulse train by 5; it is shown in the second trace of fig. 9.1.

From this point on data input and output proceed asynchronously, the former being timed by a real time clock while the latter is synchronized to the chart recorder.

The third trace in fig. 9.1 shows the data acquisition timing. Having received a transmit pulse request the timing board generates a delay of 13,3 ms before starting to issue range sampling requests. This delay allows the transmitted pulse to propagate to a range of 10 m and back. After this initial delay a range sample request is issued every 182,3 μs causing the controller to sample the amplitude of each beam, convert the sampled analog signal to a digital equivalent and store the five values in a memory location in the appropriate location in the temporary storage. The range sampling interval of 182,3 μs corresponds to a total of 1024 range cells in the

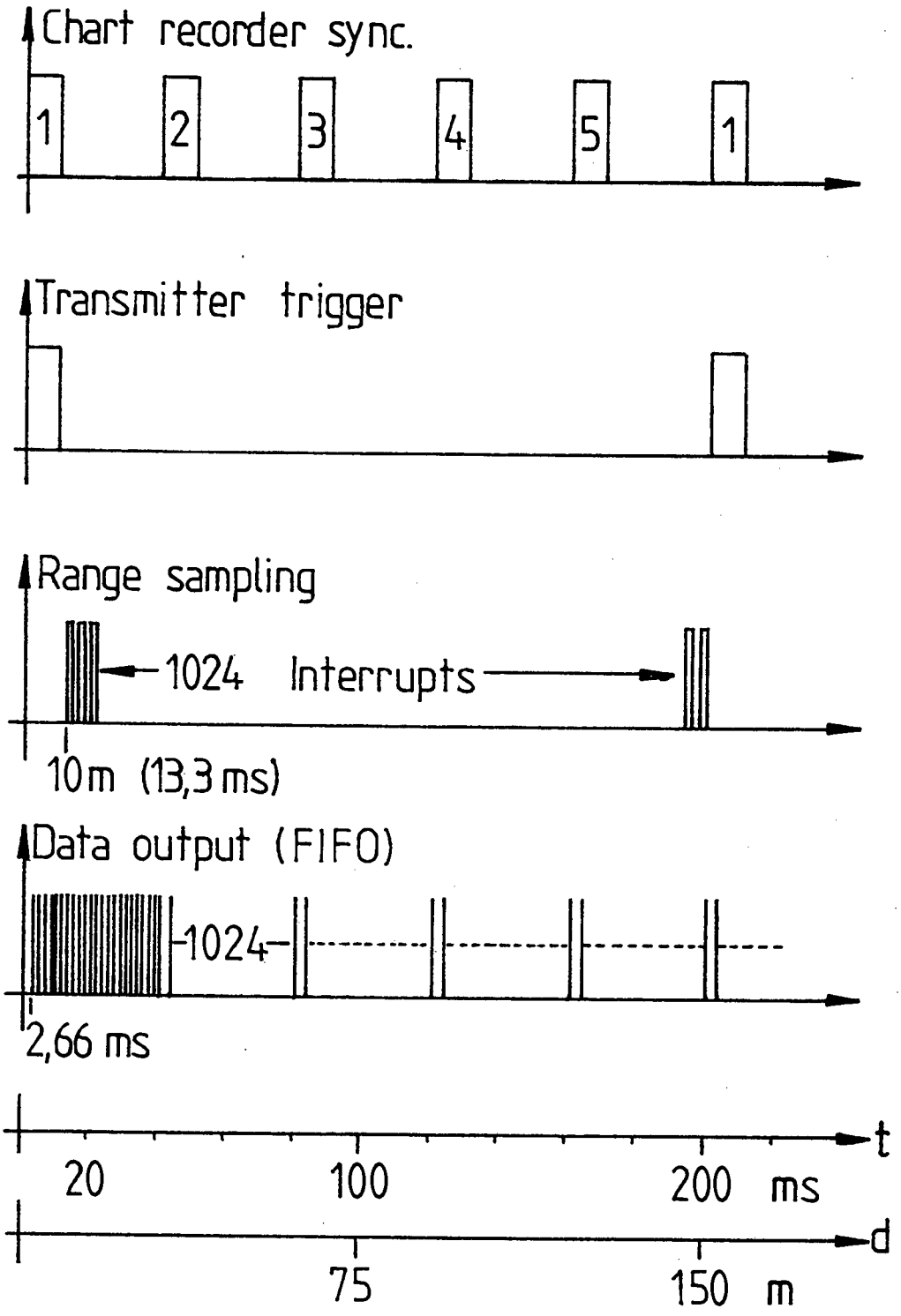

Fig. 9.1: System timing diagrams

operating range of 140 m stretching from 10 m to 150 m. The initial delay of 13,3 ms corresponds to a delay in terms of range cells of 73 cells.

9.2.3 Data output timing

Each swath is presented to the chart recorder as if it were coming from a conventional single beam sonar. After the start of swath pulse there is a delay corresponding to the round trip delay at 10 m range before data appears. The output timing pulse train is shown in the lower trace of fig. 9.1. The 13,3 ms delay before range sampling has been equally divided between the swaths, resulting in an initial delay of 2,66 ms.

This initial delay remains constant, even if the chart recorder is slowed down to allow a lower towing speed. The chart recorder is set to produce a pulse for every 20 cm of forward motion of the platform. In this way the 1 m wide sets of swaths are made to lie side by side with no gaps or overlaps. If the towing speed is halved the pulse repetition interval must be doubled, by adjusting the chart recorder.

When operating at the maximum towing speed it is essential that the data output rate is the same as the input rate. The range sampling that takes place every 182,3 μs results in the storage of 5 pixels. To maintain the same rates of data input and output the

pixels must be transferred to the chart recorder at the rate of 5 pixels every 182,3 μs or 1 pixel every 36,46 μs. This results in a time compression of the swath record as is clearly shown in fig. 9.2 where the input data (a logarithmically compressed triangle waveform) is shown along with the output from beam 1 (the upper trace). Figure 9.3 shows the situation for beam 2.

If the controller had to service the output data requests every 36 μs there would be little processing time available for anything else. This is especially true in an interrupt driven asynchronous environment. Each serviced request involves a number of program jumps and the storage of the current status. To reduce the frequency of requests (and the processing overhead of the interrupt vectoring) storage of output data is provided on the output and timing board in the form of a First In First Out (FIFO) buffer.

9.3 Timing and output hardware

The block diagram is shown in fig. 9.4. It includes a crystal controlled master clock running at a frequency of 9,837 MHz and divided by 360 to generate the required fundamental period of 36,46 μs. This clock is applied to three programmable timers to generate the timing signals.

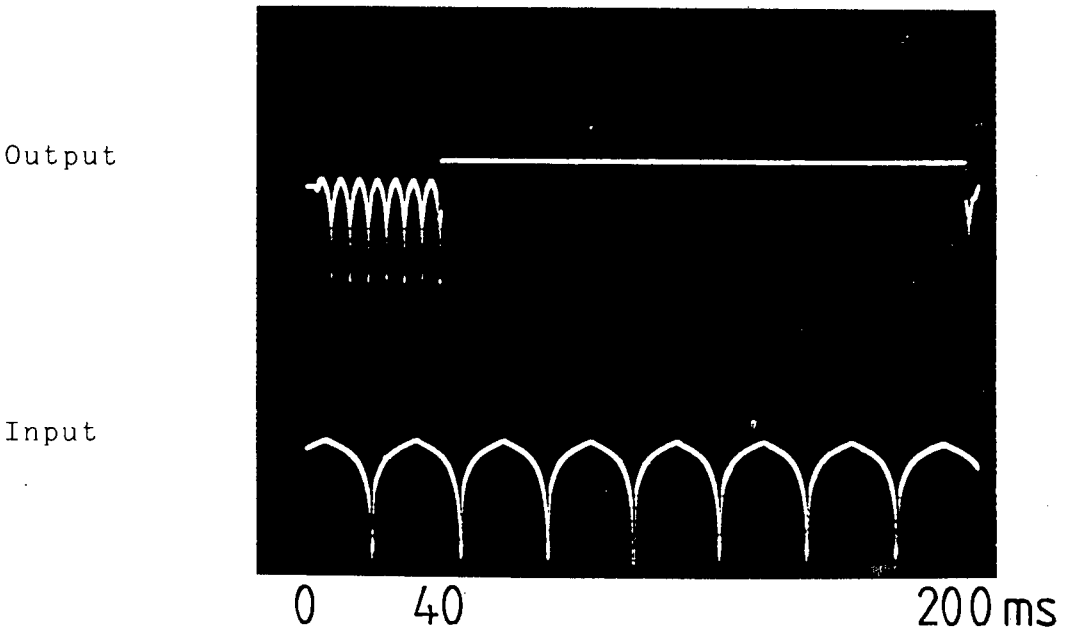

Fig. 9.2: Measured timing, beam no. 1

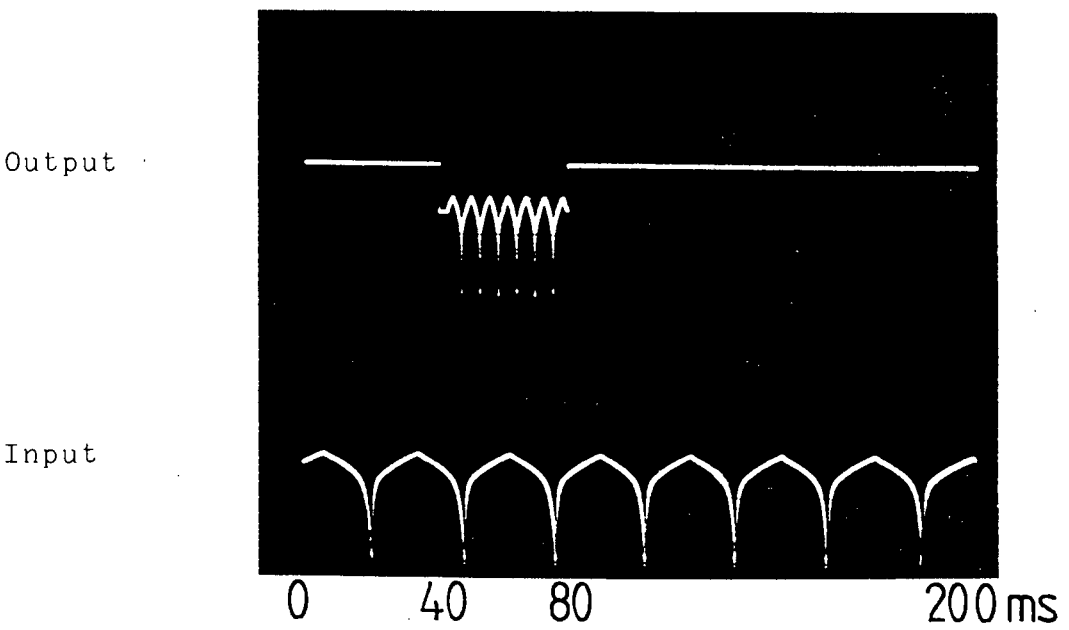

Fig. 9.3: Measured timing, beam no. 2

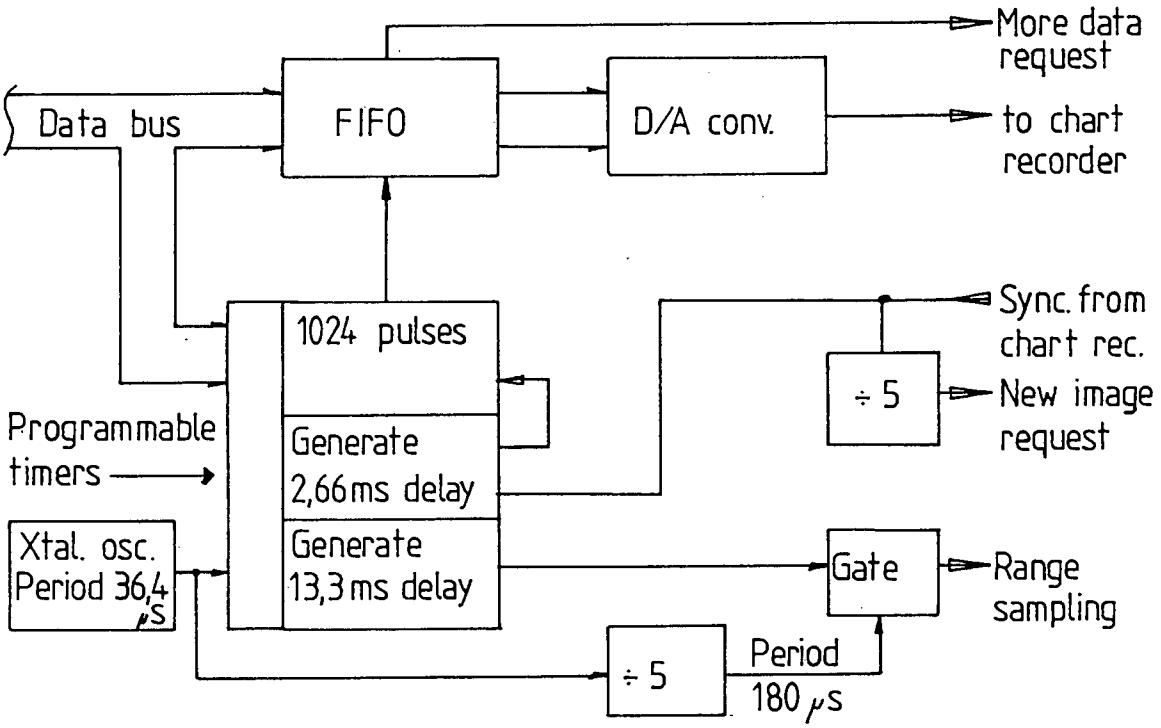

Fig. 9.4: Block diagram of timing board

The range sampling is derived by dividing the basic period by 5 to generate the range sampling interval. After 73 range cells (10 m range) a gate is opened allowing range sampling interrupts to be sent to the controller. Further range cell counting is performed in software where the count is used to determine the appropriate destination of incoming data and the storage location of the phases for the next focal zone.

Two of the programmable timers are used to generate the 1024 pulses required for the output of one swath. They are restarted with the 'start of line' signal from the chart recorder. These 1024 pulses are used to clock the data out of the FIFO buffer (which is preloaded with data from the previous swath).

The FIFO buffer has an internal flag which it raises when it is almost empty. When the controller recieves this request, in the form of an interrupt, a burst of 20 pixels is sent to the FIFO. With this arrangement there is no need to maintain a software count of the number of pixels transferred. The data clocked into the FIFO in a burst is clocked out at the regular rate of one pixel every 36,46 μs to a digital to analog converter and thence to the recorder.

A photograph of the output and timing board is shown in fig. 9.5.

Fig. 9.5: Photograph of timing board

MICROPROCESSOR

10.1 Introduction

The Intel 8085 microprocessor executes three routines (apart from the initialization etc.) in the process of beam forming. The primary (and most time consuming) is the transfer of focus, steer and gain data from ROM to the phase shifters. The other two functions - range sampling and data output - are initiated on demand since they have to be executed at specific times. The routines are described in detail along with the memory and I/O mapping and the programming rationale. Special programming techniques are required to achieve rapid execution times. The source code was written using a word processing program on an HP-86 P.C. Object code was then generated using a two pass cross assembler written in BASIC for this purpose. Although a macro facility was not included the copy function of the word processor proved to be very useful in writing the phase setting routine, which should, correctly, have been written using macros. As can be seen from the record of the CPU time (2047 s) at the end of the listing the cross assembler was not fast, but it was convenient.

The description of a program which has been written, not for elegance but for speed, is necessarily somewhat convoluted. All the rules of structured

programming have been broken. A change in one line would render all the subroutines inoperable due to the extensive parameter passing and altering. The main routine is exited via a subroutine call from which it never returns; the stack is merely restored and the system waits for the next transmit pulse.

The source code (appendix IV) has been comprehensively commented and, if read in conjunction with this chapter, should be fairly easy to follow. Where a pair of numbers separated by a colon appear in the text a specific reference is made to a particular page and line number in the listing.

10.2 Program overview

The phases required for forming the five focused beams are stored in memory. The microprocessor retrieves a set of phases and transfers them simultaneously to the phase shifters at the start of each new focal zone. There are 50 phases to be set for each focal zone thus each refocus involves the transfer of 50 pairs of coefficients. Each focal zone in turn is divided into 16 range cells. (The reason for the base 2 numbers is that binary arithmetic is faster than decimal arithmetic on the 8085).

The duration of each focal zone may be considered to be the basic time unit in the software execution. Since the two way propagation time is 186,7 ms (between

the ranges of 10 m and 150 m) the duration of a focal zone is 1/64 th of this, or 2,92 ms. During this time the microprocessor must be capable of selecting the appropriate set of phases and transferring these to the phase shifters while being interrupted 16 times to aquire and store the 80 range samples (16 samples per focal zone from each of five beams). It must also reformat the previous image, converting the parallel data to serial, and service requests for data from the output board. Since the output of data takes place at the same time as the input there are on average 80 range samples to be presented for output on request. The housekeeping in all three of these routines involves keeping track of the range cell number and the focal zone number and using these to determine the appropriate storage locations of the phase coefficients, the input data and the output data.

Clearly this is a lot of processing to be performed in 2,92 ms for a microprocessor which takes well over a microsecond to execute a single instruction. The design of the microprocessor software involved the development of the various routines and the determination of their respective execution times by counting the number of processor cycles in each routine. The routines and their interactions with each other were then optimised to take the least possible time. A small fraction of the available 2,92 ms left over after all the tasks had been completed allowed some small changes to improve the modularity and ease

of testing of the routines.

10.3 Software Description

The software is described by dividing it into the partially seperable subroutines and referring to the the pertinent flow charts and the page/line number references.

10.3.1 Main routine

The flow chart of the main routine is shown in fig. 10.1. After the basic initialization required for an image a loop is entered in which phases are set up and interupts are serviced (2:16 to 5:50).

10.3.1.1 Time varying gain

The time varying gain is implemented by transferring a single gain byte from an appropriate location in ROM to programmable amplifiers on board the beam formers. The gain is adjusted with each new focal zone; there are thus 64 gain coefficients to be found in ROM starting with location GSET. Rather than a direct transfer of this data from ROM to the gain control amplifier it is first transfered to a temporary storage in RAM, starting at location GAIN (1:31). Later, when each new set of phases is applied (7:2) the appropriate byte is taken from here and sent to the TVG amplifiers.

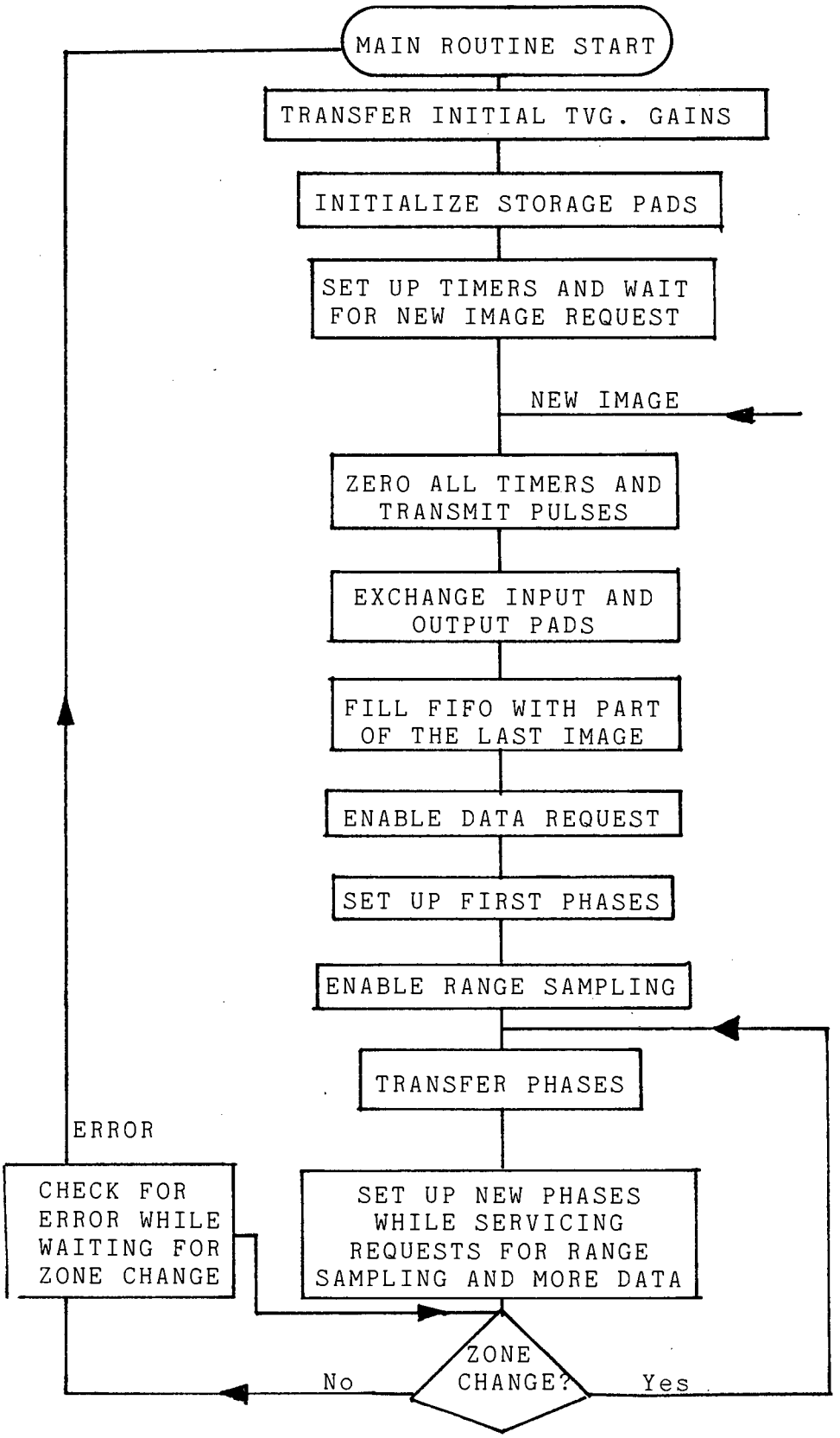

Fig. 10.1: Flow chart of Main Routine

The reason for this method of transfer is that it anticipates future system improvements and allows an adaptive TVG to be implemented using data from previous swath records and a simple digital filter routine with little change to the software. There is ample time available for such a routine in the 13,4 ms between the transmission of a pulse and the start of range sampling and phase adjusment.

10.3.1.2 Time keeping setup

During the initialization procedure (2:20) three timers are set. Their functions are described in greater detail in the section on output and timing but, for completeness a brief description follows. The first counter is the pixel count. It is preloaded with 1024, the number of pixels in a swath. When the imaging of a set of swaths is complete this counter sends a pulse to the transmit sequencing board in the fish to indicate to it that there are no further input samples to be taken and the array elements can thus be switched over to the transmit position. The reason for this timing arrangement is to allow the T/R switches (relays) time to settle.

Having completed the initialisation the processor waits for a signal from the timing board to indicate that the chart recorder is ready for a new swath and thus a new image can be initiated (2:47). This is also the reentry point for the software after one full image cycle has been completed.

10.3.1.3 Dynamic memory allocation

On receiving the start of swath indication from the timing board the transmitter is triggered and all timers are reset. Incoming and outgoing range samples are routed to dynamically allocated memory locations to permit coversion from parallel to serial format.

There are two RAM storage blocks for images. They are referred to as pad "A" and pad "B" with base addresses ABASE and BBASE. While an image is being formed and written into one pad the other stores the last complete image, from which it is read and presented to the chart recorder. The situation is represented schematically in fig. 10.2.

The location in the input pad into which an incoming byte is written is pointed to by VRIN, a variable range marker for input data. The lowest value that VRIN can have is the base address of the current input pad, a variable with the label BASIN. Similarly, the output data is refered to by the variable VROUT, starting from the base address of the output data, BASOUT.

On entering the main program the input is allocated to pad "A" (2:20). The variable BASIN is thus made equal to ABASE. Similarly BASOUT is made equal to BBASE. The variable range pointers in the input and output pads, VRIN and VROUT, are initialized to BASIN and BASOUT respectively. At the end of the completed image the input and output pads are exchanged by simply

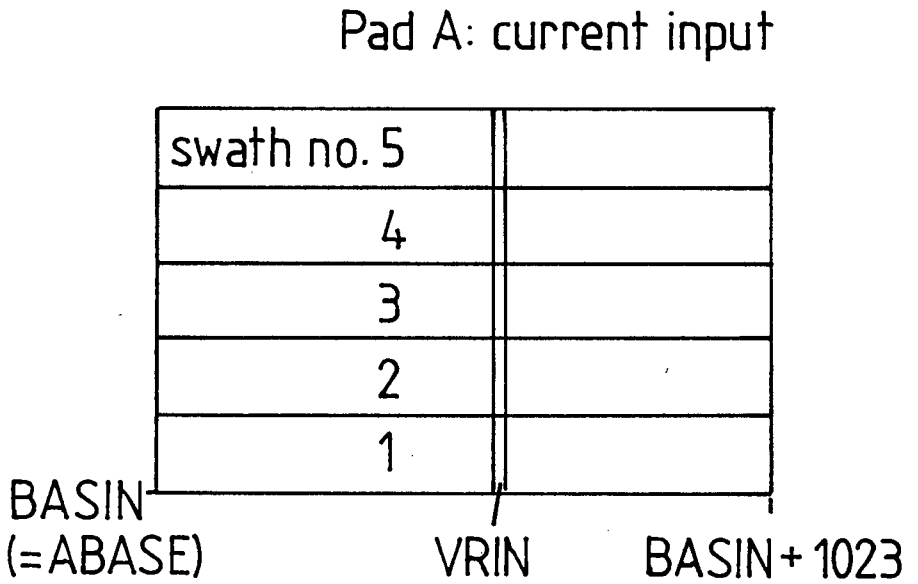

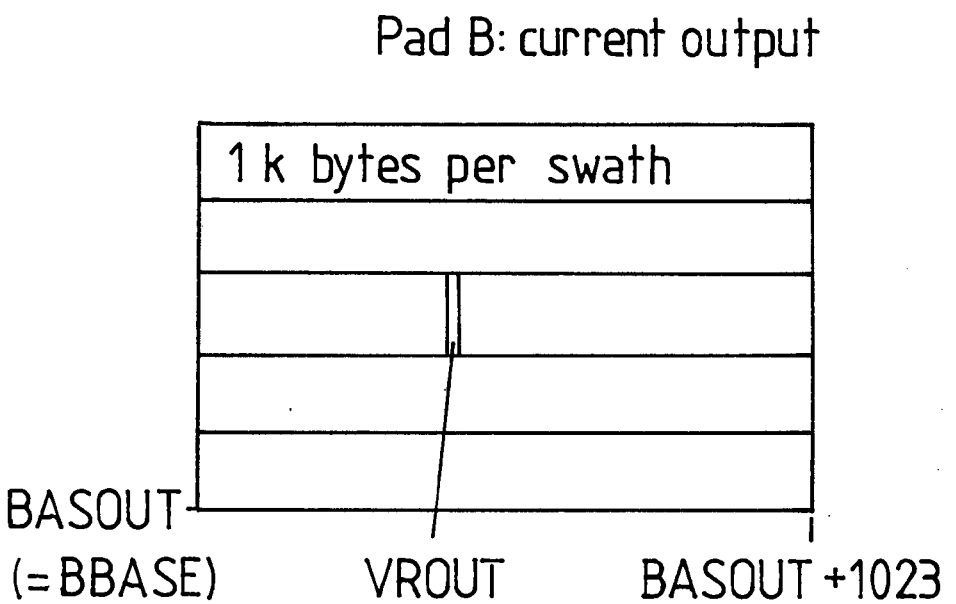

Fig. 10.2: Dynamic memory allocation

exchanging the values of the variables BASIN and BASOUT (3:7). Pad "A", previously the destination of the input data now becomes the source of the output data. The previous source of output data (pad "B"), no longer required, is overwritten by the new incoming data.

10.3.1.4 Initial output

As soon as the location of the output data has been determined data transfer begins (3:20). Since the 13,3 ms delay before range sampling starts is divided between the five swaths the start of data output occurs 2,66 ms after the start of a line on the chart recorder. Data is thus required for output before range sampling has begun. The FIFO buffer on the output board is filled with 32 bytes of data ready for output. Further data is supplied to the FIFO buffer only on request (7:27).

10.3.1.5 Initial phases

The phases for the first focal zone must be set up prior to range sampling. The coefficients are transferred from ROM to the the phase shifters and are immediately applied.

10.3.1.6 Beam forming loop

The program then enters the beam forming loop in which range sampling and data request interrupts are

serviced and the next group of phases are transferred to temporary latches on the double buffered multiplying A/D converters (5:33). A status word (STAT) is set non zero to indicate that this is a new group of phases, only to be applied after 16 range samples, when a new focal zone is entered. Should the processor complete the task of transferring the phases from ROM to temporary storage well before the last range sample in a particular focal zone it enters a loop and waits for the 16 th range cell before simultaneously changing the phases of all 50 phase shifters.

10.3.2 Phase setting

The phase setting routine is called at the beginning of each focal zone (9:8). As long as the required 100 bytes are transferred before the start of the next focal zone the exact timing of the transfer is unimportant. This routine may be interupted many times during its execution. On entry all interrupts are briefly disabled while the zone index is used to determine the ROM location of the base address (PHBASE) of the block of 100 bytes which constitute the focusing data for that focal zone. Having determined this pointer all interrupts are enabled and the rapid tranfer of phases begins.

A cursory scan of the microprocessor software listing in Appendex IV indicates that almost half the program consists of the transfer of phase data, a

repetitive process that is easy to describe as an algorithm. In order to avoid the time wasted in looping and updating loop variables the phase transfer is written as linear code. The flow chart of this routine is shown in fig. 10.3.

10.3.3 Range sampling

The range sampling routine has the highest priority of all tasks (6:1). It must be processed immediately upon request to maintain accurate range sampling. A flow chart is shown in fig. 10.4. The only possible interrupt request that may arise during the execution of this routine will be issued by the asynchronous output buffer (the FIFO) requesting more data. This request is not serviced during this routine to avoid the processing overhead of storing the many variables used and alterred by range sampling.

On entry the five bytes of pixel intensities are taken from the A/D converters and stored. The A/Dś are immediately retriggered and sample the new intensities. The incoming data is stored in memory locations spaced by 1024 bytes. Refering to fig. 10.2 the parallel storage format is evident. The processor is now finished with the image input, but there is housekeeping to be done. The range cell pointer (VRIN) is updated and, if it is a multiple of 16, the zone index (ZONE) is also updated (6:4).

On those occasions when the zone index changes, a

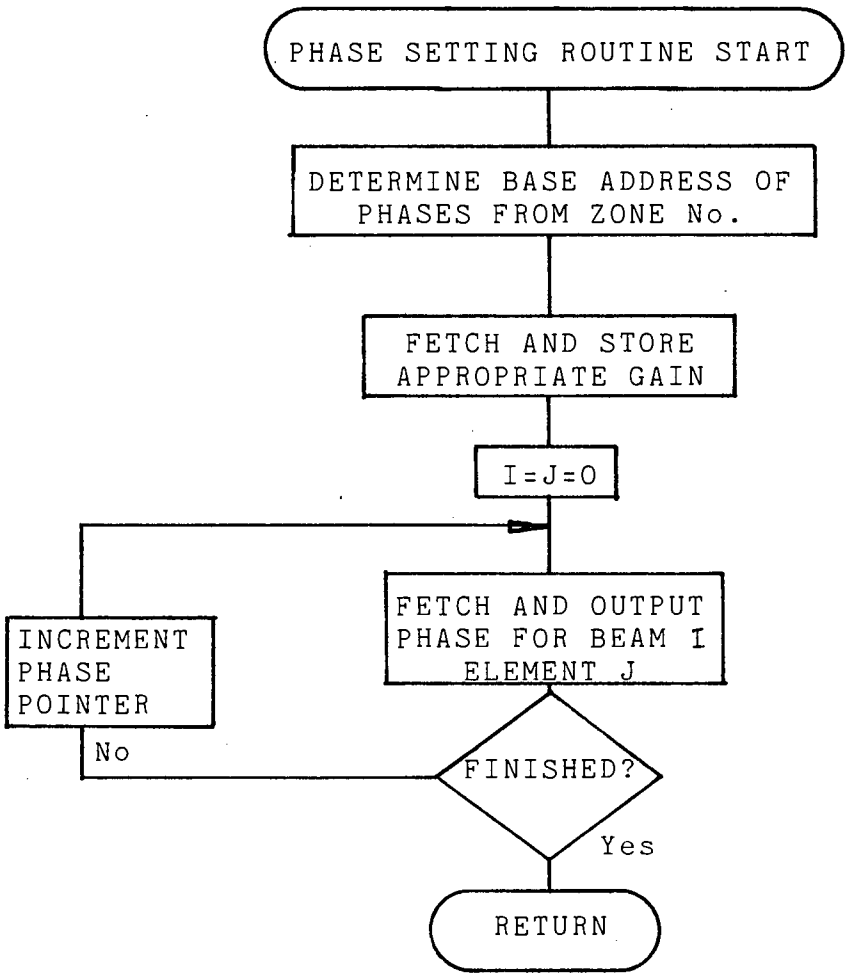

Fig. 10.3: Phase setting routine

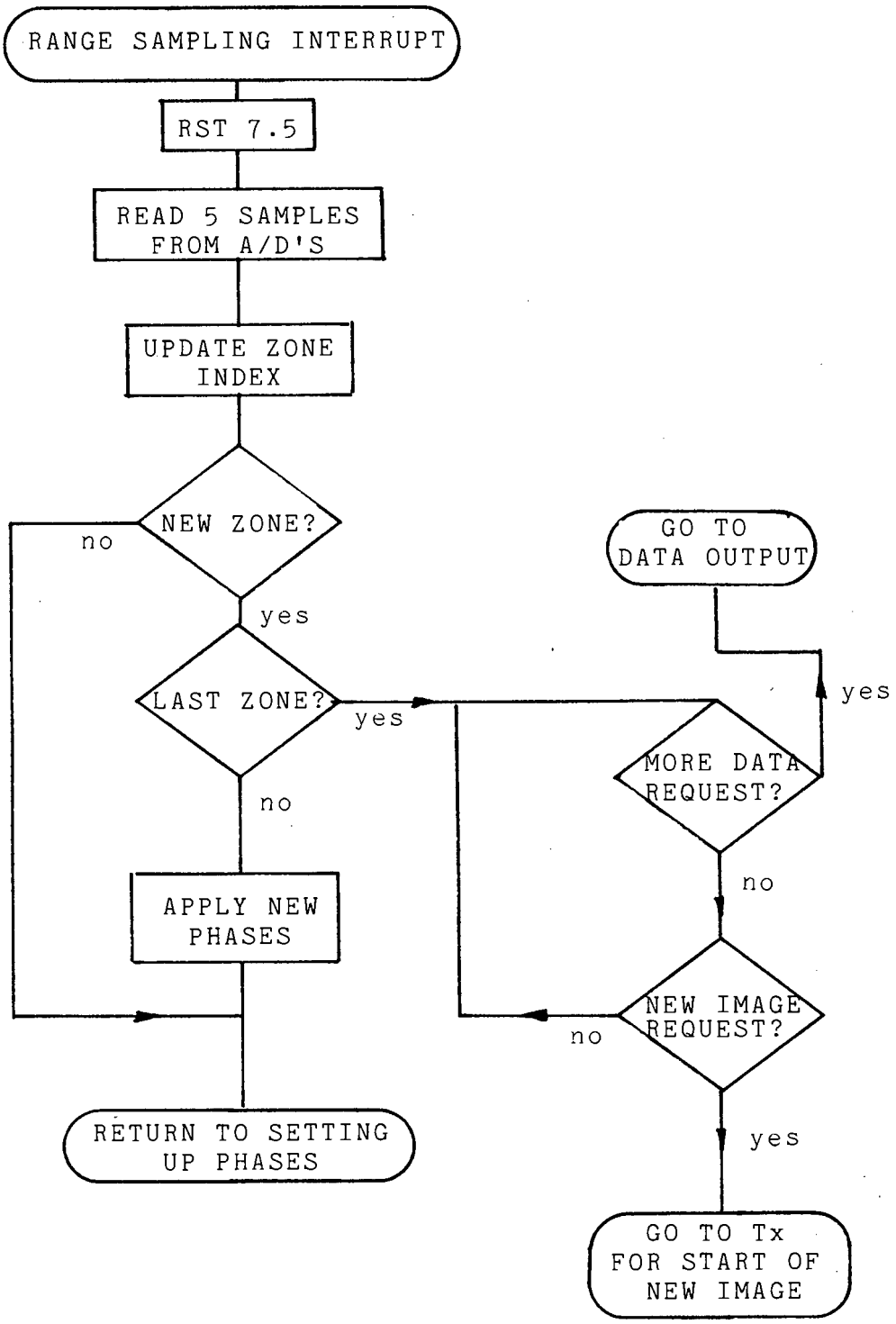

Fig. 10.4: Range sampling interrupt routine

refocusing is required. The 100 bytes waiting in the temporary latches are simultaneously transfered with a single command. The status word (STAT) used in the beam forming routine is set to zero to indicate that the phases have been applied and that the data transfer for the next focal zone can begin.

If the zone index is less than 64 the image is not complete and the processor returns to setting up phases and supplying output data after having restored all registers that were altered during the range sampling routine.

When the zone index reaches 64 the refocusing operation is complete. The last 16 range cells are sampled and image acquisition is finished. Range sampling interupts are now disabled. The output of data, on the other hand, may not be complete. If the towing speed is low and the chart recorder line speed has been decreased to prevent swath overlapping, there may be as many as 4 swaths waiting for output. The processor thus enters a loop servicing the data requests which may only be exited via a new image request from the timing board (7:15).

10.3.4 Data output

The signal from the chart recorder indicating the start of a new line is used to initiate a delay on the output and timing board. After this delay the range samples must be presented to the D/A converter for

output to the chart recorder at regular intervals corresponding to range cells. To process requests for more data at the range sampling intervals would place an unbearable demand on the processor, causing it to waste much time jumping back and forth between range sampling and data output.

For this reason the data output is buffered in a FIFO which can store 32 bytes. The FIFO requests more data whenever it has outputted 20 bytes. If the request is not immediately serviced there is ample data for a short wait. The reduction in the number of data requests is thus a factor of 20. The output routine must now transfer 20 bytes instead of 1, but the overhead of storing and restoring current status is also reduced by a factor of 20, and a significant time reduction is achieved.

The flow chart of the data request servicing routine (7:27) is shown in fig. 10.5. The routine also keeps track of the pointer in the output pad. A range sampling request may interrupt this routine, and the registers being used must be saved for later restoration.

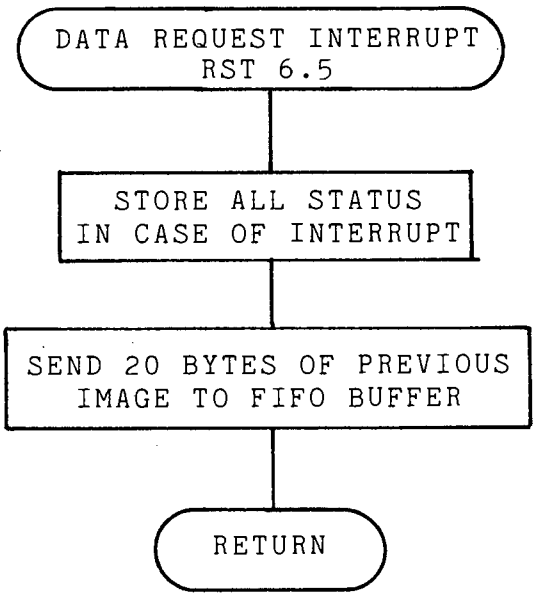

Fig. 10.5: Data request servicing

10.4 Memory map

10.4.1 Program memory

Both the program and the focus and steer information reside on a 16 k ROM card. The program starts at memory location 0 and is allocated 4 k of ROM. The rest of the ROM is reserved for data. The program at present occupies less than 1 k of the allocated space.

10.4.2 Preset data storage

The focusing and steering of the five beams requires the transfer of 100 bytes (two for each of fifty phase shifters) from ROM to the phase shifters each time a new focal zone is encountered. Since there are 64 focal zones there are 6400 bytes of this data. This data is stored in the upper part of the 4 k of ROM along with the initial gain estimates.

10.4.3 Random access memory

The RAM may conveniently be divided into four sections; these are two pads for the storage of the images (one for the current input, one for output), a scratch pad for variables (range indices, focal zone index etc.), and a block of 64 bytes of gain information (one gain setting for each focal zone).

Each image is composed of five swaths, each swath being represented in memory by a sequence of 1024 bytes (one per range cell). The completed image thus requires 5 k bytes of storage while that currently being formed will occupy 5 k bytes.

10.5 Address allocation

The assignment of memory space is shown in the table below. Memory locations are listed in hexadecimal.

	ADDRESS	LABEL	DESCRIPTION
ROM	0000	MCP	Master Control Program
	0800	PHSDAT	Phase/Focus Data
	2700	GSET	Table of initial gains
RAM	4000	ABASE	Base address image pad "A"
	5400	BBASE	Base address of image pad "B"
	6900	GAIN	Base address of gain table
	7EE0	GTEMP	Temporary storage of gain byte
	7EE1	VROUT	Variable pointer in output pad
	7EE3	VRIN	Variable pointer in input pad
	7EE5	ONE	Zone index
	7EE6	BASIN	Variable input pad base address
	7EE8	BASOUT	Variable output pad base address
	7EEA	STAT	Status word for phase transfer
	7EEB	INCHEC	Status word for range sampling
	7EEC	PHBASE	Variable address of focusing data
	7FFF	STCK	Top of stack

Table 10.1 : Memory allocation

10.6 Input/output ports

All the devices external to the microprocessor are addressed as I/O ports with addresses ranging from 00 hex to FF hex. A table of the ports, their function, and addresses is shown below.

	ADDRESS	FUNCTION
INPUTS:	28#	A/D. Beam 1
	29#	A/D. Beam 2
	2A#	A/D. Beam 3
	2B#	A/D. Beam 4
	2C#	A/D. Beam 5
OUTPUTS:		
	20# (-27#)	Gain setting
	2F#	Start A/D converters
	30#	Counter 0
	31#	Counter 1
	32#	Counter 2
	33#	Counter mode word
	34# (-37#)	Reset all timers
	38# (-3B#)	Send TX pulse
	3C# (-3F#)	Fifo load
	40# to 72#	Phase shifters SIN
	80# to B2#	Phase shifters COSINE
	E0# (-EF#)	Transfer phases

Table 10.2 : Input/output port mapping

A brief description of the functions of the various ports follows. Where addresses are shown with another address in parentheses preceeded by a dash it indicates that a valid address for that port is an optional parameter inclusive of the limits.

The input ports are the five A/D converters corresponding to the five beams. When the A/D converters are read by an input statement (e.g. IN 28#) they are reset and readied for the next start conversion instruction. The start conversion is issued immediately following a range sample interrupt and is effected with an output command (OUT 2F#).

Every fifth line on the chart recorder indicates that a new set of swaths is to be insonified and thus that the transmit sequence should be initiated. This is accomplished with an output instruction (OUT 38#).

The data request from the FIFO causes the output of the required number of bytes via the port 3C#.

During the imaging process the focusing phases are periodically updated. This is performed in the order; OUT 40# , OUT 80# , OUT 41# , OUT 81# and so on. This transfer is completed before the new phases are required and the processor then awaits the new focal zone indication, whereupon it performs a simultaneous phase transfer with the OUT E0# command.

10.7 Hardware

The system has been developed in a rack mounting frame. Six 19-inch racks are used; the upper five house groups of ten phase shifters each. The lower rack houses the beam formers and controller. By this arrangement the upper five racks may be driven by unidirectional bus buffers. Bus buffering is necessary

since the fan out of the Low Power Schottky is very much less than the fifty loads on the output bus. Each rack of phase shifters has its own bus driver; driven in turn by another buffer on the main bus in the lower rack.

The memory (RAM and ROM) cards were purchased off the shelf with the microprocessor card. A ROM based system monitor was installed during development to enable the testing of the subroutines. This monitor provided communication via a serial port from a terminal to the boards in the racks.

The signals on the rack mother boards are all digital. Analog signals are routed down the sides of the racks in 50 cables to the beam formers. Fig. 10.7 shows a photograph of the whole beam forming system.

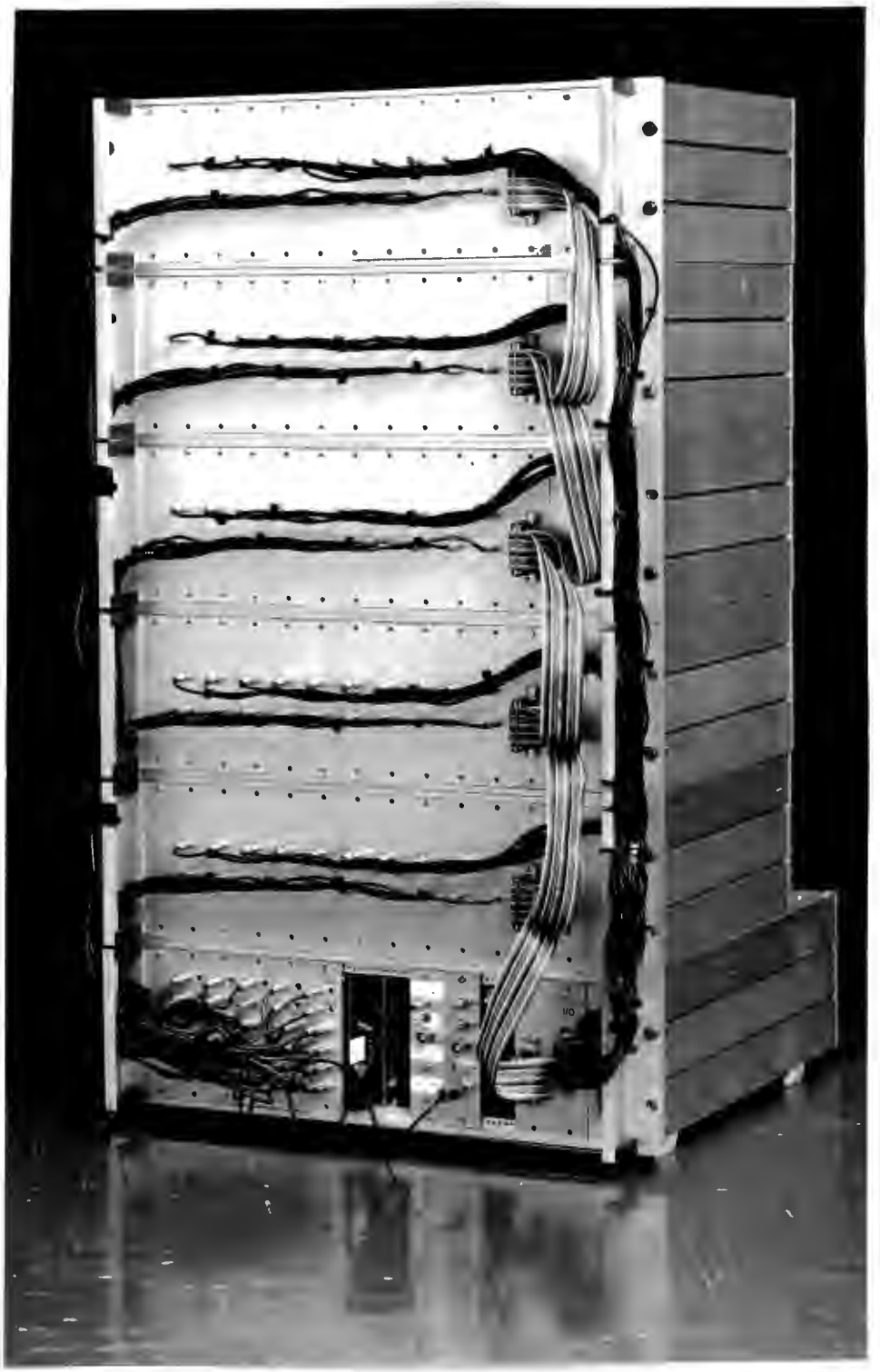

Fig. 10.7: Photograph of controller

RESULTS: BEAMWIDTHS AND SEA TRIALS

11.1 Introduction

Due to the complex system timing the measurement of beamforming performance is done in two ways. Measurements made in a tank using simulated echoes provide the most accurate method of assessing beamwidths; the results are in excellent agreement with the theoretical predictions. The maximum ranges at which beamwidths may be evaluated are limited by the tank length, although the correspondence of measured results and predictions will certainly not degrade with range.

The primary objective of the sea trials is to demonstrate that the system produces the desired resolution at a high image formation rate. The images produced, although not of good tonal quality, confirm the tank measurements of the resolution, while demonstrating the correct operation of the processes of insonification, beam forming and image reformatting.

11.2 Beamwidth measurement

Since the array processing is linear the directional discrimination (which determines the resolution) and the directivity response are essentially equivalent.

11.2.1 Experimental setup

The measurement of directivity is performed in a tank 20 m long. Depth and width are both 10 m. A small transmitting transducer is placed at various distances from the array, where it emits a short pulse at the appropriate time. The recieving array is mounted in a computer controlled rotator. The recieved signals are then extracted immediately after the summing amplifiers. This is the last linear stage in the beam former. The simulated echo is then digitized and the waveform samples are passed to a computer for the determination and plotting of the directivity response. The experimental setup is shown in fig. 11.1.

The signal emitted by the source transducer must occur at the correct time, so that when the wavefront arrives at the array the focusing and steering phases are correct for that range. This requires that the time of emission of the simulated echo be measured from the time at which a pulse would be transmitted if the system were operated normally, since the whole process of focusing begins with the transmission of a pulse.

The whole process must be orchestrated as if the overall timing were set by a chart recorder. The means by which this timing is derived are shown in fig. 11.2. The computer issues a command to the programmable waveform generator when it is ready for a measurement. The waveform generator then emits a

series of five pulses at 40 ms intervals; the intervals that would be generated by setting the chart recorder for maximum towing speed. The first pulse initiates the process of focusing and range sampling. The other four pulses are not of interest here, they merely serve to return the whole system to the known pre-transmit stage.

Between the first pulse and the transmission of the simulated echo a delay of one half the round trip time is inserted. After twice this delay the waveform recorder digitizes the received signals. In this way the returning signal appears at the same time as if it were a true echo. The range of interest is entered via the console and used to determine the delays, which are sent to the programmable delay lines.

The computer then reads the digitized waveform and converts it into the measured intensity sample. After this the computer steps the array through to the next measurement angle, and when all mechanical vibrations and oscillations have died out, the process begins again.

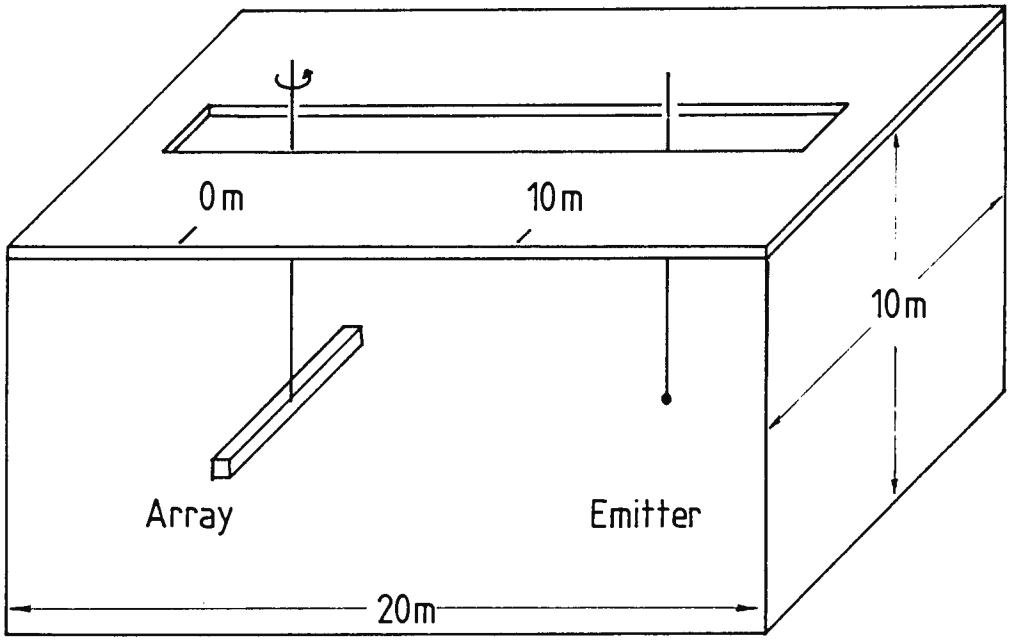

Fig. 11.1: Tank experimental set up

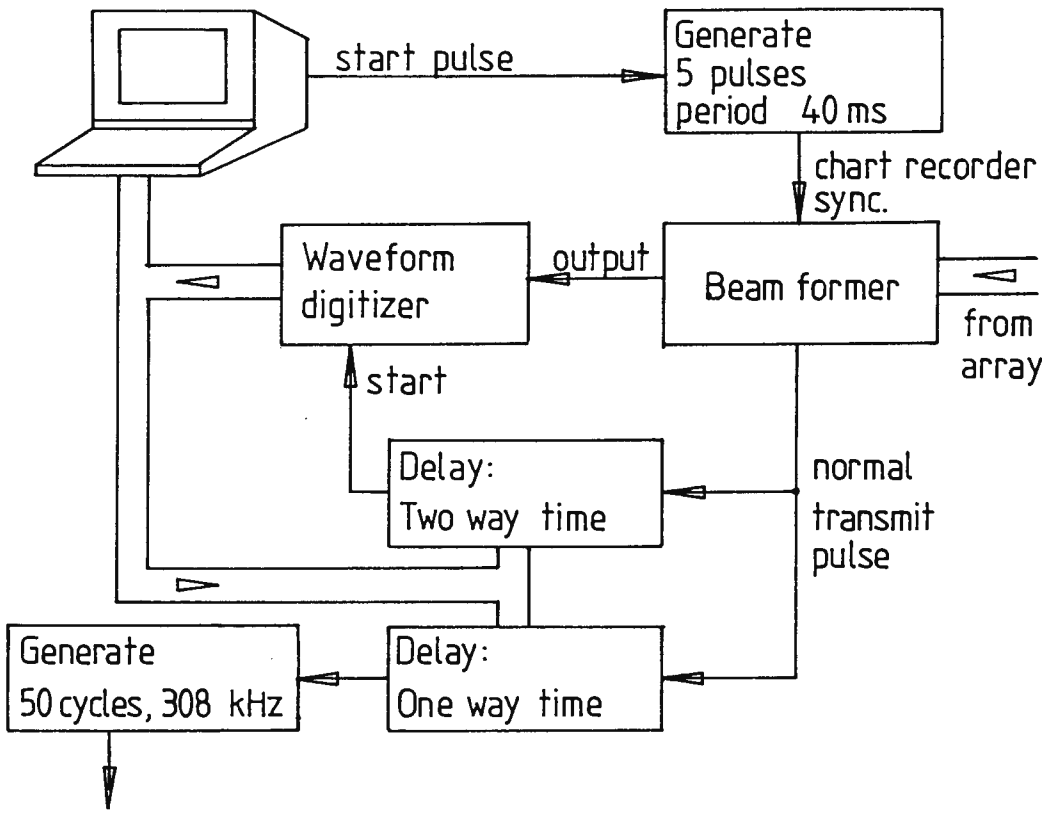

Fig. 11.2: Simulated echo timing system

11.2.2 Measurement accuracy

The major sources of inaccuracy are due to the array rotator. The array is mounted in a different position for each measurement. When the central beam is under examination the mounting is coincident with the axis of symmetry of the whole array. When any other beam is examined the array is mounted with the axis of the rotator through the axis of symmetry of that subarray. This is done to restrict the translation of the phase centre of the subarray while it is being rotated, and the effect is rendered negligible.

Angular position inaccuracies are more important. These are due to the limited step size of 0,4° and the mechanical backlash in the gearbox. Backlash is reduced to very small levels by rotating in one direction only. The step size of 0,4° is a bit larger than might be desired.

At 10 m range a resolution of 20 cm reqires a beamwidth of 1,146°. The measurement setup thus limits the number of samples to less than 3 on the main lobe width. The beamwidth at 10 m range predicted with the computer model is closer to 16 cm (see fig. 4.4).

11.3 Beamwidths

Notwithstanding the limited sampling interval the results are in close accordance with predictions. Fig 11.3 shows the directivity response of beam number 1 at 10 m range. (Beam numbering is from the trailing end of the array). Angular calibration marks at 0.5° increments have been plotted on the scale in the vicinity of the main lobe.

A conservative estimate of the -3 dB beamwidth is 1°. This corresponds to a spatial beamwidth of 17,45 cm, to be compared to the predicted value of 16 cm. More striking is the sidelobe structure. It is unsymmetrical due to the array steering as discussed earlier.

Comparing fig. 11.3 with the corresponding predicted directivity pattern shown in fig. 4.5 and fig 4.10 (both reproduced here) the sidelobes are seen to be at levels close to those predicted with a very similar angular distribution. After the directivity plot of fig. 11.3 is rotated about its vertical axis the similarity between predicted and measured directivity is striking.

Fig 11.4 shows the measured directivity of beam no. 2 at 10 m. The width of the main lobe is still less than 1° but the distribution of the sidelobes is slightly different. The directivity should be a replica of that of fig. 11.3 since the beams are

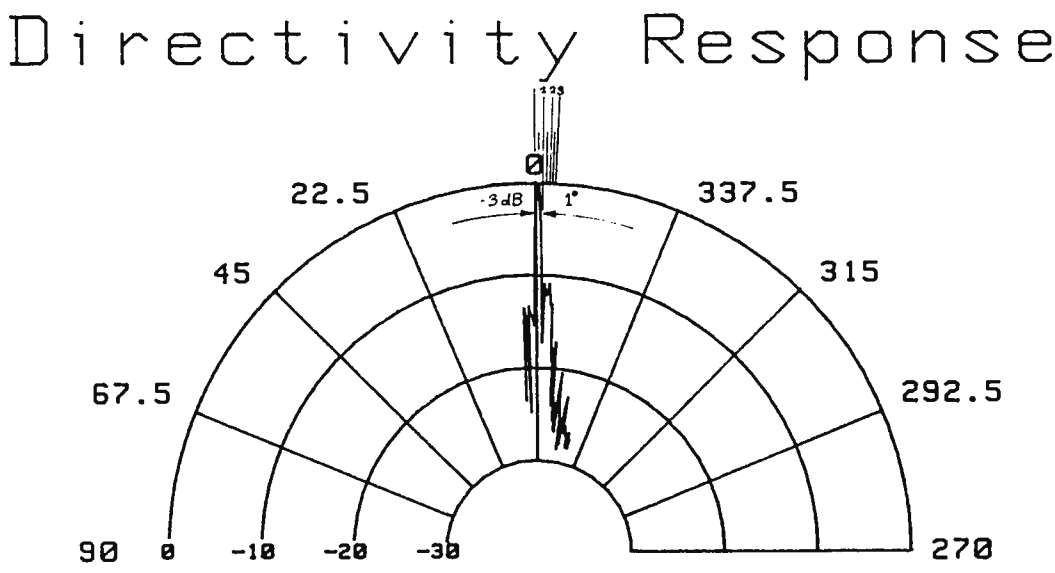

Fig. 11.3: Directivity; beam no. 1 at 10 m

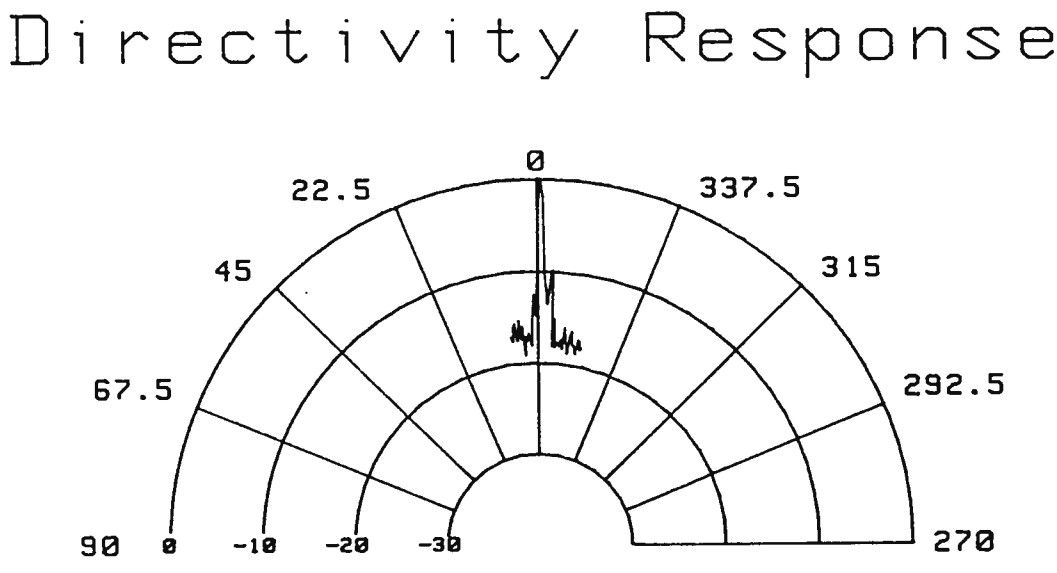

Fig. 11.4: Directivity; beam no. 2 at 10 m

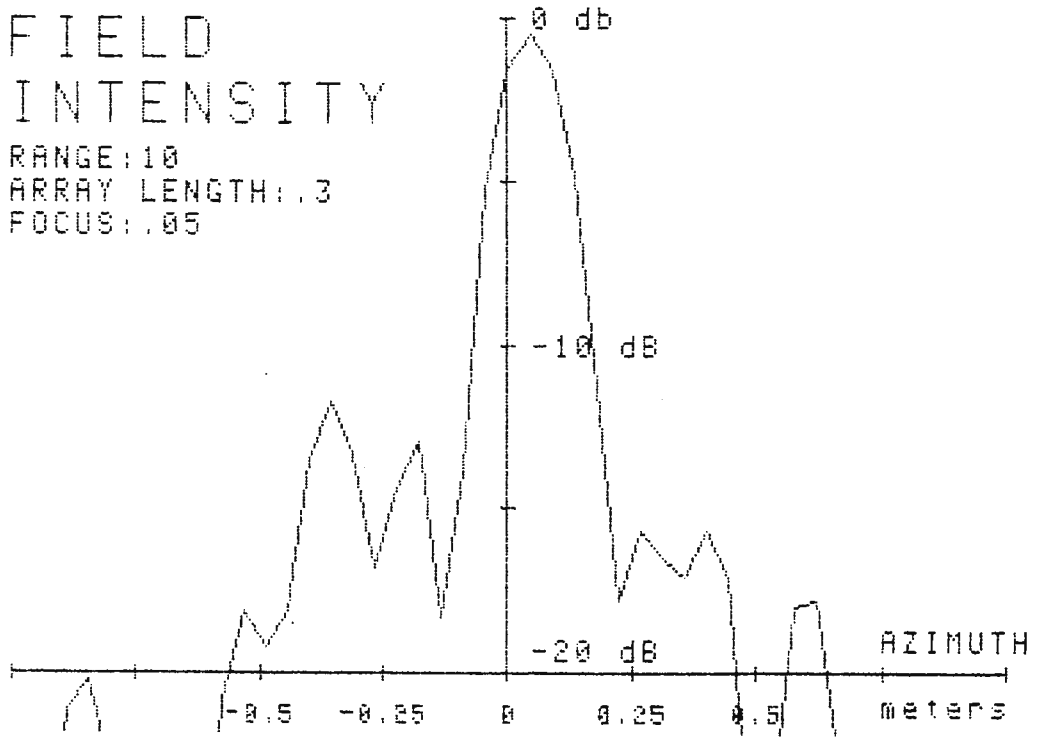

Fig. 4.5: Central beam at 10m

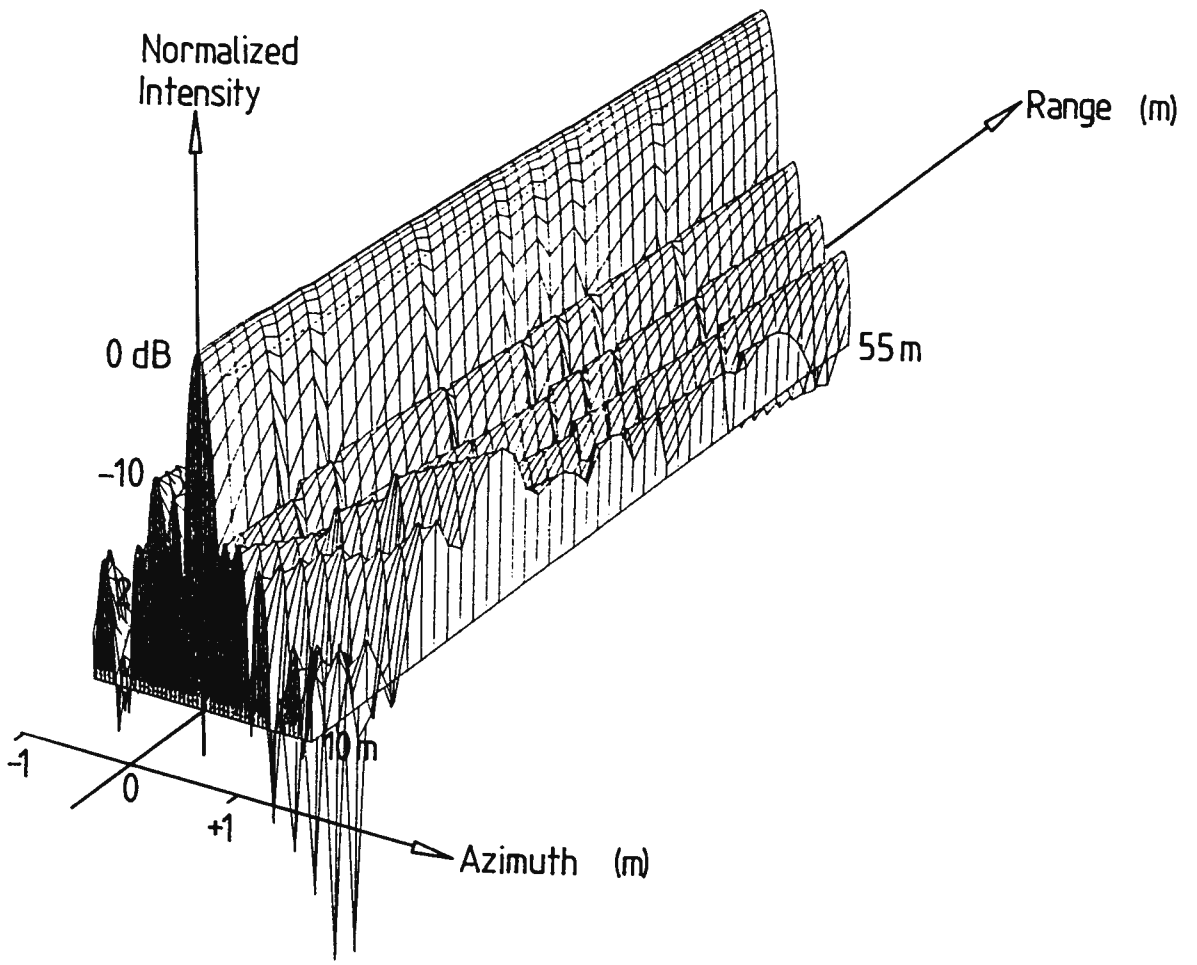

Fig. 4.10: Central beam, 10 to 55m

formed with similar subarrays. The problem may lie in the measurement system. When the directivity plot in fig. 11.3 was made great care was taken in setting up the zero position to ensure that one of the samples is taken at the peak. This proved to be very time consuming since the rotator is moved back to the starting position before a sequence of measurements is taken and the backlash is difficult to predict. The advantage is that the plots are normalized to the actual peak of the beam pattern.

For the other measurements the normalizing value is simply the largest measured value (sought by the computer). This maximum might be up to 1 dB down from the actual peak when the there are only two samples on the main lobe. This may account for the apparent 1 dB increase in the side lobe levels as shown in fig. 11.4.

Fig. 11.5 is the measured directivity of the beam no. 1 at 14.2 m range when the subarray grows to 4 elements. As expected the main lobe narrows slightly. The sidelobe levels have increased slightly, above the limit where sampling can account for them. These levels are probably due to the marked effect of beam steering on the sidelobe levels of the longer array. This topic was discussed in chapter 4 in some detail with reference to a 4 element array at 10 m. The computer modelling results presented in the "3-D" plot of 4.10 predict a sudden increase in sidelobe levels as

the extra element is included, at this range.

Figures 11.6 and 11.7 show the directivity responses of the central beam and the outside one respectively, at a range of 16,8 m, close to the maximum range at which 4 elements are used in the subarray. The sidelobes have settled down in both cases; symmetrically on the central beam since it is unsteered, and asymmetrically on the outside beam where 10 cm of beam deflection is required to put the focal point on the swath centreline.

Fig. 11.8 shows the same beam as that of fig. 11.7, but at a range of 17 m, just after the fifth element has been included in the subarray. Again there is the sudden increase in one of the sidelobes. The required beam deflection, measured from the new subarray axis, increases to 0,15 m at this range, hence the increase.

11.4 Vertical beamwidth

As mentioned earlier in connection with the transmitter the vertical beam pattern should be broad, to provide uniform sensitivity over the angular variation from the first to the last range cell. The beamwidth is chosen somewhat larger than this to eliminate the effects of any possible rolling of the array in operational use.

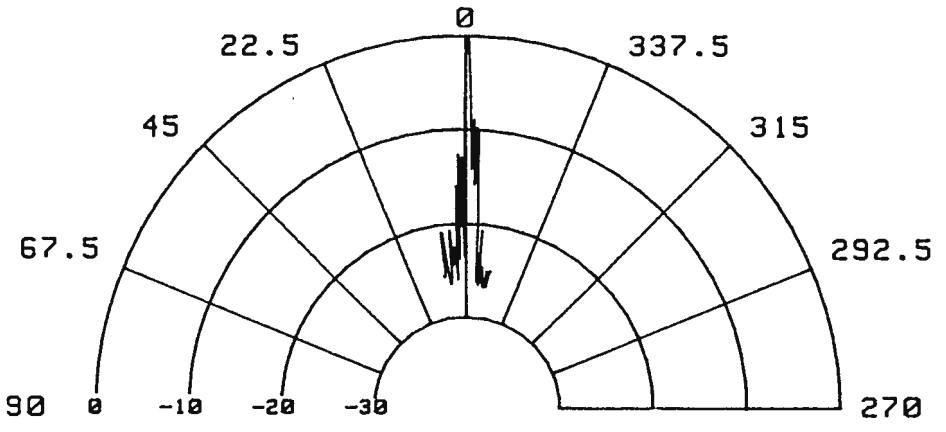

Fig. 11.5: Beam no. 1 at 14 m

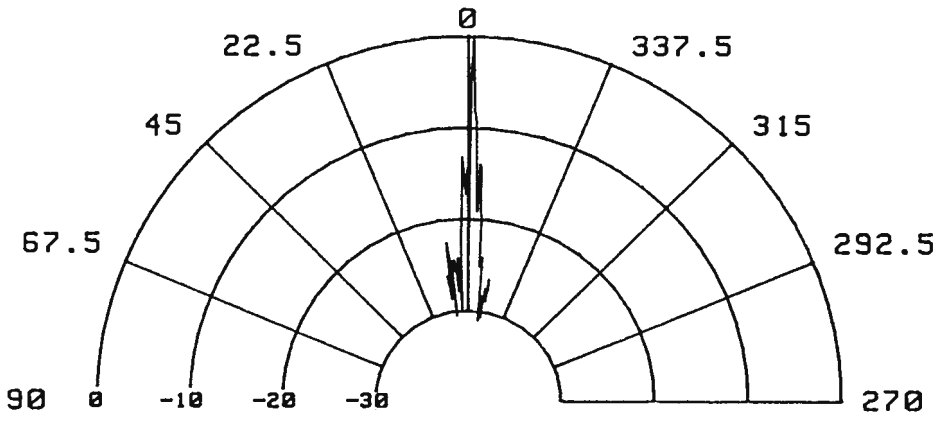

Fig. 11.6: Beam no. 3 at 16.8 m

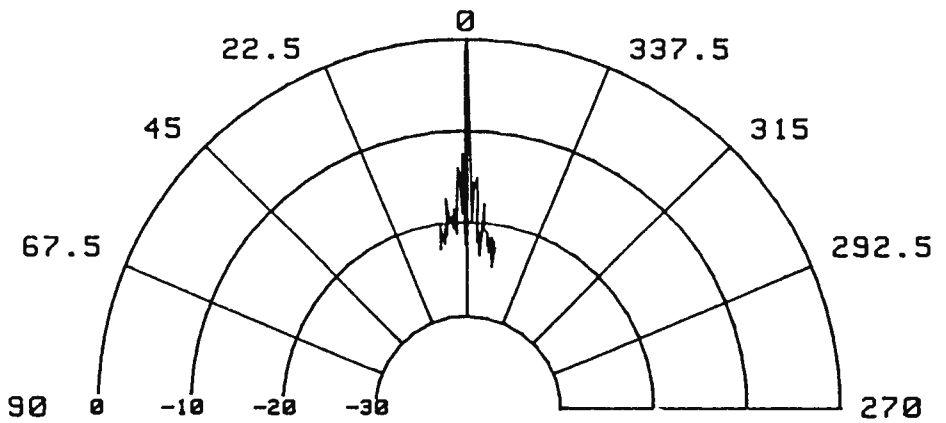

Fig. 11.7: Beam no. 1 at 16,8 m

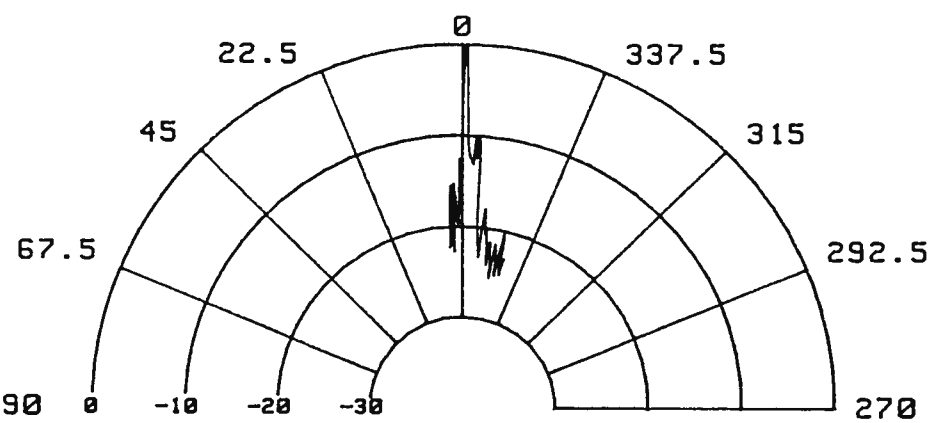

Fig. 11.8: Beam no. 1 at 17 m

Using the measurement system described above the measured 3 dB vertical beamwidth is close to 90° and there is a significant response to even greater angles, as shown in fig 11.9. The array is angled away from the sea surface to reduce the noise and reflections returned from there. To keep the angle within reasonable bounds the vertical beam pattern is adjusted with a baffle. The resulting directivity response is shown in fig. 11.10 while a crossection of the array is shown in fig. 11.11, with the baffle in place.

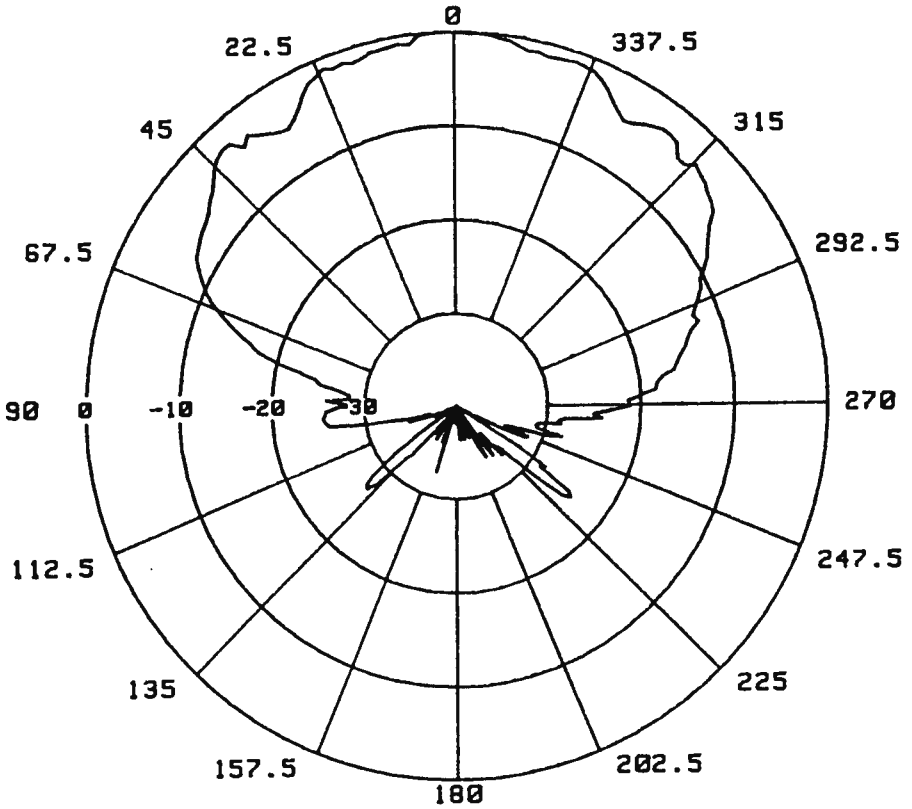

Fig. 11.9: Vertical beam pattern

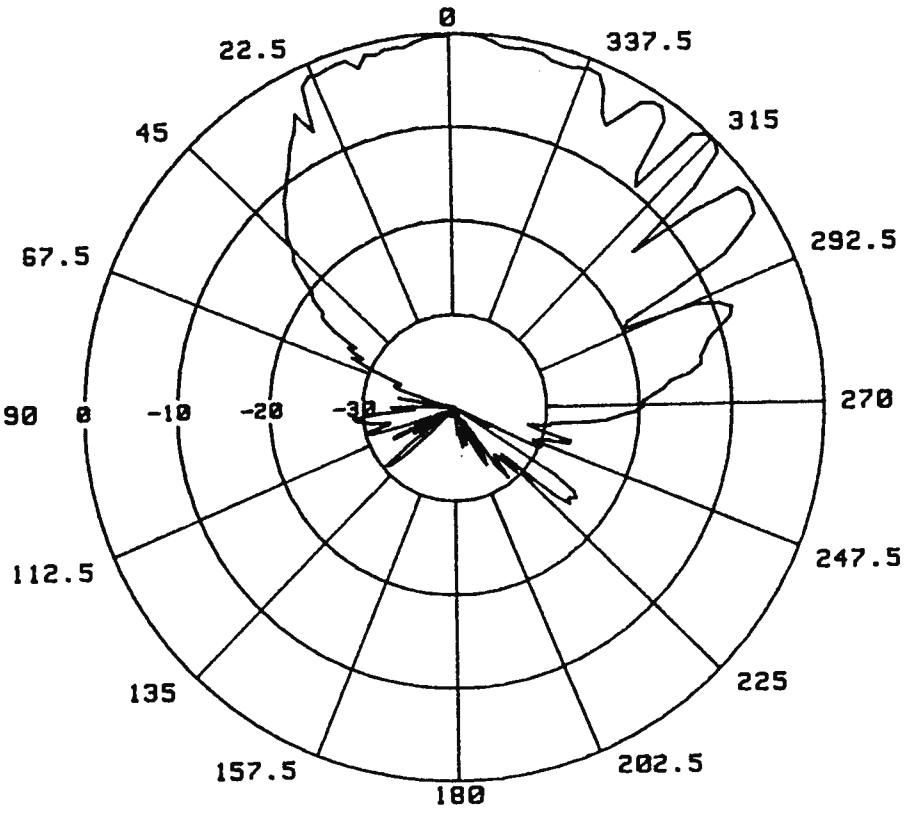

Fig. 11.10: Vertical beam pattern with baffle

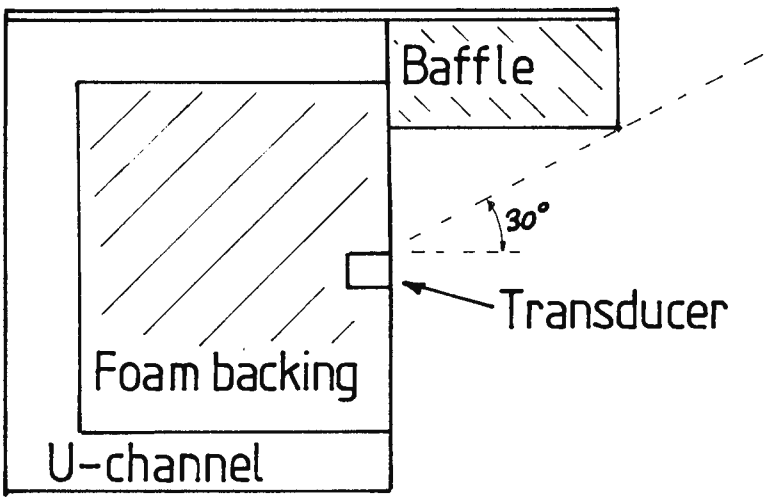

Fig. 11.11: Geometry of baffle

11.5 Reservoir tests

The best evaluation of the overall system operation is a test in a lake or at sea. A floating laboratory was used for the initial operational tests. The result is shown in fig. 11.12, which is a polar scan of the reservoir floor over 180°. The maximum range is 100 m. The results show that under these conditions an adequate signal to noise ratio is achieved. The bottom of the reservoir is mainly soft mud (with a backscattering strength close to -40 dB) and occasional fist sized rocks and metal cans. The maximum depth of 7 m lies immediately below the transducer.

Resolution is difficult to evaluate from a polar scan since the system images sets of parallel swaths. At close ranges (the exact definition of close depends on the polar scanning rate) the swaths in one set overlap those in the next. At only one range do the swaths lie contiguously. At this range the array axis describes an arc of 1 m during each interpulse period. A 180° scan made in 30 s causes this range to lie at 50 m. At greater ranges there are gaps between the surveyed areas.

Fig. 11.12: Polar scan of reservoir

11.6 Sea trials

Sea trials were performed in False Bay, aboard the "Shirley-T". This research vessel is a 10 m twin hull with a 1 m opening in the aft deck through which transducers may be lowered into the sea. Instruments and recorders are set up inside a covered cabin. This proved to be a most convenient arrangement on one of the trials when the worst hail storm in 20 years moved over False Bay accompanied by winds gusting to 30 knots.

Since a chart recorder was not available for the trials a fibre optic recorder was used. The dry process recording paper, with development taking place after exposure to ultraviolet light, was available in two grades. One provided good definition with hard contrast, while the other produced lower contrast images with a slight blurring of the individual oscillograph traces, noticeable in the enlarged images.

An external clock with a period consistent with the towing speed was used to synchronize the fibre optic recorder and the beam forming system. Some difficulty was experienced with the adjustment of the response of the fibre optic recorder while at sea. To enable these adjustments to be made in the laboratory the signals from the beam forming system were recorded on magnetic tape. The required signal bandwidth, of almost DC to 25 kHz, was accommodated using an FM channel and running the tape at 152 cm/s. This large bandwidth is

the result of the fivefold time compression of the individual swath signals.

The array was mounted in the frame shown in fig. 11.13. The frame in turn was bolted to the deck and stayed with two turnbuckles. With this arrangement, and the lack of streamlining, the resulting drag and turbulence limited the depth of the array to less than 2 m and the maximum towing speed to 4 knots.

The depth restriction places the array less than a meter from the vessels hull (at an angle of 45°) and within 2,5 m of the propellers. Noise from the propellers is a problem; marked changes in the noise level were noted whenever the vessel accelerated or changed course. This source of noise might be reduced were it possible to travel slower than the ´critical speed´ of the vessel; the speed at which propellor cavitation occurs. The noise level at high frequencies has been noted in one instance (66) to show a dramatic 50 dB increase as the speed increases above 3 knots. The minimum towing speed is constrained by the motion of the vessel and the fact that no gyrostabilization of the array has been provided. At 150 m range the axis of symmetry of the swaths is displaced by 1 m when the ships heading changes by less than half a degree. The stability of the heading may be increased by travelling faster thereby diminishing the effect of the short wavelength/short period chop which is the major cause of platform motion at low speed.

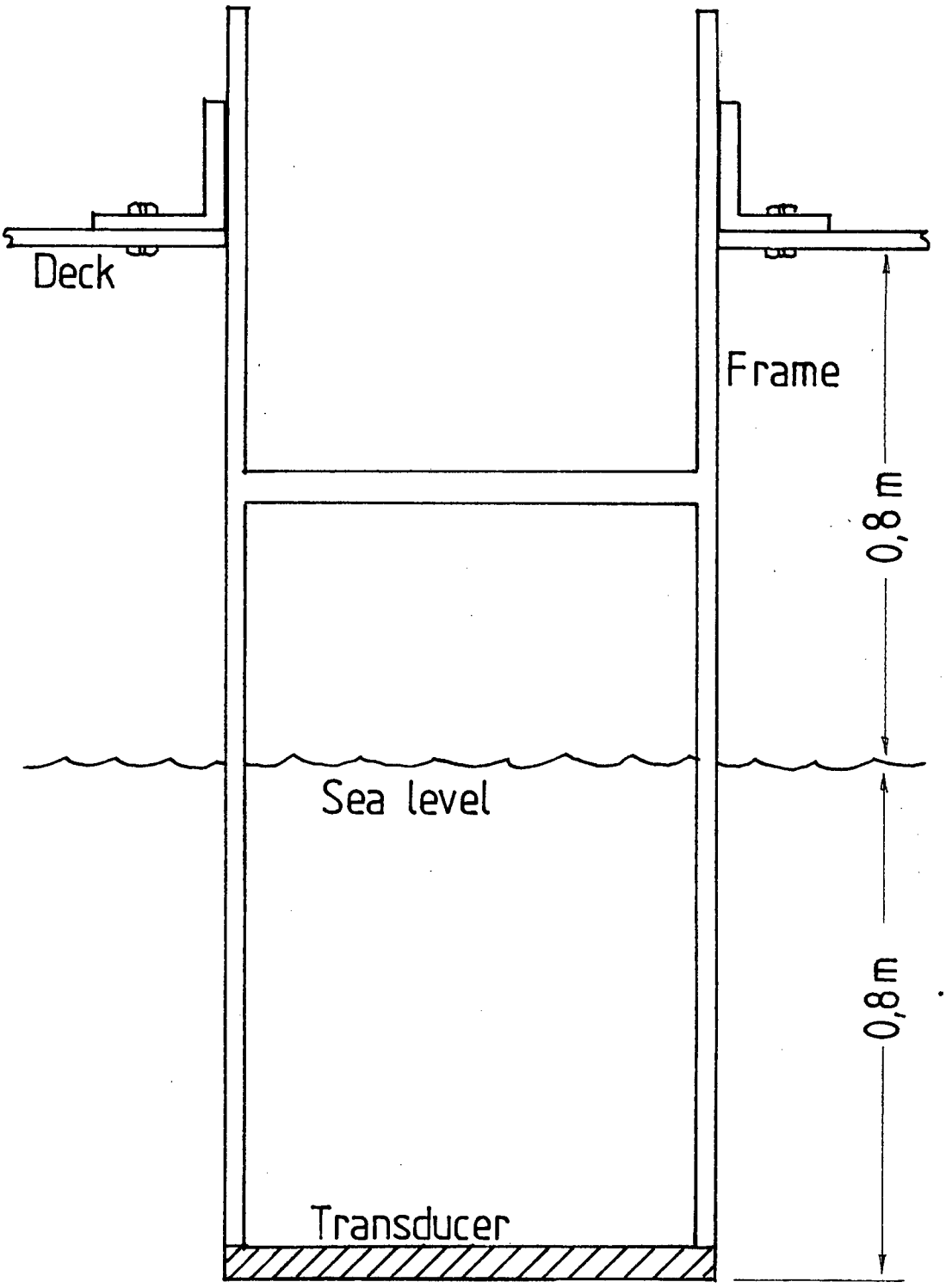

Fig. 11.13: Array mounting frame for sea trials

The evaluation of resolution is the priority and the maximum towing speed of 4 knots was adopted at the expense of signal to noise ratio.

The initial sea trials were performed in a relatively calm sea. Fig 11.14 shows the results of a scan of the wreck of the "Clan Stewart". This ship was wrecked over 100 years ago in less than 5 m of water with the shore line 75 m away. At close ranges the A/D converters are driven into saturation due to an incorrect time varying gain profile. In the vicinity of the wreck there are sand ripples, clearly revealed in the image. Each line of the image represents an along track interval of 20 cm. Between the wreck and the beach there are breaking waves and the returned signals are probably due to suspended bubbles in the water.

The time varying gain profile was adjusted and further sea trials were performed under less than idyllic conditions. Figure 11.15 shows the image of the wreck of the Clan Stewart with the improved TVG profile. The sand ripples are visible from the shortest range (at lower left) to slightly beyond the wreck. Also noticeable on these records is a slight beam amplitude imbalance, manifest as a raggedness on the edges of the wreck. No other records were made on this occasion with the improved TVG.

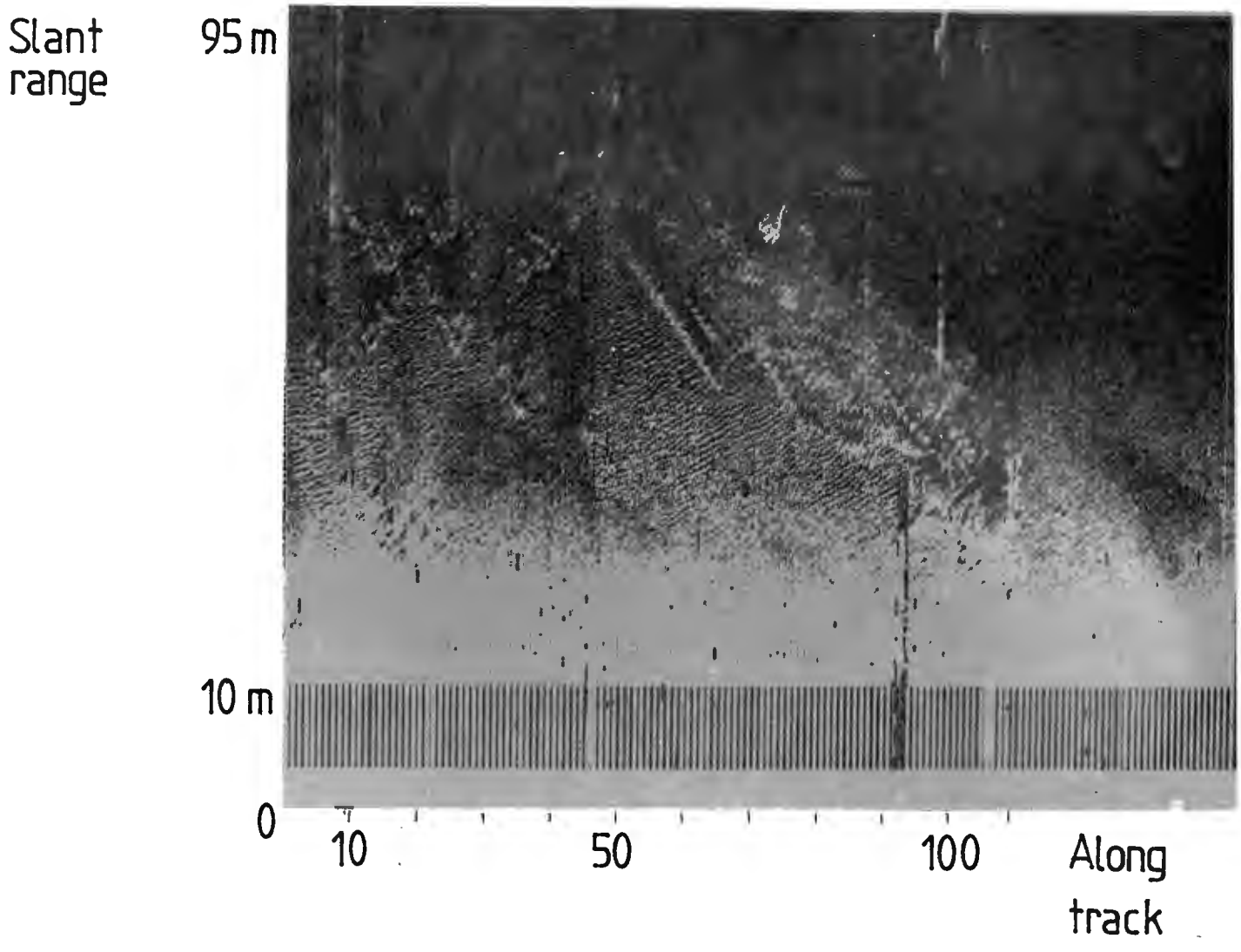

Fig. 11.14: Side scan record of wreck

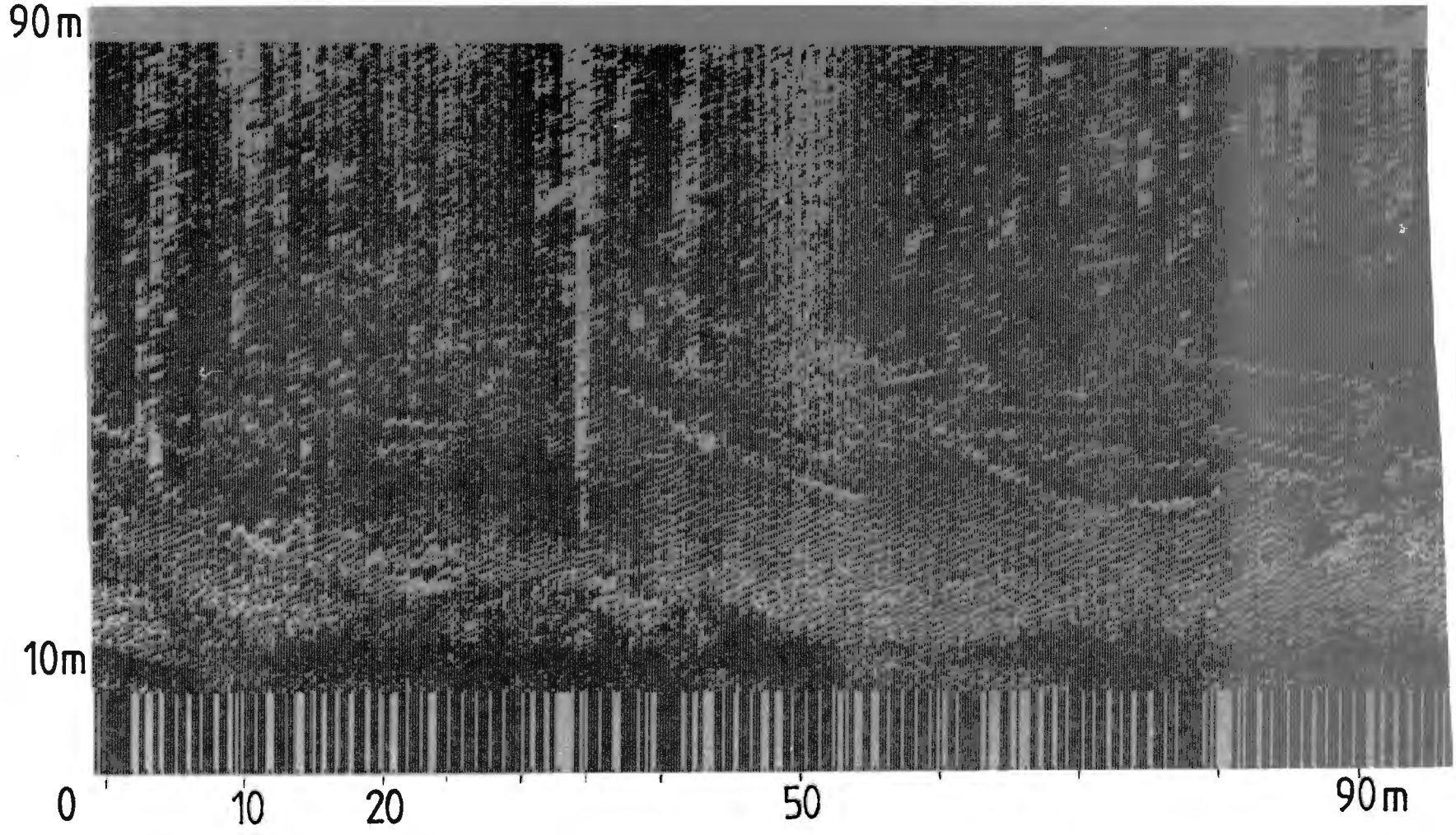

Fig. 11.15: Side scan record of wreck with improved T.V.G., made under extremely adverse weather conditions

Returning to the earlier trials, fig. 11.16 shows the base of a tower in 20 m of water while fig. 11.17 shows sand ripples in the immediate vicinity of the tower.

A sand hillock is shown in fig. 11.18. When the contrast is reduced, as shown in fig. 11.19 the image shows the detail better. The final image is the same as that of fig. 11.19 but has been expanded along track. As before each line is a swath and each swath is 20 cm.

Along the edge of the image in fig. 11.20 is a dark band with lighter lines at regular intervals. This interval represents 1 m of along track motion and marks the start of one set of swaths. The detail is seen in some places to change significantly from swath to swath; this is interpreted as a confirmation of the results obtained in the tank, namely that the predicted performance has been achieved.

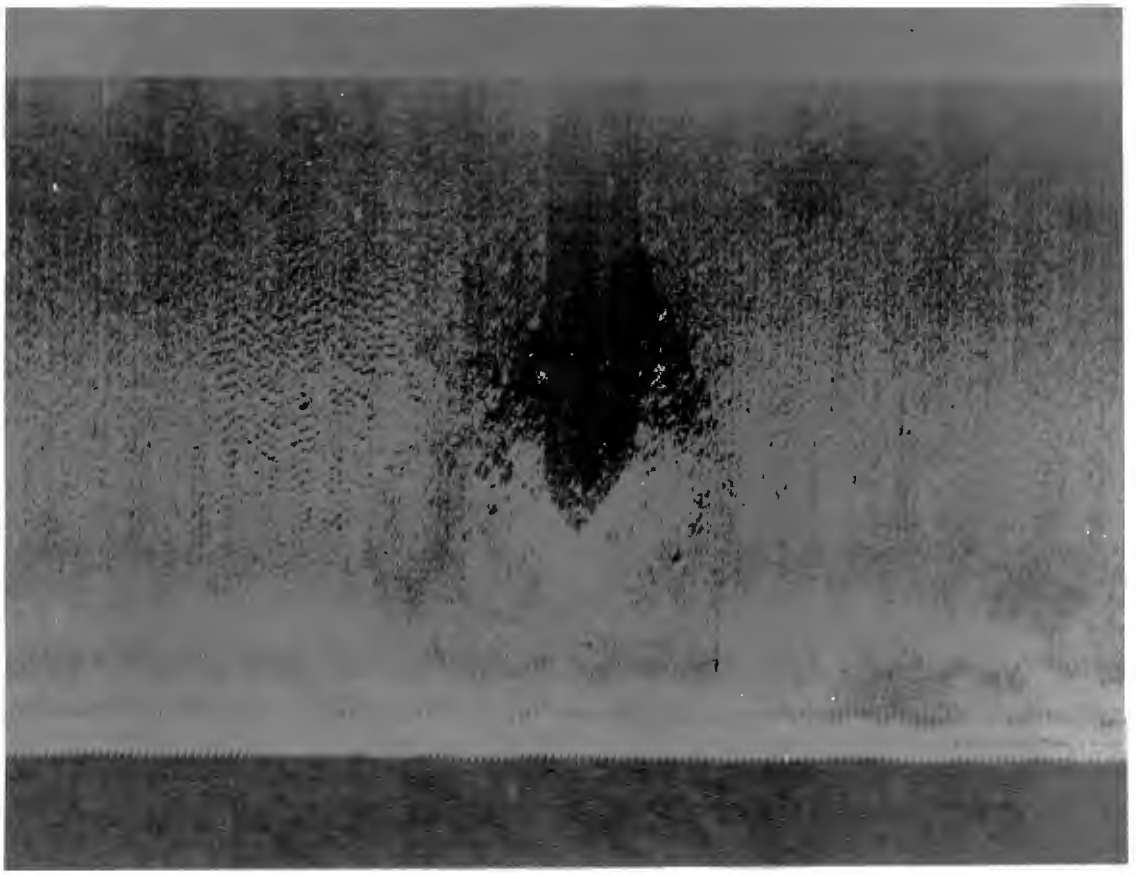

Fig. 11.16: Record of base of tower

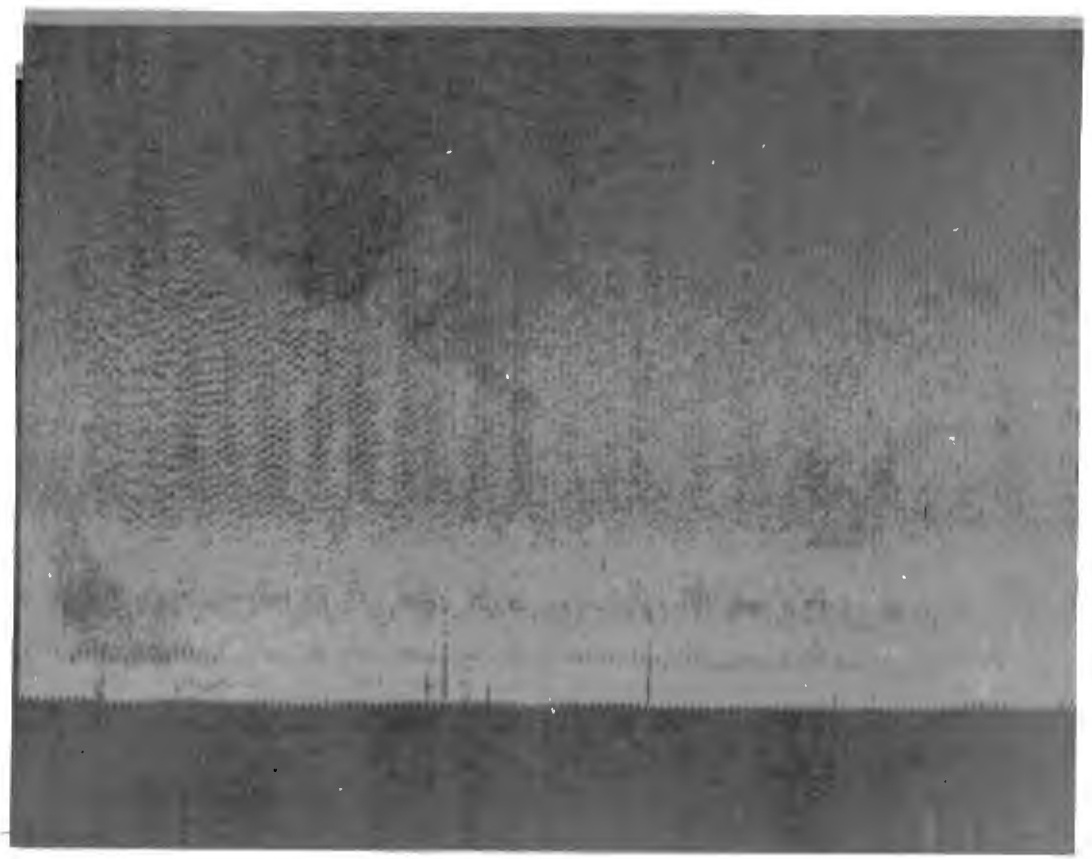

Fig. 11.17: More sand ripples

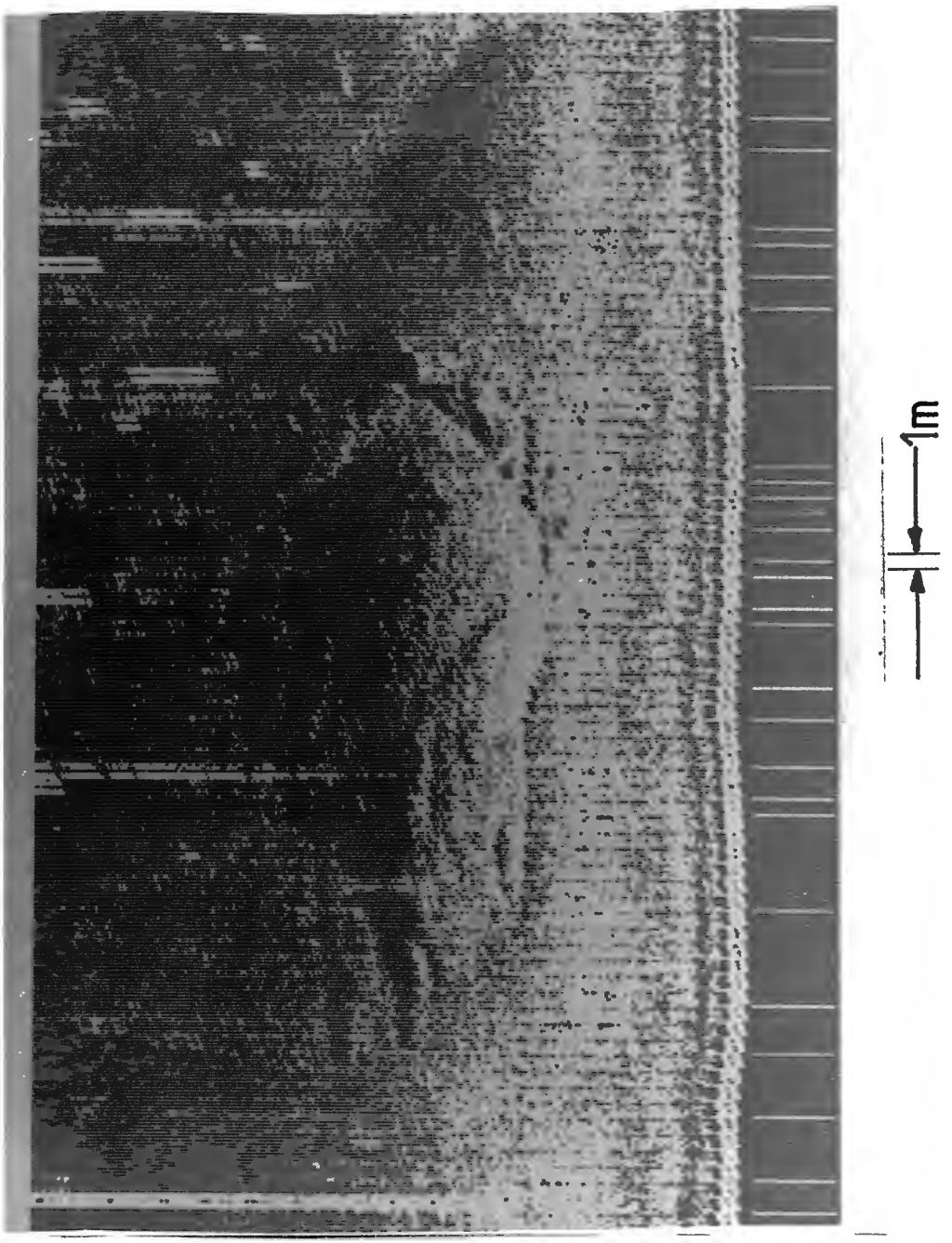

Fig. 11.18: Sand hillock

NOTE: This record is expanded along track to show resolution.

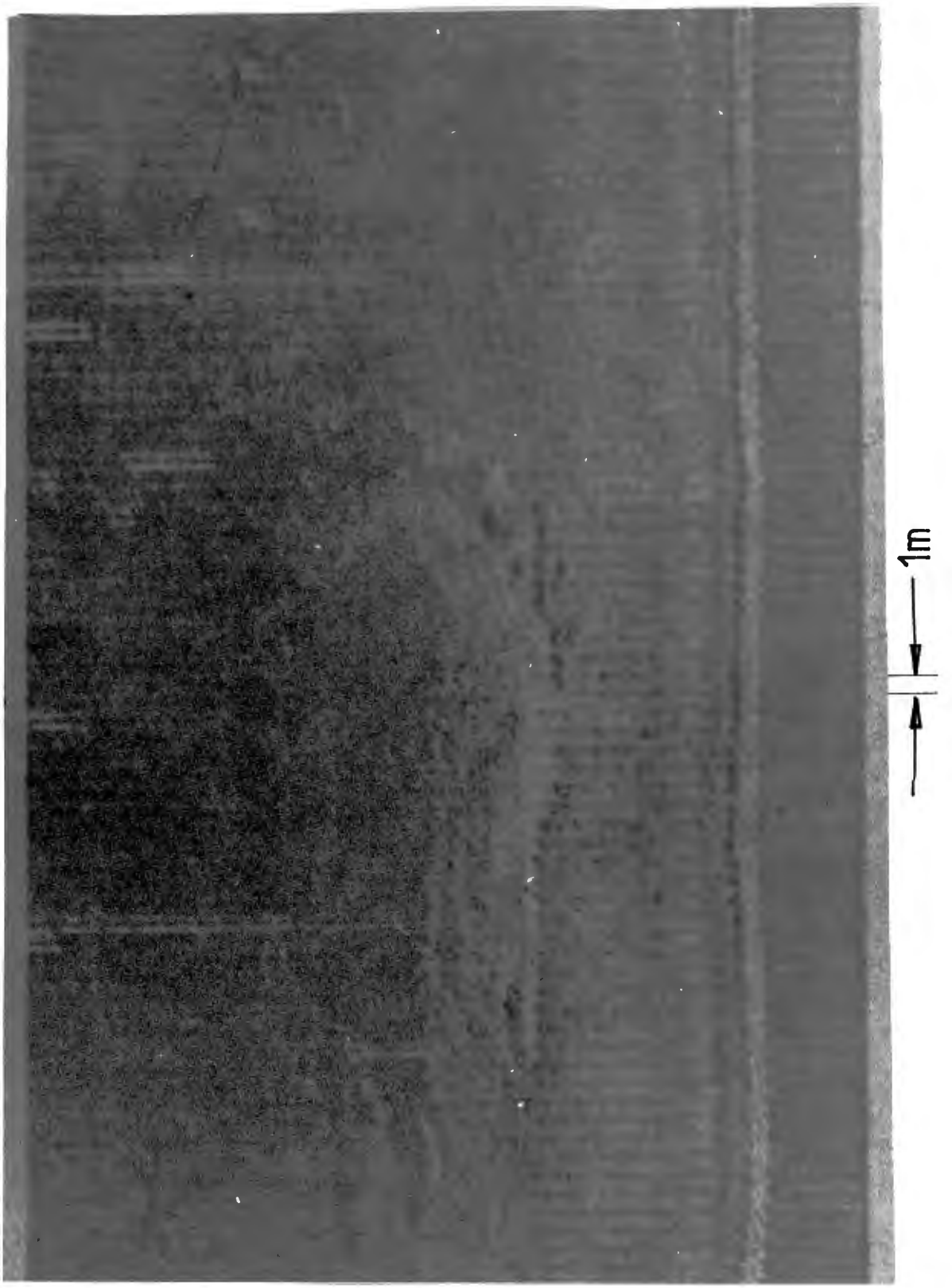

Fig. 11.19: Sand hillock, lower contrast.
NOTE: Expanded along track.

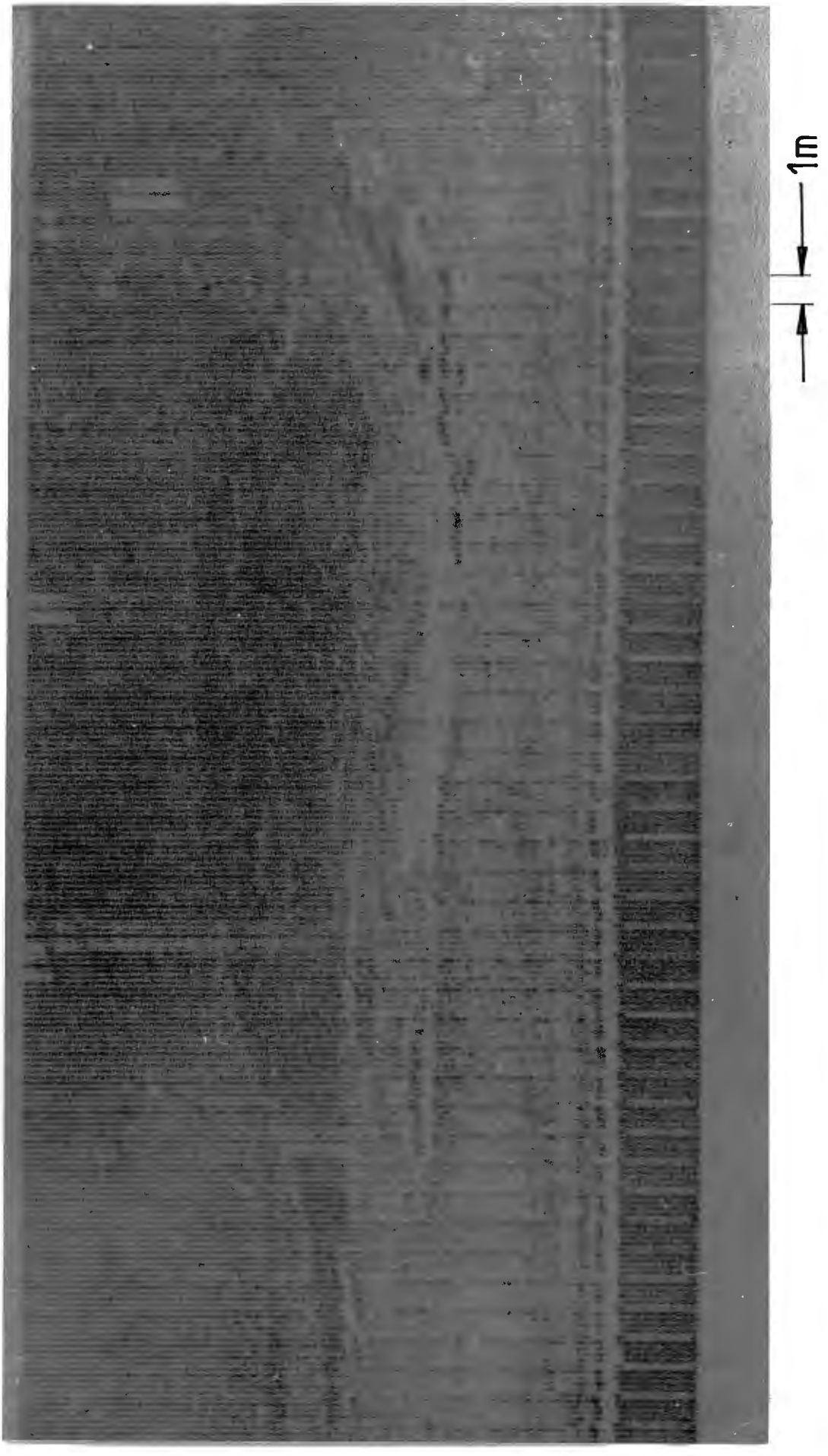

Fig. 11.20: Sand hillock

NOTE: The along track scale is greatly expanded.

CONCLUSIONS

12.1 Conclusions

The objective of the design, construction and evaluation of a high resolution microprocessor controlled dynamically focused multiple beam side scan sonar with a high image formation rate has been achieved.

By the consideration of the theoretical and practical costraints a suitable array was chosen. Theoretical analysis of the chosen array yielded an easily programmable solution to the problem of determining sub-array configurations. The results thus obtained were used as input to field modelling programs written for this purpose. From these came predictions of beam forming performance.

A programmable quadrature phase shifter was designed to provide both phase and amplitude control of the signals acquired by the array, amplified by low noise amplifiers and sent to the phase shifter via line drivers and coaxial cable. The phase shifted signals were summed, detected, logarithmically compressed and converted from analog to digital prior to their storage.

An Intel 8085 microprocessor - of low performance by today´s standards - provided the low cost control. A holistic approach to programming led to rapidly

executable code composed of interlinked subroutines which were developed and tested during the design of the associated hardware.

The timing constraints place a severe load on the microprocessor. By a judicious trade-off of software for hardware the software execution time was dramatically reduced. The major part of the data output routine is handled by a first-in-first-out buffer and a variety of timers. This circuitry, along with the overall system timing generators and the input and output connections to the chart recorder, was designed with only twenty four IC's on a single board. The alternative was a dual processor arrangement.

Tests of the phase shifters under dynamic control of the microprocessor showed the faultless updating (at intervals correspoding to two meter increases in range) of the required focusing phases and element shading.

Laboratory tests were performed on the whole system with simulated echoes in a large tank. The theoretical and computer predictions were remarkably closely approximated in these trials. Reservoir trials showed the working of the novel time domain multiplexed transmitter, and signal to noise ratios were seen to be adequate.

Sea trials produced images that, while not having good tonal qualities, clearly show detail changing from swath to swath (thus indicating that the desired

resolution has been achieved). They also, of course demonstrate the portable nature of the instrument.

The results presented demonstrate the basic operation of the system and the soundness of the assertion that such a sophisticated system can be constructed to be easy to handle while not being prohibitively costly. The full potential of the use of dynamic focusing in side scan sonars remains to be realized.

12.2 Developmental possibilities

Improvements in the contrast and tonal quality of the final image may be achieved by using a chart recorder rather than the fibre optic recorder. The signal to noise ratio may be improved by mounting the array on a towed body to minimize the interfering effects of the vessel's engine and the aeration from the propellor and the hull.

The towing cable must either have more than ten coaxial cores along with some power lines, or the signals from the array must be multiplexed onto the few available coaxial pairs (with a coherent demultiplexer to leave the relative phases unalterred).

If the multiplexing scheme were adopted it would be advantageous to provide a bank of ten phase tracking AGC amplifiers to reduce the long term dynamic range prior to modulation. Programmable attenuators have

been provided on the preamplifiers with a view to implementing this solution.

At present the time varying gain has a preset empirically determined profile. The determination of a TVG profile on the basis of the previous set of swath amplitudes would provide near optimum image acquisition. In the moments when the microprocessor is idle (there is at least 10 ms available between the transmission of a pulse and the start of a new image) a low order sampled data filter could provide estimates of the expected image amplitudes in each focal zone of the new swath. A sixteen sample uniform window moving average filter can be extremely efficiently implemented in machine code on the 8085. The values thus obtained are then used to estimate the appropriate gains.

The single byte of gain for each focal zone can be sent directly to the preamplifiers in the towed body via a slow serial line (a single twisted pair) or it may be applied after the beam forming summation, to the TVG amplifiers.

Rack mountings were used for the implementation of the card based system. The reason for this arrangement was to facilitate ease of testing and system assembly. All the digital circuitry may be quite comfortably laid out on one PC board, with the summing amplifiers and A/D converters on another.

By implementing the phase shifters in a hybrid technology each could be spaciously laid out over 5 cm^2. Placing all the phase shifters on a single board (which need be no larger than 500 cm^2), and performing the address decoding at a single location on that board significantly reduces the cost of the decoding circuitry and the associated intermediate bus buffers.

At the end of such developments this high performance side scan sonar may be placed in a truly portable package the size of a large briefcase, perhaps with a shoulder strap! The present system provides the high performance but it requires well coordinated cooperation between two men to get it from the jetty onto the vessel.

APPENDIX I

The field of any source is generally expressed as an integral over that source. The diagram below shows the geometry of a line source, of length D m. The field point of interest is the point(x_z,z); at an azimuth of x and a range of z.

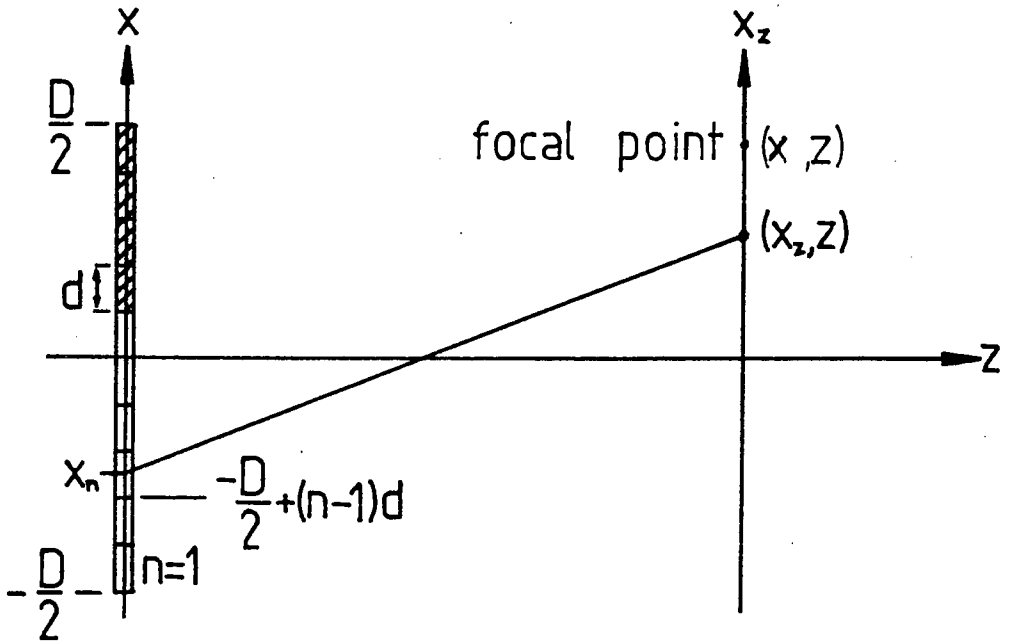

At the point of interest the field amplitude $P(x_z,z)$ is closely approximated by integrating the effects of the source distribution with a weighting accounting for the variation in spatial phase and amplitude between the source point at (x,z) and the field point at (x_z,z).

The term S(x) represents the source amplitude and phase distribution and the term $r(x,x_z,z)$ is the distance between the points.

$$P(x_z,z) = k\int_{-D/2}^{D/2} S(x)\ \frac{e^{-j\beta r(x,x_z,z)}}{r(x,x_z,z)}\ dx$$

where $r=\sqrt{(x_z-x)^2+z^2}$ and $\beta=2\pi/\lambda$.

In the Fresnel region the following approximations are usually made (41):

i) the 1/r term in the denominator is approximated by a constant 1/R, where R=z. The effect of this approximation on the array in question is small. The term $(x_z - x)$ is always less than 1 while z is greater than 10. The resulting amplitude error is less than 5%.

ii) in the phase term the range is expanded using the binomial theorem and dropping all terms but the first two, thus arriving at the simplifying approximation

$$r \simeq z + \frac{(x_z - x)^2}{2z}$$

The resulting Fresnel region field amplitude is then simply expressed as

$$P(x_z, z) = \frac{ke^{-j\beta z}}{z} \int_{-D/2}^{D/2} S(x) e^{-j\beta\left(\frac{\{x_z - x\}^2}{2z}\right)} dx$$

When the array is composed of contiguous elements, each with a constant phase and amplitude the resulting field amplitude is expressed more explicitly as

$$P(x_z, z) = \frac{ke^{-j\beta z}}{z} \sum_{n=1}^{N} S(n) \int_{-D/2+(n-1)d}^{-D/2+nd} e^{-j\beta\{(x_z - x)^2/2z\}} dx$$

The above integral is simply a sum of N integrals, each over one of the N array elements. The term S(n) represents the discrete aperture distribution. The limits of integration are from one end of an element to the other.

It is more convenient to map all the elements onto a generic element with the transformation (67)

$$x = x_n + u \quad \text{where} \quad x_n = -D/2 + (n-1)d$$

The term x_n is the distance between the centre of the n th element and the field point. The integration over the n th element

$$I_n=\int_{-D/2-(n-1)d}^{-D/2+nd} e^{-j\beta((x_z-x)^2/2z)}\,dx$$

becomes

$$I_n=\int_{-d/2}^{d/2} e^{-j\beta\left[\left((x_z-x_n)^2-2u(x_z-x_n)+u^2\right)/2z\right]}\,du$$

For the geometry under consideration the term u is half the width of an element, or 0,05 m. The square of this is significantly smaller than the term $2u(x_z-x_n)$, which may be as large as 0,095. Neglecting the u^2 term allows the integral over the element to be expressed as

$$I_n=e^{-j\beta((x_z-x_n)^2/2z)}.d\left(\frac{\sin(\beta d(x_z-x_n)/2z)}{\beta d(x_z-x_n)/2z}\right)$$

and the total field is the sum over all elements

$$P(x_z,z)=\frac{ke^{-j\beta z}}{z}\sum_{n=1}^{N} S(n)e^{-j\beta\left(\frac{(x_z-x_n)^2}{2z}\right)}.d.Sa\left(\frac{\beta d(x_z-x_n)}{2z}\right)$$

This is clearly the summed effect of N individual elements operating in their far field with their characteristic sinc function shape.

Array focusing is achieved by cancelling the phase terms in the sum. The appropriate choice of phases for each element for each focal azimuth and range is given by choosing the phase of the aperture distribution to be

$$\angle S(n)=e^{+j\beta\left(\frac{(x_z-x_n)^2}{2z}\right)}$$

The amplitude of this term is determined by requiring each element to make a contribution to the field at a point greater than some specified minimum.

The elements contribution is dependent on the azimuthal separation between the focal point and the element centre as shown by the term

$$Sa\left(\frac{\beta d(x_z-x_n)}{2z}\right) = \frac{\sin\left(\frac{\beta d(x_z-x_n)}{2z}\right)}{\beta d(x_z-x_n)/2z}$$

The half power points are at an argument of slightly less than $\pi/2$. Constraining the distance appropriately yields the inequality

$$|(x_z-x_n)| \leq \frac{z}{2d}$$

The elements in the array are 21 wavelengths long and the inequality becomes

$$|(x_z-x_n)| \leq \frac{z}{42}$$

At z=10 m the inequality is satisfied by a maximum aximuthal distance between element centre and focal point of

$$|(x_z-x_n)| \leq 0;238$$

If the focal point is at an azimuth of 0,4 m this constraint is satisfied by only the three elements at that end of the array.

The program below calculates which elements are useful at each focal point for each range and presents these values in the graphic form of Table 4.1 on page 49.

```
10 b=2*pi @ d=0.1 @ a$=" "
20 for z=10 to 150 step 2.187
30 q=pi*z/(b*d)
40 print "Range=";z
50 for xf=-0.4 to 0.4 step 0.2
60 for xn=-0.45 to 0.45 step 0.1
70 if abs(xf-xn)<0.1*int(q*10) then a$=a$&"1" else
   a$=a$&"0"
80 next xn
90 print a$
100 a$=" "
110 next xf
120 next z
130 end
```

APPENDIX II

The field modelling is performed with a discrete approximation of the integral

$$P(x_z,z)=k\int_{-D/2}^{D/2} S(x)e^{-j\beta r(x,x_z,z)}\,dx$$

where S(x) is the specified aperture illumination. The variables entered by the operator are the number of points in the discrete approximation, the array length D, the size of the elements d, the range z, and the azimuthal limits of the graphic output. The BASIC program operates in either an interactive mode or a batch mode, providing plots of normalized field intensity (directivity), at a single range. A similar program in FORTRAN was run on a Univac 1100 series to generate the "3-D" and contour plots, showing the normalized field intensity at many ranges.

```
10 ! FILE NAME ;FIELD    DISK ;THESIS (ARRAY)
20 REM ***THE FIELD INTENSITY OF A DISCRETELY FOCUSED LINE SOURCE***
30 ! PRINTER IS 701
40 ON ERROR GOTO 70
50 LOADBIN "GDUMP"
60 OPTION BASE 1
70 DIM T(50),R(50),P(50,50),Q(50),F(50),SOURCEMAG(50),U(50),MAG(10)
80 OFF ERROR
90 RAD
100 CLEAR
110 IMAGE 2D,5X D.DDD,5X DDD.DD
120 IMAGE "No. OF POINTS IN TRANSFORM=",DD,2/
130 ! B IS THE PHASE SHIFT CONSTANT
140 ! THE FREQUENCY IS 308 kHZ
150 ! WAVELENGTH IS 0.00487 m
160 B=2*PI /.00487
170 DISP "USER INPUT (Y or N)";
180 INPUT S$
190 IF S$="Y" THEN 230
200 READ T,D,W,F,Z,U,FILE$
210 FOCUS=U
220 GOTO 650
230 ! **********************************
240 ! ** DEFINE ARRAY DIMENSIONS  **
250 ! **********************************
260 DISP "ENTER THE NAME OF THE DESTINATION GRAPHICS FILE";
270 INPUT FILE$
280 DISP "INPUT DESIRED NO OF POINTS FOR TRANSFORM. MAX =50";
290 INPUT T
300 DISP "ENTER ARRAY LENGTH (m)";
310 INPUT D
320 DISP "ENTER SUBARRAY DIM.";
330 INPUT W
340 DISP "ENTER WIDTH OF OUTPUT FIELD (m)";
350 INPUT F
360 DISP "ENTER RANGE";
370 INPUT Z
380 ! ***J IS THE NUMBER OF SUBARRAYS
390 ! ***H IS THE NO OF POINTS ON THE SUBARRAYS
400 ! *** A IS THE POINT SPACING
410 ! *** ON THE ARRAY
420 ! *** E IS THE POINT SPACING ON THE FIELD
430 E=F/T
440 J=D/W
450 H=T/J
460 A=D/T
470 DISP "DO YOU WANT THE FIELD OF A FOCUSED ARRAY (Y or N)"
480 INPUT Q$
490 IF Q$="N" THEN 500 ELSE 570
500 FOR K=1 TO J
510 DISP "ENTER THE PHASE FOR ELEMENT (";K;")";
520 INPUT PHI(K)
525 PHI(K)=DTR (PHI(K))
530 DISP "ENTER THE MAGNITUDE OF ELEMENT (";K;")";
540 INPUT MAG(K)
```

```
550 NEXT K
560 GOTO 590
570 DISP "INPUT FOCAL POINT";
580 INPUT U@ Q$="Y"
590 IMAGE "ARRAY LENGTH=",DD.DD,2/
600 IMAGE "SUBARRAY DIM:",DD.DD,2/
610 IMAGE "FIELD WIDTH:",X,DD.DD,2/
620 IMAGE "PIXEL WIDTH:",X,DD.DD,2/
630 IMAGE "RANGE:",8X,DD.D,2/
640 IMAGE "FOCAL POINT X=",D.DD,2X,"Z=",DD.DD,2/
650 PRINT USING 120 ; T
660 PRINT USING 590 ; D
670 PRINT USING 600 ; W
680 PRINT USING 610 ; F
690 PRINT USING 620 ; E
700 PRINT USING 630 ; Z
710 IF Q$="N" THEN 730
720 PRINT USING 640 ; U,Z
730 ! ***********************************************
740 ! **** ENTER FOCUS AND STEER INFORMATION  ****
750 ! ***********************************************
760 IMAGE "SUBARRAY NO.",4X,"PHASE SHIFT",4X,"MAGNITUDE"
770 IMAGE 3X,DD,12X,DDD.DD,10X,D.DD
780 PRINT USING 760
790 FOR I=1 TO J
800 IF Q$="N" THEN P=PHI(I) @ GOTO 840 ELSE 810
810 V=I*W-W/2-D/2
820 MAG(I)=1 ! NO SHADING
830 P=B*(SQR ((U-V)*(U-V)+Z*Z)-Z)
840 PRINT USING 770 ; I,P/PI *180,MAG(I)
850 FOR N=(I-1)*H+1 TO I*H
860 DISP N
870 T(N)=P @ SOURCEMAG(N)=MAG(I)
880 NEXT N
890 NEXT I
900 ! ***************************************************************
910 ! *****  CALCULATE THE PHASE SHIFT FROM POINT TO POINT ******
920 ! ***************************************************************
930 !
940 FOR M=1 TO T ! FOR EACH FIELD POINT...
950 U(M)=M*E-E/2-F/2
960 FOR N=1 TO T ! ....TO EACH SOURCE POINT
970 V=N*A-A/2-D/2
980 DIST=SQR ((U(M)-V)*(U(M)-V)+Z*Z) ! THE SEPARATION BETWEEN THE POINTS
990 P(N,M)=T(N)-B*DIST ! SOURCE AND SPACE PHASE
1000 NEXT N
1010 R(M)=0
1020 Q(M)=0
1030 NEXT M
1040 ! *****************************************************
1050 ! *****  CALCULATE FIELD INTENSITY ******************
1060 ! *****************************************************
1070 PRINT
1080 IMAGE "INDEX",2X,"POS.",3X,"FIELD INTENSITY (dB)"
1090 PRINT USING 1080
1100 FOR M=1 TO T ! THE FIELDSTRENGTH AT EACH FIELD POINT IS.....
1110 FOR N=1 TO T ! ......A WEIGHTED SUM OF SOURCE CONTRIBUTIONS
1120   R(M)=SOURCEMAG(N)*COS (P(N,M))+R(M)
```

```
1130   Q(M)=SOURCEMAG(N)*SIN (P(N,M))+Q(M)
1140 NEXT N
1150 F(M)=10*LGT ((R(M)*R(M)+Q(M)*Q(M))/(T*T))
1160 ! F(M) IS THE NORMALIZED FIELD INTENSITY
1170 PRINT USING 110 ; M,U(M),F(M)
1180 NEXT M
1190 ! !**********************************************
1200 ! **** THE GRAPHICS START HERE ******************
1210 ! **********************************************
1220 GCLEAR @ GRAPHALL
1230 SCALE -1.1,1.1,-.1,1.1
1240 XAXIS 0,.25,-1,1
1250 YAXIS 0,.25,0,1
1260 FRAME
1270 CSIZE 5
1280 MOVE .05,1
1290 LORG 2
1300 LABEL "0 db"
1310 MOVE .05,.5
1320 LABEL "-10 dB"
1330 MOVE .05,.05
1340 LORG 1
1350 LABEL "-20 dB"
1360 PEN UP
1370 P=-1
1380 FOR M=1 TO T
1390 U=M*E-E/2-F/2
1400 PLOT U,1+F(M)/20
1410 NEXT M
1420 LORG 6
1430 CSIZE 4
1440 MOVE -.5,-.05
1450 LABEL "-0.5"
1460 MOVE -.25,-.05
1470 LABEL "-0.25"
1480 MOVE 0,-.05
1490 LABEL "0"
1500 MOVE .25,-.05
1510 LABEL "0.25"
1520 MOVE .5,-.05
1530 LABEL "0.5"
1540 MOVE -1,1
1550 CSIZE 10
1560 LORG 3
1570 LABEL "FIELD"
1580 MOVE -1,.9
1590 LABEL "INTENSITY"
1600 CSIZE 5
1610 MOVE -1,.8
1620 LABEL "RANGE:",VAL$ (Z)
1630 MOVE -1,.75
1640 LABEL "ARRAY LENGTH:",VAL$ (D)
1650 MOVE -1,.7
1660 IF Q$="N" THEN 1680
1670 LABEL "FOCUS:",VAL$ (FOCUS)
1680 MOVE .75,.05
1690 LORG 2
1700 LABEL "AZIMUTH"
```

```
1710 MOVE .75,-.05
1720 LABEL "meters"
1730 DUMP GRAPHICS 0,0,1
1740 GSTORE FILE$
1750 ! ##########################################
1760 ! #####  DATA FOUND HERE ##################
1770 ! ##########################################
1780 ! No. OF POINTS
1790 ! ARRAY LENGTH
1800 ! ELEMENT LENGTH
1810 ! FIELD WIDTH
1820 ! RANGE
1830 ! FOCAL POINT
1840 DATA 50,.2,.1,2,10,0,"FLOT2"
1850 DATA 45,.3,.1,2,10,0,"FLOT3"
1860 DATA 45,.3,.1,2,10,.05,"FLOT4"
1870 DATA 40,.4,.1,2,10,0,"FLOT5"
1880 DATA 40,.4,.1,2,10,.1,"FLOT6"
1890 IF S$="Y" THEN 1910
1900 GOTO 200
1910 END
```

APPENDIX III

Three programs are provided. The first determines the required focusing and steering phases for all the beams at all ranges. The second converts these values to their HEX equivalents and arranges them in focal zones, ready for transfer to the phase shifters. The third program allows the binary beam shading to be entered separately.

```
10 ! COEFFP
20 ! A PROGRAM ON DISC "THESIS"
30 ! CREATED ON 7/10/83;8/10;1/11;24/11
40 ! THE PROGRAM CALCULATES THE REQIRED FOCUSING AND STEERING
50 !  COEFFICIENTS FOR A 10 ELEMENT ARRAY FORMING 5 BEAMS
60 !  RANGE SPACING INTERVAL IS 2.1875 METERS
70 !  SHORTEST RANGE IS 10 METERS
80 ! BETA IS THE PHASE SHIFT CONSTANT
90  BETA=2*PI /.00487 ! WAVELENGTH IS 4.87 MILLIMETERS
100 OPTION BASE 1
110 DIM COEFF(20,320),X(64),Z(64),RANGE(10),PHI(10)
120 ! ELEMENT SPACING IS 0.1 METERS ; BEAM SPACING IS 0.2 METERS
130 ! STORAGE REQUIREMENT FOR DATA IS 64*20*8*5 BYTES
140 !
160 PRINT CHR$ (27)&"&l18D"
170 CLEAR
180 RINC=140/64 ! 2.1875 METERS PER FOCAL ZONE
190 RZERO=10
200 ! DATA TO ARRAY COEFF(,); FIRST BEAM 1...THEN BEAM 5
210 IMAGE 11A,2X,10(DD,5X)
220 IMAGE DDZ.DDD,4X,10(DDZ.D,2X)
230 FOR J=1 TO 5 @ ! BEEP 10,1000
240 PRINT CHR$ (12)
250 PRINT " FOCUSING PHASES FOR BEAM No. ";J
260 PRINT
270 PRINT USING 210 ; "ELEMENT No.",1,2,3,4,5,6,7,8,9,10
280 PRINT "RANGE"
290 PRINT
300 BEAM=-.4+.2*(J-1) ! 5 BEAMS STARTING AT X=-0.4 ENDING AT X=0.4
310 FOR K=1 TO 64 ! 64 FOCAL ZONES
320 Z(K)=RZERO+(K-1)*RINC
330 FOR I=1 TO 10 ! 20 COEFFICIENTS,10 PAIRS;ORDERED COS/SIN/COS ETC.
340 X(K)=.1*I-.55
350 RANGE(I)=SQR (Z(K)^2+(X(K)-BEAM)^2)-Z(K)
360 PHI(I)=BETA*RANGE(I) ! PHI IS THE REQUIRED FOCUSING PHASE IN RADIANS
370 COEFF(2*I-1,K+(J-1)*64)=COS (PI /4-PHI(I))
380 COEFF(2*I,K+(J-1)*64)=SIN (PI /4-PHI(I))
390 PHI(I)=RTD (PHI(I) MOD (2*PI ))
400 NEXT I
410 PRINT USING 220 ; Z(K),PHI(1),PHI(2),PHI(3),PHI(4),PHI(5),PHI(6),PHI(7),PHI(
8),PHI(9),PHI(10)
420 NEXT K
430 NEXT J
440 GOTO 600
450 ASSIGN# 1 TO  "COEFF1" ! OPEN DATA FILE
460 PRINT# 1 ; COEFF(,) ! STORE ARRAY
470 ASSIGN# 1 TO  * ! CLOSE FILE
480 END
```

```
10 ! PHEXCO ; Program for HEX COefficients
20 ! A PROGRAM ON DISC "THESIS"
30 ! CREATED ON 3/2/84
40 ! THE PROGRAM CALCULATES THE REQIRED FOCUSING AND STEERING
50 !  COEFFICIENTS FOR A 10 ELEMENT ARRAY FORMING 5 BEAMS IN HEX
60 !  RANGE SPACING INTERVAL IS 2.1875 METERS
70 !  SHORTEST RANGE IS 10 METERS
80 ! BETA IS THE PHASE SHIFT CONSTANT
90  BETA=2*PI /.00487 ! WAVELENGTH IS 4.87 MILLIMETERS
100 OPTION BASE 1@ DEG
110 A$="0123456789ABCDEF"
120 DIM COHEX$(340)[40],X(64),Z(64),RANGE(10),PHI(10),U$[40]
130 ! ELEMENT SPACING IS 0.1 METERS ; BEAM SPACING IS 0.2 METERS
140 ! STORAGE REQUIREMENT FOR DATA IS 64*40*5 BYTES
150 ! 64 ZONES , 5 BEAMS , 20 HEX PAIRS PER BEAM
170 ASSIGN# 1 TO  "HEXCODATA" ! OPEN DATA FILE
180 CLEAR
190 RINC=140/64 ! 2.1875 METERS PER FOCAL ZONE
200 RZERO=10
210 ! DATA TO ARRAY COHEX$; FOCAL ZONE BY ZONE , BEAMS 1 TO 5
230 FOR K=1 TO 64 ! 64 FOCAL ZONES
240 PRINT "ZONE No.:";K
250 FOR J=1 TO 5 ! 5 BEAMS PER ZONE
260 PRINT "BEAM No.:";J
270 BEAM=-.4+.2*(J-1) ! 5 BEAMS STARTING AT X=-0.4 ENDING AT X=0.4
280 Z(K)=RZERO+(K-1)*RINC
290 FOR I=1 TO 10 ! 20 COEFFICIENTS,10 PAIRS;ORDERED COS/SIN/COS ETC.
300 X(K)=.1*I-.55
310 RANGE(I)=SQR (Z(K)^2+(X(K)-BEAM)^2)-Z(K)
320 PHI(I)=BETA*RANGE(I) ! PHI IS THE REQUIRED FOCUSING PHASE IN RADIANS
330 PHI(I)=RTD (PHI(I) MOD (2*PI ))
340 C=128-127*COS (181-PHI(I))
350 S=128-127*SIN (181-PHI(I))
360 GOSUB DECTOHEX
370 L=(K-1)*5+J
380 COHEX$(L)[4*I-3,4*I-2]=C$[1,2]
390 COHEX$(L)[4*I-1,4*I]=S$[1,2]
400 NEXT I
410 PRINT COHEX$(L)[1,40]
420 U$=COHEX$(L)[1,40]
430 PRINT# 1,L ; U$ ! STORE FOCAL ZONE DATA , ONE BEAM AT A TIME
440 NEXT J
450 NEXT K
460 GOTO 480
470 ASSIGN# 1 TO  * ! CLOSE FILE
480 END
490 DECTOHEX:
500 Q=C
510 B=INT (RMD (Q,16))
520 A=Q/16-B/16
530 C$[1,1]=A$[A+1,A+1] @ C$[2,2]=A$[B+1,B+1]
540 Q=S
550 B=INT (RMD (Q,16))
560 A=Q/16-B/16
570 S$[1,1]=A$[A+1,A+1] @ S$[2,2]=A$[B+1,B+1]
580 RETURN
```

```
10 ! PHEXSHAD ; A PROGRAM TO PERFORM THE BEAM SHADING
20 ! DISC ; THESIS
30 ! CREATED ON 7/2/84
40 ! P.A.FOX
50 ! ##################################################
60 ! # THE HEX PHASE DATA IS FETCHED FROM A FILE   ###
70 ! # CALLED 'HEXCODATA'  AND SHADING IS PERFORMED ##
80 ! # THE SHADED DATA IS RETURNED TO 'HEXSHADE'    ##
90 ! ##################################################
100 DIM COHEX$(340)[40],SHADE$(340)[10]
110 !
120 !
130 !
140 ASSIGN# 1 TO  "HEXCODATA" ! OPEN SOURCE FILE
150 FOR K=1 TO 64
160 FOR J=1 TO 5
170 L=(K-1)*5+J
180 READ# 1 ; COHEX$(L)[1,40]
190 ! DISP COHEX$(L)[1,40]
200 SHADE$(L)[1,10]="0000000000"
210 NEXT J
220 NEXT K
230 ASSIGN# 1 TO  * ! CLOSE SOURCE FILE
240 !
250 !
260 FOR K=1 TO 64 ! 64 FOCAL ZONES
270 FOR J=1 TO 5 ! 5 BEAMS
280 DISP "FOCAL ZONE No.:";K,"BEAM No.:";J
290 L=(K-1)*5+J
300 DISP COHEX$(L)[1,40]
310 IF L<= 5 THEN GOTO RESHADE
320 DISP SHADE$(L-5)[1,10]
330 DISP "TYPE Y TO CHANGE SHADING";
340 INPUT ANSWER$
350 IF ANSWER$="Y" THEN GOTO RESHADE
360 SHADE$(L)[1,10]=SHADE$(L-5)[1,10] @ DISP SHADE$(L)[1,10]
370 FOR I=1 TO 10
380 SHADE=VAL (SHADE$(L)[I,I])
390 IF SHADE=1 THEN 410
400 COHEX$(L)[(I-1)*4+1,I*4]="8080" ! SHADE TO ZERO
410 NEXT I
420 DISP COHEX$(L)[1,40] @ PRINT COHEX$(L)[1,40]
430 NEXT J
440 NEXT K
450 GOTO SAVEFILE
460 !
470 !
480 !
490 RESHADE:
500 DISP "ENTER SHADING e.g. 0011000000";
510 INPUT SHADE$(L)[1,10]
520 GOTO 370
530 !
540 !
550 SAVEFILE:
```

```
560 ASSIGN# 1 TO  "HEXSHADE"
570 FOR L=1 TO 320
580 PRINT# 1 ; COHEX$(L)[1,40]
590 NEXT L
600 ASSIGN# 1 TO  # ! CLOSE FILE
610 !
620 !
630 END
```

APPENDIX IV : Microprocessor software

```
PAGE  1     FOX ASSEMBLER 8085V1/2              SOURCE FILE: IMAGE

LOC   OBJ     LINE  SOURCE STATEMENT
0000            1                               ;EDITOR FILE: MCPED
0000            2                               ;ASCII  FILE: IMAGE
0000            3                               ;
0000            4                               ;HEX FILE: IMAGE/HEX
0000            5                               ;
0000            6                               ;REVISION RECORD
0000            7                               ;1983 19/7,27/7,28/7,29/8,12/9,13/9,4/10
0000            8                               ;1984 15/1,16/1
0000            9                               ;1984 5/3,6/3,12/3,13/3,14/3
0000           10                               ;1984 4/6,5/6,6/6,7/6,12/6,13/6,14/6,22/6
0000           11                               ;1984 23/6,25/6
0000           12                               ;******************************
0000           13                               ;DEFINE VARIABLES AND POINTERS
0000           14                               ;
0000           15                               ;
0000           16  STCK:     EQU   #7FFF       ;SET STACK ON TOP OF RAM (256 BYTES)
0000           17  PHBASE:   EQU   #7EEC       ;VARIABLE BASE OF FOCAL ZONE PHASES
0000           18  INCHEC:   EQU   #7EEB       ;STATUS WORD FOR RANGE SAMPLING
0000           19  STAT:     EQU   #7EEA       ;STATUS WORD FOR PHASE TRANSFER
0000           20  BASOUT:   EQU   #7EE8       ;VARIABLE BASE ADRESS OF OUTPUT PAD
0000           21  BASIN:    EQU   #7EE6       ;VARIABLE BASE ADRESS OF INPUT PAD
0000           22  ZONE:     EQU   #7EE5       ;VARIABLE ZONE INDEX
0000           23  VRIN:     EQU   #7EE3       ;VARIABLE POINTER IN INPUT PAD
0000           24  VROUT:    EQU   #7EE1       ;
0000           25  GTEMP:    EQU   #7EE0       ;TEMPORARY STORAGE OF GAIN BYTE
0000           26  GSET:     EQU   #2700       ;ROM LOCATION OF INITIAL GAINS
0000           27  GAIN:     EQU   #6900       ;RAM LOCATION OF CURRENT GAINS
0000           28  ABASE:    EQU   #4000       ;RAM ADRESS PAD A
0000           29  BBASE:    EQU   #5400       ;RAM ADRESS PAD B
0000           30                               ;
0000           31                               ;******************************
0000           32            ORG   #0000       ;TRANSFER INITIAL GAIN BYTES ON POWER UP
0000           33                               ;
0000  063F     34            MVI   B,#3F       ;64 BYTES TO TRANSFER
0002  110069   35            LXI   D,GAIN      ;POINT TO CURRENT GAINS
0005  210027   36            LXI   H,GSET      ;POINT TO INITIAL GAINS
0008  7E       37  TRANS:    MOV   A,M         ;FETCH INITIAL
0009  12       38            STAX  D           ;STORE IN CURRENT
000A  23       39            INX   H           ;
000B  13       40            INX   D           ;
000C  05       41            DCR   B           ;
000D  C20800   42            JNZ   TRANS       ;KEEP AT IT TILL 64
0010           43                               ;
0010           44                               ;******************************
0010  C35000   45            JMP   INIT        ;JUMP OVER INTERRUPTS
0013           46                               ;******************************
0013           47                               ;INTERRUPT REDIRECTING
0013           48            ORG   #2C         ;RST 5.5 NEW IMAGE REQUEST
002C  C38B00   49            JMP   TX          ;GOTO TX
002F           50                               ;******************************
```

```
PAGE  2     FOX ASSEMBLER 8085V1/2          SOURCE FILE: IMAGE

LOC   OBJ     LINE  SOURCE STATEMENT
002F            1          ORG   #34        ;RST 6.5 REQUEST FOR MORE DATA
0034  D5          2          PUSH  D          ;SAVE D,E,A IN CASE INT OCURRS IN FAZSET
0035  F5          3          PUSH  PSW        ;
0036  C3C101      4          JMP   DOUT       ;PROCESS DATA REQUEST
0039            5                           ;*******************************
0039            6          ORG   #3C        ;RST 7.5 RANGE SAMPLE INTERRUPT
003C  47          7          MOV   B,A        ;SAVE CONTENTS OF ACC.
003D  3AEB7E      8          LDA   INCHEC     ;CHECK IF FINISHED WITH INPUT
0040  FE1C        9          CPI   #1C        ;IF YES THEN NO RANGE SAMPLING
0042  78          10         MOV   A,B        ;RESTORE ACC. WITHOUT AFFECTING FLAGS
0043  C8          11         RZ               ;
0044  E5          12         PUSH  H          ;IN CASE DATA TO FIFO IS INT.
0045  D5          13         PUSH  D          ;IN CASE DATA TO PHASE SHIFTERS IS INT
0046  F5          14         PUSH  PSW        ;
0047  C36201      15         JMP   ADIN       ;PROCESS RANGE SAMPLING
004A            16                          ;*******************************
004A            17                          ;MAIN ROUTINE
004A            18                          ;*******************************
004A            19         ORG   #0050      ;
0050  210040    20  INIT:  LXI   H,ABASE    ;FETCH ABASE ADRESS
0053  22E67E    21         SHLD  BASIN      ;AND ASSIGN AS INPUT PAD
0056  22E37E    22         SHLD  VRIN       ;SET POINTER IN INPUT PAD TO BASE
0059  210054    23         LXI   H,BBASE    ;
005C  22E87E    24         SHLD  BASOUT     ;ASSIGN OUTPUT PAD TO BBASE
005F  22E17E    25         SHLD  VROUT      ;AND INITIALIZE THE POINTER
0062            26                          ;*****
0062            27                          ;SET UP THE THREE COUNTERS
0062  3E3A      28         MVI   A,#3A      ;COUNTER 0 MODE 5
0064  D333      29         OUT   #33        ;
0066  3E49      30         MVI   A,#49      ;PRESET TO 73
0068  D330      31         OUT   #30        ;FIRST LSB
006A  3E00      32         MVI   A,#00      ;THEN  MSB
006C  D330      33         OUT   #30        ;
006E  3E7A      34         MVI   A,#7A      ;COUNTER 1 MODE 5
0070  D333      35         OUT   #33        ;
0072  3E00      36         MVI   A,#00      ;PRESET TO 1024
0074  D331      37         OUT   #31        ;
0076  3E04      38         MVI   A,#04      ;
0078  D331      39         OUT   #31        ;
007A  3EBA      40         MVI   A,#BA      ;COUNTER 2 MODE 5
007C  D333      41         OUT   #33        ;
007E  3E49      42         MVI   A,#49      ;PRESET TO 73
0080  D332      43         OUT   #32        ;
0082  3E00      44         MVI   A,#00      ;
0084  D332      45         OUT   #32        ;FINISHED SETTING COUNTERS
0086            46                          ;*******************************
0086            47                          ;READY FOR ACTION!!!!
0086  3E1E      48  READY: MVI   A,#1E      ;ENABLE ONLY RST 5.5 FOR NEW IMAGE
0088  30        49         SIM              ;
0089  FB        50         EI               ;
```

```
PAGE  3     FOX ASSEMBLER 8085V1/2                SOURCE FILE: IMAGE

LOC   OBJ     LINE  SOURCE STATEMENT
008A  76        1           HLT             ;WAIT FOR NEW IMAGE REQUEST
008B            2                           ;BEFORE TRANSMITTING PULSE
008B  D338      3  TX:      OUT   #38       ;SEND TX PULSE
008D  D335      4           OUT   #35       ;RESET ALL TIMERS
008F  21000B    5           LXI   H,#0800   ;BASE OF PHASE DATA AT #0800
0092  22EC7E    6           SHLD  PHBASE    ;TO PHBASE
0095  2AE67E    7           LHLD  BASIN     ;FETCH PREVIOUS INPUT PAD BASE
0098  EB        8           XCHG            ;KEEP IT IN D,E
0099  2AE87E    9           LHLD  BASOUT    ;FETCH PREVIOUS OUTPUT PAD BASE
009C  22E67E    10          SHLD  BASIN     ;AND EXCHANGE THEM
009F  22E37E    11          SHLD  VRIN      ;INIT. POINTER IN INPUT PAD
00A2  EB        12          XCHG            ;AND KEEP IN D,E
00A3  22E87E    13          SHLD  BASOUT    ;OUTPUT PAD POINTER IN H,L
00A6  22E17E    14          SHLD  VROUT     ;AND INIT. POINTER
00A9            15                          ;
00A9  31FF7F    16          LXI   SP,STCK   ;RESTORE STACK
00AC  3E00      17          MVI   A,#00     ;
00AE  32E57E    18          STA   ZONE      ;RESET THE ZONE INDEX
00B1  32EB7E    19          STA   INCHEC    ;AND SET THE FLAG TO ALLOW RANGE SAMPLING
00B4            20                          ;*****************************
00B4            21                          ;TRANSFER 32 BYTES TO FIFO
00B4            22                          ;H,L POINT TO OUTPUT PAD
00B4  7E        23          MOV   A,M       ;FETCH OUTPUT DATA BYTE  1
00B5  D33C      24          OUT   #3C       ;
00B7  23        25          INX   H         ;
00B8  7E        26          MOV   A,M       ;FETCH OUTPUT DATA BYTE
00B9  D33C      27          OUT   #3C       ;
00BB  23        28          INX   H         ;
00BC  7E        29          MOV   A,M       ;FETCH OUTPUT DATA BYTE
00BD  D33C      30          OUT   #3C       ;
00BF  23        31          INX   H         ;
00C0  7E        32          MOV   A,M       ;FETCH OUTPUT DATA BYTE
00C1  D33C      33          OUT   #3C       ;
00C3  23        34          INX   H         ;
00C4  7E        35          MOV   A,M       ;FETCH OUTPUT DATA BYTE  5
00C5  D33C      36          OUT   #3C       ;
00C7  23        37          INX   H         ;
00C8  7E        38          MOV   A,M       ;FETCH OUTPUT DATA BYTE
00C9  D33C      39          OUT   #3C       ;
00CB  23        40          INX   H         ;
00CC  7E        41          MOV   A,M       ;FETCH OUTPUT DATA BYTE
00CD  D33C      42          OUT   #3C       ;
00CF  23        43          INX   H         ;
00D0  7E        44          MOV   A,M       ;FETCH OUTPUT DATA BYTE
00D1  D33C      45          OUT   #3C       ;
00D3  23        46          INX   H         ;
00D4  7E        47          MOV   A,M       ;FETCH OUTPUT DATA BYTE
00D5  D33C      48          OUT   #3C       ;
00D7  23        49          INX   H         ;
00D8  7E        50          MOV   A,M       ;FETCH OUTPUT DATA BYTE  10
```

```
PAGE  4     FOX ASSEMBLER 8085V1/2              SOURCE FILE: IMAGE

LOC   OBJ     LINE  SOURCE STATEMENT
00D9  D33C       1          OUT   #3C          ;
00DB  23         2          INX   H            ;
00DC  7E         3          MOV   A,M          ;FETCH OUTPUT DATA BYTE
00DD  D33C       4          OUT   #3C          ;
00DF  23         5          INX   H            ;
00E0  7E         6          MOV   A,M          ;FETCH OUTPUT DATA BYTE
00E1  D33C       7          OUT   #3C          ;
00E3  23         8          INX   H            ;
00E4  7E         9          MOV   A,M          ;FETCH OUTPUT DATA BYTE
00E5  D33C      10          OUT   #3C          ;
00E7  23        11          INX   H            ;
00E8  7E        12          MOV   A,M          ;FETCH OUTPUT DATA BYTE
00E9  D33C      13          OUT   #3C          ;
00EB  23        14          INX   H            ;
00EC  7E        15          MOV   A,M          ;FETCH OUTPUT DATA BYTE  15
00ED  D33C      16          OUT   #3C          ;
00EF  23        17          INX   H            ;
00F0  7E        18          MOV   A,M          ;FETCH OUTPUT DATA BYTE
00F1  D33C      19          OUT   #3C          ;
00F3  23        20          INX   H            ;
00F4  7E        21          MOV   A,M          ;FETCH OUTPUT DATA BYTE
00F5  D33C      22          OUT   #3C          ;
00F7  23        23          INX   H            ;
00F8  7E        24          MOV   A,M          ;FETCH OUTPUT DATA BYTE
00F9  D33C      25          OUT   #3C          ;
00FB  23        26          INX   H            ;
00FC  7E        27          MOV   A,M          ;FETCH OUTPUT DATA BYTE
00FD  D33C      28          OUT   #3C          ;
00FF  23        29          INX   H            ;
0100  7E        30          MOV   A,M          ;FETCH OUTPUT DATA BYTE  20
0101  D33C      31          OUT   #3C          ;
0103  23        32          INX   H            ;
0104  7E        33          MOV   A,M          ;FETCH OUTPUT DATA BYTE
0105  D33C      34          OUT   #3C          ;
0107  23        35          INX   H            ;
0108  7E        36          MOV   A,M          ;FETCH OUTPUT DATA BYTE
0109  D33C      37          OUT   #3C          ;
010B  23        38          INX   H            ;
010C  7E        39          MOV   A,M          ;FETCH OUTPUT DATA BYTE
010D  D33C      40          OUT   #3C          ;
010F  23        41          INX   H            ;
0110  7E        42          MOV   A,M          ;FETCH OUTPUT DATA BYTE
0111  D33C      43          OUT   #3C          ;
0113  23        44          INX   H            ;
0114  7E        45          MOV   A,M          ;FETCH OUTPUT DATA BYTE  25
0115  D33C      46          OUT   #3C          ;
0117  23        47          INX   H            ;
0118  7E        48          MOV   A,M          ;FETCH OUTPUT DATA BYTE
0119  D33C      49          OUT   #3C          ;
011B  23        50          INX   H            ;
```

```
PAGE  5     FOX ASSEMBLER 8085V1/2                SOURCE FILE: IMAGE

LOC   OBJ     LINE  SOURCE STATEMENT
011C  7E        1           MOV    A,M          ;FETCH OUTPUT DATA BYTE
011D  D33C      2           OUT    #3C          ;
011F  23        3           INX    H            ;
0120  7E        4           MOV    A,M          ;FETCH OUTPUT DATA BYTE
0121  D33C      5           OUT    #3C          ;
0123  23        6           INX    H            ;
0124  7E        7           MOV    A,M          ;FETCH OUTPUT DATA BYTE
0125  D33C      8           OUT    #3C          ;
0127  23        9           INX    H            ;
0128  7E       10           MOV    A,M          ;FETCH OUTPUT DATA BYTE  30
0129  D33C     11           OUT    #3C          ;
012B  23       12           INX    H            ;
012C  7E       13           MOV    A,M          ;FETCH OUTPUT DATA BYTE
012D  D33C     14           OUT    #3C          ;
012F  23       15           INX    H            ;
0130  7E       16           MOV    A,M          ;
0131  D33C     17           OUT    #3C          ;OUTPUT DATA BYTE NUMBER 32
0133  23       18           INX    H            ;INCREMENT VROUT BEFORE REPLACING
0134  22E17E   19           SHLD   VROUT        ;REPLACE VARIABLE OUTPUT PAD POINTER
0137           20                                ;END OF INITIAL DATA TRANSFER
0137           21                                ;
0137  3E1D     22           MVI    A,#1D        ;ENABLE RST 6.5 FOR DATA REQUEST (1101)
0139  30       23           SIM                 ;
013A  FB       24           EI                  ;
013B           25                                ;**********************************
013B           26                                ;SET UP FIRST SET OF PHASES
013B  CD2202   27  FAZIT:   CALL   FAZSET        ;TRANSFER THE PHASES
013E  D3E0     28           OUT    #E0          ;
0140  3AE07E   29           LDA    GTEMP        ;FETCH GAIN BYTE AND TRANSFER
0143  D320     30           OUT    #20          ;
0145           31                                ;
0145           32                                ;
0145  3E19     33  DATIN:   MVI    A,#19        ;ENABLE DATA REQ. AND RANGE SAMPLE INTS. (1001)
0147  32EA7E   34           STA    STAT         ;SET PHASE STATUS WORD NON ZERO
014A  30       35           SIM                 ;
014B  FB       36           EI                  ;ENABLE RST 6.5 AND 7.5
014C  CD2202   37           CALL   FAZSET       ;START SETTING UP NEXT PHASES
014F           38                                ;
014F           39                                ;
014F  21FFFF   40  TIMOUT:  LXI    H,#FFFF      ;WAIT A LIMITED TIME AFTER PHASE TRANSFER
0152  3AEA7E   41  LOOP:    LDA    STAT         ;WHILE CHECKING IF PHASES HAVE BEEN APPLIED
0155  A7       42           ANA    A            ;PHASES ARE APPLIED EVERY 16 RANGE SAMPLES
0156  CA4501   43           JZ     DATIN        ; DURING EXECUTION OF SAMPLING ROUTINE
0159  2B       44           DCX    H            ;
015A  7D       45           MOV    A,L          ;
015B  B4       46           ORA    H            ;
015C  C25201   47           JNZ    LOOP         ;
015F           48                                ;
015F           49                                ;
015F  C35000   50           JMP    INIT         ;ERROR CONDITION GOTO INIT AND TRY AGAIN
```

```
PAGE  6     FOX ASSEMBLER 8085V1/2              SOURCE FILE: IMAGE

LOC   OBJ     LINE  SOURCE STATEMENT
0162            1                               ;*****************************
0162            2                               ;A ROUTINE TO READ THE A/D CONVERTORS
0162            3                               ;ALTERS REGISTERS A B C H L
0162            4                               ;THIS ROUTINE IS NOT INTERUPTABLE
0162            5                               ;A/D's ARE STARTED AFTER BEING READ
0162            6                               ;ZONE NUMBER IS DETERMINED AND UPDATED
0162            7                               ;IF ZONE CHANGES THE PHASES ARE APPLIED
0162            8                               ;STAT IS SET TO ZERO TO INDICATE THAT NEW
0162            9                               ; PHASES MAY NOW BE SET UP
0162            10                              ;GAIN TRANSFER FOLLOWS ON PHASES
0162            11                              ;
0162  2AE37E    12  ADIN:   LHLD   VRIN         ;POINT TO CURRENT INPUT PAD
0165  010004    13          LXI    B,#0400      ;LOAD 1024 TO B,C
0168  DB28      14          IN     #28          ;READ BEAM SAMPLE
016A  77        15          MOV    M,A          ;STORE IN INPUT PAD
016B  09        16          DAD    B            ;MOVE TO NEXT SWATH
016C  DB29      17          IN     #29          ;READ BEAM 2 SAMPLE
016E  77        18          MOV    M,A          ;STORE IN INPUT PAD
016F  09        19          DAD    B            ;MOVE TO NEXT SWATH
0170  DB2A      20          IN     #2A          ;READ BEAM 3 SAMPLE
0172  77        21          MOV    M,A          ;STORE IN INPUT PAD
0173  09        22          DAD    B            ;MOVE TO NEXT SWATH
0174  DB2B      23          IN     #2B          ;READ BEAM 4 SAMPLE
0176  77        24          MOV    M,A          ;STORE IN INPUT PAD
0177  09        25          DAD    B            ;MOVE TO NEXT SWATH
0178  DB2C      26          IN     #2C          ;READ BEAM 5 SAMPLE
017A  77        27          MOV    M,A          ;STORE IN INPUT PAD
017B            28                              ;
017B  D32F      29          OUT    #2F          ;RETRIGGER THE A/D CONVERTORS
017D  7C        30          MOV    A,H          ;FETCH HI BYTE OF INPUT POINTER
017E  D610      31          SUI    #10          ;SUBTRACT 4096 AND RETURN POINTER
0180  67        32          MOV    H,A          ; TO H,L
0181  23        33          INX    H            ;INCREMENT INPUT POINTER
0182  22E37E    34          SHLD   VRIN         ;AND RETURN TO VRIN
0185            35                              ;
0185  7D        36          MOV    A,L          ;DETERMINING NEW ZONE INDEX
0186  E60F      37          ANI    #0F          ;FROM LOW BYTE OF INPUT POINTER
0188  C2AD01    38          JNZ    NEXT         ;IF NO NEW ZONE THEN CONTINUE WITHOUT REFOCUS
018B            39                              ;
018B            40                              ;
018B  2AEC7E    41  RCHK:   LHLD   PHBASE        ;FETCH PREVIOUS BASE OF PHASE DATA
018E  016400    42          LXI    B,#0064      ;
0191  09        43          DAD    B            ;ADD A 100 BYTE OFFSET FOR NEW ZONE
0192  22EC7E    44          SHLD   PHBASE       ;
0195  3AE57E    45          LDA    ZONE         ;FETCH CURRENT ZONE INDEX
0198  C601      46          ADI    #01          ;AND INCREMENT IT
019A  32E57E    47          STA    ZONE         ;
019D  FE40      48          CPI    #40          ;IF ZONE No. IS 64 THEN THE IMAGE IS COMPLETE
019F  CAB501    49          JZ     INFIN        ;EXIT INPUT ROUTINE
01A2            50                              ;
```

```
PAGE  7     FOX ASSEMBLER 8085V1/2          SOURCE FILE: IMAGE

LOC   OBJ     LINE  SOURCE STATEMENT
01A2            1                          ;
01A2  D3E0      2  PHOUT:   OUT   #E0       ;APPLY PHASES
01A4  3AE07E    3          LDA   GTEMP      ;FETCH GAIN FROM TEMP STORAGE
01A7  D320      4          OUT   #20        ;REPROGRAM GAIN
01A9  AF        5          XRA   A          ;
01AA  32EA7E    6          STA   STAT       ;SET STAT TO ZERO TO INDICATE PHASES APPLIED
01AD            7                           ;
01AD  3E19      8  NEXT:   MVI   A,#19      ;REENABLE RANGE AND DATA INTERRUPTS (1001)
01AF  30        9          SIM              ;
01B0  F1        10         POP   PSW        ;
01B1  D1        11         POP   D          ;
01B2  E1        12         POP   H          ;
01B3  FB        13         EI               ;
01B4  C9        14         RET              ;RETURN TO SETTING UP PHASES
01B5            15                          ;**********************************************
01B5            16                          ;AT END OF SWATH INPUT SERVICE ONLY NEW IMAGE AND
01B5            17                          ;MORE DATA REQESTS
01B5  3E1C      18 INFIN:  MVI   A,#1C       ;ENABLE ONLY RST 5.5 AND 6.5
01B7  30        19         SIM              ;
01B8  32EB7E    20         STA   INCHEC     ;SET THE INPUT CHECK FLAG NON ZERO
01BB            21                          ;
01BB  FB        22         EI               ;
01BC  76        23         HLT              ;WAIT FOR INT.
01BD  F3        24         DI               ;DISABLE RANGE SAMPLING ON RETURN
01BE  C3B501    25         JMP   INFIN      ;AND GO WAIT FOR NEW DATA REQUEST
01C1            26                          ;EXIT ONLY VIA  NEW IMAGE REQUEST
01C1            27                          ;******************************************
01C1            28                          ;DATA OUTPUT ROUTINE
01C1            29                          ;
01C1            30                          ;******************************************
01C1            31                          ;REGISTERS H L A ARE AFFECTED
01C1            32                          ;A REQUEST FOR DATA HAS BEEN RECIEVED FROM FIFO
01C1            33                          ;OUTPUT 20 BYTE OF PREVIOUS IMAGE
01C1            34                          ;FORMATTING IS PERFORMED HERE
01C1  3E0B      35 DOUT:   MVI   A,#0B       ;ENABLE RANGE SAMPLING INT. WITHOUT RESETTING
01C3  30        36         SIM              ;BUT ONLY AFTER AT LEAST ONE BYTE IS TRANSFERRED
01C4            37                          ;
01C4  2AE17E    38         LHLD  VROUT      ;SET UP H,L TO POINT TO OUTPUT PAD
01C7  7E        39         MOV   A,M        ;FETCH OUTPUT DATA BYTE  1
01C8  D33C      40         OUT   #3C        ;
01CA  FB        41         EI               ;
01CB  23        42         INX   H          ;
01CC  7E        43         MOV   A,M        ;FETCH OUTPUT DATA BYTE
01CD  D33C      44         OUT   #3C        ;
01CF  23        45         INX   H          ;
01D0  7E        46         MOV   A,M        ;FETCH OUTPUT DATA BYTE
01D1  D33C      47         OUT   #3C        ;
01D3  23        48         INX   H          ;
01D4  7E        49         MOV   A,M        ;FETCH OUTPUT DATA BYTE
01D5  D33C      50         OUT   #3C        ;
```

```
PAGE  8     FOX ASSEMBLER 8085V1/2              SOURCE FILE: IMAGE

LOC   OBJ     LINE  SOURCE STATEMENT
01D7  23        1           INX   H             ;
01D8  7E        2           MOV   A,M           ;FETCH OUTPUT DATA BYTE  5
01D9  D33C      3           OUT   #3C           ;
01DB  23        4           INX   H             ;
01DC  7E        5           MOV   A,M           ;FETCH OUTPUT DATA BYTE
01DD  D33C      6           OUT   #3C           ;
01DF  23        7           INX   H             ;
01E0  7E        8           MOV   A,M           ;FETCH OUTPUT DATA BYTE
01E1  D33C      9           OUT   #3C           ;
01E3  23       10           INX   H             ;
01E4  7E       11           MOV   A,M           ;FETCH OUTPUT DATA BYTE
01E5  D33C     12           OUT   #3C           ;
01E7  23       13           INX   H             ;
01E8  7E       14           MOV   A,M           ;FETCH OUTPUT DATA BYTE
01E9  D33C     15           OUT   #3C           ;
01EB  23       16           INX   H             ;
01EC  7E       17           MOV   A,M           ;FETCH OUTPUT DATA BYTE  10
01ED  D33C     18           OUT   #3C           ;
01EF  23       19           INX   H             ;
01F0  7E       20           MOV   A,M           ;FETCH OUTPUT DATA BYTE
01F1  D33C     21           OUT   #3C           ;
01F3  23       22           INX   H             ;
01F4  7E       23           MOV   A,M           ;FETCH OUTPUT DATA BYTE
01F5  D33C     24           OUT   #3C           ;
01F7  23       25           INX   H             ;
01F8  7E       26           MOV   A,M           ;FETCH OUTPUT DATA BYTE
01F9  D33C     27           OUT   #3C           ;
01FB  23       28           INX   H             ;
01FC  7E       29           MOV   A,M           ;FETCH OUTPUT DATA BYTE
01FD  D33C     30           OUT   #3C           ;
01FF  23       31           INX   H             ;
0200  7E       32           MOV   A,M           ;FETCH OUTPUT DATA BYTE  15
0201  D33C     33           OUT   #3C           ;
0203  23       34           INX   H             ;
0204  7E       35           MOV   A,M           ;FETCH OUTPUT DATA BYTE
0205  D33C     36           OUT   #3C           ;
0207  23       37           INX   H             ;
0208  7E       38           MOV   A,M           ;FETCH OUTPUT DATA BYTE
0209  D33C     39           OUT   #3C           ;
020B  23       40           INX   H             ;
020C  7E       41           MOV   A,M           ;FETCH OUTPUT DATA BYTE
020D  D33C     42           OUT   #3C           ;
020F  23       43           INX   H             ;
0210  7E       44           MOV   A,M           ;FETCH OUTPUT DATA BYTE
0211  D33C     45           OUT   #3C           ;
0213  23       46           INX   H             ;
0214  7E       47           MOV   A,M           ;FETCH OUTPUT DATA BYTE  20
0215  D33C     48           OUT   #3C           ;
0217  23       49           INX   H             ;INCREMENT AND...
0218  22E17E   50           SHLD  VROUT         ;REPLACE VARIABLE OUTPUT PAD POINTER
```

```
PAGE  9     FOX ASSEMBLER 8085V1/2                SOURCE FILE: IMAGE

LOC   OBJ     LINE  SOURCE STATEMENT
021B  3E19       1          MVI    A,#19        ;REENABLE DATA REQUESTS AND RANGE SAMPLING
021D  30         2          SIM                 ;
021E  F1         3          POP    PSW          ;
021F  D1         4          POP    D            ;
0220  FB         5          EI                  ;
0221  C9         6          RET                 ;
0222             7                              ;
0222             8                              ;**********************************
0222             9                              ;
0222            10                              ;THIS ROUTINE SETS UP THE PHASES
0222            11                              ;PRIOR TO THEIR APPLICATION TO THE ARRAY
0222            12                              ;A SINGLE GAIN BYTE FOR THE ZONE IS FETCHED
0222            13                              ;H,L ARE USED BRIEFLY WHILE INTS ARE OFF
0222            14                              ;D,E ARE USED THROUGHOUT , MUST NOT BE ALTERRED
0222            15                              ;
0222            16                              ;
0222  F3        17  FAZSET:   DI                ;INTS ARE DISABLED WHILE THE ZONE INDEX IS USED
0223  2AEC7E    18          LHLD   PHBASE       ;FETCH CURRENT BASE ADRESS OF PHASE DATA
0226  EB        19          XCHG                ;
0227            20                              ;D,E NOW POINTS TO THE SET OF PHASES
0227  3AE57E    21          LDA    ZONE         ;
022A  210069    22          LXI    H,GAIN       ;
022D  85        23          ADD    L            ;
022E  6F        24          MOV    L,A          ;POINT TO GAIN BYTE FOR THIS ZONE
022F  7E        25          MOV    A,M          ;FETCH GAIN BYTE
0230  32E07E    26          STA    GTEMP        ;PLACE IN TEMPORARY STORAGE
0233            27                              ;
0233  FB        28          EI                  ;FINISHED WITH H,L RENABLE INTS.
0234            29                              ;START OF TRANSFER
0234            30                              ;
0234  1A        31          LDAX   D            ;BEAM 1 ELT 1
0235  D340      32          OUT    #40          ;
0237  13        33          INX    D            ;
0238  1A        34          LDAX   D            ;
0239  D380      35          OUT    #80          ;
023B  13        36          INX    D            ;
023C            37                              ;
023C  1A        38          LDAX   D            ;BEAM 1 ELT 2
023D  D341      39          OUT    #41          ;
023F  13        40          INX    D            ;
0240  1A        41          LDAX   D            ;
0241  D381      42          OUT    #81          ;
0243  13        43          INX    D            ;
0244            44                              ;
0244  1A        45          LDAX   D            ;BEAM 1 ELT 3
0245  D342      46          OUT    #42          ;
0247  13        47          INX    D            ;
0248  1A        48          LDAX   D            ;
0249  D382      49          OUT    #82          ;
024B  13        50          INX    D            ;
```

```
PAGE  10      FOX ASSEMBLER 8085V1/2                SOURCE FILE: IMAGE

LOC   OBJ     LINE  SOURCE STATEMENT
024C            1                                   ;
024C  1A        2           LDAX   D                ;BEAM 1 ELT 4
024D  D343      3           OUT    #43              ;
024F  13        4           INX    D                ;
0250  1A        5           LDAX   D                ;
0251  D383      6           OUT    #83              ;
0253  13        7           INX    D                ;
0254            8                                   ;
0254  1A        9           LDAX   D                ;BEAM 1 ELT 5
0255  D344     10           OUT    #44              ;
0257  13       11           INX    D                ;
0258  1A       12           LDAX   D                ;
0259  D384     13           OUT    #84              ;
025B  13       14           INX    D                ;
025C           15                                   ;
025C  1A       16           LDAX   D                ;BEAM 1 ELT 6
025D  D345     17           OUT    #45              ;
025F  13       18           INX    D                ;
0260  1A       19           LDAX   D                ;
0261  D385     20           OUT    #85              ;
0263  13       21           INX    D                ;
0264           22                                   ;
0264  1A       23           LDAX   D                ;BEAM 1 ELT 7
0265  D346     24           OUT    #46              ;
0267  13       25           INX    D                ;
0268  1A       26           LDAX   D                ;
0269  D386     27           OUT    #86              ;
026B  13       28           INX    D                ;
026C           29                                   ;
026C  1A       30           LDAX   D                ;BEAM 1 ELT 8
026D  D347     31           OUT    #47              ;
026F  13       32           INX    D                ;
0270  1A       33           LDAX   D                ;
0271  D387     34           OUT    #87              ;
0273  13       35           INX    D                ;
0274           36                                   ;
0274  1A       37           LDAX   D                ;BEAM 1 ELT 9
0275  D348     38           OUT    #48              ;
0277  13       39           INX    D                ;
0278  1A       40           LDAX   D                ;
0279  D388     41           OUT    #88              ;
027B  13       42           INX    D                ;
027C           43                                   ;
027C  1A       44           LDAX   D                ;BEAM 1 ELT 10
027D  D349     45           OUT    #49              ;
027F  13       46           INX    D                ;
0280  1A       47           LDAX   D                ;
0281  D389     48           OUT    #89              ;
0283  13       49           INX    D                ;
0284           50                                   ;************  NEXT BEAM
```

```
PAGE  11      FOX ASSEMBLER 8085V1/2                SOURCE FILE: IMAGE

LOC   OBJ     LINE  SOURCE STATEMENT
02B4  1A        1           LDAX   D          ;BEAM 2 ELT 1
02B5  D34A      2           OUT    #4A        ;
02B7  13        3           INX    D          ;
02B8  1A        4           LDAX   D          ;
02B9  D38A      5           OUT    #8A        ;
02BB  13        6           INX    D          ;
02BC            7                              ;
02BC  1A        8           LDAX   D          ;BEAM 2 ELT 2
02BD  D34B      9           OUT    #4B        ;
02BF  13       10           INX    D          ;
0290  1A       11           LDAX   D          ;
0291  D38B     12           OUT    #8B        ;
0293  13       13           INX    D          ;
0294           14                              ;
0294  1A       15           LDAX   D          ;BEAM 2 ELT 3
0295  D34C     16           OUT    #4C        ;
0297  13       17           INX    D          ;
0298  1A       18           LDAX   D          ;
0299  D38C     19           OUT    #8C        ;
029B  13       20           INX    D          ;
029C           21                              ;
029C  1A       22           LDAX   D          ;BEAM 2 ELT 4
029D  D34D     23           OUT    #4D        ;
029F  13       24           INX    D          ;
02A0  1A       25           LDAX   D          ;
02A1  D38D     26           OUT    #8D        ;
02A3  13       27           INX    D          ;
02A4           28                              ;
02A4  1A       29           LDAX   D          ;BEAM 2 ELT 5
02A5  D34E     30           OUT    #4E        ;
02A7  13       31           INX    D          ;
02A8  1A       32           LDAX   D          ;
02A9  D38E     33           OUT    #8E        ;
02AB  13       34           INX    D          ;
02AC           35                              ;
02AC  1A       36           LDAX   D          ;BEAM 2 ELT 6
02AD  D34F     37           OUT    #4F        ;
02AF  13       38           INX    D          ;
02B0  1A       39           LDAX   D          ;
02B1  D38F     40           OUT    #8F        ;
02B3  13       41           INX    D          ;
02B4           42                              ;
02B4  1A       43           LDAX   D          ;BEAM 2 ELT 7
02B5  D350     44           OUT    #50        ;
02B7  13       45           INX    D          ;
02B8  1A       46           LDAX   D          ;
02B9  D390     47           OUT    #90        ;
02BB  13       48           INX    D          ;
02BC           49                              ;
02BC  1A       50           LDAX   D          ;BEAM 2 ELT 8
```

```
PAGE  12      FOX ASSEMBLER 8085V1/2                SOURCE FILE: IMAGE

LOC   OBJ     LINE  SOURCE STATEMENT
02BD  D351       1          OUT    #51          ;
02BF  13         2          INX    D            ;
02C0  1A         3          LDAX   D            ;
02C1  D391       4          OUT    #91          ;
02C3  13         5          INX    D            ;
02C4             6                               ;
02C4  1A         7          LDAX   D            ;BEAM 2 ELT 9
02C5  D352       8          OUT    #52          ;
02C7  13         9          INX    D            ;
02C8  1A        10          LDAX   D            ;
02C9  D392      11          OUT    #92          ;
02CB  13        12          INX    D            ;
02CC            13                              ;
02CC  1A        14          LDAX   D            ;BEAM 2 ELT 10
02CD  D353      15          OUT    #53          ;
02CF  13        16          INX    D            ;
02D0  1A        17          LDAX   D            ;
02D1  D393      18          OUT    #93          ;
02D3  13        19          INX    D            ;
02D4            20                              ;BEAM 3
02D4  1A        21          LDAX   D            ;ELT 1
02D5  D354      22          OUT    #54          ;
02D7  13        23          INX    D            ;
02D8  1A        24          LDAX   D            ;
02D9  D394      25          OUT    #94          ;
02DB  13        26          INX    D            ;
02DC            27                              ;
02DC  1A        28          LDAX   D            ;
02DD  D355      29          OUT    #55          ;
02DF  13        30          INX    D            ;
02E0  1A        31          LDAX   D            ;
02E1  D395      32          OUT    #95          ;
02E3  13        33          INX    D            ;
02E4            34                              ;
02E4  1A        35          LDAX   D            ;ELT 3
02E5  D356      36          OUT    #56          ;
02E7  13        37          INX    D            ;
02E8  1A        38          LDAX   D            ;
02E9  D396      39          OUT    #96          ;
02EB  13        40          INX    D            ;
02EC            41                              ;
02EC  1A        42          LDAX   D            ;
02ED  D357      43          OUT    #57          ;
02EF  13        44          INX    D            ;
02F0  1A        45          LDAX   D            ;
02F1  D397      46          OUT    #97          ;
02F3  13        47          INX    D            ;
02F4            48                              ;
02F4  1A        49          LDAX   D            ;ELT 5
02F5  D358      50          OUT    #58          ;
```

```
PAGE  13      FOX ASSEMBLER B0B5V1/2              SOURCE FILE: IMAGE

LOC   OBJ     LINE  SOURCE STATEMENT
02F7  13        1           INX    D            ;
02F8  1A        2           LDAX   D            ;
02F9  D398      3           OUT    #98          ;
02FB  13        4           INX    D            ;
02FC            5                                ;
02FC            6                                ;
02FC  1A        7           LDAX   D            ;
02FD  D359      8           OUT    #59          ;
02FF  13        9           INX    D            ;
0300  1A       10           LDAX   D            ;
0301  D399     11           OUT    #99          ;
0303  13       12           INX    D            ;
0304           13                                ;
0304  1A       14           LDAX   D            ;ELT 7
0305  D35A     15           OUT    #5A          ;
0307  13       16           INX    D            ;
0308  1A       17           LDAX   D            ;
0309  D39A     18           OUT    #9A          ;
030B  13       19           INX    D            ;
030C           20                                ;
030C  1A       21           LDAX   D            ;
030D  D35B     22           OUT    #5B          ;
030F  13       23           INX    D            ;
0310  1A       24           LDAX   D            ;
0311  D39B     25           OUT    #9B          ;
0313  13       26           INX    D            ;
0314           27                                ;
0314  1A       28           LDAX   D            ;ELT 9
0315  D35C     29           OUT    #5C          ;
0317  13       30           INX    D            ;
0318  1A       31           LDAX   D            ;
0319  D39C     32           OUT    #9C          ;
031B  13       33           INX    D            ;
031C           34                                ;
031C  1A       35           LDAX   D            ;
031D  D35D     36           OUT    #5D          ;
031F  13       37           INX    D            ;
0320  1A       38           LDAX   D            ;
0321  D39D     39           OUT    #9D          ;
0323  13       40           INX    D            ;
0324           41                                ;BEAM 4
0324  1A       42           LDAX   D            ;ELT 1
0325  D35E     43           OUT    #5E          ;
0327  13       44           INX    D            ;
0328  1A       45           LDAX   D            ;
0329  D39E     46           OUT    #9E          ;
032B  13       47           INX    D            ;
032C           48                                ;
032C  1A       49           LDAX   D            ;
032D  D35F     50           OUT    #5F          ;
```

```
PAGE  14      FOX ASSEMBLER 8085V1/2              SOURCE FILE: IMAGE

LOC   OBJ     LINE  SOURCE STATEMENT
032F  13        1           INX    D            ;
0330  1A        2           LDAX   D            ;
0331  D39F      3           OUT    #9F          ;
0333  13        4           INX    D            ;
0334            5                                ;
0334  1A        6           LDAX   D            ;ELT 3
0335  D360      7           OUT    #60          ;
0337  13        8           INX    D            ;
0338  1A        9           LDAX   D            ;
0339  D3A0      10          OUT    #A0          ;
033B  13        11          INX    D            ;
033C            12                               ;
033C  1A        13          LDAX   D            ;
033D  D361      14          OUT    #61          ;
033F  13        15          INX    D            ;
0340  1A        16          LDAX   D            ;
0341  D3A1      17          OUT    #A1          ;
0343  13        18          INX    D            ;
0344            19                               ;
0344  1A        20          LDAX   D            ;ELT 5
0345  D362      21          OUT    #62          ;
0347  13        22          INX    D            ;
0348  1A        23          LDAX   D            ;
0349  D3A2      24          OUT    #A2          ;
034B  13        25          INX    D            ;
034C            26                               ;
034C  1A        27          LDAX   D            ;
034D  D363      28          OUT    #63          ;
034F  13        29          INX    D            ;
0350  1A        30          LDAX   D            ;
0351  D3A3      31          OUT    #A3          ;
0353  13        32          INX    D            ;
0354            33                               ;
0354  1A        34          LDAX   D            ;ELT 7
0355  D364      35          OUT    #64          ;
0357  13        36          INX    D            ;
0358  1A        37          LDAX   D            ;
0359  D3A4      38          OUT    #A4          ;
035B  13        39          INX    D            ;
035C            40                               ;
035C  1A        41          LDAX   D            ;
035D  D365      42          OUT    #65          ;
035F  13        43          INX    D            ;
0360  1A        44          LDAX   D            ;
0361  D3A5      45          OUT    #A5          ;
0363  13        46          INX    D            ;
0364            47                               ;
0364  1A        48          LDAX   D            ;ELT 9
0365  D366      49          OUT    #66          ;
0367  13        50          INX    D            ;
```

```
PAGE  15      FOX ASSEMBLER 8085V1/2                SOURCE FILE: IMAGE

LOC   OBJ     LINE  SOURCE STATEMENT
0368  1A        1           LDAX   D          ;
0369  D3A6      2           OUT    #A6        ;
036B  13        3           INX    D          ;
036C            4                              ;
036C  1A        5           LDAX   D          ;
036D  D367      6           OUT    #67        ;
036F  13        7           INX    D          ;
0370  1A        8           LDAX   D          ;
0371  D3A7      9           OUT    #A7        ;
0373  13        10          INX    D          ;
0374            11                             ;BEAM 5
0374  1A        12          LDAX   D          ;ELT 1
0375  D368      13          OUT    #68        ;
0377  13        14          INX    D          ;
0378  1A        15          LDAX   D          ;
0379  D3A8      16          OUT    #A8        ;
037B  13        17          INX    D          ;
037C            18                             ;
037C  1A        19          LDAX   D          ;
037D  D369      20          OUT    #69        ;
037F  13        21          INX    D          ;
0380  1A        22          LDAX   D          ;
0381  D3A9      23          OUT    #A9        ;
0383  13        24          INX    D          ;
0384            25                             ;
0384  1A        26          LDAX   D          ;ELT 3
0385  D36A      27          OUT    #6A        ;
0387  13        28          INX    D          ;
0388  1A        29          LDAX   D          ;
0389  D3AA      30          OUT    #AA        ;
038B  13        31          INX    D          ;
038C            32                             ;
038C  1A        33          LDAX   D          ;
038D  D36B      34          OUT    #6B        ;
038F  13        35          INX    D          ;
0390  1A        36          LDAX   D          ;
0391  D3AB      37          OUT    #AB        ;
0393  13        38          INX    D          ;
0394            39                             ;
0394  1A        40          LDAX   D          ;ELT 5
0395  D36C      41          OUT    #6C        ;
0397  13        42          INX    D          ;
0398  1A        43          LDAX   D          ;
0399  D3AC      44          OUT    #AC        ;
039B  13        45          INX    D          ;
039C            46                             ;
039C  1A        47          LDAX   D          ;
039D  D36D      48          OUT    #6D        ;
039F  13        49          INX    D          ;
03A0  1A        50          LDAX   D          ;
```

```
PAGE  16      FOX ASSEMBLER 8085V1/2              SOURCE FILE: IMAGE

LOC   OBJ     LINE  SOURCE STATEMENT
03A1  D3AD       1            OUT    #AD          ;
03A3  13         2            INX    D            ;
03A4             3                                 ;
03A4  1A         4            LDAX   D            ;ELT 7
03A5  D36E       5            OUT    #6E          ;
03A7  13         6            INX    D            ;
03A8  1A         7            LDAX   D            ;
03A9  D3AE       8            OUT    #AE          ;
03AB  13         9            INX    D            ;
03AC            10                                 ;
03AC  1A        11            LDAX   D            ;
03AD  D36F      12            OUT    #6F          ;
03AF  13        13            INX    D            ;
03B0  1A        14            LDAX   D            ;
03B1  D3AF      15            OUT    #AF          ;
03B3  13        16            INX    D            ;
03B4            17                                 ;
03B4  1A        18            LDAX   D            ;
03B5  D370      19            OUT    #70          ;
03B7  13        20            INX    D            ;
03B8  1A        21            LDAX   D            ;
03B9  D3B0      22            OUT    #B0          ;
03BB  13        23            INX    D            ;
03BC            24                                 ;
03BC  1A        25            LDAX   D            ;
03BD  D371      26            OUT    #71          ;
03BF  13        27            INX    D            ;
03C0  1A        28            LDAX   D            ;
03C1  D3B1      29            OUT    #B1          ;
03C3  13        30            INX    D            ;
03C4            31                                 ;
03C4  C9        32            RET                 ;FINISHED SETTING UP THE PHASES
03C5            33                                 ;
03C5            34                                 ;THIS IS THE END !!!!!

USER SYMBOLS

ABASE =#4000   ADIN  =#0162   BASIN =#7EE6   BASOUT=#7EE8
BBASE =#5400   DATIN =#0145   DOUT  =#01C1   FAZIT =#013B
FAZSET=#0222   GAIN  =#6900   GSET  =#2700   GTEMP =#7EE0
INCHEC=#7EEB   INFIN =#01B5   INIT  =#0050   LOOP  =#0152
NEXT  =#01AD   PHBASE=#7EEC   PHOUT =#01A2   RCHK  =#018B
READY =#0086   STAT  =#7EEA   STCK  =#7FFF   TIMOUT=#014F
TRANS =#0008   TX    =#008B   VRIN  =#7EE3   VROUT =#7EE1
ZONE  =#7EE5

USER ERRORS 0

CPU TIME = 2047.426 SECONDS
```

QUADRATURE PHASE SHIFTER

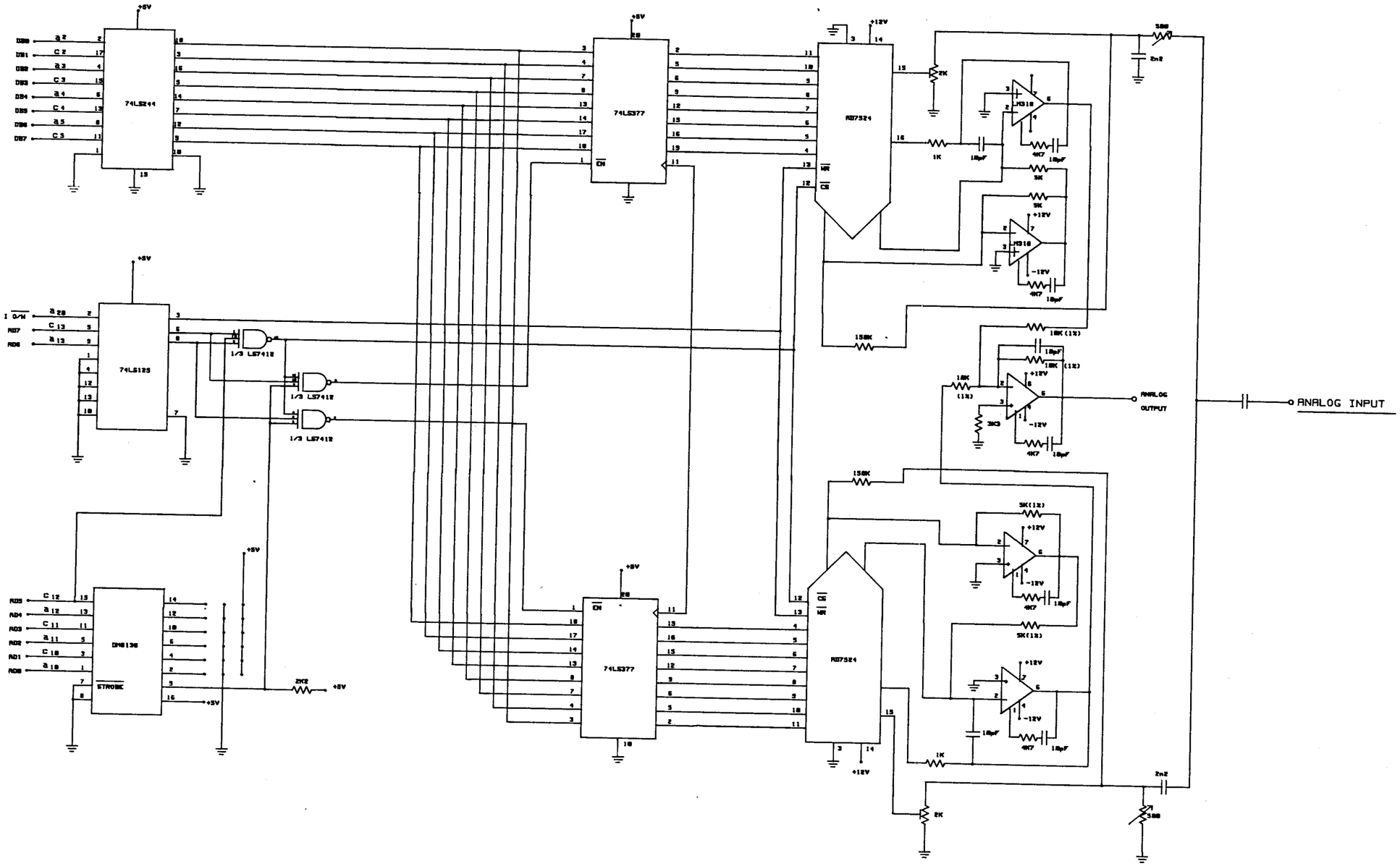

SUMMING AMPLIFIER AND A/D CONVERTER

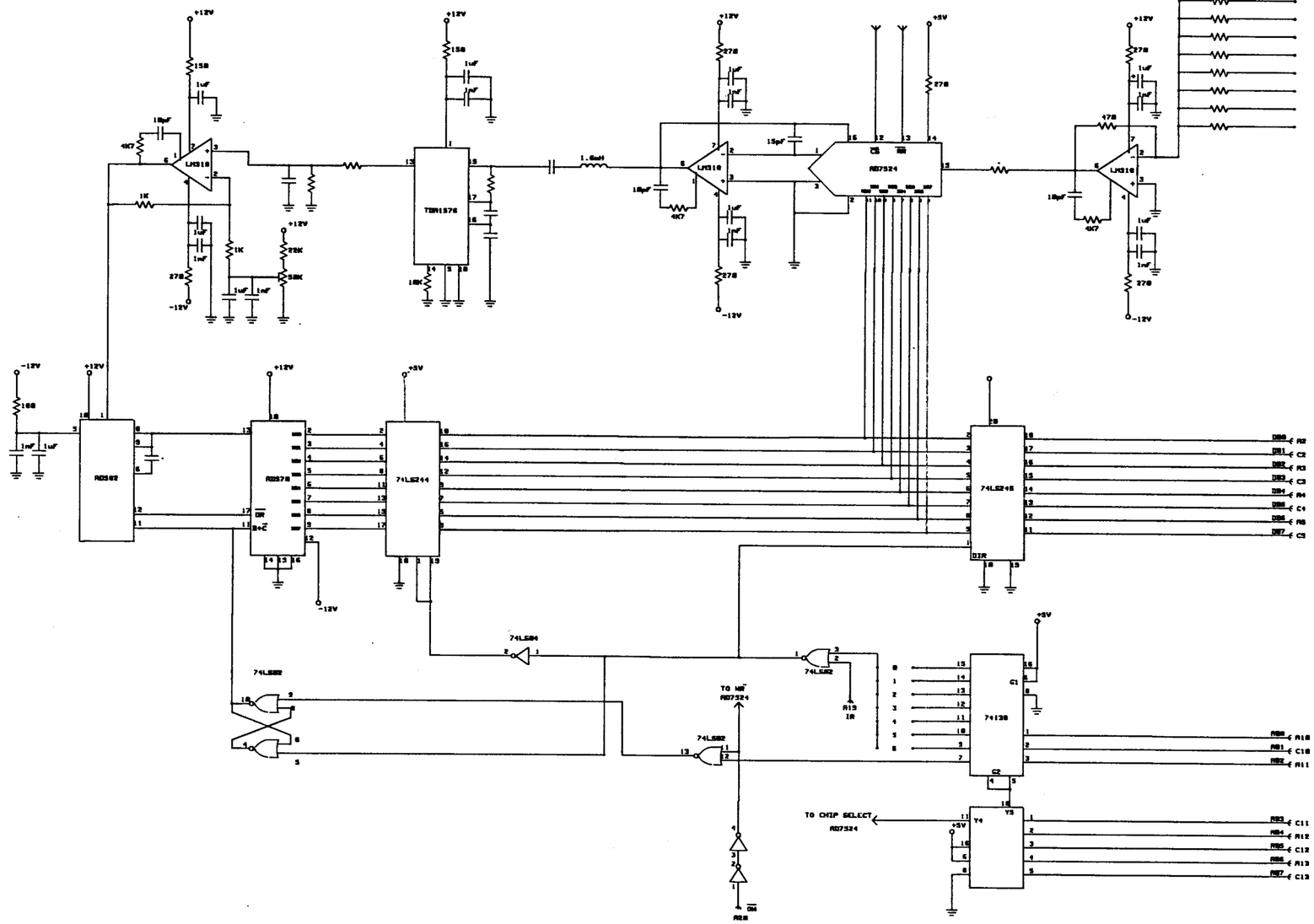

PRE AMPLIFIER

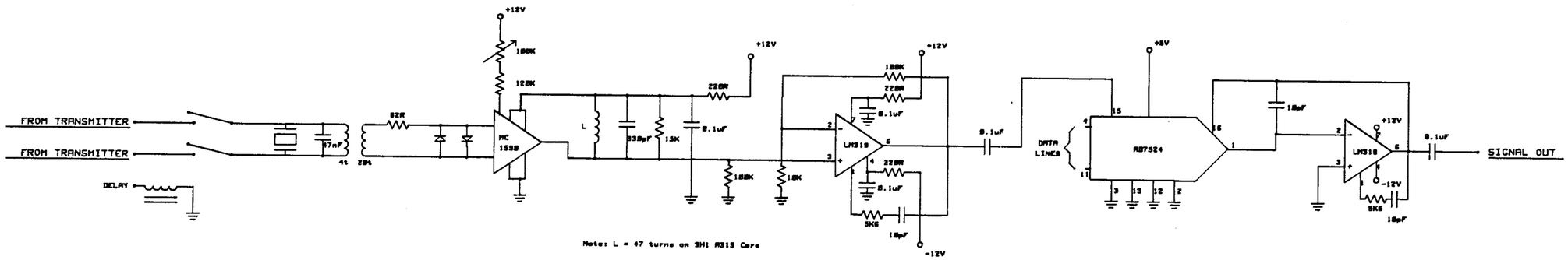

TRANSMIT SEQUENCE CONTROL

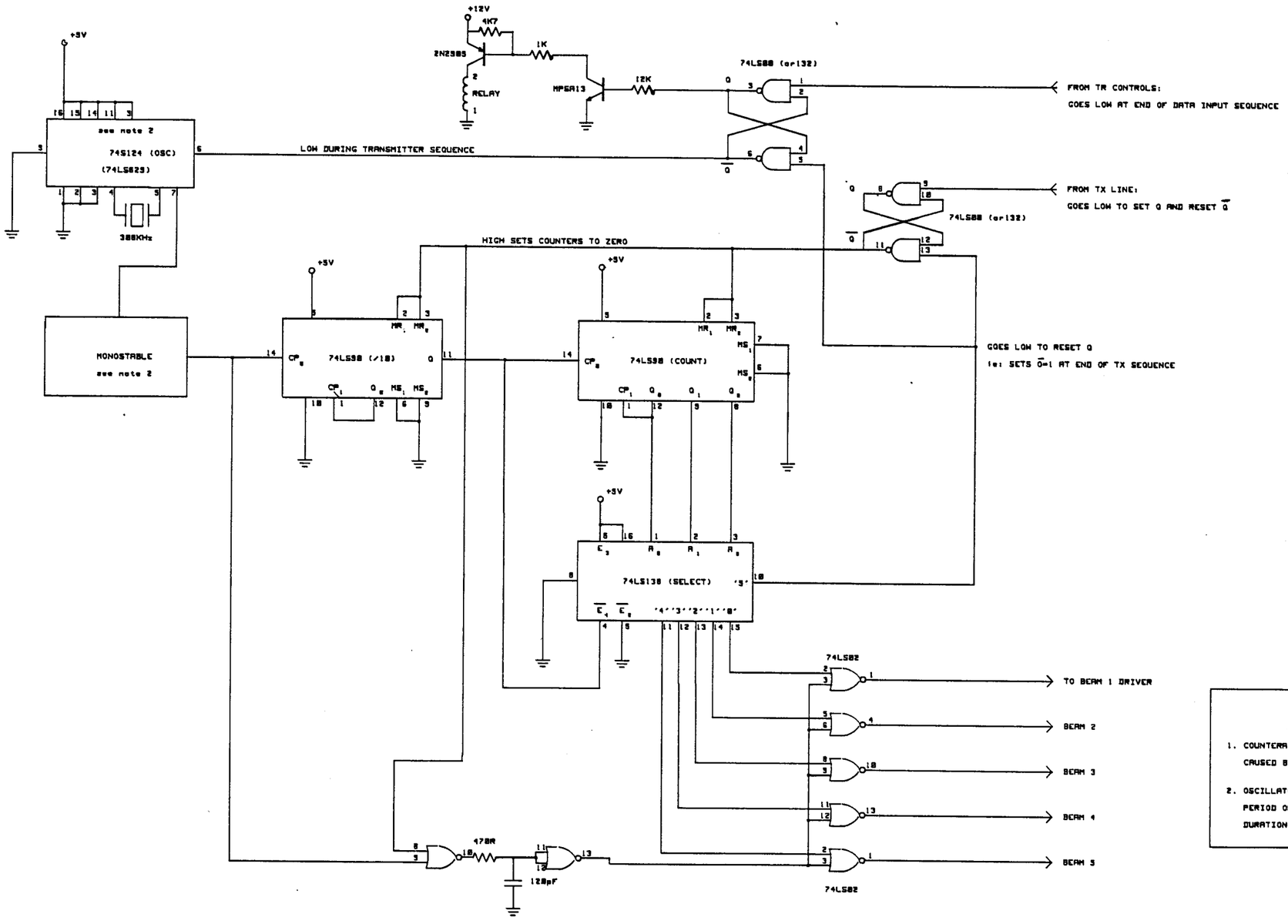

NOTES

1. COUNTERACTS THE GLITCH CAUSED BY UNEQUAL DELAYS
2. OSCILLATOR MUST PRODUCE A PERIOD OF 3.25uS WITH PULSE DURATION OF 288nS

TRANSMITTER DRIVER

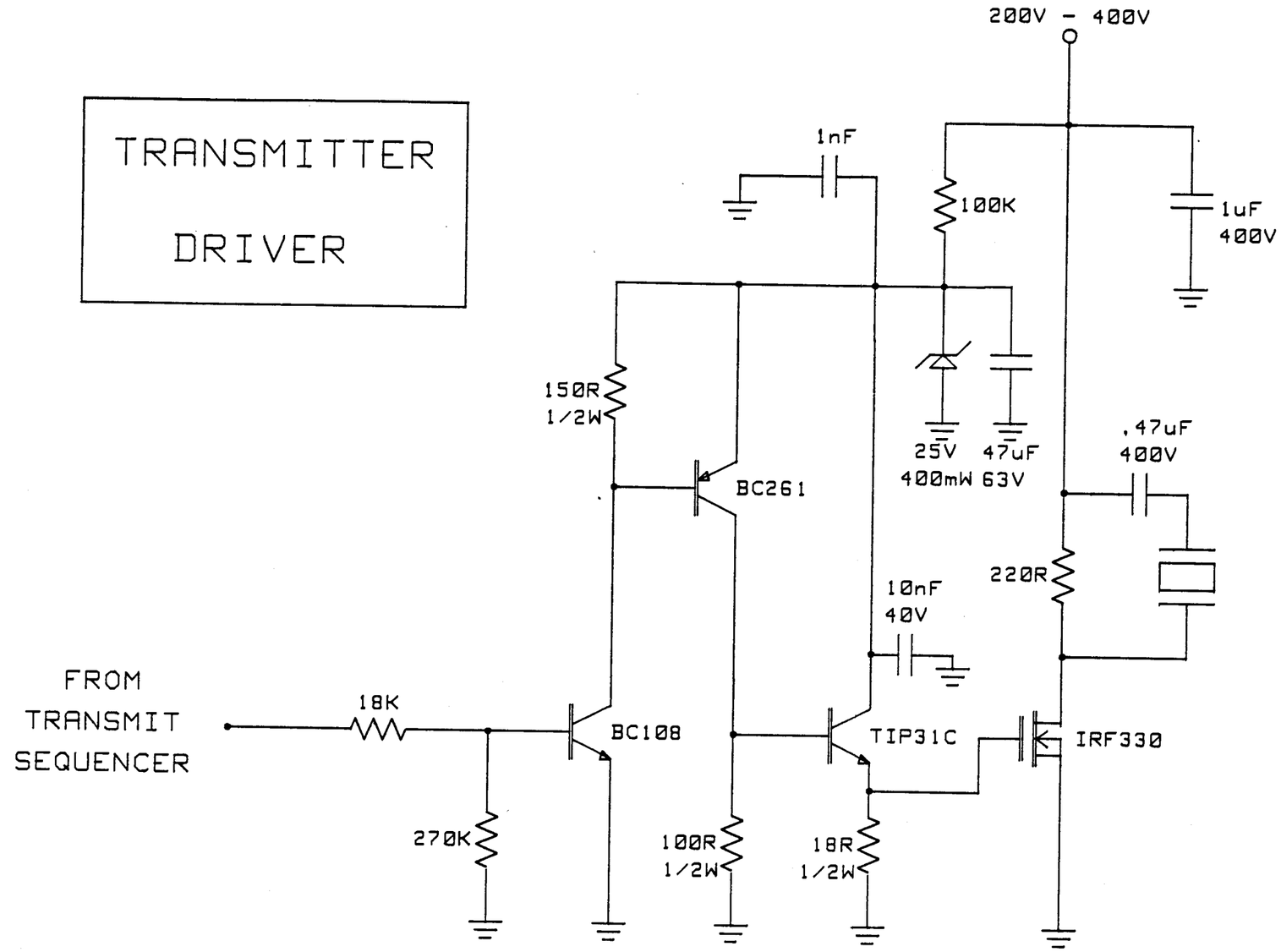

OUTPUT AND TIMING BOARD

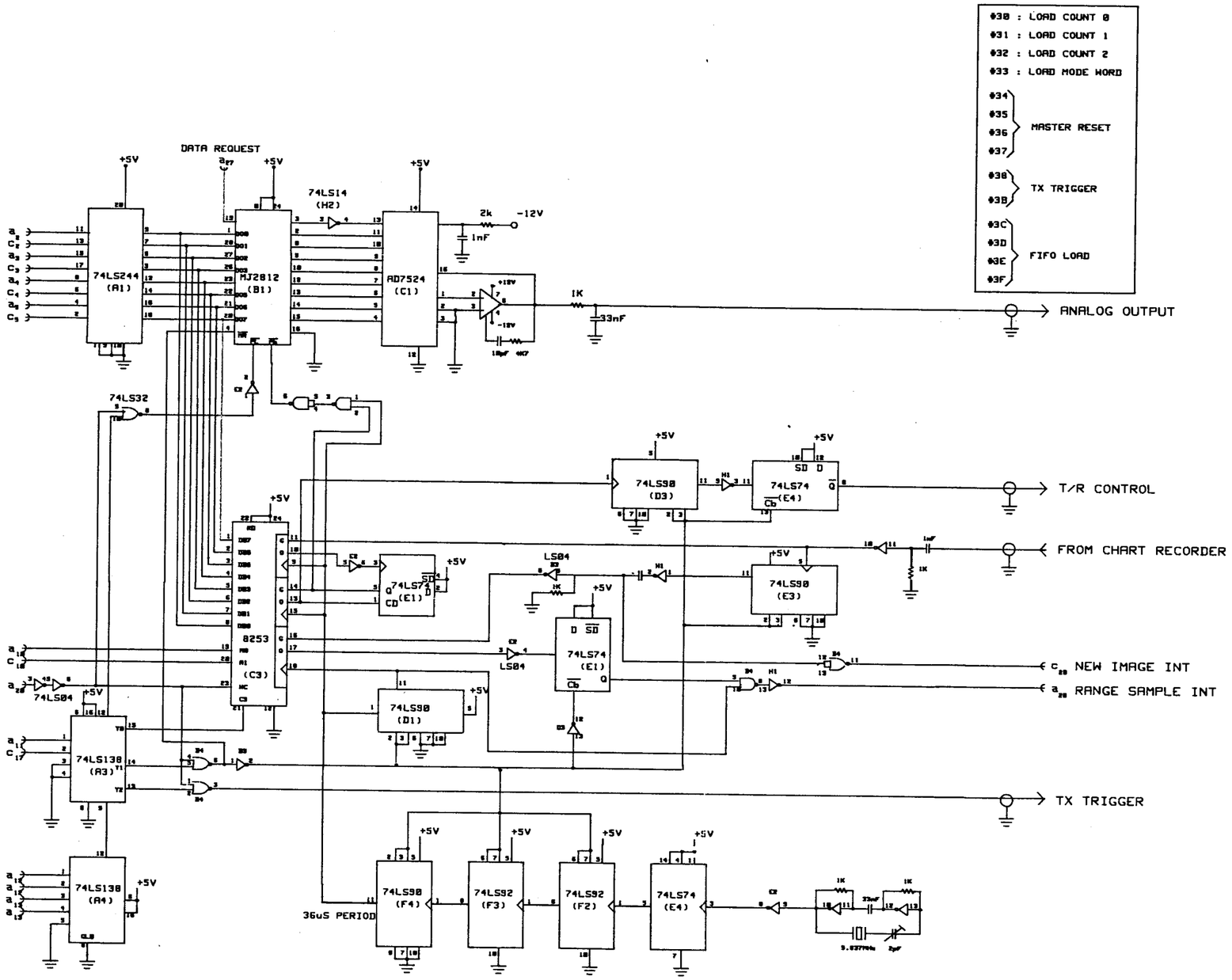

APPENDIX VI

The paper reproduced on the following pages describes the status of this project in early 1983 after the preliminary design phase.

The paper appears in:

"Acoustics and the Sea-Bed",
Proceedings of an Institute of Acoustics,
Underwater Acoustics Group Conference,
Edited by N.G. Pace,
Bath University Press,
Bath, U.K., (1983).

Electronically Focussed, Multibeam Side Scan Sonar

P. A. Fox, P. N. Denbigh
University of Cape Town, South Africa)

SUMMARY

The system constraints of a high resolution electronically focussed sidescan sonar are discussed. A design is described which provides a good compromise in terms of resolution and signal processing complexity. The necessary phase shifting is obtained using programmable gain amplifiers under microprocessor control.

INTRODUCTION

In side scan sonar systems the factor determining the operating frequency is the required maximum operating range. This paper describes a sidescan sonar aimed at an operating range of 150 meters. A system calculation (Denbigh and Flemming, 1982) using appropriate source levels, figures for sound attenuation, backscattering strengths, etc. show that a suitable operating frequency is 320 kHz. Having determined the operating frequency the resolution is determined by the length of the transducer. For a line source of length D meters, and a wavelength of λ meters, the beam diverses with an angle of λ/D radians (Macovski, 1979). Increasing D will lead to a decrease in beamwidth and a corresponding improvement in along-track resolution. Unfortunately the resolution in the near-field of a transducer array is approximately equal to its own length. Since the near-field extends to a range (Macovski, 1979) of D^2/λ it is apparent that the resolution cannot be arbitrarily increased unless the transducer is focussed. See Fig. 1.

For a 1 meter transducer, operating at 320 kHz, the nearfield extends to over 200 meters. In order to realise the available resolution of such a transducer over an operating range of 10-150 meters, it is necessary to focus the transducer onto the point to be imaged. The realization of an imaging system with an along-track resolution of approximately 0.2 meters is not without problems. Since the imaging must be performed out to a maximum range of 150 meters, and the corresponding two way propagation delay of an ultrasonic pulse in water is 200 ms, it follows that a single swath can only be imaged every 200 ms in order to avoid range ambiguities. This constrains the maximum towing speed of the 'fish' bearing the transducer to 0.2 meters in 200 ms, or 1 meters per second. This is considered to be too slow.

The focussing of a transducer array is achieved by dividing a transducer into an array of smaller transducers, and then applying a phase shift to the individual elements which varies quadratically over the length of the array. This realization leads to the possibility of steering the beam by applying, over and above the quadratic phase shift, a linear phase shift. Multiple non-overlapping beams can easily be realized by forming a number of beams, focussed at the same range, but having different linear phase shifts so as to image adjacent swaths. By imaging 5 adjacent swaths simultaneously, the imaging rate increases from 0.2 m in 200 ms to 1 m in 200 ms, or 5 meters per second. See Fig. 2.

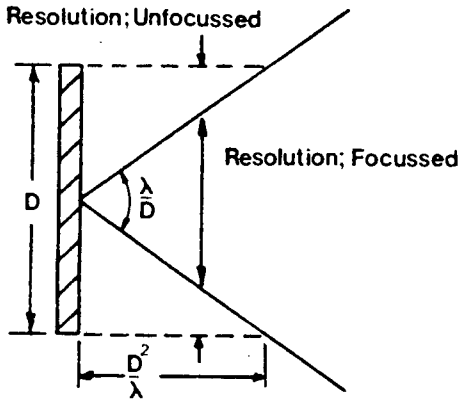

Fig.1.

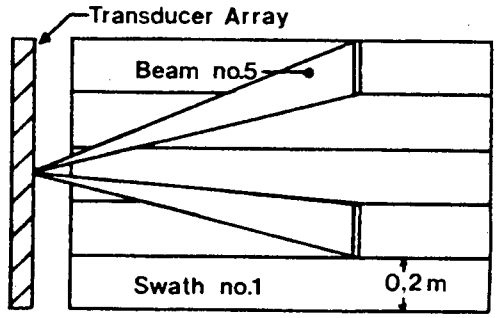

Fig.2.

The focussing and steering of a multibeam array in real time is a task well suited for a microprocessor. To this end a sidescan sonar is currently under construction. This uses a 1 meter long ten element transducer array, in conjunction with a bank of digitally controlled phase shifters and a microprocessor, to realize a dynamically focussed and steered transducer array forming 5 simultaneous beams.

TRANSDUCER ARRAY

The transducer is a contiguous array of ten elements, each 10 cm in length. For each element the radiated beam (or equivalently the beam of sensitivity) has, to a first approximation a constant beamwidth of 10 cm in the near field, i.e. to a range of 8 meters. Beyond this range the beam associated with each individual element diverges with an angle of Θ = 0.047 radians.

Focussing and beam steering with N elements can only be achieved in that zone in which the N elements have beams that overlap. This is illustrated in Fig. 3 for the case of three elements.

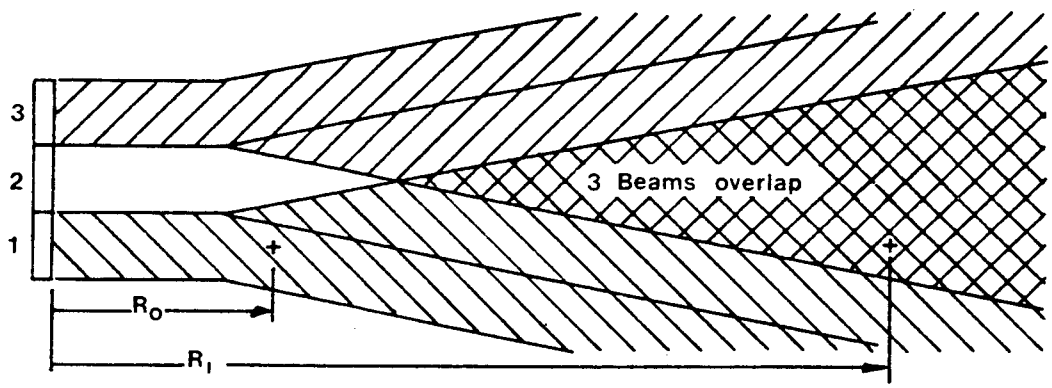

Fig.3.

Fig. 3 shows two image points or pixels which lie on the same swath but at different ranges R_0 and R_1. It is clear from the diagram that an echo from the pixel at range R_0 is only received by the transducer element labelled 1. An echo from a pixel at range R_1, well within the 3 dB beamwidths of all three elements, will provide approximately equal amplitude signals from each of the three elements. These signals will only differ in phase. By applying the correct phase shifts to the received signals they can be made to add in phase, thus realizing a focussed, steered beam. (See appendix A for further details).

It is apparent from the above discussion that not all the elements in a ten element array are useful in imaging at short ranges. Therefore, for each of the beams formed, the number of elements should be made to progressively increase with range, commencing with only one element at very short range, and increasing to the use of all ten elements at maximum range. In order to focus an array, a minimum of three elements are necessary. Two element arrays may be steered but not focussed. It follows that at those ranges where two elements are used, the best resolution obtainable corresponds to the near-field resolution of an unfocussed linear array two elements long. The near-field resolution of a two element array is the length of two elements, or 20 cm, in the system under construction. The along-track resolution thus varies from one element length at short ranges where only one element is used, to two element lengths at slightly greater ranges. Beyond the near field distance associated with a two element array, at ranges where the beams of N elements overlap, the optimum resolution becomes that of a focussed array N elements in length. At 150 meters this corresponds to the product of range and far-field beamwidth. This is 0.7 meters for a 1 meter array operating at 320 kHz. It is interesting to note that if the array length were increased to 2 meters, comprised of ten elements of 20 cm, the resolution at 150 meters would be improved to 0.35 m. However, at those lesser ranges where two elements only are used, the resolution would equal two element lengths which would now be 40 cm. For a ten channel processor the 1 m array is considered to provide the more attractive system.

The procedure used to determine the number of active elements for a given range is outlined in Appendix B. The results are shown in Table 1.

TABLE 1

RANGE	NO. OF ELEMENTS	ACTIVE ARRAY LENGTH	RESOLUTION
10-14 meters	3	0.3 meters	0.14-0.25 meters
14-17	4	0.4	0.17-0.22
17-25	5	0.5	0.18-0.22
25-31	6	0.6	0.18-0.20
31-34	7	0.7	0.17-0.21
34-37	8	0.8	0.18-0.21
37-44	9	0.9	0.18-0.21
44-150	10	1.0	0.19-0.70

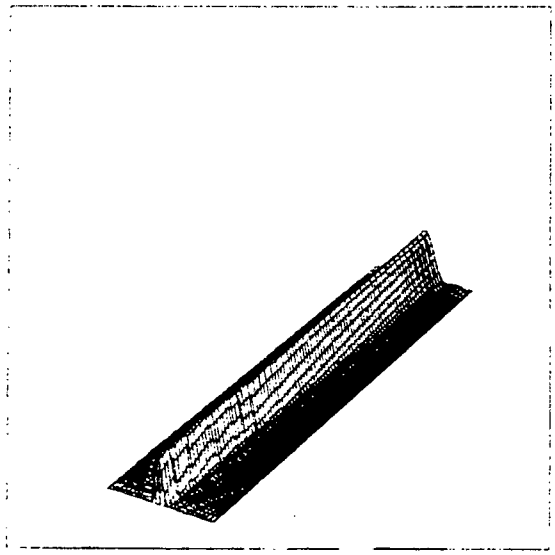

Fig. 4a.
FIELD INTENSITY OF FOCUSSED TRANSDUCER

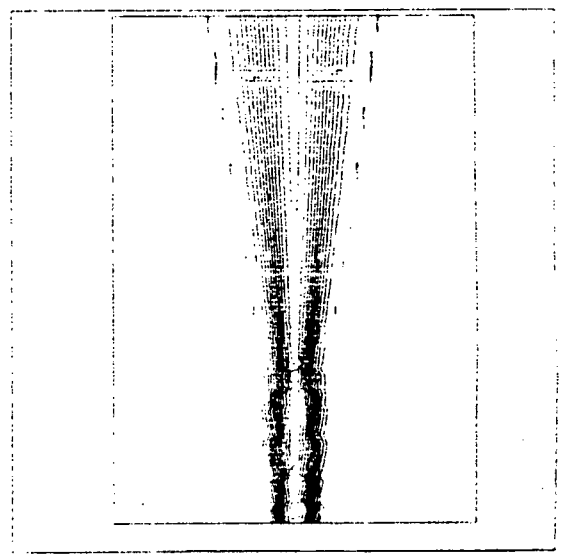

Fig. 4b.
FIELD INTENSITY OF FOCUSSED TRANSDUCER

A three dimensional plot of the radiation pattern of the array described above is shown in Fig. 4a, while contours of constant field intensity are shown in 4b.

PROGRAMMABLE PHASE SHIFTERS

The phase and amplitude of each element is controlled by passing the received signal from the element through a programmable phase shifter, which has been designed in such a way as to make amplitude control possible. A block diagram of a single phase shifter is shown in Fig. 5.

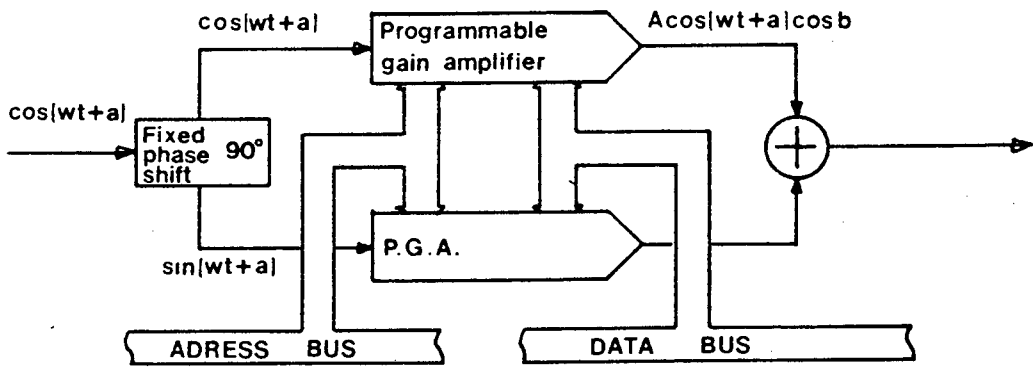

Fig.5.

The phase and amplitude control is achieved by passing the signal, say $\cos(\omega t+a)$, through a 90 degree phase shifter, so as to obtain the quadrature signals, $\cos(\omega t+a)$ and $\sin(\omega t+a)$. These signals are then passed through two programmable gain amplifiers. The cos term is multiplied by $A\cos(b)$ and the sin term by $A\sin(b)$. These two gain constants are read from a lookup table by the microprocessor and outputted to the amplifiers. The two scaled quadrature signals are then added, the result being

$$A\cos(\omega t+a)\cos(b)+A\sin(\omega t+a)\sin(b)$$

or $$A\cos(\omega t+a+b) \quad .$$

The multiplying constants are quantized into two 8-bit bytes. At unity gain the phase resolution is optimum and one degree phase increments are readily obtained. The phase resolution decreases with decreasing gain. This is not, however, a problem since the contribution of an element with less gain is smaller, thus allowing less need for an accurate phase shifter. A photograph of the completed phase shifter is shown in Fig. 6.

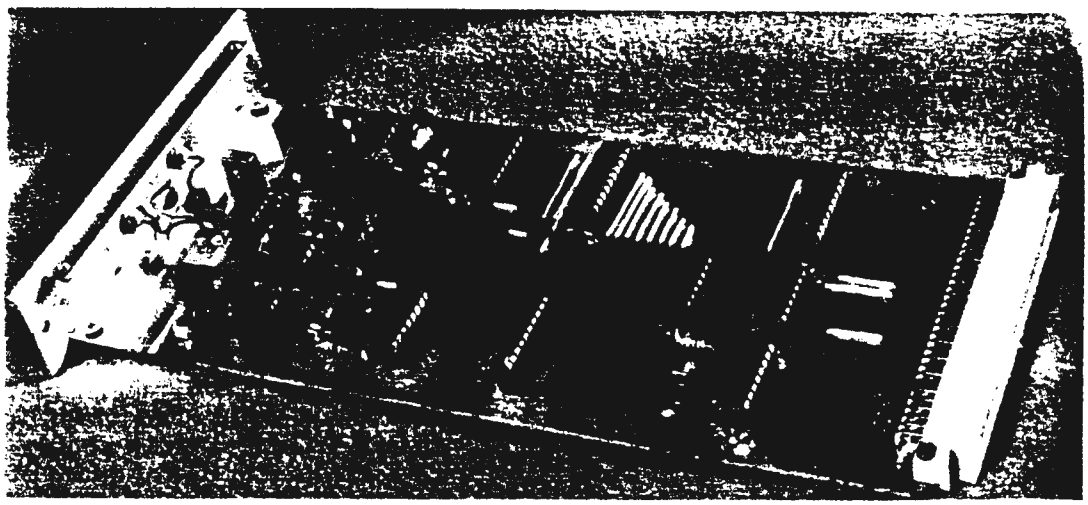

Fig.6.

MULTIPLE BEAM FORMATION

As mentioned in the introduction, the achievement of high resolution, and the constraints of towing speeds necessitates the formation of multiple beams. By imaging 5 swaths simultaneously a 5 times increase in towing speed is achieved. The required hardware for the formation of these multiple beams is shown in Fig. 7.

The focussing and steering of a single beam synthesized with a ten element array requires ten phase shifters. To focus and steer 5 beams requires 50 phase shifters.

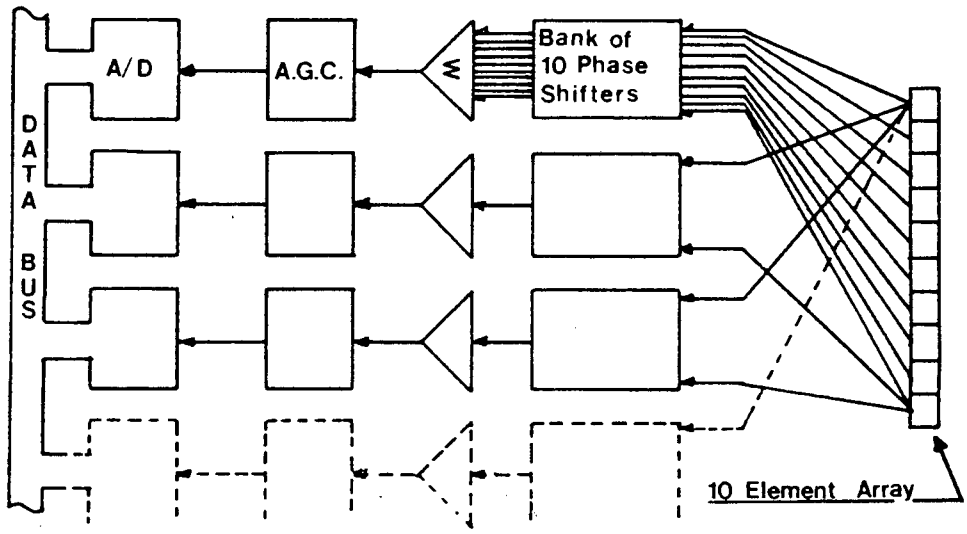

Fig.7.

TOWING SPEED VARIATIONS

The use of a microprocessor for setting up the required phases has the advantage of flexibility. This is used to great advantage in dealing with variations in towing speed. Consider the problem of the array being towed at twice the design speed. In this case the array moves 2 meters between transmitted pulses. Since the imaged swath is only 1 meter wide, it follows that there will be 1 meter wide gaps in the image. This is considered to be unacceptable. If a higher imaging rate is required, resolution must be sacrificed in the interests of obtaining an image of contiguous swaths. This is achieved by having a number of lookup tables of focus and steer data, one for each range of towing velocity. At the larger towing speeds the beams are defocussed (i.e. the swaths become wider) and steered to image more widely separated swaths. This is illustrated in Fig. 8a and 8b for towing speeds of 5 and 10 m/s respectively. A similar problem exists when the array is towed slower than 5 m/s. In this case the beams are steered inward without defocussing, so as to image a smaller total along-track swath with each pulse.

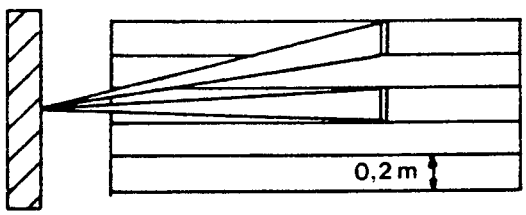

Fig.8a.

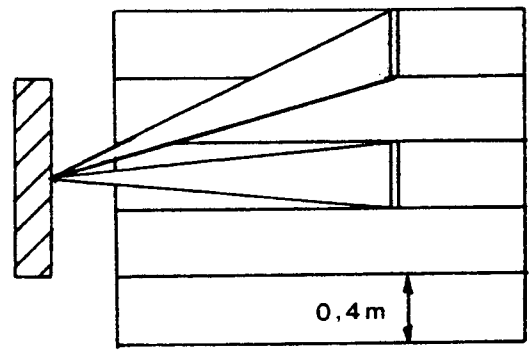

Fig.8b.

IMAGE STORAGE AND DISPLAY

After the 5 beams have been formed in the summing amplifiers shown in Fig. 7 the resulting signals are passed through an A.G.C. network to a sample-and-hold amplifier and thence to an analog-to-digital converter. The digitized image of the 5 swaths is then stored in a random access memory. It is desirable for standardization purposes to have the image available in a format compatible with a chart recorder.

A standard chart recorder forms an image line by line. The multi-beam imaging process, on the other hand, forms the image 5 lines at a time. It is thus necessary to store the image in one 'page' of random access memory while it is being formed. When the image of the 5 swaths is complete, it is transferred to an output buffer, from which the pixels are read out in order of increasing range, line by line. The 8-bit words, corresponding to the echo intensity at that pixel, are read into a digital-to-analog converter and the resulting analog levels are then used to intensity modulate the chart recorder. Thus the image is formed a negligible 150 ms, later than real time.

MICROPROCESSOR SYSTEM

The required phase shifts for each pixel are stored in a read only memory (or lookup table), where they are accessed by the microprocessor and placed in temporary latches. The temporary latches are required in order that the phase shifts are applied simultaneously to all elements. Since each phase shifter requires two bytes, it follows that the setting up of 50 phase shifts requires the microprocessor to access and output 100 bytes. The access and output of a single byte takes over 7 microseconds. Thus over 700 microseconds are required to set up all the phase shifters for a given range. Fortunately the depth of field of the focussed beam is significantly greater than a single range cell and focussing thus does not have to be updated for every range cell. While the image is being formed over a number of range cells, the data required for focussing is placed in the temporary latches. As soon as the 100 bytes have been read out a single command transfers the data to the programmable gain amplifiers in the phase shifters, thus achieving an instantaneous change of focussing and steering.

In summary then, the total system comprises the following subsystems:

1. Microprocessor
2. Two pages of random access memory
3. A lookup table of focus and steer data for each towing speed
4. 50 phase shifters
5. 5 summing amplifiers and A/D converters
6. One D/A for image output
7. Transducer array of ten, 10 cm elements
8. Transmitter
9. A towed 'fish' bearing the array.

The system configuration is shown below in Fig. 9.

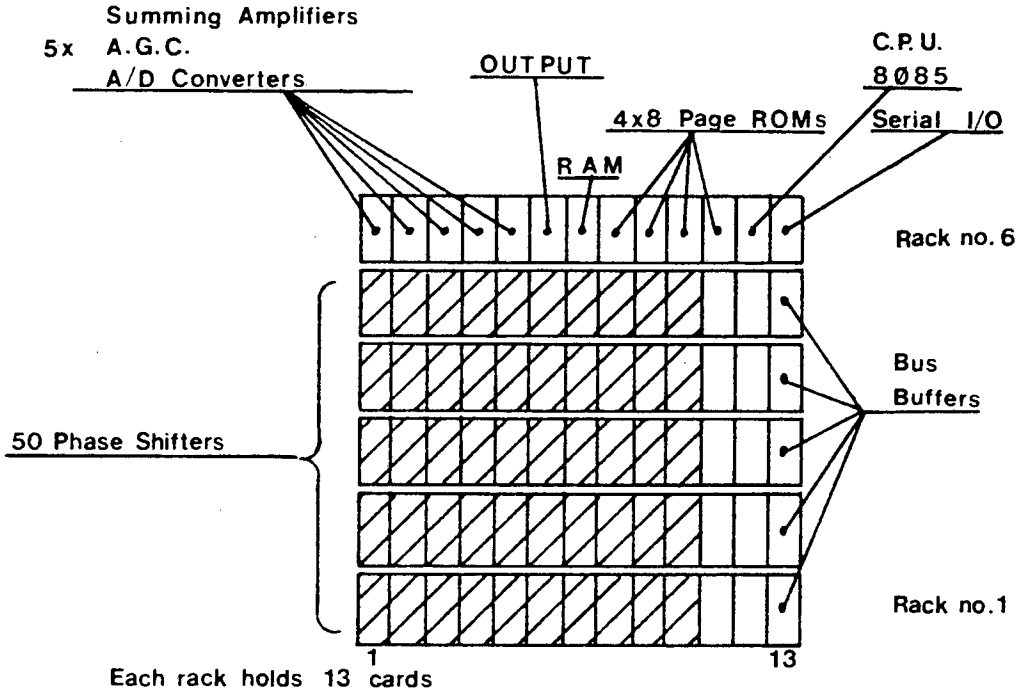

Fig.9.

APPENDIX A: Consider the geometry in Fig. 1. A monopole source at position (u,o) has a radial velocity $S(u)$ at its surface. It sets up a pressure $p(v,z)$ on a plane at range z meters.

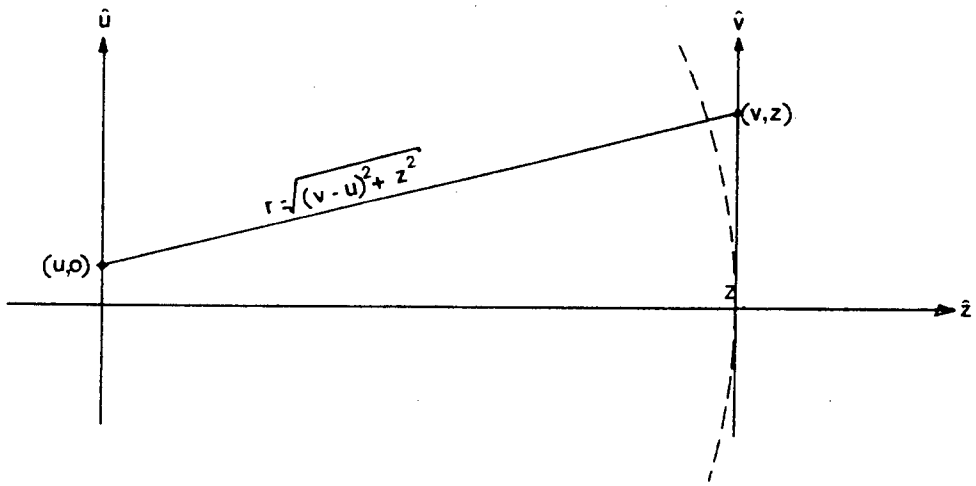

Fig.1.

The resulting pressure at (v,z) is related to the source through an amplitude term that varies as $^1/_r$ and a phase term that varies as

$\exp(-j\beta\sqrt{(v-u)^2+z^2})$

Thus (Clay and Medwin, 1977) $p(v,z)=\frac{k}{r}S(u)\exp(-j\beta\sqrt{(v-u)^2+z^2})$

Assuming that the $^1/r$ term varies significantly more slowly with r than the phase term the approximation

$$p(v,z)=k_1S(u)\exp(-j\beta\sqrt{(v-u)^2+z^2})$$

can be made on the plane of interest.

The field of a continuous array is described by an integral over the source

$$p(v,z)=k_1\int_{-\infty}^{+\infty}S(u)\exp(-j\beta\sqrt{(v-u)^2+z^2})du$$

For an array of N point sources with spacing Δu the resulting field is described by

$$p(v,z)=k_2\sum_{m=1}^{N}S(m\Delta u)\exp(-j\beta\sqrt{(v-m\Delta u)^2+z^2})$$

The required phases for focussing an array are found by setting $\Delta u = d$ where d is the element spacing and N is thus the number of elements. $S(md)$ is then determined such that the sum above is a maximum. The result is

$$S(md)=\exp(+j\beta\sqrt{(v-md)^2+z^2})$$

A table of $S(md)$ for the points (v,z) is stored in the ROM.

APPENDIX B: Having determined the phases required for focussing for various values of N (from $N=3$ elements to $N=10$) the field intensities are calculated for ranges from 10 to 150 m.

The contour lines of field intensity are plotted and the 0,2 meter wide swath is drawn in. The technique of selecting the number of elements is to use the minimum number of elements consistent with the -3dB intensity lying within a 0.2 metre swath. The three element array is found to be useful over the range from 10 to 14 meters at which point the -3dB contours diverge out of the 0,2 m swath. At this stage another element is introduced and the -3dB contours are found to remain within the desired limits until a range of 17 meters. This procedure is adopted until all 10 elements are being used.

REFERENCES.

Denbigh, P.N. and Flemming, B.W. (1982). Range Prediction and Calibration in Side Scan Sonar.
In: Recent Developments in Side Scan Sonar Techniques. (W.G.A. Russell-Cargill, ed.), pp. 81 - 100. Cape Town: W.G.A. Russell-Cargill.

Clay, C.S. and Medwin, H. (1977). Acoustical Oceanograph. New York: John Wiley and Sons.

Macovski, A. (1979). Ultrasonic Imaging Using Arrays. Proceedings of the IEEE, Vol. 67, No. 4, April 1979, 484 - 495.

REFERENCES

1. RICHARDSON, L.F., "Apparatus for Warning a Ship at Sea of its Nearness to Large Objects Wholly or Partly Under Water", British Patent Office, No.11,125 (1912).

2. FESSENDEN, H.M., "Fessenden, builder of tomorrows", Coward-McCann, New York, 1973, Ch.XXIX.

3. LANGEVIN, P. and CHILOWSKI, M.C., "Procedes et appareils pour la production de signaux sous-marins direges pour la localisation a distance dóbstacles sous-marins", French Patent 502913, (1916).

4. URICK, R.J., "Backscattering of Sound from a Harbour Bottom", J.A.S.A., Vol. 26:231, (1954).

5. URICK, R.J., "The Processes of Sound Scattering at the Ocean Surface and Bottom", Journal of Marine Research 15:134 (1956).

6. AHRENS, E., "Horizontallotung im Fischfang" Archiv fur Fischereiwissenschaft 6, Heft 3/4 s.230, (1955).

7. AHRENS, E., "Use of Horizontal Sounding for Wreck Detection", Int. Hyd. Rev., 34, (1957), p.73-81.

8. KUNZE, W., "General aspects of Application of Horizontal Echo Sounding Method to Shipping ", Int. Hyd. Rev., 34, (1957), p.63-72.

9. CHESTERMAN, W.D., CLYNICK, P.R. and STRIDE, A.H., "An Acoustic aid to Seabed Survey", Acoustica, 8, (1958), p.285-290.

10. HAINS, R.G., "Developments in Ultrasonic Instruments", Int. Hyd. Rev., 40:1, (1963), p.49-57.

11. RUSBY, S., "A Long Range Side Scan Sonar for use in the Deep Sea (GLORIA project)", Int.Hyd.Rev., 47:2, (1970), p.25-39.

12. GAZEY, B.K. and CREASEY, D.J., "A Very Short Range High Resolution Sidescan Sonar", British Acoustical Society, Side Scan Sonar Applications, 70:122, (1971).

13. FLEMMING, B.W., "A historical introduction to underwater acoustics with special reference to echo sounding, sub bottom profiling and side scan sonar", in "Recent developments in side scan sonar", Russel-Cargill, W.G.A., Editor, W.G.A. RUSSELL-CARGILL, University of Cape Town (1982), p.3.

14. SCHELKUNOFF, S.A., "A Mathematical Theory of Linear Arrays", Bell. Sys. Tech. J., 22, Jan., (1943), p.80-107.

15. WOODWARD, P.M., "A Method of Calculating the Field over a Plane Aperture required to produce a given Polar Diagram", J. Inst. Electrical Engns., 93:3a, (1946), p.1554.

16. SKOLNIK, M.I., "Introduction to radar systems", 2nd. Ed., McGraw-Hill, (1981), p.278.

17. SOMERS, M.L. and STUBBS, A.R., "Side scan Sonar", IEE Proc., 131, part F, No.3, (1984).

18. TUCKER, D.G., WELSBY, V.G. and KENDELL, R., "Electronic Sector Scanning", J. Brit. I.R.E., August (1958), p.465-484.

19. VOGLIS, G.M., "A General Treatment of Modulation Scanning as Applied to Acoustic Linear Arrays", Part 1: Ultrasonics, July (1971); Part 2 : Ultrasonics, October (1971).

20. TUCKER. D.G., WELSBY, V.G., KAY, L., TUCKER, M.J., STUBBS, A.R. and HENDERSON, J.G., "Underwater Echo-Ranging with Electronic Sector Scanning: Sea Trials on R.R.S. Discovery 2", J. Brit. I.R.E., November (1959), p.681-686.

21. WELSBY, W.G. and TUCKER, D.G., "Multiplicative Recieving Arrays", J. Brit. I.R.E., 19, June (1959), p.369.

22. McCARTNEY, B.S., "An Improved Electronic Sector Scanning Sonar Reciever", J. Brit. I.R.E., 22:6, December (1961), p.481-488.

23. WELSBY, V.G. and DUNN, J.R., "A High Resolution Electronic Sector-Scanning Sonar", J. Brit. I.R.E., September (1963), p.205-208.

24. KARRER, H.E., DIAS, J.F., LARSON, J.D. and PERING, R.D., "A Phased Array Acoustic Imaging System For Medical use", Acoustical Imaging and Holography, 10, Plenum, New York, (1980), p.47-63.

25. WELSBY, V.G., CREASEY, D.J. and BARNICKLE, N., "Narrow Beam Focused Array for Electronically Scanned Sonar: Some Experimental Results", J. Sound Vib., 30, no.2, (1973), p.237-248.

26. FREEDMAN, A., "Sound Field of a Rectangular Piston", J.A.S.A., 32, no. 2, February (1960), p.197-209.

27. KAY, L. and BISHOP, M.J., "The Effect of a Linear Phase Taper on the Near Field of an Ultrasonic Multi-element Array", The Radio and Electronic Engineer, April (1965), p.207-212.

28. WELSBY, V.G., "Electronic Scanning of Focused Arrays", J. Sound Vib., 8, no. 3, (1968), p.390-394.

29. TUCKER, D.G., "Near Field Effects in Electronic Scanning Sonar", J. Sound Vib., 8, no. 3, (1968), p.355-363.

30. SOMER, J.C., "Electronic sector scanning for Ultrasonic Diagnosis", Ultrasonics, July (1968), p.153-159.

31. SOMER, J.C., "New processing techniques for instantaneous Cross-sectional Echo-pictures and for improving angular resolution by smaller beams", Proceedings of the Forth Conference of the International Society for Ultrasonic Diagnosis in Opthalmology, May 6-9 (1971), Paris, France.

32. THURSTONE, F.L. and VON RAM, O.T.,"A new Ultrasound Imaging Technique Employing Two Dimentional Electronic Beam Steering", Acoustical Holography and Imaging, Vol. 5, Plenum, New York, (1973), p.249-259.

33. HOLLEY, M.L., MITSON, R.B. and PRATT, A.R., "Developments in Sector Scanning Sonar", IERE. Proc., 32, (1975), p.139-153.

34. SHERMAN, C.H., "Underwater Sound - A Review" IEEE Trans. on Sonics and Ultrasonics, SU-22, no. 5, September (1975).

35. BARTRAM, J.F., RAMSEYER, R.R. and HEINES, J.M., "Fifth Generation Digital Sonar Signal Processing", IEEE J. of Oceanic Eng., vol. OE-2, no. 4, October (1977), p.337-343.

36. KNIGHT, W.C., PRIDHAM, R.G. and KAY, S.M., "Digital Signal Processing for Sonar", IEEE Proc., vol. 69, no. 11, November (1981).

37. ANDERSON, V.C., "Digital Array Phasing", J.A.S.A., 32, (1960), p.867.

38. MANES, G.F., ATZENI, C. and SUSINI, C., "Design of Simplified Delay Systems for Ultrasound Phased Array Imaging", IEEE. Trans. Sonics and Ultrasonics, vol. SU-30, no. 6, (1983), p.350-354

39. KEATING, P.N., "Acoustical Holography-A Comparison with Phased Array Sonar", Acoustical Holography and Imaging, Vol. 5, (1973), p.231-237.

40. COOLEY, J.W. and TUKEY, J.W., "An Algorithm for the Machine Calculation of Complex Fourier Series", Math. Comput., 19, (1965), p.297.

41. SHERMAN, J.W., "Properties of Focused Apertures in the Fresnel Region", IRE. Trans. Ant. and Prop., July (1962), p.399-408.

42. DUCK, F., JOHNSON, S., GREENLEAF, J. and SAMAYOA, W., "Digital Image Focusing in the Near Field of a Sampled Acoustic Aperture", Ultrasonics, March (1977), p.83-88.

43. CORL, P.D., KINO, G.S., DESILETS, C.S. and GRANT P.M., "A Digital Synthetic Focus Acoustic Imaging System", Acoustical Imaging, Vol. 8., Plenum, New York, (1978), p.39-53.

44. LINDEN, D.A., "A Discussion of Sampling Theorems", Proc. IRE, 47, July (1959), p.1219-1226.

45. CURTISS, T.E. and WARD, R.J., "Digital beam forming for sonar systems", IEE Proc., 127, part F, No. 2, April (1980).

46. PRIDHAM, R.G. and MUCCI. R.A., "Shifted Sideband Beam Forming", IEEE. Trans. Acoust. Speech and Signal Processing, ASSP-27, 713-722, Dec. (1979).

47. MUCCI, R.A., "A Comparison of Efficient Beamforming Algorithms", IEEE Trans., ASSP-32, No. 3, June (1984).

48. DIX, J.F., DEAN, N., WIDDIWSON, J. and MAVOR, J., "Applications of CCDś to Sonar Systems", IEE Proc., Vol.127, Part F, No. 2, April (1980).

49. DOORNBOS, P. and SOMER, J.C., "An electrically variable analogue delay achieved fast consecutively commutated capacitors", Prog. Rep. 3, Inst. Med. Phys., TNO. Da Costakade 45, Utrecht, The Netherlands, (1972).

50. WALKER, J.T., "Doppler Wavefront Distortion Effects due to Continuous Dynamic Array Focusing", Acoustical Imaging, vol. 8, Plenum, New York, (1978), p.39-53.

51. POWERS, J.E., PHILLIPS, D.J., BRANDESTINI, M.A. and SIGELMANN, R.A., "Ultrasound Phased Array Delay Lines Based on Quadrature Sampling Technique", IEEE Trans., vol. SU-27, No. 6, November (1980).

52. EATON, M.D., MELEN, R.D. and MEINDL, J.D., "A Flexible Real Time System for Experimentation in Phased Array Ultrasound Imaging", Acoustical Imaging, vol. 8, Plenum, New York, (1978), p.55-67.

53. SHOTT, J.D., MELEN, R.D., MEINDL, J.D., "Charge-coupled devices for use in electronically-focused ultrasonic imaging systems", IEE Proc., Vol. 127, part F, No. 2, April (1980).

54. MANES, G.F., ATZENI, C., SUSINI, C. and SOMER, J.C., "A new Delay Technique with application to Ultrasound Phased Array Imaging systems", Ultrasonics, 17, September (1979), p.225-229.

55. HAVLICE, J.F., KINO, G.S., KOFOL, J.S. and QUATE, C.F., "An electronically focused acoustic imaging device", Acoustical Holography and Imaging, vol. 5, Plenum, New York, (1973), p.317-333.

56. SCHULKIN, M. and MARSH, H.W., "Absorbtion of Sound in Sea Water", J. Brit. IRE., 25:493, (1963).

57. URICK, R.J., "Principles of Underwater Sound", chap. 7, McGraw-Hill, (1975).

58. McKINNEY, C.M., and ANDERSON, C.D., "Measurements of Backscattering of Sound From The Ocean Bottom", J.A.S.A., vol. 36, (1964), p.158-163.

59. DENBIGH, P.N. and FLEMMING, B.W., "Range prediction and calibration in side scan sonar", in "Recent developments in side scan sonar", Russell-Cargill, Editor, W.G.A. RUSSELL-CARGILL, University of Cape Town (1982), p.81.

60. MILLER, E.B., SMITH, S.W. and THURSTONE, F.L., "A Study of Near Fieald Ultrasonic Beam Patterns from a Pulsed Linear Array", Acoustical Holography and Imaging, vol. 5, Plenum, New York, (1973), p.261-281.

61. MAGEUR, P., GELLY, J.F., MAERFELD, C. and CRALL, G., "An Underwater Focused Imaging System", Acoustic Imaging, vol. 10, Plenum, New York, (1982), p.607.

62. MACOVSKI, A., "Ultrasonic Imaging Using Arrays", Proc. IEEE, vol. 67, No. 4, April (1979).

63. SILVER, S., "Microwave Theory and Design", MIT. Rad. Lab. Ser., McGraw-Hill, New York (1949), vol. 12, p.173.

64. RUZE, J, "Antenna Tolerance Theory-A Review", Proc. IEEE, vol. 54, April (1966), p.633-640.

65. ZEMANEK, J., "Beam Behavior within the Near Field of a Vibrating Piston", J.A.S.A., 49, January (1971), p.181-191.

66. URICK, R.J., "Principles of Underwater Sound", chap. 9, McGraw-Hill, U.S.A., (1975).

67. CLAY, C.S. and MEDWIN, H., "Acoustical Oceanography", John Wiley and Sons, U.S.A., (1977).

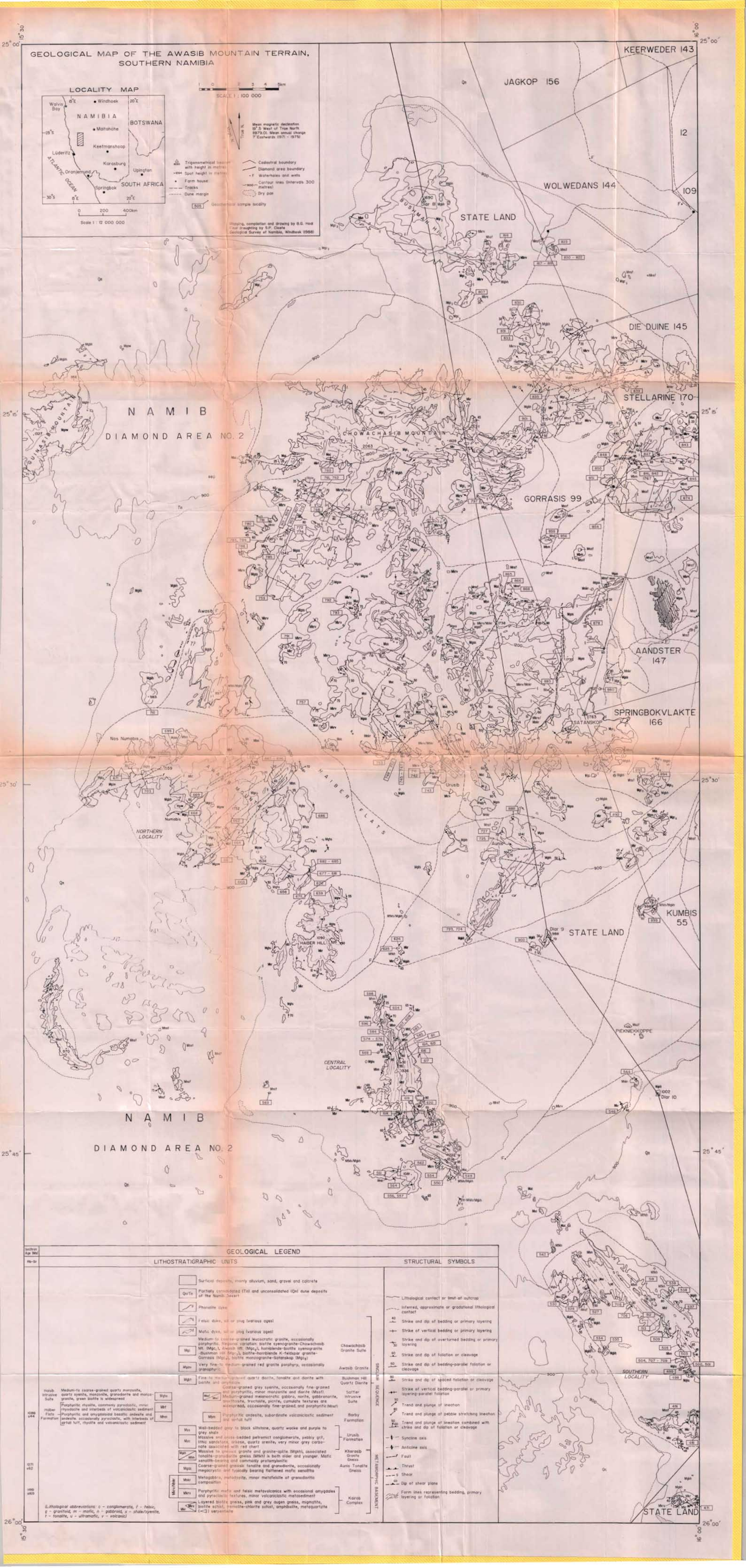
GEOLOGICAL MAP OF THE AWASIB MOUNTAIN TERRAIN, SOUTHERN NAMIBIA
LOCALITY MAP
Walvis Bay
Windhoek
NAMIBIA
BOTSWANA
Maltahöhe
Keetmanshoop
Lüderitz
Karasburg
Upington
Oranjemund
Springbok
SOUTH AFRICA
ATLANTIC OCEAN
SCALE 1 : 100 000
Mean magnetic declination 19°.5 West of True North (1973.0). Mean annual change 7' Eastwards (1971 - 1975)
Trigonometrical beacon with height in metres
Spot height in metres
Farm house
Tracks
Dune margin
Cadastral boundary
Diamond area boundary
Waterholes and wells
Contour lines (intervals 300 metres)
Dry pan
Geochemical sample locality
Mapping, compilation and drawing by B.G. Hall
Final draughting by S.P. Cleaife
Geological Survey of Namibia, Windhoek (1988)
KEERWEDER 143
JAGKOP 156
12
WOLWEDANS 144
109
STATE LAND
DIE DUINE 145
STELLARINE 170
NAMIB
DIAMOND AREA NO. 2
CHOWACHASIB MOUNTAIN
2063
GORRASIS 99
AANDSTER 147
SPRINGBOKVLAKTE 166
SATANKOP
Awasib
Nos Numabis
HAIBER FLATS
Urusib
Aunis
NORTHERN LOCALITY
KUMBIS 55
STATE LAND
HAIBER HILL
PIEKNEKKOPPE
CENTRAL LOCALITY
SOUTHERN LOCALITY
GEOLOGICAL LEGEND
LITHOSTRATIGRAPHIC UNITS
STRUCTURAL SYMBOLS
Surficial deposits, mainly alluvium, sand, gravel and calcrete
Partially consolidated (Tsl) and unconsolidated (Qn) dune deposits of the Namib Desert
Phonolite dyke
Felsic dyke, sill or plug (various ages)
Mafic dyke, sill or plug (various ages)
Chowachasib Granite Suite
Awasib Granite
Bushman Hill Quartz Diorite
Sorbie Intrusive Suite
Barby Formation
Urusib Formation
Kharasib Granite Gneiss
Aunis Tonalite Gneiss
Karas Complex
SWAKOP SEQUENCE
BASEMENT COMPLEX
Lithological contact or limit of outcrop
Inferred, approximate or gradational lithological contact
Strike and dip of bedding or primary layering
Strike of vertical bedding or primary layering
Strike and dip of overturned bedding or primary layering
Strike and dip of foliation or cleavage
Strike and dip of bedding-parallel foliation or cleavage
Strike and dip of spaced foliation or cleavage
Strike of vertical bedding-parallel or primary layering-parallel foliation
Trend and plunge of lineation
Trend and plunge of pebble stretching lineation
Trend and plunge of lineation combined with strike and dip of foliation or cleavage
Syncline axis
Anticline axis
Fault
Thrust
Shear
Dip of shear plane
Form lines representing bedding, primary layering or foliation